

# Sheffield Hallam University

*The role of the CNS endothelium in the pathogenesis of multiple sclerosis.*

PLUMB, Jonathan.

Available from the Sheffield Hallam University Research Archive (SHURA) at:

<http://shura.shu.ac.uk/20237/>

## A Sheffield Hallam University thesis

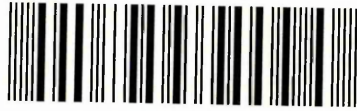
This thesis is protected by copyright which belongs to the author.

The content must not be changed in any way or sold commercially in any format or medium without the formal permission of the author.

When referring to this work, full bibliographic details including the author, title, awarding institution and date of the thesis must be given.

Please visit <http://shura.shu.ac.uk/20237/> and <http://shura.shu.ac.uk/information.html> for further details about copyright and re-use permissions.

101 826 195 8



**Fines are charged at 50p per hour**

07 NOV 06 4.14pm

22 FEB 2007 4pm

- 8 MAY 2007

28 APR 2007 5pm

**REFERENCE**

ProQuest Number: 10700882

All rights reserved

INFORMATION TO ALL USERS

The quality of this reproduction is dependent upon the quality of the copy submitted.

In the unlikely event that the author did not send a complete manuscript and there are missing pages, these will be noted. Also, if material had to be removed, a note will indicate the deletion.



ProQuest 10700882

Published by ProQuest LLC (2017). Copyright of the Dissertation is held by the Author.

All rights reserved.

This work is protected against unauthorized copying under Title 17, United States Code  
Microform Edition © ProQuest LLC.

ProQuest LLC.  
789 East Eisenhower Parkway  
P.O. Box 1346  
Ann Arbor, MI 48106 – 1346

# **The Role of the CNS endothelium in the pathogenesis of Multiple Sclerosis**

**Jonathan Plumb**

A thesis submitted in partial fulfilment of the requirements of  
Sheffield Hallam University for the degree of Doctor of Philosophy

August 2005

## Abstract

Multiple sclerosis (MS) is an inflammatory demyelinating disease of the central nervous system (CNS) causing neurological disability in young adults. The neuropathological features of MS include large perivascular inflammatory cell infiltrates, microglia activation, antigen presentation and reactive astrogliosis. The CNS is protected by highly regulated blood-brain barrier (BBB) that is breached in MS as detected by MRI. Formation and regulation of the BBB involves the interactions of the interendothelial tight junction-associated proteins, occludin, ZO-1 and claudin. The results from this study suggest that the BBB is disrupted at the molecular level with alterations in ZO-1 and occludin expression being observed in blood vessels from MS tissue compared with normal control white matter. Tight junction (TJ) disruption was observed predominantly within vessels from active MS lesion however disruption was also observed within the normal appearing white matter and chronic lesions. The results of this study suggest that TJ disruption plays a critical role in disease progression as TJ abnormalities were observed in conjunction with serum protein leakage and large inflammatory infiltrates. BBB leakage as gauged by MRI is reported to cease after an attack however this study shows that a low level of persistent serum protein leakage occurs in chronic lesions.

The recruitment of circulating leukocytes and resident glial cells to sites of CNS inflammation is dependant on the interaction of adhesion molecules, chemokines and their receptors and cytokines and their receptors. A disintegrin and metalloproteinase-17 (ADAM-17) is an enzyme that has been shown to mediate proteolytic cleavage of some of these inflammatory components. The results in this study have described the constitutive expression of ADAM-17 by the cerebral endothelial cells in human and rat CNS. ADAM-17 is also shown to be expressed by resident glia and inflammatory cells and is elevated in active MS lesions and in the spinal cords of rats during peak phase of experimental autoimmune encephalomyelitis suggesting a pathogenic role for ADAM-17 in these disease processes. *In vitro* studies confirmed the production of ADAM-17 by cerebral endothelial cells and astrocytes. ADAM-17 expression is increased under pro-inflammatory conditions whereas its natural inhibitor TIMP3 is decreased. Release of TNF from GP8 cell surface is induced following treatment with TNF and LPS.

## Contents

Abstract	i
Contents	ii
List of figures	xi
List of tables	xiv
Directory of Suppliers	xv
Abbreviations	xvii
References relevant to the thesis	xxi
Acknowledgements	xxii

## Chapter 1

### Introduction

1.1 Multiple sclerosis	1
1.1.1 Epidemiology of MS	1
1.1.2 Genetics and gene association studies in MS	2
1.1.3 Clinical symptoms of MS	4
1.1.4 Diagnosis of MS	5
1.1.4.1 Magnetic resonance imaging	5
1.1.4.2 Analysis of CSF in MS	9
1.1.5 Disease course in MS	9
1.2 Cellular constituents of the CNS	11
1.2.1 Cerebral endothelia and the BBB	11
1.2.2 Microglia	14
1.2.3 Astrocytes	15
1.2.4 Oligodendrocytes	16
1.3 Pathology of MS	17
1.3.1 Heterogeneity of MS lesions	19
1.3.2 Axonal pathology	21
1.3.3 Oligodendrocyte pathology	22
1.3.4 Remyelination	25

1.4 Inflammation and the BBB	26
1.4.1. BBB in Multiple Sclerosis and other CNS disorders	30
1.5 Immunology of MS	31
1.5.1 Immune cell response in MS	31
1.5.1.1 T cells	31
1.5.1.2 B cells	34
1.5.1.3 Microglia	35
1.5.1.4 Astrocytes	37
1.5.2 Cytokines in MS	37
1.5.2.1 Tumor necrosis factor family	38
1.5.2.1.1 <i>In vivo</i> evidence for TNF involvement in MS	39
1.5.2.1.2 Autopsy tissue evidence for TNF involvement in MS	39
1.5.2.1.3 <i>In vitro</i> evidence for TNF involvement in MS	40
1.5.3 Chemokines in MS	41
1.6 Matrix metalloproteinases	43
1.6.1 MMPs and multiple sclerosis	43
1.6.1.1 <i>In vivo</i> evidence for MMP involvement in MS	44
1.6.1.2 Autopsy tissue evidence for MMP involvement in MS	44
1.6.1.3 <i>In vitro</i> evidence for MMP involvement in MS	44
1.7. ADAM family proteins	45
1.7.1 Domain structure of the ADAM family	45
1.7.2. ADAM proteins in biology	48
1.8 Experimental autoimmune encephalomyelitis an experimental model of MS	50
1.8.1 Autoantigens in EAE	50
1.8.2 MOG as an autoantigen in EAE	51
1.9 Pathology of EAE	51
1.9.1 Pathological comparisons to MS	52
1.9.2 Cellular and immune responses in EAE	52

1.9.2.1 Cytokines	52
1.9.2.1.1 TNF and IFN $\gamma$ in EAE	53
1.9.2.1.2 IL-1 in EAE	53
1.9.2.1.3 IL-12 in EAE	54
1.9.2.1.4 IL-4 and IL-10 in EAE	54
1.9.2.2 Chemokines	54
1.9.2.3 Adhesion molecules	55
1.10 The aim of this thesis	56

## **Chapter 2**

### Endothelial tight junction-associated proteins of the blood-brain barrier in multiple sclerosis

2.1 Introduction	58
2.1.1 Molecular composition of the BBB tight junction (TJ)	58
2.1.1.1 Transmembrane proteins	58
2.1.1.2 Cytoplasmic sub-membranous plaque associated proteins of the TJ	61
2.1.1.3 The adherens junction	62
2.1.2 Regulation of TJs	62
2.1.3 Aim of study	63
2.2 Materials and Methods	65
2.2.1 Selection of tissue for TJ study	65
2.2.1.1 Formalin fixed paraffin embedded tissue	67
2.2.1.1.1 Microwave antigen retrieval	67
2.2.1.1.2 Proteinase K	67
2.2.1.2 Snap-frozen tissue	67
2.2.2 Tissue characterisation	68
2.2.2.1 Single label immunofluorescence staining	68

2.2.2.2 Dual label immunofluorescence staining	70
2.2.3 Imaging	71
2.2.3.1 Confocal scanning laser microscopy	71
2.2.3.2 Data collection	74
2.2.3.3 Data analysis	74
2.2.3.4 Statistical analysis	76
2.2.3.5 Digital photography	76
2.3 Results	76
2.3.1 Optimisation of immunostaining protocols for TJ study	76
2.3.2 Characterisation of snap frozen tissue	78
2.3.3 Indirect immunofluorescence	81
2.3.3.1 TJ expression in normal and OND controls	81
2.3.3.2 TJ expression in MS	81
2.3.3.3 Extent of abnormal ZO-1 expression in MS	83
2.3.3.4 TJ abnormalities and vessel size	83
2.3.4 Correlation of TJ abnormalities with other aspects of MS pathology	86
2.3.4.1 TJ abnormality and evidence of recent myelin breakdown	86
2.3.4.2 TJ abnormality and macrophage/microglial activation	86
2.3.4.3 TJ abnormality and lymphocytic infiltration	89
2.3.4.4 TJ abnormality and serum protein leakage	89
2.3.5 Influence of Death-autopsy interval on TJ abnormalities and serum protein leakage	93
2.4 Discussion	96

## Chapter 3

### Expression of ADAM-17 in the CNS in MS: a pathogenic role

3.1 Introduction	104
3.1.1. ADAM-17	104
3.1.1.1 ADAM-17 in disease	106
3.1.1.2 ADAM-17 and MS	107
3.1.2. TIMP3	107
3.1.3. Aim of study	108
3.2 Materials and methods	110
3.2.1 Tissue characterisation	110
3.2.1.1. Immunohistochemistry	110
3.2.2 Indirect Immunofluorescence staining	112
3.2.2.1. Semi quantitative analysis of ADAM-17 immunoreactivity	114
3.2.2.2 Tyramide Signal Amplification	114
3.2.3 Imaging	115
3.2.3.1 Confocal scanning laser microscopy	115
3.2.3.2 Digital photography	115
3.2.4 Protein and mRNA extraction	115
3.2.4.1 Bicinchoninic acid (BCA) Assay	116
3.2.5 SDS PAGE and western blotting	116
3.2.6 mRNA analysis	118
3.2.6.1 Reverse transcriptase PCR	118
3.3 Results	120

3.3.1 Tissue characterisation	120
3.3.2. ADAM-17 immunoreactivity within control and MS white matter	123
3.3.3 TIMP3 immunoreactivity within control and MS white matter	128
3.3.4 Western blot analysis of ADAM-17 and TIMP3 from human CNS tissue homogenates	135
3.3.5 Identification of ADAM-17 and TIMP3 mRNA in MS and normal control tissue	135
3.4 Discussion	140

## **Chapter 4**

### ADAM-17 expression within rat spinal cords of experimental autoimmune encephalitis, an experimental model of MS

4.1 Introduction	147
4.1.1 The use of EAE as a therapeutic model for MS treatment	147
4.1.2 Aim of study	148
4.2 Materials and methods	149
4.2.1 Experimental autoimmune encephalomyelitis tissue	149
4.2.2 Immunohistochemistry	149
4.2.3 Indirect Immunofluorescence staining	150
4.2.3.1 Single label immunofluorescence	150

4.2.3.2 Dual label immunofluorescence	150
4.2.4 Imaging	151
4.2.5 Quantification	151
4.2.5.1 ADAM-17 and ED1 grading	151
4.2.5.2 Co-localisation	151
4.2.6 Protein and RNA extraction	151
4.2.7 Western blotting for ADAM-17 and TIMP3	152
4.2.8 RNA analysis for ADAM-17 and TIMP3	152
4.2.8.1 Reverse transcriptase PCR	152
4.2.8.2 Real-time PCR	152
4.3 Results	155
4.3.1 Characterisation of rat spinal cord histopathology	155
4.3.2 Indirect immunofluorescence	157
4.3.2.1 ADAM-17 expression in EAE and control rat spinal cord	157
4.3.2.2 TIMP3 expression in EAE and control rat spinal cord	159
4.3.2.3 Cellular localisation of ADAM-17	159
4.3.3 ADAM-17 and TIMP3 protein levels in EAE and control rat spinal cord white matter	164
4.3.4 Detection of ADAM-17 and TIMP3 mRNA at various stages of EAE disease course	166
4.3.4.1 RT-PCR	166
4.3.4.2 qRT-PCR	166
4.4 Discussion	170

## Chapter 5

### Expression and regulation of ADAM-17 and TIMP3 in endothelial cells *in vitro*

5.1 Introduction	176
5.1.1. <i>In vitro</i> cultures of cerebral endothelial cells	176
5.1.2 Aim of study	177
5.2 Materials and Methods	178
5.2.1 Cell cultures	178
5.2.1.1 Collagen coating	178
5.2.1.2 Subculture	179
5.2.1.3 Culture on coverslips	179
5.2.2 Indirect immunofluorescence	179
5.2.2.1 Dual label immunofluorescence	180
5.2.2.2 Imaging	180
5.2.3 Cytokine stimulation of GP8 endothelial cells	182
5.2.4 Protein extraction	182
5.2.4.1 Western blot	182
5.2.5 TNF enzyme linked-immuno-sorbent assay	183
5.3 Results	184
5.3.1 Characterisation of cell cultures	184
5.3.2 ADAM-17 and TIMP3 expression within cell cultures	184
5.3.2.1 ADAM-17 expression in cell cultures	184
5.3.2.2 TIMP3 expression in cell cultures	187

5.3.3 Cytokine regulation of ADAM-17 and TIMP3 expression in GP8 endothelial cells	192
5.3.4 Cytokine regulation of TNF release by GP8 cells	192
5.4 Discussion	197
<b>Chapter 6</b>	
General Discussion	
Discussion	202
Future Work	210
Summary	212
<b>Chapter 7</b>	
Appendix	214
References	225

## List of figures

### Chapter 1

1.1 MRI scan	7
1.2 Disease course in MS	10
1.3 Schematic representation of the blood-brain barrier	12
1.4 MS pathologies	18
1.5 Schematic representation of axon degeneration	23
1.6 Schematic representation of adhesion molecules and transendothelial migration	27
1.7 Schematic representation of T cell-APC interaction	32
1.8 Schematic representation of the domain structure of ADAM proteins	46
1.9 Schematic representation of pathological mechanisms in the CNS during MS	57

### Chapter 2

2.1 Schematic representation of the molecular components of the TJ at the BBB	59
2.2 Schematic representation of different antibody detection methods	69
2.3 Schematic representation of the detection principles in CSLM	72
2.4 ZO-1 detection using different tissues and fixatives	77
2.5 Grading of MS lesion activity	80
2.6 Normal and abnormal TJ protein expression	82
2.7 Assessing blood vessel integrity with TJ proteins	84
2.8a Extent of TJ disruption in all tissue categories	85
2.8b Extent of TJ disruption in all tissue categories from each case	85
2.9 Comparison of TJ abnormality and blood vessel sizes	87
2.10 TJ abnormality and cellular activation within active MS lesions	88
2.11 TJ abnormality associated with inflammatory cells	90
2.12 Serum protein leakage and TJ disruption	91
2.13 TJ abnormality and fibrinogen leakage	92
2.14 Association of TJ disruption with serum protein leakage	94
2.15 Association of death-autopsy interval with TJ disruption and serum protein leakage	95

## **Chapter 3**

3.1 Comparison of immunostaining for ADAM-17 using different fixatives and antibodies	124
3.2 Co-localisation of the monoclonal (Amgen) and polyclonal (Abcam) antibodies to ADAM-17	125
3.3 ADAM-17 expression within control and MS white matter	126
3.4 ADAM-17 immunoreactivity grading system	127
3.5 Extent of ADAM-17 immunoreactivity in all tissue groups	129
3.6 Expression of ADAM-17 in lesions displaying active disease process	130
3.7a ADAM-17 co-localisation with the endothelial marker, von Willebrand factor	131
3.7b ADAM-17 co-localisation with the endothelial marker, von Willebrand factor	132
3.8 ADAM-17 co-localisation with the astrocytic marker GFAP	133
3.9 ADAM-17 co-localisation with MHC class II expressing microglia and macrophages	134
3.10 Western blot analysis of ADAM-17 and TIMP3 protein expression in MS and control white matter	136
3.11 ADAM-17 mRNA expression in MS and normal control white matter using RT-PCR	137
3.12 TIMP3 mRNA expression in MS and normal control white matter using RT-PCR	138
3.13 GAPDH mRNA expression in MS and normal control white matter using RT-PCR	139

## **Chapter 4**

4.1 ED1 expression within naïve and EAE spinal cords	158
4.2 ADAM-17 expression within naïve and EAE spinal cord	160
4.3 ADAM-17 co-localisation with the astrocytic marker GFAP in EAE spinal cords	161
4.4 ADAM-17 co-localises with the macrophage marker ED1 in EAE	162
4.5 ADAM-17 co-localises with the endothelial marker von Willebrand factor in EAE	163

4.6 Western blot analyses of ADAM-17 and TIMP3 expression during the disease course of EAE	165
4.7 RT-PCR products for ADAM-17 in naïve and EAE spinal cords	167
4.8 RT-PCR products for TIMP3 in naïve and EAE spinal cords	168
4.9 qRT-PCR analysis of ADAM-17 and TIMP3 mRNA expression	169
<b>Chapter 5</b>	
5.1 Characterisation of cell cultures	185
5.2 Single label immunofluorescence for ADAM-17 and cytoskeletal markers in GP8 endothelial cells and 1° human astrocytes	186
5.3 Cellular localisation of ADAM-17 in GP8 endothelial cell cultures	188
5.4 ADAM-17 co-localises with actin filaments in GP8 endothelial cells	189
5.5 Dual label immunofluorescence for ADAM-17 and markers for Golgi apparatus and tubulin in GP8 endothelial cells	190
5.6 ADAM-17 and TIMP3 protein expression in GP8 endothelial and primary human astrocyte cell cultures	191
5.7 ADAM-17 expression in GP8 cells following pro-inflammatory stimulation	193
5.8 ADAM-17 expression by GP8 endothelial cells under control and inflammatory conditions	194
5.9 TIMP3 expression in GP8 cells following pro-inflammatory stimulation	195
5.10 Release of soluble TNF from GP8 endothelial cells following pro-inflammatory stimulation	196
<b>Chapter 6</b>	
6.1 Schematic representation of the possible roles for ADAM-17 in the CNS during MS pathogenesis	207

## List of tables

### Chapter 1

1.1 Selected scores from the Kurtzke expanded disability status scale	6
1.2 Phenotypic markers of oligodendrocyte development	16

### Chapter 2

2.1 Summary of individual details of all the cases used in the TJ study	66
2.2 TJ and fibrinogen scoring grades	75
2.3 Description and distribution of scoring for cellular activation within the MS tissue samples studied	79

### Chapter 3

3.1 Case details of subjects in this study	111
3.2 Summary of primary antibodies used for indirect immunofluorescence staining	113
3.3 Individual block characterisation for lesion activity and ADAM-17 expression	121
3.4 Description and distribution of scoring for cellular activation within the MS tissue samples studied	122

### Chapter 4

4.1 Rat specific primer sequences as used during qRT-PCR to assess mRNA in EAE	153
4.2 ADAM-17 and ED1 immunoreactivity grades EAE rats	156
4.3 Ratio of ADAM-17 and TIMP3 protein levels at four stages of EAE, as determined by western blotting	164

### Chapter 5

5.1 Primary antibodies used for immunocytochemistry in the cell culture study	181
---	-----

Directory of suppliers for the reagents used in this thesis

Supplier	Address
Abcam	332 Cambridge Science Park, Milton Rd, Cambridge, CB4 0FW, UK
Amersham	Pollards Wood, Nightingales Lane, Chalfont St Giles, Bucks, HP8 4SP, UK
BDH (now VWR international)	Merck House, Poole, Dorset, BH15 1TD, UK
Bioline	16 The Edge Business Centre, Humber Rd, London, NW2 6EW, UK
Bio-Rad	Bio-Rad House, Maylands Ave, Hemel Hempstead, Hertfordshire, HP2 7TD, UK
Biosource	542 Flynn Rd, Camarillo, CA 93012, USA
Chemicon	The Science Centre, Eagle Close, Chandlers Ford, Hampshire, S053 4NF, UK
Dako	Denmark House, Angel Drove, Ely, Cambridgeshire, CB7 4ET, UK
Invitrogen	3 Fountain Drive, Inchinnan Business Park, Paisley, PA4 9RF, UK
Millipore	Upper Mills Industrial Estate, Bristol Rd, Stonehouse. Gloucestershire, GL10 2BJ, UK
Molecular Probes	Now supplied by Invitrogen Ltd
Novocastra	Balliol Business Park West, Benton Lane, Newcastle Upon Tyne, NE12 8EW, UK
Oncogene	10394 Pacific Centre Court, San Diego, CA 92121, USA
Peptotech	Peptotech House, 29 Margravine Rd, London, W6 8LL, UK
R&D Systems	19 Barton Lane, Abingdon Science Park, Abingdon, OX14 3NB, UK
Roche	Bell Lane, Lewes, East Sussex, BN7 1LG, UK
Santa Cruz	2145 Delaware Ave, California, 95060, USA
Serotec	22 Bankside, Station Approach, Kidlington, Oxford, OX5 1JE, UK

Sigma	The Old Brickyard, New Road, Gillingham, Dorset, SP8 4XT, UK
Vector laboratories	3 Accent Park, Bakewell Rd, Orton Southgate, Peterborough, PE2 6XS, UK
Zymed	Cambridge BioScience, 24-25 Signet Court, Newmarket Rd, Cambridge, CB5 8LA, UK

## List of abbreviations

ADAM	A disintegrin and metalloproteinase
ALD	Adrenoleukodystrophy
APC	Antigen presenting cell
ApoE	Apolipoprotein E
APP	Amyloid precursor protein
BBB	Blood brain barrier
BCA	Bicinchoninic acid
BCR	B cell receptor
BMEC	Brain microvascular endothelial cell
Bp	Base pair
BSA	Bovine serum albumin
cDNA	Complementary deoxyribonucleic acid
CNPase	2', 3'-cyclic nucleotide-3-phosphohydrolase
CNS	Central nervous system
CREAE	Chronic relapsing EAE
CSF	Cerebrospinal fluid
CSLM	Confocal scanning laser microscope
Da	Daltons
DAB	3, 3' diaminobenzidine
DAI	Death autopsy interval
DAPI	4',6-diamidino-2-phenylindole
DC	Dendritic cell
DMEM	Dulbecco's modified Eagles medium
EAE	Experimental autoimmune encephalomyelitis
EBV	Epstein Bar Virus
ECM	Extracellular matrix
EDSS	Expanded disability status scale
EGF	Epidermal growth factor
EPO	Erythropoietin
FCS	Fetal calf serum
FFPE	Formalin fixed paraffin embedded

FITC	Fluorescein Isothiocyanate
GalC	Galactocerebroside
GAMES	Genetic analysis of multiple sclerosis in Europeans
GAPDH	Glyceraldehyde-3-phosphate dehydrogenase
Gd-DTPA	Gadolinium-diethylenetriaminepentaacetic acid
GMCSF	Granulocyte macrophage colony stimulating factor
GFAP	Glial fibrillary acidic protein
H&E	Haematoxylin and eosin
HHV	Human herpes virus
HIV	Human immune deficiency virus
HLA	Human leukocyte antigen
HUVEC	Human umbilical vein endothelial cell
ICAM	Intercellular adhesion molecule
IFN	Interferon
Ig	Immunoglobulin
IL	Interleukin
IOD	Integrated optical density
IP-10	Interferon gamma inducible protein-10
IPx	Immunoperoxidase
Jak	Janus kinase
JAM	Junctional adhesion molecule
LCA	Leukocyte common antigen
LT	Lymphotoxin
LFA	Lymphocyte function antigen
LPS	Lipopolysaccharide
MAb	Monoclonal antibody
MBP	Myelin basic protein
MCP	Monocyte chemoattractant protein
MHC	Major histocompatibility complex
MIG	Monokine induced by gamma-interferon
MIP	Macrophage inflammatory protein
MMP	Matrix metalloproteinase
MOBP	Myelin oligodendrocyte basic protein
MOG	Myelin oligodendrocyte glycoprotein

MRI	Magnetic resonance imaging
MRS	Magnetic resonance spectroscopy
MS	Multiple Sclerosis
MTI	Magnetic transfer imaging
MT-MMP	Membrane type MMP
NAA	N-acetyl aspartate
NAWM	Normal appearing white matter
OND	Other neurological disease
OPC	Oligodendrocyte progenitor cell
ORO	Oil red O
PBMC	Peripheral blood monocytes
PBS	Phosphate buffered saline
PI	Propidium Iodide
PLP	Proteolipid protein
PPMS	Primary progressive MS
qRT-PCR	Quantitative real time polymerase chain reaction
RANTES	Regulated upon activation, normal T cell expressed and secreted
RNA	Ribonucleic acid
RRMS	Relapsing remitting MS
RT	Room temperature
RT-PCR	Reverse transcriptase polymerase chain reaction
SDS	Sodium dodecyl sulphate
SF	Snap frozen
SPMS	Secondary progressive MS
SSPE	Subacute sclerosing panencephalomyelitis
STAT	Signal transducer activating transcription
SVMP	Snake venom metalloprotease
TACE	TNF alpha converting enzyme
TBS	Tris buffered saline
TCR	T cell receptor
TEER	Transendothelial electrical resistance
Th	T helper
TIMP	Tissue inhibitor of metalloproteinase
TNF	Tumor necrosis factor

TNFR	TNF receptor
VCAM	Vascular cell adhesion molecule
VEP	Visual evoked potential
VLA	Very late antigen
VWF	von Willebrand factor

### ***Publications relevant to the thesis***

1. Plumb, J., McQuaid S., Mirakhur, M., Kirk, J. Abnormal endothelial tight junctions in active lesions and normal-appearing white matter in multiple sclerosis. *Brain Pathology*, 2002; 12:154-69.
2. Kirk J., Plumb J., Mirakhur M., McQuaid S. Tight junctional abnormality in multiple sclerosis white matter affects all calibres of vessel and is associated with blood-brain barrier leakage and active demyelination. *J Pathology* 2003; 201:319-27.
3. Plumb, J., Cross, AK., Surr, J., Haddock, G., Smith, T., Bunning, RAD., Woodroffe, MN. ADAM-17 protein and mRNA expression in the spinal cord of rats with acute experimental autoimmune encephalomyelitis. *J Neuroimmunology*, 2005; 164:1-9
4. Plumb J., McQuaid S., Cross AK., Surr J., Haddock G., Bunning RAD., Woodroffe MN. Upregulation of ADAM-17 expression in active lesions in multiple sclerosis. *Multiple Sclerosis*, 2005, in press.

## Acknowledgements

The work described within this thesis would not have been possible without the assistance and guidance to whom I owe many thanks.

To my supervisors Prof N Woodroffe and Dr R Bunning, whose encouragement, guidance and assistance was invaluable.

To all the members of staff and students of the BMRC (past and present), for all their help, encouragement, and making the last three years so memorable, especially Jessica, Gail, Alison and Clare.

To Dr S McQuaid, from the department of neuropathology, Royal Group of Hospitals Trust, Belfast, whose supervision of the tight junction project and introduction to MS research have lead me to where I am today. I am forever grateful for his continued friendship and encouragement.

The undertaking of this study would not have been possible without the financial backing of the MS society of the UK and Ireland.

A special thanks is extended to my MS buddies, Margaret, Roger and Linda for their extremely positive encouragement and inspiration.

Finally to my wife Rose who is always there for me during the long character changing months of the write up, her encouragement and belief in me have been vital.

### 1.1 Multiple sclerosis

Multiple sclerosis (MS) is described as a chronic inflammatory autoimmune demyelinating disease of the central nervous system (CNS). This description encompasses a number of aspects that are either generalised or based on supposition from research using animal models. MS was first described by a French neurologist, Jean Martin Charcot, in 1868. Charcot described the pathology of patients, who had intermittent episodes of neurological dysfunction, as having an accumulation of inflammatory cells in a perivascular distribution affecting both the brain and spinal cord white matter (Hafler, 2004). Charcot termed his findings as *sclérose en plaque disseminées*, or multiple sclerosis (Thompson and McDonald, 1996; Hafler, 2004). MS symptoms and neurological disability arise from inflammation, demyelination, reduction in axonal function and loss of axons within the CNS (DeLuca *et al.*, 2004). These demyelinated areas of the CNS are referred to as lesions or plaques.

#### 1.1.1 Epidemiology of MS

Mean age of onset occurs during early adulthood (30 years old), however the distribution actually shows a bimodal distribution with a peak age of onset at 21-25 years and a lesser peak at 41-45 years old (Thompson and McDonald, 1996). However childhood onset, though uncommon, has been reported along with a diagnosis in patients over 70 years old. As MS begins in early adult life it carries major consequences on careers, family and social life (Thompson and McDonald, 1996). MS, like many other autoimmune diseases is more common in females than males, in a ratio of 3:2. Over 1 million people suffer from MS worldwide (Barcellos and Thomson, 2003). MS has a prevalence of approximately 85,000 cases within the UK with an incidence of about 2,500 new cases a year. The prevalence of MS is varied worldwide and has been shown to be more prevalent in temperate countries and areas of northern latitudes, suggesting that an environmental factor may have an influence on a person's likelihood of

developing MS. Prevalence varies geographically in the UK, with the south of England having approximately 50 cases /100,000 of the population while the Shetland and Orkney Isles having 300 cases /100,000 of the population (Swingler and Compston, 1986). Japan, although geographically would be expected to have a high prevalence of MS, actually has a very low prevalence, indicating a genetic role in MS susceptibility. Following migrational studies, individuals emigrating from an area of high prevalence to an area with a lower prevalence before the onset of puberty adopt the prevalence of their new residence. People emigrating after the age of onset of puberty retain the prevalence risk factor of their original country (Gale and Martyn, 1995) further implicating the influence of environmental factors in the development of disease.

### *1.1.2 Genetics and gene association studies in MS*

It is widely believed that susceptibility to MS is determined by a complex interaction of susceptibility genes and the environment (Willer *et al.*, 2003). Genetic factors are further suggested by twin studies in which monozygotic twins have a higher concordance rate (30%) than dizygotic twins (4%) (Ebers *et al.*, 1986; McFarland, 1993; Willer *et al.*, 2003; Lindsey, 2005). It has recently been suggested that twins with MS share a systemic condition called the MS trait, in which an environmental trigger is required to transform the trait into the disease (Poser, 2004).

Family studies assessing the risk of MS to twins, siblings, half siblings and adoptees to parents with MS have clearly shown a familial aggregation for the disease suggesting genetic and environmental factors in MS aetiology (Herrera and Ebers, 2003; Dymont *et al.*, 2004). Half sibling studies support the notion that shared genetics rather than family environment is critical for familial aggregation of MS (Sadovnick *et al.*, 1996). The recurrence rate of offspring born of conjugal parentage (both parents with MS) is significantly higher (30.5) in comparison to offspring from one parent with MS (2.49%) (Dymont *et al.*, 2004). The recurrence rate for family members and concordance rates for twins indicate that the genetics of MS is complicated and not associated with the presence of a single disease gene or Mendelian trait (Barcellos and Thompson, 2003). A recent cohort study in Sardinia has

reported an association between MS and insulin-dependent diabetes mellitus (Marrosu *et al.*, 2002). People with MS in Sardinia had a 5 times greater prevalence of diabetes than the general public and 3 times higher prevalence than their siblings (Marrosu *et al.*, 2002).

### *Gene association studies in MS*

Association screening or linkage disequilibrium studies are applied to determine genes with small or modest effect in complex traits (Risch, 2000). Recently large multicentre studies in America, Canada and the UK have carried out full genome searches for candidate genes in MS (Dyment and Ebers, 2004; Sotgiu *et al.*, 2004). Based on the assumption that MS is an autoimmune disease, genetic studies have concentrated on the immune-related genes (Herrera and Ebers, 2003; Sotgiu *et al.*, 2004). The major histocompatibility complex (MHC) is unambiguously associated with MS (Dyment *et al.*, 2004). There are over 200 genes in the MHC that play important roles in the development and maturation of the T cell repertoire (Dyment *et al.*, 2004). The first genetic association with MS was reported to involve human leukocyte antigen (HLA) class I antigens (Jersild *et al.*, 1972). More recently HLA class II antigens have been commonly and repeatedly reported as having associations with MS (Olerup and Hillert, 1991). In northern Europeans DRB1\*1501, DQA1\*0102 and DQB2\*0602 haplotypes of the HLA molecule have been shown to be linked to MS susceptibility (Herrera and Ebers, 2003), in addition DRB1\*13-DQB1\*0603 was found to have a protective effect in Finland (Herrera and Ebers, 2003). As well as having a role in MS susceptibility the HLA DRB1\*15 haplotype has been associated with an earlier age of onset (Hensiek *et al.*, 2002).

The genetic analysis of multiple sclerosis in Europeans (GAMES) carried out linkage screens across 15 countries involving nearly 10,000 MS patient DNA samples using large panels of PCR-based microsatellites and pooled DNA samples (Barcellos and Thompson, 2003; Sawcer and Compston, 2003). GAMES revealed associations in 19q13 and 6p21 regions but the most promising regions highlighted by GAMES were 11q23 and 17q11 (Barcellos and Thompson, 2003). 17q11 was also reported to have the highest evidence of linkage following meta-analysis of the Canadian and

American screen samples (Dyment *et al.*, 2004). However caution remains since it has been noted that following a positive genetic association in candidate studies, the report of a positive association is commonly followed by a negative report (Colhoun *et al.*, 2003). It is suggested that 95% of initial positive associations are then shown to be negative (Colhoun *et al.*, 2003).

Functional candidate gene analyses have studied genes coding for cytokines, chemokines, interleukins, myelin antigens, HLA and T cell receptors, however no functional link has consistently been demonstrated in MS (Kenealy *et al.*, 2003; Herrer and Ebers, 2003; Dymment *et al.*, 2004). Apolipoprotein E (apoE) is a major carrier protein that has been reported to be an anti-inflammatory agent and is associated with regeneration of axons and myelin following lesion formation (Kenealy *et al.*, 2003; Herrer and Ebers, 2003). CNS and intrathecal concentrations of apoE are decreased in MS compared with controls (Kenealy *et al.*, 2003; Herrer and Ebers, 2003). The gene encoding for apoE is located on chromosome 19 (19q13) of which there are 3 variants:  $\epsilon 2$ ,  $\epsilon 3$  and  $\epsilon 4$  (Herrer and Ebers, 2003). The  $\epsilon 4$  allele is associated as a risk factor in Alzheimer's disease and also affects disease course in MS (Kenealy *et al.*, 2003; Herrer and Ebers, 2003). People with MS carrying the  $\epsilon 4$  allele are reported to have shorter disease duration, more annual relapses and reach a higher expanded disability status scale (EDSS) score sooner (Herrer and Ebers, 2003). Although the genetic aspect of MS has been known for a long time, identification of strong susceptibility gene(s) remains unknown. The use of new high throughput technologies like gene microarray analysis and using single nucleotide polymorphisms (SNPs) for association studies should help unravel the complex genetic interactions involved in MS.

### 1.1.3 Clinical symptoms of MS

Initial onset of MS is monosymptomatic in 85% of patients. Presenting symptoms vary between individuals and are correlated to the location of the lesion(s) within the CNS. The most common clinical presentations are optic neuritis, sensory disturbance of the limbs, leg weakness, fatigue and ataxia. As MS is not the only demyelinating disease of the CNS, careful diagnosis and classification is vital when deciding upon the therapeutic direction (Poser

and Brinar, 2004). People with MS each experience varying degrees of disability throughout the course of the disease. It is important that these symptoms are carefully monitored throughout the disease progression. The Kurtzke EDSS (Table 1.1) enables neurologists to determine the extent of the neurological impairment which allows them to determine how progressive the disease is and also to determine if treatments are of any clinical benefit (Kurtzke, 1983).

#### *1.1.4 Diagnosis of MS*

Although MS was first described over 130 years ago, diagnosis of MS remains problematic with no single conclusive laboratory based immunological assay available (Poser and Brinar, 2004). Over the years numerous diagnostic criteria have been implemented, the most recent of which being the McDonald criteria (McDonald *et al.*, 2001). The McDonald criteria incorporate many of the original Poser criteria (Poser *et al.*, 1983) with the addition of the use of magnetic resonance imaging (MRI). Poser suggested that MS can be diagnosed on the basis of impaired visual evoked potential (VEP), the presence of oligoclonal IgG bands in the cerebrospinal fluid (CSF) and a detailed clinical history (Poser *et al.*, 1983). Demyelination of the optic nerve and the clinical presentation of optic neuritis is the most common initial symptom of MS making VEP very useful in the diagnosis of MS (Thompson and McDonald, 1996). MRI has become a very important tool in the diagnosis of MS and is the optimal imaging technique for MS (Figure 1.1) however results from MRI are not necessarily MS specific (Miller *et al.*, 1998; Poser and Brinar, 2004).

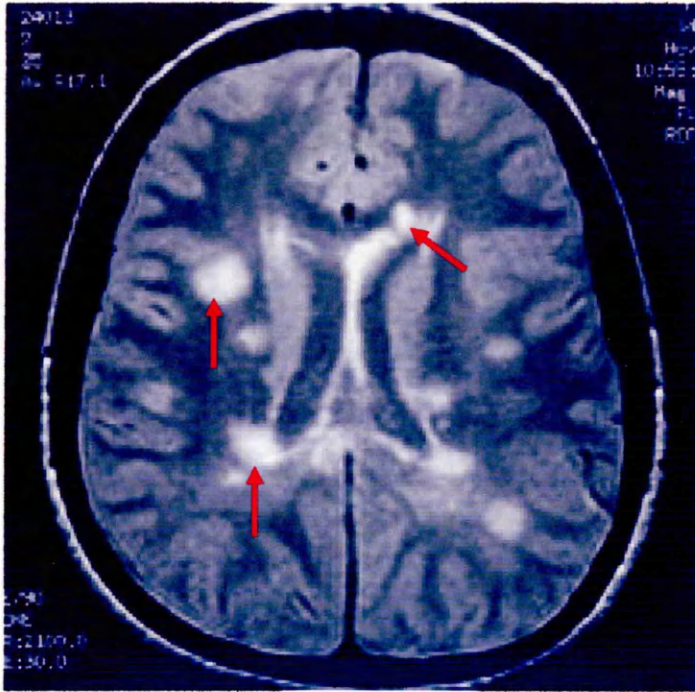
##### *1.1.4.1 Magnetic resonance imaging*

Conventional MRI is a sensitive technique for the detection of MS lesions and has been adopted to support clinical evidence for the diagnosis of MS and is used in the management and the monitoring treatment effects in MS (Miller *et al.*, 1998; McDonald *et al.*, 2001; Moore, 2003; Zivadinov and Bakshi, 2004; Korteweg *et al.*, 2005). A hyperintense lesion detected by conventional T2 weighted MRI is primarily related to increased water content and therefore does not distinguish between inflammation,

Table 1.1 Selected scores from the Kurtzke expanded disability status scale (EDSS), rating neurological impairment in MS (Kurtzke, 1983).

0	Normal neurologic exam
1.0	No disability, minimal signs in one functional system
1.5	No disability, minimal signs in more than one functional system
2.0	Minimal disability in one functional system
2.5	Minimal disability in two functional systems
6.0	Intermittent or unilateral constant assistance (cane, crutch or brace) required to walk about 100 meters with or without resting
6.5	Constant bilateral assistance (canes, crutches or braces) required to walk about 20 meters without resting
7.0	Unable to walk beyond 5 meters even with aid. Essentially restricted to a wheelchair. Wheels self in standard wheelchair and transfers alone. Active in wheelchair about 12 hours a day
7.5	Unable to take more than a few steps. Restricted to wheelchair. May need aid to transfer. Wheels self but cannot carry on in standard wheelchair a full day. May require a motorized wheelchair
9.0	Helpless bed patient. Can communicate and eat
9.5	Totally helpless bed patient. Unable to communicate effectively or eat/swallow
10	Death due to multiple sclerosis

Figure 1.1 MRI scan from a patient with MS



A typical MRI from a person with MS displaying hyperintense T2 lesions (arrows) in periventricular locations. Specifically, the periventricular lesions and the more peripheral white matter lesions near the grey matter–white matter junction are typical MRI findings in MS.

[www.emedicine.com/ radio/topic461.htm](http://www.emedicine.com/radio/topic461.htm)

edema, demyelination and axonal loss (Werring *et al.*, 2000; Zivadinov and Bakshi, 2004). The contrast agent gadolinium-diethylenetriaminepentaacetic acid (Gd-DTPA) improves the pathological specificity of MRI (Werring *et al.*, 2000). Areas of enhancement with Gd-DTPA MRI reflect inflammatory infiltrate induced blood-brain barrier (BBB) disruption and neovascularisation (Bruck *et al.*, 1997; Miller *et al.*, 1998). Magnetic transfer imaging (MTI) has been shown to detect changes in the normal appearing white matter (NAWM) at the site of future MS lesions (Moore, 2003). It has been reported that focal changes in MTI may exist up to one month before being detected by Gd-DTPA MRI (Moore, 2003). Diffusion MRI techniques enable the detection of subtle changes in motion (diffusion) of water molecules within the brain and has been reported to display changes in the NAWM up to 6-8 months prior to Gd-DTPA MRI detection (Werring *et al.*, 2000).

A lack of correlation between conventional MRI and MS disability (Kurtzke scale) has been reported however the advent of new MRI techniques have allowed histopathological and MRI correlates to be obtained (Fillipi *et al.*, 1995; Moore, 2003; Zivadinov and Bakshi, 2004). Magnetic resonance spectroscopy (MRS) allows the identification of specific compounds within specific structures. N-acetyl aspartate (NAA), an axonal/neuronal specific marker, has been used to determine axonal loss and pathology within MS lesions. NAA has been shown to be decreased in chronic MS plaques correlating with axonal loss in pathologic studies (Trapp *et al.*, 1998; Fu *et al.*, 1998). MRS has also been used to detect ongoing demyelination. Abnormal lipid peaks in MRS are representative of myelin breakdown into neutral lipid during demyelination (Moore, 2003). MRI continues to evolve and non-conventional MRI techniques now provide a powerful tool to non-invasively study pathological substrates of lesions and NAWM (Zivadinov and Bakshi, 2004). However it is important to note that diagnosis of MS cannot be made solely on MRI as other neurologic diseases such as glioma gives similar MRI to MS lesions. Similarly a normal MRI cannot rule out the diagnosis of MS as approximately 5% of patients with confirmed MS can show normal MRI (Poser and Brinar, 2004).

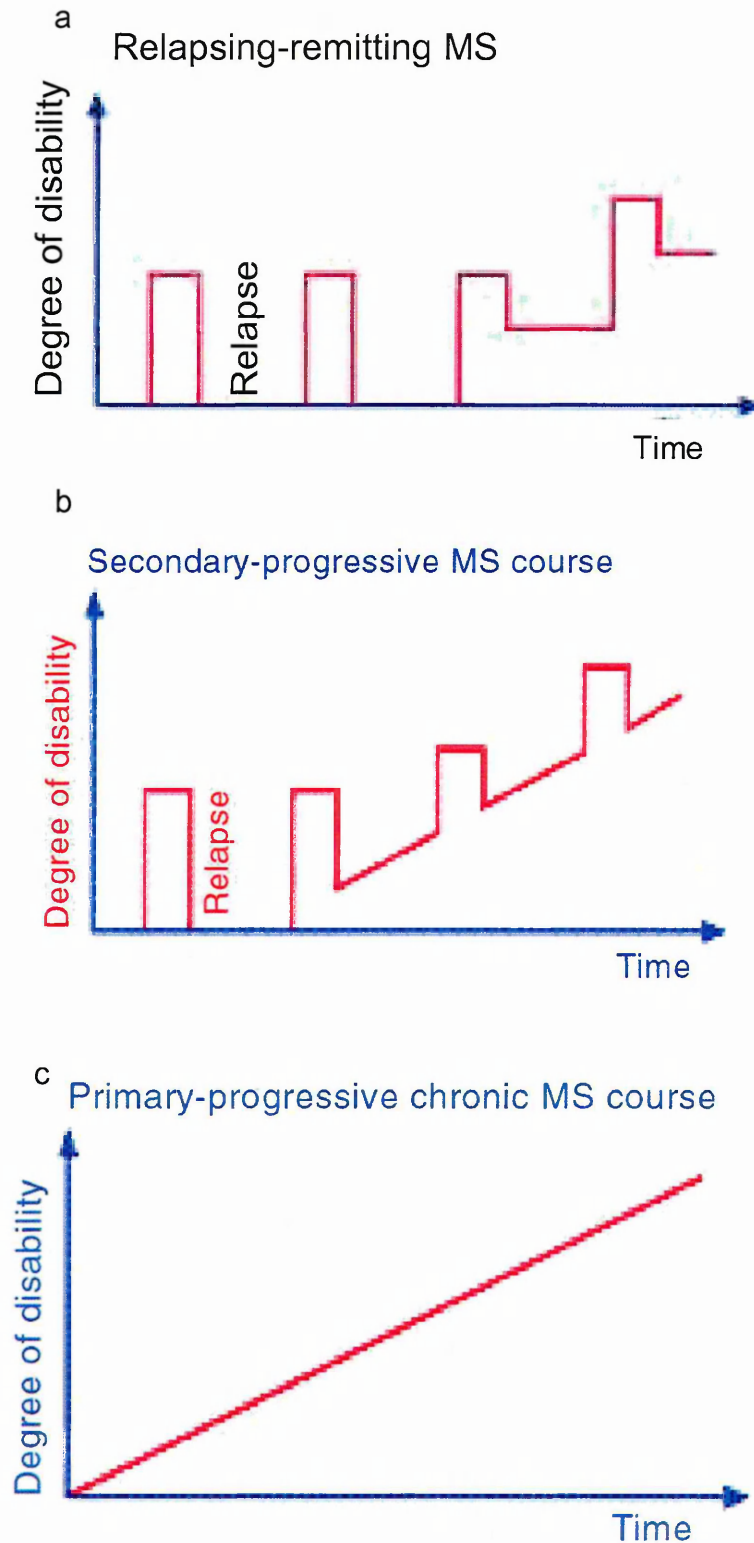
#### 1.1.4.2 Analysis of CSF in MS

The CSF of MS patients is examined to detect an increase in the  $\gamma$ -globulin/albumin ratio and  $\gamma$ -globulin oligoclonal bands on isoelectric focussing (Brosnan and Raine, 1996; Hickey, 2001). Presence of oligoclonal bands occurs in pathological conditions where B cells enter the CNS, following alterations of the BBB. B cells, clonally expand, differentiate into plasma cells and secrete antibody into the extracellular fluid of the CNS and is therefore detected in the serum and CSF as clonally restricted IgG bands (Hickey, 2001).

#### 1.1.5 Disease course in MS

MS presents and manifests in a number of different clinical disease courses (Figure 1.2). The most common course of MS occurs when an individual experiences an episode of neurological dysfunction (relapse), onset of which can be rapid (overnight) or eventual (over a week), for a duration of 4-6 weeks then the symptoms regress to a baseline of normal function (remission). The remission stages can last variable durations from months to several years. This pattern of MS is called relapsing remitting MS (RRMS) and is accountable for approximately 85% of MS patients (Weinshenker, 1994; Hohol *et al.*, 1995). After 15 years approximately 65% of RRMS patients will develop secondary progressive MS (SPMS). As the name suggests SPMS is secondary to RRMS and only occurs in people who have had RRMS. During SPMS the neurological dysfunction fails to return to normal and the MS patient experiences subtle but definite deterioration in their level of function (Weinshenker, 1994; Hohol *et al.*, 1995). In some cases however people with RRMS fail to develop SPMS and continue to have relapses that return to the baseline of normal function, this is benign MS. People are generally only diagnosed with benign MS when they have not developed any new symptoms 10-15 years after initial attack. Primary progressive MS (PPMS) is different to the other forms of MS in that people with PPMS do not experience attacks or remissions but begin with subtle problems that slowly worsen over time. People with an older age of onset are mainly affected by PPMS which accounts for approximately 15% of the people with MS. PPMS is clinically associated with a lack of response to any

Figure 1.2 Graphical representation of the different clinical courses of MS



The majority of people with MS (approx 80%) experience a disease with a relapsing and remitting course (a). After 15 years approximately 65% of RRMS patients will develop secondary progressive MS (b). People with PPMS do not experience attacks or remissions but begin with subtle problems that slowly worsen over time (c)

form of immunotherapy (Hohol *et al.*, 1995). Following a 25 year population based study, the progressive phase of PPMS and SPMS were reported to display remarkable similarities (Ebers, 2004).

## 1.2 Cellular constituents of the CNS

The CNS is composed of the cerebral endothelium and the BBB, neurons, oligodendrocytes, astrocytes and microglia. The cells within the CNS communicate via various ion channels, transporter mechanisms and signalling pathways helping to maintain homeostasis within the CNS.

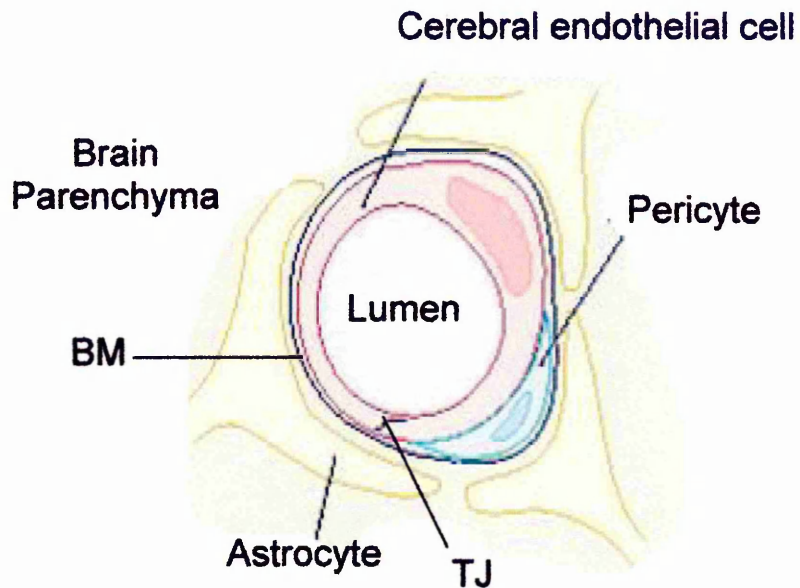
### 1.2.1 Cerebral endothelia and the BBB

The BBB is a complex cellular system that plays a crucial role in regulating cell trafficking and maintaining homeostasis within the extracellular microenvironment of the CNS (Petty and Lo, 2002; Wolburg and Lippoldt, 2002). The BBB, once regarded as a static physical barrier between the vascular system and the CNS, is now considered as a complex dynamic structure that is capable of rapid modulation (Huber *et al.*, 2001).

The BBB is comprised of capillary endothelial cells resting on a thin but multilayered basal membrane which separates them from closely adherent pericytes, perivascular microglia and the astrocytic foot-processes (Prat *et al.*, 2001; Ballabh *et al.*, 2004) (Figure 1.3).

Perivascular astrocytes extend large cellular processes (end-feet) that abut and cover most of the ab-luminal surface of the cerebral capillary wall (Prat *et al.*, 2001). This close contact acts as a structural support for the BBB and as a two way signalling pathway between the endothelium and the surrounding neuroenvironment (Ballabh *et al.*, 2004). Close contact between the astroglia and the endothelium is deemed essential for establishing and maintaining an optimal barrier (Hirase *et al.*, 1997; Prat *et al.*, 2001). Astrocytes are also reported to confer a protective role on the BBB against hypoxia and aglycemia (Abbruscato and Davis, 1999). Although little studied, pericytes are also believed to have a protective role as well as roles in: angiogenesis, maintaining the structural integrity of the vessel and the formation of tight junctions (TJ) (Hori *et al.*, 2004). It is reported that all these

Figure 1.3 Schematic representation of the BBB



The BBB is comprised of the inter-endothelial tight junctions (TJ) of the vascular endothelial cells. The endothelial cells are in intimate contact with astrocytic end feet, pericytes and the basement membrane (BM). (Adapted from Terasaki et al., 2003).

cellular components of the BBB are essential for normal function and stability of the BBB (Ballabh *et al.*, 2004).

The microvascular endothelium of the BBB differs from and is more specialised than the peripheral endothelium throughout the rest of the body due to;

- lack of fenestrations,
- has fewer endocytic vesicles,
- possesses a higher mitochondrial volume fraction and
- forms extensive TJs
- a high transendothelial electrical resistance (Prat *et al.*, 2001; Petty and Lo, 2002; Ballabh *et al.*, 2004)

An important characteristic of the BBB endothelial phenotype is the possession of a high transendothelial electrical resistance (TEER), in the range of 1000-5000 $\Omega\text{cm}^2$  in comparison to the 'non-barrier' placental endothelial cells which have an electrical resistance of 22-52 $\Omega\text{cm}^2$  (Huber *et al.*, 2001; Petty and Lo, 2002). High electrical resistance in the CNS microvasculature is a consequence of the extreme structural specialization of the endothelium, in particular its minimal 'pore' size, this enables the cerebral endothelia of the BBB to regulate the passage of molecules and cells to the parenchyma (Romero *et al.*, 2003).

The function of the BBB is to protect the brain microenvironment from the potentially damaging effects of substances in the blood, whilst ensuring a supply of nutrients by the action of specific transport systems (Petty and Lo, 2002). Passage across the BBB can occur either through the endothelial cell via the transcellular route, or between adjacent endothelial cells via the paracellular route (Fanning *et al.*, 1999; Tsukita and Furuse, 1999; Dallasta *et al.*, 1999; Huber *et al.*, 2001; Petty and Lo, 2002). Only lipophilic substances of a molecular weight less than 450, can cross the BBB via the transcellular route by passive diffusion (Petty and Lo, 2002). There is however active transport of some large hydrophilic molecules into the brain via the transcellular pathway (Huber *et al.*, 2001; Petty and Lo, 2002;). Ions and solutes normally diffuse down their concentration gradient between

adjacent endothelial cells by the paracellular pathway, however at the BBB this pathway is blocked by cell-cell contacts at the apical region of the endothelial cells. These contacts are the inter-endothelial TJs of the BBB (Huber *et al.*, 2001; Petty and Lo, 2002; Ballabh *et al.*, 2004;). Control of paracellular diffusion by the TJs is also known as the barrier function. TJs also restrict protein movement within the plane of the endothelial membrane (so called 'fence' function ), thereby ensuring that the apical and basolateral membrane domains remain distinct allowing active transport of nutrients (Tsukita and Furuse, 1999; Fanning *et al.*, 1999).

### 1.2.2 Microglia

Microglia, derived from monocytes from the bone marrow, are ubiquitously distributed within the CNS, where they are spaced out evenly throughout the brain and spinal cord and account for approximately 12% of the cells in the CNS (Minagar *et al.*, 2002; Streit, 2005). In the normal uninjured CNS the microglial cells are referred to as resting microglia and morphologically are highly branched or ramified. These cells are the primary immune effector cells of the CNS, responding to biochemical or bioelectrical alterations within the microenvironment (Hickey, 2001; Minager *et al.*, 2002;). Resting microglia express the macrophage phenotypic marker CD11b and constitutively exhibit low levels of expression of MHC Class II and the co-stimulatory molecules CD86 and CD40 (Ponomarev *et al.*, 2005). The microglia are both targets and sources of numerous cytokines and chemokines. Activated microglia have shortened cell processes and may conform to a bushy macrophage-like morphology and are capable of phagocytosis. Activated microglia, as observed in areas of inflammation and trauma can express both MHC class I and II, B7 co-stimulatory molecules, ICAM-1 and Fc receptors suggesting a role for these cells in antigen presentation (Minagar *et al.*, 2002; Mack *et al.*, 2003). *Ex-vivo* murine microglia have been shown to differentiate into dendritic cells *in vitro* following stimulation with granulocyte macrophage colony stimulating factor, thus increasing the efficacy of antigen presentation within the CNS (Ponomarev *et al.*, 2005). Activated microglia release the cytokines, interleukin (IL)-1, IL-4, IL-6, IL-12 and tumor necrosis factor (TNF) and

interact with Th1 and Th2 cells inducing clonal expansion and cytokine release (Minagar *et al.*, 2002). Interestingly the chemokine fractalkine (CX3CL1) is expressed on neurons whilst its receptor CX3CR1 is expressed on the microglia (Nishiyori *et al.*, 1998; Garton *et al.*, 2001). This distinct separation in cellular location of CX3CL1 and CX3CR1 suggests a role for fractalkine in mediating neuron-microglia interactions in basal conditions and in disease (Streit, 2005). The microglial plasma membrane is complex with a large repertoire of potentially immunogenic surface antigens resulting in the detection of microglia by numerous antibodies detected in cells from a monocytic lineage (Streit, 2005). Microglia can be detected with antibodies to lymphocytic antigens including lymphocyte function antigen (LFA) and leukocyte common antigen (LCA) as well as detection of MHC. However within the CNS MHC expression is not limited to microglia but is also expressed by macrophages and endothelial cells (Streit, 2005). It has been reported that distinction can be made using flow cytometric analyses where resident microglia express CD11b/c<sup>+</sup> CD45<sup>low</sup> whereas parenchymal macrophages have been described as being CD11b/c<sup>+</sup> CD45<sup>hi</sup> (Ford *et al.*, 1995).

### 1.2.3 Astrocytes

Astrocytes are the major cellular components of the CNS outnumbering neurons 10:1 (Okada *et al.*, 2005). Astrocytes were traditionally considered as structural elements of the CNS as they are in close contact with several cellular components of the brain parenchyma (Pellerin and Magistretti, 2005). However astrocytes are now considered to be more dynamic and are reported to play an important role in the homeostasis of the CNS, release neurotrophic factors, contribute to neurotransmitter metabolism and regulate extracellular pH and K<sup>+</sup> levels (Dong and Benveniste, 2001; Kettenmann and Steinhauser, 2005; Pellerin and Magistretti, 2005). Astrocytes are also reported to play a major role in the formation and regulation of the BBB (Hamm *et al.*, 2004). Astrocytes are reported to take up extracellular glutamate, an excitatory neurotransmitter of the CNS (Pellerin and Magistretti, 2005). Astrocytes lack the capacity to deliver co-stimulatory signals to T cells and therefore cannot function as competent

antigen presenting cells (APC) (Dong and Benveniste, 2001). Astrocytes express functional IL-4 receptors and upon exposure to IL-4 they secrete the neurotrophins, nerve growth factor and brain derived growth factor, supporting axonal growth (Minagar *et al.*, 2002; Pellerin and Magistretti, 2005). Astrocytes can be detected *in vivo* and *in vitro* by immunohistochemistry using antibodies against glial fibrillary acidic protein (GFAP) and S-100 (Zheng *et al.*, 2000).

#### 1.2.4 Oligodendrocytes

Oligodendrocytes are responsible for the synthesis and maintenance of myelin within the CNS. Myelin membranes are extended out from the oligodendrocytes and wrap around axons, forming a multi-lamella myelin sheath, thereby increasing nerve conductance velocity (Franklin and Blakemore, 1997). Each oligodendrocyte, unlike their peripheral nervous system counterparts, Schwann cells, is able to myelinate more than one axon however one oligodendrocyte does not myelinate the same axon more than once (Jessen and Mirsky, 2005). In addition to myelinating oligodendrocytes, non-myelinating satellite oligodendrocytes and adult oligodendrocyte progenitor cells (OPCs) are also evident within the CNS (Scolding *et al.*, 1998; Dawson *et al.*, 2000). Throughout the CNS oligodendrocytes have been detected at different stages of maturation expressing distinct phenotypic markers, listed below (Armstrong *et al.*, 1992; Norton, 1996; Levine *et al.*, 2001).

Table 1.2 Phenotypic markers of oligodendrocyte maturation

<b>Maturation stage</b>	<b>Phenotype</b>
Progenitor cell	NG2, A2B5 <sup>+</sup> and G <sub>D3</sub> <sup>+</sup>
Pre-oligodendrocyte	O4 <sup>+</sup> , A2B5 <sup>+</sup> and G <sub>D3</sub> <sup>+</sup>
Immature oligodendrocyte	GC <sup>+</sup> , A2B5 <sup>-</sup> and G <sub>D3</sub> <sup>-</sup>
Mature oligodendrocyte	O4 <sup>+</sup> , GC <sup>+</sup> , PLP <sup>+</sup> , MBP <sup>+</sup> and CNP <sup>+</sup>

Phenotypic markers for oligodendrocytes include expression of chondroitin sulphate proteoglycans (NG2), surface gangliosides (A2B5 and G<sub>D3</sub>) and the

myelin proteins myelin basic protein (MBP), proteolipid protein (PLP), galactocerebroside (GalC) and 2', 3'-cyclic nucleotide-3-phosphohydrolase (CNPase).

### 1.3 Pathology of MS

Demyelination is regarded as the pathological hallmark of MS along with inflammation, through BBB breakdown. However other pathologies exist in the MS lesion including axonal loss, oligodendrocyte loss and astrogliosis. (Bjartmar *et al.*, 2003).

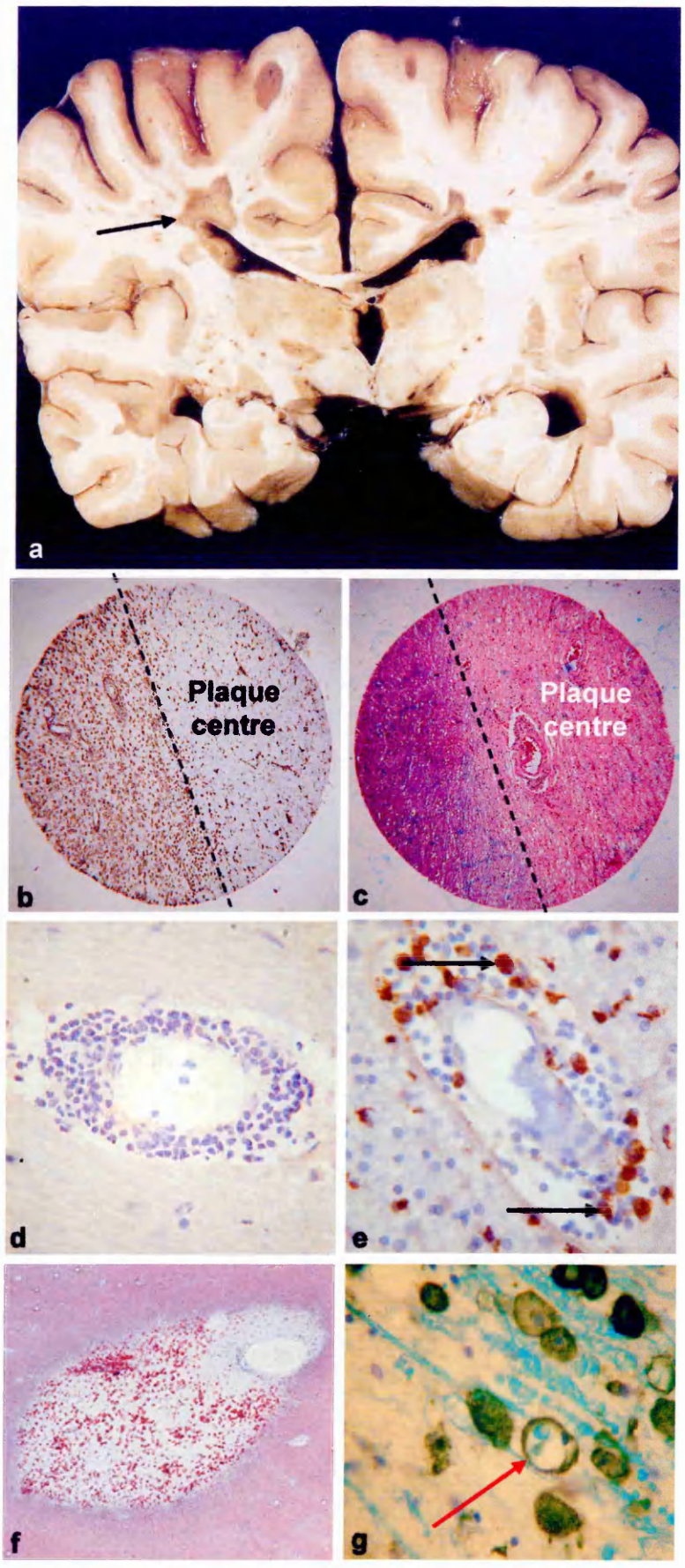
The classical hallmarks of MS are demyelinated lesions, disseminated throughout the CNS but with an apparent predilection to the optic nerves, white matter tracts of the periventricular regions, the brain stem and the spinal cord (Hafler, 2004). Macroscopically, lesions of the autopsied brain are grossly visible, irregular in shape and size and can be clearly distinguished by the discolouration of the white matter (Figure 1.4). Recently formed lesions appear pink or even yellow due to the hyperemia and lipid breakdown and neutral fat production, whereas older more chronic lesions have a darker grey-tan appearance (Thompson and McDonald, 1996; Hickey, 1999; Hafler, 2004). Developing an understanding of the pathogenesis of MS lesion formation is problematic as most cases are presented at the end stage of the disease at autopsy where the majority of lesions are old, chronic and inactive, and may bear no significance to the underlying pathogenic mechanisms involved. The CNS of a person with MS may contain lesions that are disseminated in time and as such at different stages of lesion activity.

Lesion classification with regards to activity has been reported as being of great importance in pathological studies investigating early lesion development (Lassmann, 1998). In general there are three main ages of lesions described based on histological appearance; active lesions, chronic active lesions and chronic inactive lesions (Figure 1.4) (Lassmann, 1998, Trapp *et al.*, 1999):

- Active lesions are early lesions with active demyelination occurring throughout the lesion. Macrophages containing myelin proteins are evenly spread throughout the lesion. Active lesions containing

Macroscopic appearance of discoloured periventricular white matter lesions (arrow) (a). (b) Clearly demarcated active lesion edge (dashed line) of a chronic active lesion with an abundance of HLA-DR<sup>+</sup> foamy macrophages. A comparable demyelinated area of chronic active lesions stained with luxol fast blue (LFB) (c). Histologically large perivascular cuffs are observed within lesions and NAWM (d) that contain CD68<sup>+</sup> macrophages (arrows) (e). Large vascular associated active lesion with an abundance of ORO lipid laden macrophages throughout the lesion (f). Evidence of LFB<sup>+</sup> myelin debris within a HLA-DR<sup>+</sup> macrophage (g). Images were obtained from archival MS autopsy material from the Belfast Brain Bank, Pathology Department, Royal Group of Hospitals Trust, Belfast, N Ireland.

Figure 1.4 Digital photographs of pathological hallmarks of MS



acrophages with myelin immuno-reactive protein are considered to be very recent, 2-3 weeks (Trapp *et al.*, 1999) (Figure 1.4a).

- Chronic active plaques are generally characterized by an enrichment of MHC class II positive lipid laden foamy macrophages along a clearly demarcated hypercellular border (Figure 1.4b).
- In inactive lesions the area of demyelination is hypocellular with very few MHC class II positive cells. Myelin is replaced by reactive astrocytes forming gliotic scar tissue.
- A key feature of active MS plaques is the presence of large perivascular cuffs, areas containing various lymphocytic inflammatory cells (Figure 1.4d). The majority of MS plaques are centred on an associated venule. The cellular constituents of the perivascular cuff vary throughout lesion development and are discussed later (Section 1.5.1.2).

### 1.3.1 Heterogeneity of MS lesions

Recently the idea that all MS lesions evolve using the same mechanism has been revised (Lucchinetti *et al.*, 2000). MS lesions, not surprisingly considering the clinical differences in progression, severity and duration of MS, have been shown to be heterogeneous. By examining 235 actively demyelinating lesions from both autopsy and biopsy material, four distinct lesion patterns have been described that may be indicative of different underlying pathogenic mechanisms (Lucchinetti *et al.*, 2000; Kornek and Lassmann, 2003).

Lesion patterns I & II: In these lesions it is reported that the myelin sheath is the main target of the destructive process (Lucchinetti *et al.*, 2000). Pattern I & II lesions are typically centred on small veins and venules with clearly demarcated borders. Demyelination in pattern I is suggested to be mediated by macrophage released toxins such as TNF and reactive oxygen species, whereas in pattern II demyelination is suggested to be specifically antibody and complement mediated (Lucchenitti *et al.*, 2000; Kornek and Lassmann, 2003).

Lesion pattern III: In comparison to patterns I & II, pattern III lesions are not associated with small veins and venules. Indeed preservation of myelin surrounding blood vessels within the lesion was reported. This lesion pattern of active demyelination displays diffuse borders that spread into the surrounding white matter. Another distinguishing characteristic of pattern III is that the oligodendrocytes appear to be the main target. Surprisingly myelin associated glycoprotein (MAG) appeared to be preferentially lost while other myelin proteins appeared to be unaffected. The loss of MAG is associated with oligodendrocytes undergoing apoptosis (Lucchinetti *et al.*, 2000), similar to pathology observed in acute white matter in stroke (Kornek and Lassmann, 2003).

Lesion pattern IV: This pattern type of lesion has a clearly demarcated lesion border, with oligodendrocyte loss that is associated with the periplaque white matter. Oligodendrocytes are described as apoptotic due to the fragmentation of the DNA, however no morphological aspects of apoptosis were described. This type of lesion pattern was only identified in samples that were obtained from people who had suffered from PPMS (Kornek and Lassmann, 2003).

All lesions were reported to have inflammatory infiltrates of T cells and macrophages, the lesions were segregated based on distribution of myelin loss, plaque geography, the pattern of oligodendrocyte destruction, and the immunopathological evidence of immunoglobulin and activated complement deposits (Lucchinetti *et al.*, 2000; Kornek and Lassmann, 2003). MS lesions are heterogeneous between individual MS patients however it was reported that each individual contained only one lesion pattern (Lucchinetti *et al.*, 2000). Others have reported five lesion types following multifactorial cluster analysis incorporating detailed immunocytochemical analysis of CD4<sup>+</sup> CD8<sup>+</sup> T cell and plasma cell populations, macrophage morphology as well as parenchymal fibrinogen staining, indicative of BBB disruption (Gay *et al.*, 1997). Lucchinetti's description of lesion type is highly regarded in the literature however it is not accepted universally by all researchers as it fails to include the presence or extent of axon loss which has been described in

MS pathology for over a century (Charcot, 1867; Evangelou *et al.*, 2000; DeLuca, 2004) (Section 1.3.2).

### 1.3.2 Axonal pathology

Axonal loss has been observed in MS for a long time however new insights into the timing and functional consequences of axonal loss have brought axonal research to the fore again (DeLuca *et al.*, 2004). It has been suggested that the cumulative loss of axons is a major determinant in the progression from RRMS to the SPMS, where aspects of the neurological dysfunction become irreversible (Trapp *et al.*, 1998, Bjartmar *et al.*, 2000 & 2003). MS patients are reported to contain a mean axonal loss of 68% (range 45-84%) compared with controls. A supporting role for axonal degeneration in irreversible neurological disability is suggested as MS patients in this study had an EDSS  $\geq 7.5$  (Bjartmar and Trapp, 2001).

Acute axonal damage can be determined immunohistochemically by the presence of amyloid precursor protein (APP) (Ferguson *et al.*, 1997; Kornek *et al.*, 2000; Kuhlmann *et al.*, 2002). APP is a neuronal protein, transported by fast antegrade axonal transport and can only be detected when axoplasmic flow is compromised (Ferguson, *et al.*, 1997). Following axonal transection the transport of APP is interrupted leading to an accumulation of APP in the proximal axonal ends (Ferguson *et al.*, 1997; Kuhlmann *et al.*, 2002) as such very little APP is detected in normal brains (Kronek *et al.*, 2000). Transected axons appear as axonal ovoids or axonal bulbs that are reported to be an early event in lesion formation, with the highest amount of acute axonal damage associated with active demyelination and inflammation (Ferguson *et al.*, 1997; Trapp *et al.*, 1998; Bitsch *et al.*, 2000b; Kornek *et al.*, 2000). A quantitative study reported axonal bulbs being more abundant and larger in active lesions (11,236/mm<sup>3</sup>) than either the active rim (3138/mm<sup>3</sup>) or lesion centre (875/mm<sup>3</sup>) of chronic active lesions (Trapp *et al.*, 1998). Axonal bulbs were also reported in the NAWM (17/mm<sup>3</sup>) and control white matter (1/mm<sup>3</sup>) but to a far lesser extent (Trapp *et al.*, 1998). Acute axonal loss is also reported to be at its highest in the early stages of disease progression in RRMS and SPMS with the highest number of APP<sup>+</sup> axons observed in patients with a disease duration  $\leq 1$  year

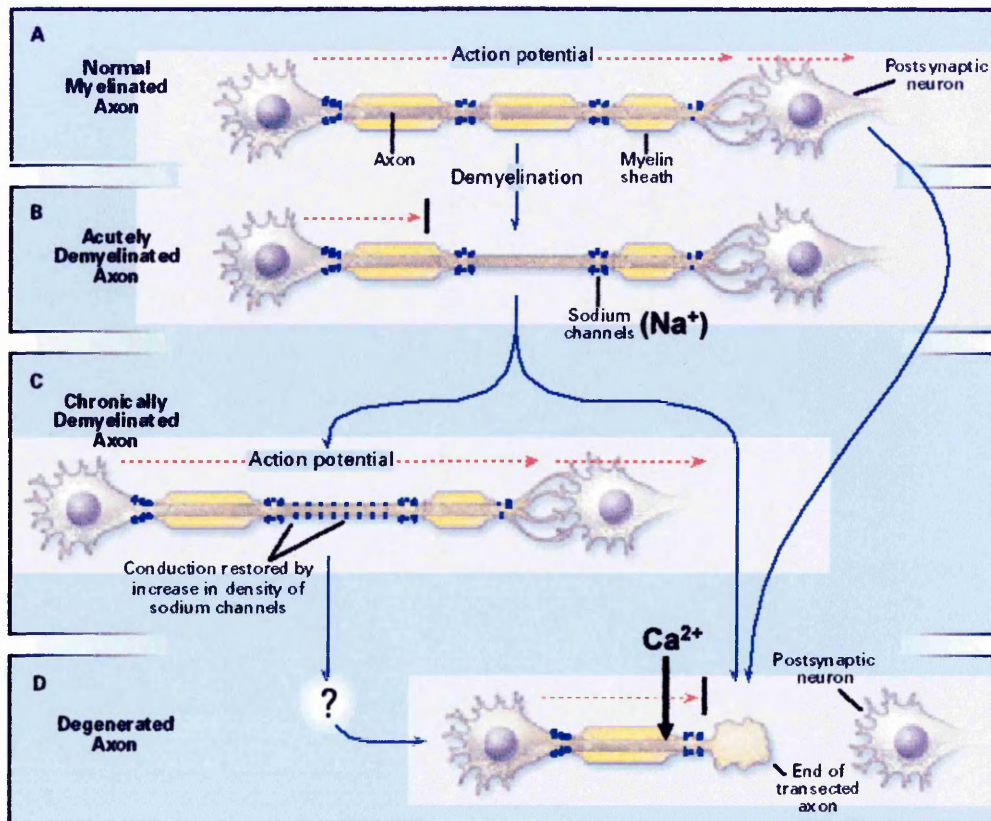
(Kuhlmann *et al.*, 2002; Fillipi *et al.*, 2003). A recent study confirmed the appearance of extensive axon loss early in disease however it suggested that no correlation exists between the amount of axon loss and disease duration (DeLuca *et al.*, 2004). In a lesion matched immunohistopathological study, acute MS white matter displayed more APP<sup>+</sup> axons than in chronic MS cases (Kornek *et al.*, 2000). The amount of acute axonal loss in PPMS is lower than that observed in RRMS and does not change significantly over time (Bitsch *et al.*, 2000b; Kuhlmann *et al.*, 2002). Investigation of the periplaque white matter has demonstrated acute axonal damage associated with CD8<sup>+</sup> T cells but without evidence of demyelination (Bitsch *et al.*, 2000b; Kornek *et al.*, 2000; Kuhlmann, *et al.*, 2002). These findings suggest that some axonal loss may be independent of demyelination or even may precede demyelination (Bitsch *et al.*, 2000; Bjartmar and Trapp, 2001; Kuhlmann *et al.*, 2002). Axonal loss has been demonstrated within the lumbar regions of the corticospinal tracts correlating with spasticity and paralysis of the lower limbs in MS. Axonal loss was also reported to be prevalent in the small nerve fibres ( $\leq 3\mu\text{m}$  diameter) with larger nerve fibres preserved (Bjartmar and Trapp, 2001; DeLuca *et al.*, 2004).

Demyelinated axons are reported to have an increased expression of Na<sup>+</sup> channels leading to a high Na<sup>+</sup> load within the axon reversing the Na<sup>+</sup>/Ca<sup>2+</sup> exchanger resulting in an influx of Ca<sup>2+</sup> into the axon which activates Ca<sup>2+</sup> dependant degenerating enzymes which destroys the axon (Craner *et al.*, 2004; Brand-Schieber and Werner, 2004; Bechtold and Smith, 2005) (Figure 1.5). In a recent study the myelin associated neurite outgrowth inhibitor, Nogo-A and its receptor NgR, have been demonstrated in chronic active demyelinating lesions (Sato *et al.*, 2005). The presence of Nogo-A and NgR may prevent axonal regeneration following injury in MS (Sato *et al.*, 2005).

### 1.3.3 Oligodendrocyte pathology

Oligodendrocytes are susceptible to damage by a variety of immune effector mechanisms during an inflammatory response (Selmaj and Raine 1988; Merrill and Scolding, 1999). Oligodendrocytes have been suggested as being the primary target for destruction in the demyelinating process in

Figure 1.5 A schematic representation of axon degeneration in MS



The normal myelinated axon (A) is demyelinated as a result of a direct or indirect immune attack (B) and nerve signals no longer transmit along the axon. Demyelinated axons are reported to have increased expression of Na<sup>+</sup> channels (C) leading the axons to become loaded with Na<sup>+</sup> temporarily restoring nerve conduction. Increased axonal Na<sup>+</sup> triggers Ca<sup>2+</sup> entry which activates Ca<sup>2+</sup> dependant degenerating enzymes which destroy the axon (Craner et al., 2004) which becomes transected and is detected histologically by an accumulation of amyloid precursor protein in the proximal axonal ends (D). [www.albany.net/~tjc/myelaxon.html](http://www.albany.net/~tjc/myelaxon.html)

MS (Ozawa *et al.*, 1994; Merrill and Scolding, 1999; Lucchinetti *et al.*, 1999; Wolswijk, 2000). The presence of both p55 and p75 tumor necrosis factor receptors on oligodendrocytes along the leading edge of active plaques suggests a role for TNF induced oligodendrocyte death via apoptosis in lesion formation (Raine *et al.*, 1998).

In a large quantitative study of oligodendrocytes in MS lesions, two distinct patterns were observed based on the presence or absence of oligodendrocyte recruitment in the lesion (Lucchinetti, *et al.*, 1999) (See section 1.3.1).

In acute MS lesions, demyelination has been associated with a loss of oligodendrocytes however some mature oligodendrocytes are preserved (Ozawa *et al.*, 1994). During early exacerbations of chronic MS, complete preservation of oligodendrocytes is observed, however in late developing lesions demyelination is accompanied by almost total destruction of oligodendrocytes (Ozawa *et al.*, 1994). Two morphologically distinct populations of oligodendrocytes have been reported in MS lesions (Kuhlmann *et al.*, 1999; Wolswijk, 2000). The first type of oligodendrocyte cell has been described as large process-bearing GalC<sup>+</sup>, MOG immature oligodendrocyte, suggesting that they were derived from a pool of OPCs. These cells were mainly associated with lesion borders and not the surrounding white matter. The second type described was small, round, non-myelinating GalC<sup>+</sup> MOG<sup>+</sup> oligodendrocytes believed to be mature oligodendrocytes that have lost their myelinating processes due to continued episodes of demyelination (Wolswijk, 2000). The small mature rounded oligodendrocytes were reported to be most abundant in the centre of lesions where recent demyelination had taken place (Wolswijk, 2000). Loss of oligodendrocytes is reported to be correlated with an increased number of macrophages suggesting that cytotoxins released by macrophages may play a pathogenic role in oligodendrocyte death (Lucchinetti *et al.*, 1999).

Recently a new type of lesion pathogenesis has been proposed following the study of a very early lesion (Barnett and Prineas, 2004). This report came from an MS patient who died within 24 hours of the onset of a new symptomatic and fatal brainstem lesion (Cannella and Raine, 2004). It has been suggested that apoptotic cell death of oligodendrocytes is the initial

event in lesion development preceding an inflammatory response (Barnett and Prineas, 2004). Leukocyte infiltration was proposed to occur after myelin breakdown to remove the large amount of myelin debris that has resulted from oligodendrocyte cell death (Barnett and Prineas, 2004).

#### 1.3.4 Remyelination

Remyelination has been described in many MS lesions either at the lesion edge or even extending throughout the entire lesion where it becomes a shadow plaque (Lassmann *et al.*, 1997; Stangel and Hartung, 2002; Bruck *et al.*, 2003). Incomplete remyelination usually occurs at the lesion edge where it forms a transition zone between the NAWM and the lesion centre. Shadow plaques appear as areas of myelin pallor within the NAWM (Bruck *et al.*, 2003). The process of remyelination has been suggested to be a recapitulation of developmental myelination (Capello *et al.*, 1997) however others have reported differences between the two processes (Stangel and Hartung, 2002). The hallmarks of remyelination are the shortened internodes and a decrease in the axon diameter: myelin thickness ratio (Adams, 1989). Areas of remyelination have been shown to coexist with areas of active demyelination (Lassmann *et al.*, 1997).

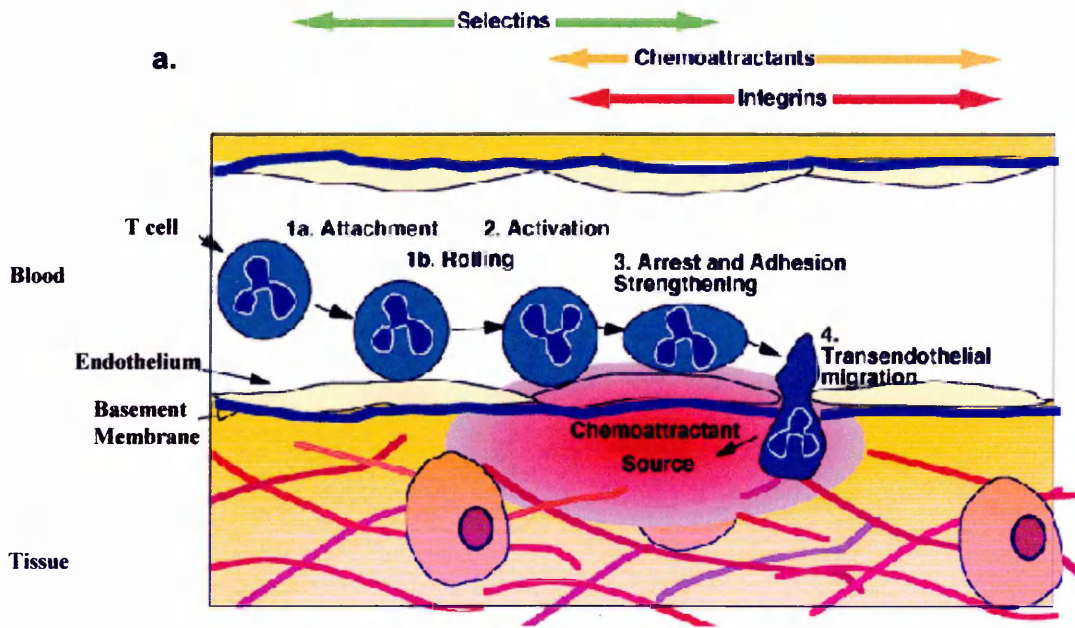
Remyelination within MS lesions is correlated to the number of oligodendrocytes surviving within the lesions (Ozawa *et al.*, 1994; Lassmann *et al.*, 1997). The anti-apoptotic protein Bcl-2 has been suggested as an influencing factor in oligodendrocyte survival (Kuhlmann, *et al.*, 1999). Bcl-2<sup>+</sup> MOG<sup>+</sup> oligodendrocytes have been reported to be at their most abundant in remyelinating lesions especially remyelinating lesions of RRMS patients (Kuhlmann *et al.*, 1999). However the source and origin of the cells responsible for remyelination remains unclear. Remyelinating cells may be derived from a pool of OPC or are mature oligodendrocytes that have survived the demyelinating attack (Lassmann *et al.*, 1997; Keirstead and Blakemore, 1999; Blakemore and Keirstead, 1999; Wolswijk, 2000). Ultimately remyelination in MS fails (Franklin, 2002). A number of explanations have been proposed however none have been categorically proven. It has been proposed that OPC fail to migrate into lesions to remyelinate, however OPC have been identified within early active plaques.

OPC appear to be of a finite supply (Blakemore and Franklin, 1997; Chang *et al.*, 2002) and numbers of OPC tend to decrease with lesion progression (Wolswijk, 2000; Chang *et al.*, 2002). OPC may fail to differentiate into myelinating mature oligodendrocytes due to possible lack of growth factor stimulation or actual attack by the disease process (Franklin, 2002). More recently it has been suggested that the myelinating properties of oligodendrocytes have been turned off by the Notch pathway, or that the axons themselves are not responsive to remyelination (Chang *et al.*, 2002; Mastronardi and Moscarello, 2004). Paradoxically it has been suggested that the inflammatory environment may actually promote remyelination (Franklin, 2002).

#### 1.4 Inflammation and the BBB

During basal conditions the BBB acts as a barrier limiting the entry of immune cells into the parenchyma. A multistep model for leukocyte transmigration has been proposed that involves the sequential interaction of selectins, chemokines and integrins in a process that involves tethering rolling, adhesion and transmigration (Springer, 1990, 1994, Butcher, 1991). Circulating lymphocytes are tethered (captured) where they transiently adhere to the vascular bed where they then roll along the vessel wall until they can become attached to the endothelium by interactions of selectins (L-selectin, E-selectin and P-selectin) (Figure 1.6). T cells upregulate their cell surface expression of  $\beta 2$  integrin lymphocyte function associated antigen-1 (LFA-1) and  $\alpha 1$  integrin very late activation antigen (VLA-4) when activated (Vora *et al.*, 1997; Ransohoff, 1999; Laschinger *et al.*, 2002; Kohm and Miller, 2003). Chemokines activate and mediate the directional migration of T cells along their concentration gradient. The attachment of these cells is then further strengthened by interactions of their integrins and the endothelial adhesion molecules, which are upregulated upon activation of the cerebral endothelium by chemokines and cytokines (Johnston and Butcher, 2002). VCAM-1 is the major ligand for VLA-4, whereas intercellular adhesion molecule-1 and -2 (ICAM-1 and ICAM-2) are the major endothelial ligands for LFA-1 (Bo *et al.*, 1996; Ransohoff, 1999; Kohm and Miller, 2003;

Figure 1.6 Schematic representation of the mechanisms involved in cellular infiltration across the BBB



b.

<i>Endothelial Cell</i>	<i>Lymphocyte</i>
<b>VCAM-1</b>	VLA-4
<b>ICAM-1</b>	LFA-1
<b>E selectin</b>	L selectin

Schematic representation of the stages (a) and adhesion molecules (b) involved in the transmigration of inflammatory cells across the BBB in MS. Activated endothelial cells and lymphocytes upregulate their expression of adhesion molecules and ligands allowing the firm attachment to the endothelial wall. Activated lymphocytes enter the brain parenchyma following a chemotactic gradient to the areas of inflammation.

Eikelenboom *et al.*, 2005). Cells migrate between or through the endothelial cell layer and matrix metalloproteinases (MMPs) degrade the basement membrane and extracellular matrix allowing cells to enter the brain following chemokine gradients (Ransohoff, 1999; Avolio *et al.*, 2003). Recently another stage has been added in the transmigration of monocytes into the brain. Following the attachment of monocytes to the vascular endothelium, they then move from the site of firm adhesion to the nearest junction in order to begin diapedesis, a process called locomotion (Schenkel *et al.*, 2004; Ancuta *et al.*, 2004).

Endothelial adhesion molecules are now believed to play a more important role in transendothelial migration than just cellular adhesion (Greenwood *et al.*, 2002, Lyck *et al.*, 2003, Turowski *et al.*, 2005). ICAM-1 has a very short cytoplasmic tail, approximately 28 amino acids in humans, however it is capable of eliciting intracellular signals that are vital for transendothelial migration (Greenwood *et al.*, 2002, Turowski *et al.*, 2005). *In vitro* studies have illustrated that the extracellular domain of ICAM-1 is sufficient to support T cell attachment whereas transendothelial migration was strictly dependant of the cytoplasmic tail (Lyck *et al.*, 2003). Intracellular ICAM-1 signalling is triggered by multimerization leading to signalling cascades that result in cytoskeletal rearrangement that facilitates transmigration (Greenwood *et al.*, 2002). ICAM-1 molecules can interact directly with components of the actin and microtubule cytoskeleton, namely  $\alpha$ -actinin and  $\beta$ -tubulin (Carpen *et al.*, 1992). ICAM-1 also interacts with the actin cytoskeleton through the ERM proteins ezrin, radixin and moesin (Turowski *et al.*, 2005). Consequently ICAM-1 cross linking lead to cytoskeletal rearrangement in the formation of actin stress fibres and the phosphorylation of the cytoskeletal-associated proteins focal adhesion kinase (FAK), paxillin and p130<sup>Cas</sup> (Etienne *et al.*, 1998). *In vitro* data has demonstrated that src activity and the phosphorylation of cortactin increases significantly, as a result of Ca<sup>2+</sup> signalling through a protein kinase-dependant pathway, following ICAM-1 cross-linking or T cell adhesion (Etienne-Manneville *et al.*, 2000). ICAM-1 cross linking and T cell adhesion has lead to reported increases in endothelial Rho proteins and activation of Rho GTPases (Adamson *et al.*, 1999). Inhibition of Rho proteins have

prevented the cytoskeletal changes in endothelial cultures and attenuated the clinical signs of EAE suggesting a central role for Rho proteins in ICAM-1 dependant transendothelial migration (Walters *et al.*, 2002, Adamson *et al.*, 1999).

Immunohistochemical studies of endothelial cell associated adhesion molecules have shown an increase in ICAM-1, VCAM-1 and E-selectin on the cell surface of the vascular endothelial cells in MS lesions compared to NAWM and control sample white matter (Sobel *et al.*, 1990; Washington *et al.*, 1994; Bo *et al.*, 1996; Dobbie *et al.*, 1999; Etienne-Manneville *et al.*, 2000). This up-regulation of adhesion molecules is suggested to be a result of TNF actions as *in vitro* models of the BBB report an upregulation in ICAM-1, VCAM-1 and E-selectin following TNF stimulation (Wong and Dorovini-Zis, 1992 & 1995). MS lesions contain a large number of VLA-4<sup>+</sup> and LFA-1<sup>+</sup> lymphocytes (Bo *et al.*, 1996).

Cleaved adhesion molecules in their soluble form are believed to act as inhibitors of adhesion with respect to the membrane bound form, by a competitive mechanism (Avolio *et al.*, 2003). Soluble ICAM-1 is reported to block lymphocyte attachment to cerebral endothelial cells. Serum levels of soluble VCAM-1 in people with relapsing-remitting MS are increased with a decrease in MRI activity, suggesting a role for endothelial VCAM-1 in disease progression (Calabresi *et al.*, 1997; Rieckmann *et al.*, 1998; Avolio *et al.*, 2003). A member of the a disintegrin and metalloproteinase (ADAM) family, ADAM-17, may also influence lymphocytic infiltration as it has been shown to be the mediator of the cleavage and shedding of adhesion molecules L-selectin, and VCAM-1 (Borland *et al.*, 1999; Garton *et al.*, 2003).

During inflammatory conditions such as stroke, human immunodeficiency virus-1 encephalitis and MS, disruption of the BBB integrity occurs associated with infiltration of activated monocytes, lymphocytes or neutrophils (Kwon and Prineas, 1994; Perry *et al.*, 1997; Boven *et al.*, 2000). Increased leukocyte migration has been reported to induce BBB breakdown and loss of the tight-junction associated proteins ZO-1 and occludin of the cerebral endothelial cells in an *in vivo* rat model (Bolton *et al.*, 1998). Other researchers however report that ZO-1 and occludin

remain associated with the endothelial cell borders and are not degraded following neutrophil adhesion and migration *in vitro* (Burns *et al.*, 2000).

During human immune deficiency virus-1 encephalitis (HIVE), HIV-1 infected monocytes infiltrate the parenchyma and are associated with a breakdown in BBB and alterations in the tight junction associated proteins occludin and ZO-1 (Dallasta *et al.*, 1999). Loss of ZO-1 and occludin expression are claimed to be associated with evidence of serum protein leakage in HIVE (Dallasta *et al.*, 1999). TJ disruption is also reported in HIV-1 associated dementia and simian immunodeficiency virus encephalitis, with ZO-1 alterations related to monocyte infiltration and CD68<sup>+</sup> perivascular macrophages (Boven *et al.*, 2000; Luabeya *et al.*, 2000).

TNF may exert an influence on TJ by reorganisation of the associated actin cytoskeleton (Wolburg and Lippoldt, 2002) resulting in the formation of intracytoplasmic aggregates of F-actin (Walsh *et al.*, 2000). Transendothelial permeability is increased across the cerebral microvasculature of Wistar-Furth rats and brain endothelial monolayers *in vitro* following stimulation with TNF (Blum *et al.*, 1997, Prat *et al.*, 2001; Mayhan, 2002).

Immunocytochemical studies have demonstrated BBB breakdown and dysfunction in HIVE, human cerebral malaria and experimental neutrophil induced BBB breakdown (Bolton *et al.*, 1998; Dallasta *et al.*, 1999; Brown *et al.*, 1999; Luabeya *et al.*, 2000; Boven *et al.*, 2000). The structural basis for these BBB permeability changes were shown to lie at the level of the TJ (Luabeya *et al.*, 2000).

#### 1.4.1. BBB in Multiple Sclerosis and other CNS disorders

Breakdown of the BBB has been suggested as an invariable and perhaps obligatory event in new lesion development in relapsing-remitting MS or secondary progressive MS (Lai *et al.*, 1996). A phase of gross but focal dysfunction of the BBB has consistently been demonstrated *in vivo* using Gd-GTPA MRI (Kermode *et al.*, 1990 a&b; McDonald, 1994; Paty and Moore, 1998) suggesting BBB breakdown precedes clinical signs and is a prominent event in the pathogenesis of MS (Claudio *et al.*, 1995). Furthermore BBB leakage has been recorded in many old chronic plaques

(Kwon and Prineas, 1994), even persisting in the absence of active inflammation, at levels which are not detected by routine MRI (Claudio *et al.*, 1995; Paty and Moore, 1998). BBB breakdown in people with relapsing-remitting MS is a common phenomenon usually associated with more aggressive disease and a younger age of onset (Stone *et al.*, 1995). TNF, present in perivascular cuffs in MS (Woodroffe and Cuzner, 1993), is also postulated to be responsible for the redistribution of VE-cadherin and JAM, and for the formation of intercellular gaps between cells (Walsh *et al.*, 2000)

### 1.5 Immunology of MS

Based on observations from the experimental model of MS, experimental autoimmune encephalomyelitis (EAE), which are described further in Chapter 4, MS has been described as a T cell mediated disease. T cells transmigrate across the BBB where they interact with macrophages resulting in myelin destruction, which in turn leads to a perpetuating cycle of damaging inflammatory responses (Hohlfeld *et al.*, 1995; Bar-Or *et al.*, 1999). Currently however MS pathogenesis is believed to involve a synergy between the immune responses of B-cells, monocytes, microglia and macrophages along with T cells (Archelos *et al.*, 2000).

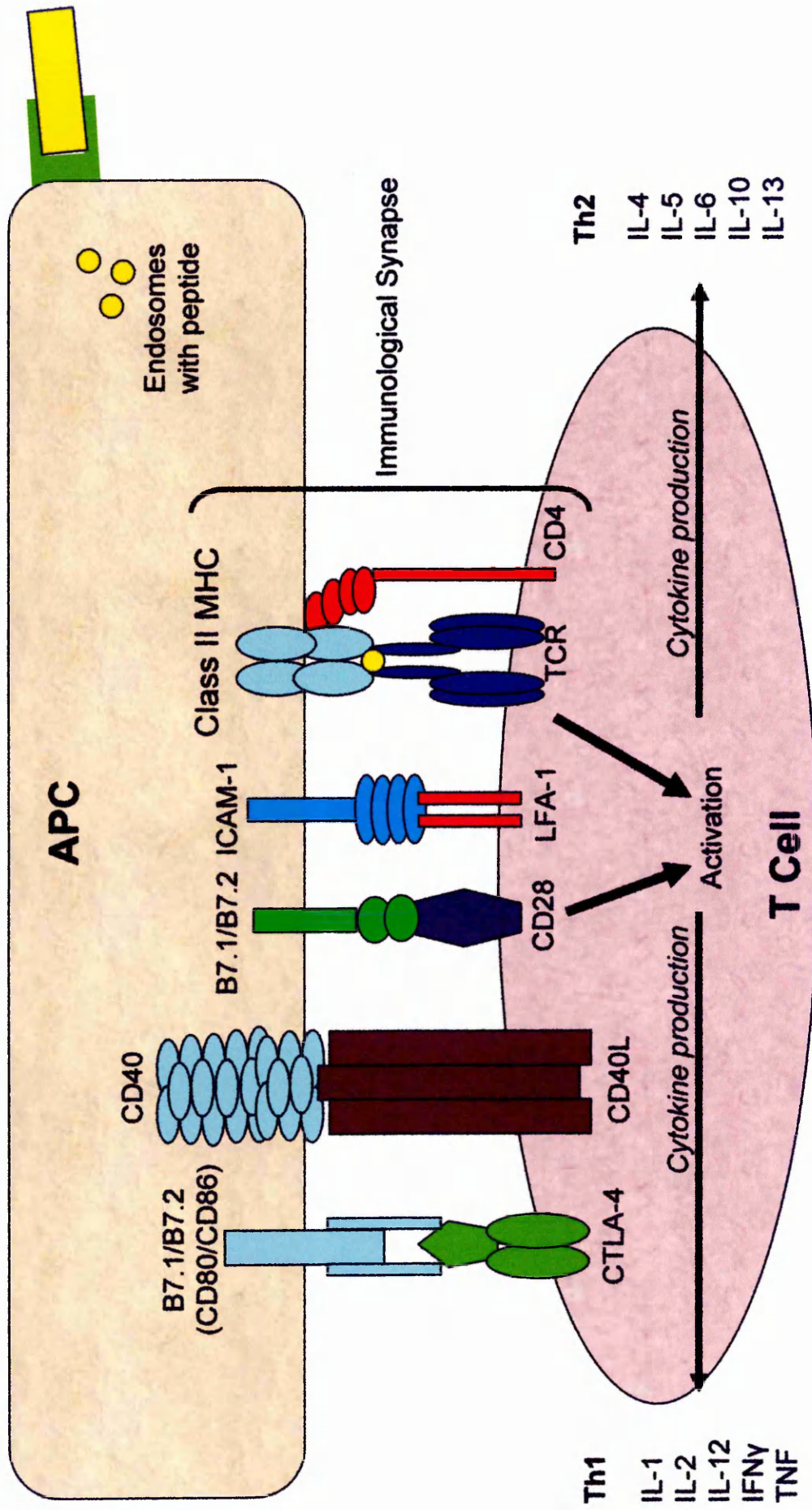
#### 1.5.1 Immune response in MS

##### 1.5.1.1 T cells

Activated T cells secrete various cytokines depending on the required response (Figure 1.7). CD4+ T helper cells (Th1) are associated with pro-inflammatory cytokines TNF, IFN $\gamma$ , lymphotoxin (LT) IL-12 and IL-1 $\beta$  resulting in a Th1 response that enhances APC activation, which in MS results in the destruction and removal of myelin. Secretion of anti-inflammatory cytokines IL-4, IL-10 and IL-13 induces a Th2 response. It has been suggested that the disease processes in lesion formation is controlled by both Th1 and Th2 cells (Kleine *et al.*, 2003). A large group of Th1 and Th2-type receptors (IL-12R, IL-18R, and IFN $\gamma$ R, IL-4R, IL-10R and IL-6R) have recently been described to be ubiquitously and constitutively expressed by oligodendrocytes in MS lesions and normal control white matter (Cannella and Raine, 2004). Expression of the corresponding cytokine ligands by the

Antigen presenting cells (APCs) phagocytose antigen and break it down in lysosomes into peptides which are then presented on the cell surface in a complex with class II MHC molecules. Initial interaction between T cells and APCs involves the interaction between the adhesion molecule ICAM-1 on the surface of the APC with its reciprocal ligand LFA-1 on the T cell surface. High affinity clusters between the TCR and the MHC class II-peptide complex in conjunction with the CD4 accessory molecule forming the immunological synapse. Formation of the immunological synapse induces the expression of CD40L on the T cell and enhances the expression of CD40 on the surface of the APC. CD40-CD40L interaction induces APC to synthesise and express CD80/CD86 co-stimulatory molecules which interact with the constitutively expressed CD28 on the T cells resulting in T cell clonal expansion and either Th1 or Th2 responses. Co-stimulation provided by CD80 is reported to be important in the induction of a Th-1 response, whereas co-stimulation by CD86 is down-regulatory of the Th-1 response. Antigen presentation in the absence of co-stimulatory molecules is insufficient to activate naïve T cells and results in clonal anergy. (Adapted from Dong and Benveniste, 2001).

Figure 1.7 Molecular interactions involved in APC activation of T cells



microglia is proposed to represent a novel innate immune network within the CNS between the oligodendrocytes and microglia (Cannella and Raine, 2004). The role of pro-inflammatory cytokines in EAE, has led to the belief that MS is a Th1 mediated disease and elevated levels of TNF and LT have been detected in MS (Selmaj and Raine, 1988; Hofman *et al.*, 1989). The role of cytokines in MS is complex, indeed subpathological levels of TNF have been suggested as being protective (Raivich and Banati, 2004) and it is believed that both Th1 and Th2 responses coexist. Presence of both Th1 and Th2-type cytokine receptors suggests that no pathway predominates but any outcome results from a shift in the local cytokine balance (Cannella and Raine, 2004).

T cells have been identified in peripheral blood from MS patients that are reactive to epitopes from myelin basic protein (MBP), proteolipid protein (PLP), and MOG (Ota *et al.*, 1990; Stinissen *et al.*, 1998; Bar-Or *et al.*, 1999; Lindert *et al.*, 1999; Iglesias *et al.*, 2001). The same myelin reactive T cells are also known to be part of the regular repertoire in normal control subjects, however certain epitopes are reported to be immunodominant in MS patients only (Ota, *et al.*, 1990; Lunemann *et al.*, 2004). T cell epitope spreading has been reported in MS, whereby an initial response against a defined epitope diversifies with time to be directed to other epitopes on the same molecule (intramolecular) or different molecules (intermolecular) (Vanderlugt *et al.*, 1998). Spreading of responses to different epitopes of PLP has been reported in patients with demyelinating syndromes who eventually developed MS (Tuohy *et al.*, 1997). MBP reactive T cells from MS patients are reported to be in a higher state of activation than those from control. T cells are activated upon presentation of antigen associated with MHC class II by APCs (Figure 1.7).

Microglia and macrophages have been shown to be MHC class II positive within MS lesions suggesting a role in antigen presentation (Hayes *et al.*, 1987) however dendritic cells (DC), known as the professional APC, are the most potent APC. DCs have been shown to be present in the perivascular infiltrate in active MS lesions (Plumb *et al.*, 2003). The presence of DCs within the perivascular cuffs of MS lesions may allow the stimulation of naïve T cells infiltrating the inflamed brain (Plumb *et al.*, 2003). Several

groups have examined the phenotype of T cells within perivascular cuffs. The predominant T cell within the perivascular infiltrate has been reported as being CD4<sup>+</sup> T cells (Compston *et al.*, 1991) however others have reported CD8<sup>+</sup> T cells (Esiri *et al.*, 1989; Gay *et al.*, 1997) as the predominant cell, whilst others have reported an equal distribution of CD4<sup>+</sup> and CD8<sup>+</sup> T cells within the perivascular cuffs (Woodrooffe *et al.*, 1986). Effective antigen presentation also requires the expression of costimulatory or accessory molecules on the surface of the APC binding to their receptor counterparts on the T cell (Windhagen *et al.*, 1995) (Figure 1.7). All CD4<sup>+</sup> and CD8<sup>+</sup> T cells express CD28 constitutively, interactions of CD28 with the costimulatory molecules, CD80 (B7.1) or CD86 (B7.2), induce differentiation of naïve T cells into either Th1 (CD80-CD28) or Th2 (CD86-CD28) cells. CD80 expression has been demonstrated in active MS lesions to be associated with inflammatory macrophages and lymphocytes (Windhagen *et al.*, 1995). CD86 expression was observed in areas of MS lesion and stroke infarct within the same brain suggesting that costimulation with CD86 results in induced scar tissue with fibrosis and not demyelination (Windhagen *et al.*, 1995).

To prevent an autoimmune attack, the CNS regulates autoreactive T cells by inducing T cell apoptosis (Pender and Rist, 2001). T cell apoptosis is mediated through the Fas pathway and the death receptor pathways such as TNF receptor pathway (Brunner *et al.*, 1995). Apoptotic T cells are removed via phagocytosis by the CNS glial cells (Nguyen and Pender, 1998; Pender and Rist, 2001).

#### 1.5.1.2 B cells

Physiologically B cells function as effector cells through their differentiation into plasma cells and secretion of antibodies, release of cytokines and mutual T cell activation. Normal individuals have non-pathological autoantibodies, although their function is unclear (Archelos *et al.*, 2000). Memory B cells can become activated by a T cell-independent mechanism in the presence of IL-2, IL-4, IL-10 and TNF (Hodgkin and Basten, 1995), all of which have been identified within MS lesions. An increase in BBB permeability allows activated B and T cells to enter the CNS

where they have been detected in the perivascular cuff along with plasma cells and macrophages in the Virchow-Robin space (Prineas and Wright, 1978; Esiri, 1977; Esiri and Gay, 1990;). Myelin specific autoantibody may bind to the myelin sheath leading to macrophage-dependent demyelination (Van der Goes *et al.*, 1999). Autoantibodies against MOG have been reported within acute MS lesions (Genain *et al.*, 1999). Antibody-mediated demyelination involves the activation of complement (Weerth *et al.*, 2003; Lassmann, 1998). Deposition of complement activation products have been shown in MOG induced EAE and a subset of MS patients (Storch *et al.*, 1998; Lassmann, 1998). The presence of oligoclonal bands in the CSF of MS patients provides supportive evidence of clonal B cells producing IgG (Hickey, 2001).

Molecular mimicry has been proposed as a possible mechanism involving T cells and B cells in the pathogenesis of MS (Bar-Or *et al.*, 1999; Archelos *et al.*, 2000). Many bacterial and viral proteins share partial sequence similarity to MBP in their genome (Wucherpfennig and Strominger, 1995). Hepatitis B virus and MBP contain sequence similarity and this sequence was encephalitic in rabbits (Wucherpfennig and Strominger, 1995, Wucherpfennig, 2001a). Vaccination with Hepatitis B vaccine has also been reported to activate previously existing MS and the appearance of CNS demyelination, consistent with MS (Faure, 2005). Two other micro-organisms, human herpes virus 6 and *Chlamydia pneumoniae* have been reported to be associated with molecular mimicry in MS (Swanborg *et al.*, 2003). MS patients with high EDSS scores were reported to have *Chlamydia pneumoniae* detected within their CSF (Sriram *et al.*, 1998). Treatment with antibiotics was reported to coincide with neurological improvement however other investigators have disputed the role of *Chlamydia pneumoniae* in MS (Swanborg *et al.*, 2003). HHV-6 has been demonstrated to be expressed within MS plaques and in the CSF of people with RRMS (Soldan *et al.*, 1997; Swanborg *et al.*, 2003).

### 1.5.1.3 Microglia

The activation of microglia and secretion of inflammatory cytokines are important events in the pathogenesis of MS lesion formation (Woodroffe

*et al.*, 1986; Brosnan and Raine, 1996). Microglia have homeostatic and reparative responsibilities and respond rapidly to physiological and stress stimuli (Aloisi, 2001). A small population of monocytes are reported to be able to migrate into the brain parenchyma where they differentiate into microglia (Stroll and Jander, 1999, Priller *et al.*, 2001). The presence of dying cells and cellular debris transforms ramified and highly branched resting microglia into rounded phagocytic macrophages (Aloisi, 2001, Raivich and Banati, 2004). In MS, activated microglia and macrophages are associated with the upregulation of molecules involved in antigen presentation, myelin and tissue breakdown, and the production of reactive oxygen species (Jack *et al.*, 2005, Raivich and Banati, 2004). Microglia also secrete cytokines, chemokines, growth factors and components of the complement cascade (Raivich and Banati, 2004). Microglia have been reported to express increased levels of the costimulatory molecules B7.1 and CD40 in MS lesions, suggesting a role in T cell antigen presentation (De Simone *et al.*, 1995; Jack *et al.*, 2005). Activated microglia have been shown to express IL-1, TNF, IFN $\gamma$ , MCSF, GMCSF and IL-12, which have been shown to have disease promoting activities. Monocytes can develop into either DC or phagocytic macrophages depending on their migration pattern through the endothelium (Randolph *et al.*, 1998). Monocytes can switch between these two differentiation pathways until a late stage of commitment (Palucka *et al.*, 1998). The entry of monocytes into the brain to establish a population of perivascular microglia is well recognised (Hickey and Kimura, 1988; Stoll and Jander, 1999).

It has been proposed that presence of the numerous CNS signalling receptors on microglia indicates that they are regulated by neuronal signals (Philips and Lampson, 2000). Neurotrophins have been shown to decrease microglial expression of MHC class II and costimulatory molecules *in vitro* (Neumann *et al.*, 1998). Microglia and neurons act cooperatively to downregulate brain inflammation by inducing the anti-inflammatory cytokines IL-13 and IL-4. Following their release microglia undergo apoptosis (Shin *et al.*, 2004; Park *et al.*, 2005).

#### 1.5.1.4 Astrocytes

As a component of the BBB the astrocyte is likely to be the first glial cell to encounter and react to inflammation in MS (Ayers *et al.*, 2004). Reactive gliosis and glial scar formation are pathological characteristics of the MS lesion and are characterised by an increased intensity of staining for GFAP, corresponding to the increased density of astroglial processes relative to normal parenchyma (Holley *et al.*, 2003; Ayers *et al.*, 2004). Astrocytes have been shown to proliferate in response to TNF stimulation (Selmaj *et al.*, 1990; 1991c) and have been demonstrated to express TNF and LT at sites of lesions in MS and EAE (Hofman *et al.*, 1989; Plant *et al.*, 2004). Activated astrocytes express vascular cell adhesion molecule-1 (VCAM-1) *in vitro* and within the spinal cord of mice with EAE (Hurwitz *et al.*, 1992; Gimenez *et al.*, 2004). This expression of VCAM-1 is suggested to facilitate the migration of T cells into the CNS with subsequent pathological consequences (Gimenez *et al.*, 2004).

#### 1.5.2 Cytokines in MS

Cytokines are small secreted proteins that are critical components of the immune inflammatory process and enable communication between cells (Imitola *et al.*, 2005). A single cytokine can be expressed by more than one cell type and communicate via cytokine receptors. The Janus kinase and signal transducer/transcription-activating (Jak/STAT) family play an important role in the signalling of many cytokine receptors (Imitola *et al.*, 2005). Cytokines have been reported to play an important role in the pathogenesis of MS and EAE (Brosnan *et al.*, 1995; Laman *et al.*, 1998; Yang *et al.*, 2002). TNF has long been associated with the pathogenesis of multiple sclerosis as described further in section 1.5.2.1.1. IL-12 is critical for the differentiation of Th1 cells and is reported to play an important role in MS (Miller *et al.*, 2004). Increased IL-12 mRNA expression was demonstrated within acute MS plaques (Windhagen *et al.*, 1985). In MS patients, IL-12 expression by peripheral blood mononuclear cells is associated with increased EDSS and disease activity as measured by MRI (Makhlouf *et al.*, 2001). IL-12 has the ability to induce IFN $\gamma$  production by Th1 cells (Miller *et al.*, 2004). IFN $\gamma$  is typically produced by Th1 cells and is a marker for a Th1 response and was

shown to be expressed by perivascular cuffs in MS lesions and is secreted by T cells from people with RRMS and SPMS (Woodroffe and Cuzner, 1993; Balashov *et al.*, 2000). Administration of IFN $\gamma$  to people with MS increased their relapse rate (Panitch *et al.*, 1987).

IL-10 is a key endogenous inhibitor of pro-inflammatory Th1 cytokines produced primarily by Th2 cells (Miller *et al.*, 2004; Imitola *et al.*, 2005) and expressed by astrocytes in MS lesions (Brosnan *et al.*, 1995; Hulshof *et al.*, 2002; Cannella and Raine, 2004). Decreased levels of IL-10 mRNA were detected in peripheral blood mononuclear cells from patients with RRMS and SPMS (Karp *et al.*, 2001). Serum levels of IL-10 protein are reported to be decreased in samples from RRMS, however levels were reported to increase in correlation with the resolution of Gd-DTPA MRI lesions (van Boxel-Dezaire *et al.*, 1999). Another Th2 cytokine associated with MS is IL-4, which is expressed by microglia and foamy macrophages in acute and chronic active MS lesions (Brosnan *et al.*, 1995; Hulshof *et al.*, 2002; Cannella and Raine, 2004).

#### 1.5.2.1 Tumor necrosis factor family

TNF has been associated with inflammation and cell injury, with the TNF/TNFR family also being involved in such diverse processes as host defence, apoptosis, inflammation, autoimmunity and organogenesis (Wallach *et al.*, 1999; Young and Eliopoulos, 2004). TNF is associated with the pathogenesis of a number of different human inflammatory diseases including rheumatoid arthritis, Crohn's disease, diabetes and MS. TNF binds to two membrane bound receptors, TNFR1 (p55) and TNFR2 (p75), the combination of each receptor ligand complex inducing different T cell responses and pathological outcomes (Akassoglou *et al.*, 1998 & 2003; Kassiotis and Kollias, 2001). Different expression patterns of TNFR have been observed within the CNS. TNFR expression has been reported to be associated with glia, neurons, and vascular endothelium, which may be critical in determining whether TNF will activate, induce proliferation or cytotoxicity in these cells and ultimately determine whether the outcome is pathogenic (Akassoglou *et al.*, 2003). TNFR p55 and p75 are also present in soluble forms, which have been shown to influence TNF activity *in vitro* and

*in vivo* (Jureicz *et al.*, 1999). TNF has long been associated with the pathogenesis of multiple sclerosis (Brosnan *et al.*, 1988; Selmaj and Raine, 1988; Hofman *et al.*, 1989; Merrill *et al.*, 1989; Selmaj *et al.*, 1990; 1991a&b).

#### 1.5.2.1.1 *In vivo* evidence for TNF involvement in MS

Increased TNF levels in the cerebrospinal fluid (CSF) and serum samples of MS patients have been reported to be associated with the pathogenesis of the disease (Maimone *et al.*, 1991; Drulovic *et al.*, 1997), however the significance in relation to disease activity is unresolved as contradictory reports have also been made (Franciotta *et al.*, 1989). TNF was detectable within the CSF of MS patients and not within samples from non-inflammatory neurological disorders (Maimone *et al.*, 1991; Drulovic *et al.*, 1997). TNF was only associated with the CSF of patients with active MS, with the TNF CSF concentrations being directly correlated with the degree of patient's disability (Drulovic *et al.*, 1997). However another study involving approximately 120 samples, 50 of which were MS, reported no significant differences in CSF TNF levels between MS and control samples, suggesting that TNF was not involved in the maintenance of the disease, however the possibility of TNF being involved in the initiation of the disease process was not ruled out (Franciotta *et al.*, 1989). Increased shedding of TNFR p75 was found in MS patients in comparison to healthy volunteers, together with decreased p55 shedding, measured in serum (Jurewicz *et al.*, 1999). In another study however, no differences were observed in p55 and p75 in serum samples of MS and control patients (Martino *et al.*, 1997).

#### 1.5.2.1.2 *Autopsy tissue* evidence for TNF involvement in MS

Immunohistochemical studies have identified the presence of TNF within MS autopsy material (Hofman *et al.*, 1989; Woodrooffe and Cuzner, 1993; Brosnan *et al.*, 1995; Cannella and Raine, 1995; Bitsch *et al.*, 2000a). TNF immunoreactivity has been identified as being associated with astrocytes, macrophages (Hofman *et al.*, 1988; Selmaj *et al.*, 1991a) and microglial cells (Cannella and Raine, 1995). TNF immunoreactivity has not been reported in other neurological diseases such as Alzheimer's and Parkinson's disease, however it has been demonstrated, albeit to a lesser extent than in MS, in

subacute sclerosing panencephalomyelitis (SSPE) and adrenoleukodystrophy (ALD) (Selmaj *et al.*, 1991a). Careful classification of MS lesion autopsy and MS biopsy material allowed interpretation of TNF involvement in lesion formation (Selmaj *et al.*, 1991a; Bitsch *et al.*, 2000a). Very little TNF was detected in chronic inactive plaques, whereas TNF<sup>+</sup> cells were observed in all areas of active lesions (Selmaj *et al.*, 1991a). Further evidence for a role for TNF in MS lesion formation is offered by the presence of both p55 and p75 TNFRs on oligodendrocytes along the leading edge of active plaques (Raine *et al.*, 1998). Presence of TNFR on peri-plaque oligodendrocytes correlated with reported oligodendrocyte pathology in MS lesions (Ozawa *et al.*, 1994).

#### 1.5.2.1.3 *In vitro* evidence for TNF involvement in MS

*In vitro* studies have investigated the effects of TNF on oligodendroglial, astroglial and endothelial cells. TNF mediated the death of oligodendrocytes *in vitro* (Selmaj and Raine, 1988; Selmaj *et al.*, 1991b; Andrews *et al.*, 1998; Buntix *et al.*, 2004a&b). Some researchers found that TNF induced oligodendrocyte necrosis (Selmaj and Raine, 1988) whereas others reported oligodendrocytes undergoing TNF mediated apoptosis (Buntinx *et al.*, 2004a&b). Further debate lies with the efficacy of TNF to induce oligodendroglial cell death, as it has been reported that TNF can act directly on oligodendrocytes (Selmaj *et al.*, 1991b) however others report that TNF potentiates the toxicity of IFN $\gamma$  (Andrews *et al.*, 1998) another cytokine that has been shown to play a role in the pathogenesis of MS (Raine, 1995). TNF had less of an effect on cells of oligodendrocyte lineage, the more differentiated the cells were (Andrews *et al.*, 1998). However *in vivo* studies have shown increases in TNF mRNA correlated with a decrease in mature MOG<sup>+</sup> oligodendrocytes, whereas there was no such correlation between TNF mRNA and PLP<sup>+</sup> oligodendrocyte precursor cells (Bitsch *et al.*, 2000). TNF does not affect oligodendrocyte proliferation (Selmaj *et al.*, 1990)

TNF induces astrocyte cell proliferation (Selmaj *et al.*, 1990; 1991c; Merrill, 1991) and reactivity (Tzeng *et al.*, 1999). This proliferative response to TNF may contribute to the reactive gliosis that is a pathological hallmark of MS.

TNF effects on the cerebral endothelial cells of the microvasculature are vital in the disruption of the BBB. *In vitro* studies on endothelial cell cultures suggest that the reported up-regulation of vascular adhesion molecules in MS is mediated by TNF (Wong and Dorovini-Zis, 1992; 1995; Cannella and Raine, 1995; Dobbie *et al.*, 1999; Freyer *et al.*, 1999).

Further evidence for a pathogenic role of TNF in MS is provided in studies that investigated treatment of MS patients with IFN- $\beta$ . Treatment with IFN- $\beta$  shows a decrease in adhesion molecule expression at the BBB with an increased level of soluble VCAM-1 within the serum. Loss of adhesion molecules at the BBB correlated with improved symptoms and a decrease in the number of enhancing lesions on MRI (Calabresi *et al.*, 1997; Rieckmann *et al.*, 1998). It has been suggested therefore that the TNF-induced increase in adhesion molecules at the BBB correlates with worsening of disease (Calabresi *et al.*, 1997; Rieckmann *et al.*, 1998). The formation of soluble adhesion molecules within the serum is suggested to have originated from the proteolytic cleavage of the membrane bound parent molecule by ADAM-17 (Avolio *et al.*, 2003).

### 1.5.3 Chemokines in MS

Chemokines are chemoattractant cytokines that belong to a super family of small secreted proteins (8-14 kDa) that were originally associated with regulating leukocyte trafficking. To date there are over 40 members of the chemokine family (Cartier *et al.*, 2005). The chemokine family is divided into four subgroups based upon the number and spacing of their conserved cysteine residues in their sequences. The chemokine families are C, CC, CXC, and CX3C, where X represents the number of amino acids between the first 2 cysteines (Murphy *et al.*, 2000; Bajetto *et al.*, 2001; Cartier *et al.*, 2005). Chemokines have been implicated in numerous functions including cell adhesion, cytokine secretion, cell proliferation, cell activation and apoptosis (Cartier *et al.*, 2005). Chemokines exert their biological effect through chemokine receptors. Chemokine receptors belong to the superfamily of seven-transmembrane domain receptors that signal through heterotrimeric GTP-binding proteins (Bajetto *et al.*, 2001). One chemokine can activate more than one receptor and conversely one receptor can be

activated by more than one chemokine (Bajetto *et al.*, 2001, Cartier *et al.*, 2005). However unique chemokine-chemokine receptor relationships do occur, e.g. CX3CL1-CX3CR1, CCL20-CCR6 and CXCL12-CXCR4 (Bajetto *et al.*, 2001; Cartier *et al.*, 2005).

CX3CL1 (fractalkine) and CXCL12 (SDF-1 $\alpha$ ) are the only chemokines to be constitutively expressed within the CNS, however 8 chemokine receptors have been reported to be constitutively expressed (Rottmann *et al.*, 1997; van der Meer *et al.*, 2000; Xia *et al.*, 2000; Goldberg *et al.*, 2001). Chemokines and their receptors have been reported to be elevated in MS especially in the perivascular cuff, in lesion formation and disease progression (Simpson *et al.*, 2000; Zhang *et al.*, 2000; Ying *et al.*, 2000; Trebst *et al.*, 2001 & 2003; Mahad *et al.*, 2002; 2003 & 2004; Kivisaak *et al.*, 2004;). Three members of the monocyte chemoattractant protein family -1, -2 and -3 (CCL2, CCL7 and CCL8) have been associated with hypertrophic astrocytes and inflammatory cells within acute and chronic MS lesions (McManus *et al.*, 1998; Van der Voorn *et al.*, 1999). As could have been predicted their corresponding receptors (CCR1-3 and CCR5) have been described to be associated with foamy macrophages and activated microglia in chronic active lesions (Simpson *et al.*, 2000a; Trebst *et al.*, 2001). RANTES (CCL5) has been proposed to be involved in the recruitment of T cells into the CNS, and has been shown to be associated with perivascular T cells along the edge of active plaques and upregulated within the CSF from people with MS compared with controls (Sørensen *et al.*, 1999; Ying *et al.*, 2000). Other chemokines suggested to have a pathogenic role in MS are the macrophage inflammatory proteins (MIP-1 $\alpha$ /CCL3 and MIP-1 $\beta$ /CCL4), interferon gamma inducible protein-10 (IP-10/CXCL10) and monokine induced by gamma-interferon (MIG/CXCL9) (Sørensen *et al.*, 1999; Simpson *et al.*, 2000b; Zhang *et al.*, 2000). Recently CCR7 and CCR8, receptors for CCL21, CCL19, CCL17, CCL1 and CCL4 have been reported to be upregulated in active MS lesions (Kivisaak *et al.*, 2004) and are associated with phagocytic macrophages (Trebst *et al.*, 2003).

## 1.6 Matrix metalloproteinases

The MMP family is a group of Zn-dependent proteolytic enzymes that are involved in the remodelling of the extracellular matrix (ECM) in a variety of physiological and pathological processes (Yong *et al.*, 1998; Rosenberg, 2002; Mandal *et al.*, 2003). Based upon their main substrates, the MMP family is divided into collagenases, gelatinases, stromelysins and membrane type MMPs (MT-MMP) and are members of the matrixin subgroup of the metzincin family. MMPs are synthesized as zymogens with an inhibitory N-terminal pro-peptide sequence with a cysteine residue that chelates the enzymatic Zn<sup>+</sup> ion in the active site (Leppert *et al.*, 2001). Conformational changes resulting in a cysteine switch followed by an autocatalytic cleavage of the pro-peptide activates MMPs (Yong *et al.*, 1998; Leppert *et al.*, 2001; Rosenberg, 2002). MMPs play a pathogenic and detrimental role in a range of CNS diseases including, bacterial meningitis, cerebral ischemia, tumor invasion and metastasis, Alzheimer's disease and MS (Yong *et al.*, 1998; Romanic *et al.*, 1998; Leib *et al.*, 2001; Leppert *et al.*, 2001; Shapiro *et al.* 2003; Meli *et al.*, 2004).

As MMPs can degrade all of the protein constituents of the ECM their activity is tightly regulated (Yong *et al.*, 1998; Leppert *et al.*, 2001). MMP activity is regulated at four levels; gene expression, pro-enzyme activation, enzyme secretion and inhibition by specific tissue inhibitors of metalloproteinases (TIMPs) (Leppert *et al.*, 2001; Visse and Nagase, 2003). TIMPs, of which there are four (TIMP1, 2, 3, 4), are specific endogenous inhibitors of MMPs and form non-covalent bonds with MMPs in a 1:1 stoichiometry inhibiting the pro- and active forms of MMPs (Leppert *et al.*, 2001; Visse and Nagase, 2003).

### 1.6.1 MMPs and multiple sclerosis

MMPs have been suggested to play a number of roles in the pathogenesis of MS, including facilitating transmigration of immune cells across the BBB and through the ECM as well as the attack and breakdown of the myelin sheath (Maeda and Sobel, 1996; Cuzner *et al.*, 1996; Cossins *et al.*, 1997; Chandler *et al.*, 1997; Lepert *et al.*, 1998; Lichtinghagen *et al.*,

1999; Lee *et al.*, 1999; Kieseier *et al.*, 1999; Kouwenhoven *et al.*, 2001; Lindberg *et al.*, 2001; Rosenberg, 2002).

#### *1.6.1.1 In vivo evidence for MMP involvement in MS*

Increased MMP9 levels have been reported in CSF samples from people with MS in comparison to controls (Gijbels *et al.*, 1992; Leppert *et al.*, 1998). Studies on peripheral blood monocytes (PBMC) have demonstrated increased mRNA levels for MMP1, 3, 7 and 9 as well as TIMP1 in patients with MS compared with OND and normal controls (Lee *et al.*, 1999; Lichtinghagen *et al.*, 1999; Kouwenhoven *et al.*, 2001). However no significant differences were observed in the number of TIMP1 and TIMP2 mRNA expressing PBMC in serum samples from active MS in comparison with stable disease and normal controls (Lee *et al.*, 1999; Lichtinghagen *et al.*, 1999). In another study however, the numbers of TIMP1 mRNA expressing monocytes were elevated in serum samples from patients with MS (Kouwenhoven *et al.*, 2001). Further evidence for the involvement of MMPs in MS comes from the reduction in the abnormally high level of MMP9 activity in the CSF of MS patients following methylprednisolone therapy (Rosenberg *et al.*, 1996).

#### *1.6.1.2 Autopsy tissue evidence for MMP involvement in MS*

Immunohistochemical studies have revealed that macrophages in active lesions and to a lesser extent in chronic lesions, express MMP1, 2, 3 and 9 (Maeda and Sobel, 1996; Cuzner *et al.*, 1996; Lindberg *et al.*, 2001). MMP7 and MMP9 expression is increased in areas of NAWM in comparison to controls and is associated with the endothelium of the microvasculature (Lindberg *et al.*, 2001). All TIMPs are reported to be constitutively expressed in control brains (Lindberg *et al.*, 2001).

#### *1.6.1.3 In vitro evidence for MMP involvement in MS*

It has been suggested that one of the major producers of MMPs are monocytes and macrophages (Kouwenhoven *et al.*, 2001). Lymphocyte migration across a barrier *in vitro*, representing the basal lamina, has been shown to be mediated by MMP9 and it is believed that MMPs expressed by

monocytes mediate their transmigration across the BBB into the brain parenchyma by ECM remodelling and disruption of the barrier (Leppert *et al.*, 1995).

### *1.7. ADAM family proteins*

The ADAMs are related to the family of MMPs and MT-MMPs which comprise the matrixin subfamily of the metzincins (Killar *et al.*, 1999). The ADAM family of proteins, include the adamalysin subfamily of the metzincins along with the snake venom metalloproteases (SVMP) (Killar *et al.*, 1999). Adamalysins are similar to the matrixins in their metalloproteinase domain, but differ by the presence of a unique integrin receptor-binding disintegrin domain. The ADAM family are a large group of type I integral membrane proteins of which to date there are 40 family members reported (Seals and Courtneidge, 2003).

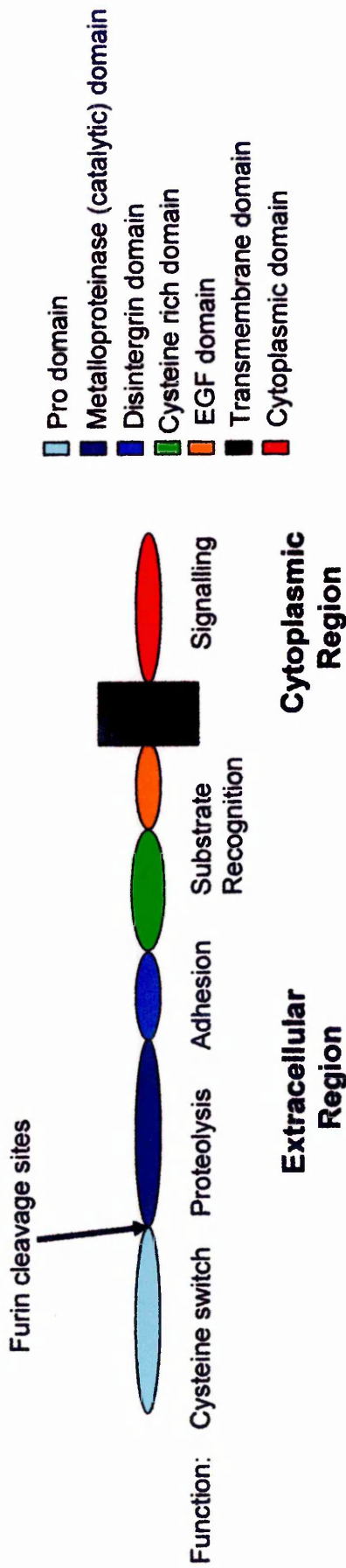
#### *1.7.1 Domain structure of the ADAM family*

Members of the ADAM family are structurally similar and phylogenically well conserved and are comprised of: prodomain; metalloproteinase domain; disintegrin domain; cysteine-rich domain; and EGF-like domain; transmembrane domain and a cytoplasmic tail (Yamamoto *et al.*, 1999) (Figure 1.8). The presence of the transmembrane and cytoplasmic domains in ADAMs but not SVMP proteins indicates that all the ADAMs exist as membrane bound forms whereas all the SVMPs are secreted (Killar *et al.*, 1999).

#### *The prodomain*

The prodomain consists of about 200 amino acid residues that are separated from the metalloproteinase domain by one or more furin cleavage sites. Primarily the prodomain keeps the metalloproteinase site of the ADAMs inactive, through a cysteine switch mechanism (Van Wart and Birkedal-Hansen, 1990). Furin, or furin-like proprotein convertases, cleave the prodomain from the rest of the protein, releasing it and switching the zinc coordination to the metalloproteinase domain making it available for catalytic activity (Killar *et al.*, 1999, Seals and Courtneidge, 2003). A further function

Figure 1.8 General schematic representation of the domain structure of ADAM proteins



Schematic representation of the structural domains and functions of ADAM proteins. All ADAMs contain a transmembrane and cytosolic domain indicating that all ADAMs have a membrane bound form (adapted from Black, 2002).

of the prodomain is to chaperone the proper folding of the protein (Milla *et al.*, 1999; Leonard *et al.*, 2005). Constructs of ADAM 10 and ADAM 17 devoid of a prodomain are reported to be enzymatically inactive *in vivo* (Milla *et al.*, 1999; Anders *et al.*, 2001).

#### *The metalloproteinase domain*

The metalloproteinase or catalytic domain consists of approximately 200 amino acid residues that contain three conserved histidine residues (**HEXGHXXGXXHD**) that coordinate the catalytic Zn<sup>2+</sup> in the active site (Killar *et al.*, 1999; Seals and Courtneidge 2003).

#### *The disintegrin domain*

The disintegrin domain was named after its presence within the SVMPs where it is involved in binding to platelet integrin receptors, preventing platelet aggregation at wound sites (Seals and Courtneidge, 2003). Structurally there is little known about the disintegrin domain of the ADAM proteins (Seals and Courtneidge, 2003) or whether or not all ADAM proteins can bind to integrins (Moss *et al.*, 2001). The disintegrin domain in ADAMs consists of approximately 90 amino acid residues, with 15 cysteines, including a 14 residue 'disintegrin loop' with 3 cysteines, one each at the start, middle and end of the loop (Moss *et al.*, 2001).

#### *The cysteine rich and EGF domains*

Little is known about the structure and function of the cysteine rich and EGF domains. These domains are comprised of approximately 160 and 40 amino acids with each also containing 14 and 6 cysteine residues respectively. It has been suggested that these domains are involved with substrate recognition and specificity, complementing the binding capacity of the disintegrin domain (Moss *et al.*, 2001, Seal and Courtneidge, 2003). The cysteine rich domain of human ADAM12 has been shown to interact with syndecan in tumor cells *in vitro* (Iba *et al.*, 1999), whereas the cysteine-rich domain of ADAM13 has been reported to bind to both fibronectin and  $\beta$ 1-containing integrins (Gaultier *et al.*, 2002).

### *The transmembrane domain*

All ADAM proteins are anchored to cell membranes via the transmembrane domain near the C-terminus. Several ADAM proteins however also have an alternatively spliced form that diverges before the transmembrane domain, thus leading to the production of a soluble secreted form (Moss *et al.*, 2001). The ADAM family members with a thrombospondin motif (ADAMTS) lack a transmembrane domain and are therefore all secreted.

### *The cytoplasmic domain*

The cytoplasmic tail of ADAM proteins is highly variable in both length and sequence (Seals and Courtneidge, 2003). The cytoplasmic tail contains SH3 binding domains and potential phosphorylation sites suggesting a signalling function (Killar *et al.*, 1999). Cell culture studies have demonstrated the importance of interaction of the cytoplasmic tail of ADAM-9 with protein kinase C, thereby upregulating its cleavage of pro-heparin binding epidermal growth factor (HB-EGF) (Moss *et al.*, 2001). Recent studies have implicated ADAM-17 as a physiological HB-EGF convertase (Hinkle *et al.*, 2004).

### *1.7.2. ADAM proteins in biology*

ADAM proteins have the potential to mediate a variety of functions including proteolysis, adhesion, fusion, and signalling (Killar *et al.*, 1999). Expression of ADAM mRNAs is wide and differentiated suggesting that these are multipotential proteins (Kärkkäinen *et al.*, 2000). ADAMs 1-3 play a pivotal role in the fertilisation of the ovum by a sperm (Evans 2001). ADAMs - 9, -12, and -19 are suggested to play a role in myogenesis and osteogenesis, whereas ADAM-13 is proposed to be involved with neural crest migration in *Xenopus* (Killar *et al.*, 1999; Seals and Courtneidge, 2003). Adhesion protein-mediated communication between cells and between cells and the extracellular matrix (ECM), together with the proteolytic processing and remodelling of cellular and extracellular proteins are essential for the structure and function of the CNS (Kärkkäinen *et al.*, 2000). In neurogenesis, ADAM-10 has been shown to mediate cell fate decisions by

activation of the Notch signalling pathway (Pan and Rubin, 1997) initiating lateral inhibition (Killar *et al.*, 1999).

A number of ADAM proteins have been found to be involved with immune responses and as a result are suggested to have pathogenic roles in numerous inflammatory conditions. ADAM-8 is suggested to play a role in the degradation of vascular basement membranes and has been demonstrated to be expressed on monocytes and macrophages and is upregulated upon cellular activation (Yoshiyama *et al.*, 1997; Yamamoto *et al.*, 1999; Killar *et al.*, 1999). Immunohistochemical studies have demonstrated ADAM-15 expression by macrophages associated with the endothelium in atherosclerosis (Herren *et al.*, 1997) suggesting a possible pathogenic role.

ADAM-10 was the first member of the ADAM family to be described as having proteolytic activity (Howard *et al.*, 1996). ADAM-10 has close homology with ADAM-17 (Described in detail in Chapter 3) however it is more closely related to Kuzbanian, its *Drosophila* homologue (Killar *et al.*, 1999, Moss *et al.*, 2001). ADAM-10 mRNA has been demonstrated to be expressed in hematopoietic cells and chondrocytes (Dallas *et al.*, 1999) and within the adult CNS (Kärkkäinen *et al.*, 2000; Kieseier *et al.*, 2003). ADAM-10 is reported to cleave myelin basic protein and type IV collagen *in vitro* (Howard *et al.*, 1996). Further *in vitro* studies have also demonstrated ADAM-10 to be capable of cleaving TNF however it is not the main physiological convertase (Lun *et al.*, 1997; Killar *et al.*, 1999). One of the pathological hallmarks of Alzheimer's disease is the presence of large extracellular amyloid plaques within the brain. The pathological formation of amyloid plaques requires the cleavage of amyloid precursor protein (APP) by both  $\beta$ -secretase (BACE) and  $\gamma$ -secretase (presenilin-1) (Numan and Small, 2000; Skovronsky *et al.*, 2001; Asai *et al.*, 2003; Kojro and Fahrenholz, 2005). ADAM-9 and ADAM-10 are  $\alpha$ -secretases of APP and may process APP down a non-amyloidogenic pathway, acting as a protective factor in Alzheimer's disease (Allinson *et al.*, 2003; Kojro and Fahrenholz, 2005).

## 1.8 Experimental autoimmune encephalomyelitis an experimental model of MS

EAE can be induced in animals by active immunization with CNS components in adjuvant, by the passive transfer of myelin-specific activated T cells into the blood stream or by viral infection (Lipton *et al.*, 1979; van Noort, 1996; Begolka *et al.*, 1998). Depending on the animal strain and type of immunization and induction, either an acute, monophasic or chronic relapsing EAE disease course can be induced (van Noort, 1996; Rausch *et al.*, 2003). Acute EAE manifests as an inflammatory disease where evidence of demyelination is minimal. Demyelination is a pathological feature of chronic EAE however, where multiple phases of tissue inflammation are followed by persistent damage to the myelin sheath (Rausch *et al.*, 2003). Demyelination is also a pathological hallmark of Theiler's murine encephalomyelitis virus induced EAE (Lipton *et al.*, 1979). Susceptibility to EAE induction varies between strains of different species due to differences in the MHC genes of different strains of animals (Rausch *et al.*, 2003; Behi *et al.*, 2005). Clinical progression of EAE is characterised by weight loss and hind limb weakness that can progress to bilateral hind limb paralysis. In most species, the disease recovers spontaneously (Badovinac *et al.*, 1998). In rat and marmoset, demyelination is strictly antibody dependant whereas in mice demyelination can be mediated by a TNF dependant mechanism (Iglesias *et al.*, 2001).

### 1.8.1 Autoantigens in EAE

EAE was originally termed experimental allergic encephalomyelitis as it was believed that the inflammation observed was an allergic response to exogenous neuronal tissue however more recent evidence has suggested an autoimmune response to a self antigen as the pathogenic mechanism. As myelin is a primary target in demyelination the protein constituents of myelin were regarded as encephalitogenic. Myelin basic protein (MBP), is the major protein constituent of myelin and was long believed to be "the" encephalitogenic protein of the CNS in EAE. Moreover other myelin proteins have been deemed encephalitogenic including PLP, MAG, MOG and myelin oligodendrocyte basic protein (MOBP) (Leber *et al.*, 1986; Sobel *et al.*, 1986;

Linington and Lassmann, 1987 Weerth *et al.*, 1999; Kaye *et al.*, 2000; Von Budingen *et al.*, 2001).

### 1.8.2 MOG as an autoantigen in EAE

MOG is now regarded as having one of the strongest encephalitogenic properties of all the myelin proteins (Von Budingen *et al.*, 2001, Brok *et al.*, 2001; Iglesias *et al.*, 2001). MOG, formally known as M2 protein (Linington *et al.*, 1984), is expressed and incorporated into the outermost lamellae of the myelin sheath, making it an ideal target for antibody mediated demyelination (Iglesias *et al.*, 2001; Brok *et al.*, 2001). MOG is developmentally regulated and is deemed a marker for mature oligodendrocytes and is the only myelin protein not to be expressed outside the CNS (Von Budingen *et al.*, 2001). MOG is unique in that it is the only myelin autoantigen that is able to induce both an encephalitogenic T cell response and a demyelinating response in EAE. In the absence of a specific antibody response, MOG induces a purely inflammatory pathology that can be altered to an inflammatory response with demyelination following intravenous injection of MOG-specific monoclonal antibody (Iglesias *et al.*, 2001). MOG by itself has been able to induce EAE in inbred mice, rats and nonhuman primates (Von Budingen *et al.*, 2001).

### 1.9 Pathology of EAE

The classic pathology of a myelin autoantigen induced EAE is of an acute monophasic T cell inflammatory process. However different autoantigens, in different species and strains can induce varying pathologies, which are useful in investigating the different underlying mechanisms involved in MS. Acute EAE displays an intense inflammatory response with large perivascular cuffs composed of T cells and ED-1<sup>+</sup> activated macrophages with a distinct reduction or lack of demyelination (Pender, 1988, Ahmed *et al.*, 2001, Rausch *et al.*, 2003). In chronic relapsing models of EAE (CREAE) inflammatory demyelination and axonopathy are prominent, especially within the spinal cord (Lublin, 1985; Baker *et al.*, 1990; Kornek *et al.*, 2000; Ahmed *et al.*, 2001; Brok *et al.*, 2001). In IL-12-induced serial relapses, levels of inflammatory cuffs were recorded to be highest

during the first relapse and were subsequently reduced during following relapses (Ahmed *et al.*, 2001). Levels of CD4<sup>+</sup> T cells and ED1<sup>+</sup> macrophages were also at their highest during the first relapse and returned to normal levels, compared with acute EAE, during subsequent relapses (Ahmed *et al.*, 2001). High levels of axons with an accumulation of  $\beta$ -APP were seen in lesions with active inflammatory activity in a CREAE model in marmosets and rats (Kornek, *et al.*, 2000; Brok *et al.*, 2001). In a non-human primate model of EAE, animals killed during the chronic, relapsing remitting phase displayed sharply defined areas of demyelination with minimal mononuclear cell infiltration and extensive astrogliosis comparative to chronic MS plaques (Genain and Hauser, 1997; Laman *et al.*, 1998).

### *1.9.1 Pathological comparisons to MS*

Overall the pathologies reported in different EAE models correlates with those observed within MS. However each induced EAE model has a specific disease course and known pathology, whereas the pathology of MS is heterogeneous (Lucchinetti *et al.*, 2000). Four patterns of MS lesion have been proposed however only two of these can be replicated in experimental models (Lucchinetti *et al.*, 2000; Brok *et al.*, 2001; Kornek and Lassmann, 2003). T cell mediated and T cell plus antibody mediated lesion formation are observed in MS and EAE, however lesions which are a result of oligodendrocyte loss from direct microbial infection or cytotoxicity have not been demonstrated in an experimental model (Brok *et al.*, 2001). Lesions within MS are disseminated throughout the brain and spinal cord, whereas in Lewis rats with EAE the affected area is mainly the spinal cord (Villarroya *et al.*, 1996), however in marmosets with EAE, periventricular demyelinated lesions have been reported (Laman *et al.*, 1998). Lesions in marmoset EAE tissue constantly display vesicular myelin disruption that is also evident in acute MS lesions (Raine *et al.*, 1999).

### *1.9.2 Cellular and immune responses in EAE*

#### *1.9.2.1 Cytokines*

EAE is a T cell mediated autoimmune disease that involves a complex cascade of pro-inflammatory chemokines and cytokines leading to a

breakdown in the BBB. Pro- and anti-inflammatory cytokines coexist in EAE during active disease in concordance with findings in MS (Cannella and Raine 1995; Laman *et al.*, 1998), suggesting that a balance of relative expression of disease inducing pro-inflammatory cytokines and the downmodulatory anti-inflammatory cytokines determines the level of clinical signs (Laman *et al.*, 1998; Yang *et al.*, 2002).

#### 1.9.2.1.1 TNF and IFN $\gamma$ in EAE

TNF activity has been demonstrated to be elevated in serum samples from Lewis rats with EAE, with peak levels corresponding to peak disease symptoms (Villarroya *et al.*, 1996). *In situ* hybridization for TNF mRNA shows expression levels that parallel clinical signs, indicating a possible deleterious role for TNF in EAE (Issazadeh *et al.*, 1995b; Villarroya *et al.*, 1996; Begolka *et al.*, 1998; Glabinski *et al.*, 2003). However TNF and LT double knockout mice were still susceptible to EAE (Frei *et al.*, 1997). In another study both p55 TNFR and p75 TNFR knockout mice were reported to still develop MOG induced EAE suggesting that other cytokines may also play a pathogenic role in EAE induction (Kassiotis *et al.*, 1999; Schiffenbauer *et al.*, 2000). IFN $\gamma$  mRNA expression in spinal cord correlates with clinical signs in EAE (Issazadeh *et al.*, 1995a; Glabinski *et al.*, 2003). Furthermore intraventricular injection of IFN $\gamma$  induced further relapses in rats with EAE (Tanuma *et al.*, 1999).

#### 1.9.2.1.2 IL-1 in EAE

IL-1 receptor (IL-1R) knockout mice failed to develop MOG induced EAE (Schiffenbauer *et al.*, 2000). IL-1 positive astroglial like cells have been reported in the parenchyma of EAE animals (Laman *et al.*, 1998). Treatment of EAE with soluble IL-1R and IL-1R antagonist reduced the clinical severity of the disease implicating IL-1 in playing a major pathogenic role in EAE (Martin and Near, 1995; Badovinac *et al.*, 1998). Presence of IL-1R antagonist during *in vitro* priming of T-cells reduced the efficacy of inducing EAE by adoptive transfer (Badovinac *et al.*, 1998). These results suggest that IL-1R and by inference IL-1 are essential for the development of EAE (Schiffenbauer *et al.*, 2000).

#### 1.9.2.1.3 IL-12 in EAE

Endogenous production of IL-12 is essential for Th1 cell generation and also promotes IFN $\gamma$  production by T cells (Issazadeh *et al.*, 1995b). Administration of IL-12 to Lewis rats, following recovery from acute EAE induces a further paralytic relapse with associated demyelination and axonal loss (Ahmed *et al.*, 2001). Only limited expression of IL-12 however was observed in marmosets with acute EAE (Laman *et al.*, 1998).

#### 1.9.2.1.4 IL-4 and IL-10 in EAE

IL-4 and IL-10 are Th2 cytokines that are reported to be associated with remission and recovery from acute EAE (Racke *et al.*, 1994; Begolka *et al.*, 1998; Yang *et al.*, 2002) and ameliorate the disease when administered *in vivo* (Racke *et al.*, 1994; Rott *et al.*, 1994). However another report suggests that IL-4 expression levels do not correlate with disease activity and that it is only detected at a very low level (Issazadeh *et al.*, 1995a). Increased levels of IL-10 were reported to occur after initial onset of disease recovery, suggesting that IL-10 rather than initiating disease recovery actually acts by keeping the animal free from relapses by suppressing cytokine synthesis by Th1 cells (Issazadeh *et al.*, 1995b).

#### 1.9.2.2 Chemokines

Several chemokines have been proposed as being involved in the pathogenesis of EAE (Ransohoff *et al.*, 1993; Godiska *et al.*, 1995; Karpus, 2001; Jee *et al.*, 2002; Glabinski *et al.*, 2003; Klein, 2004). During acute EAE, MCP-1, IP-10, RANTES, MIP-1 $\alpha$  and MIP-1 $\beta$  are upregulated at the beginning of the active stage of the disease (Godiska *et al.*, 1995; Jee *et al.*, 2002). In CREAE, MCP-1, IP-10, RANTES, MIP-1 $\alpha$  and T-cell activation gene 3 (TCA-3) are increased during relapses of the disease (Ransohoff *et al.*, 1993; Jee *et al.*, 2002; Glabinski *et al.*, 2003) suggesting a pathological involvement for these chemokines. CNS chemokine mRNA expression correlated with histological signs of inflammation, as expression was not detected in the absence of leukocyte infiltration (Godiska *et al.*, 1995). Functional studies have shown that antibodies to MIP-1 $\alpha$  and MCP-1 ameliorate EAE and MCP-1 deficient mice display reduced macrophage

recruitment to inflammatory areas and have a significantly milder form of EAE (Karpus *et al.*, 1995; Kennedy *et al.*, 1998; Huang *et al.*, 2001). CC chemokine receptor 2 (CCR2), the main receptor for MCP-1, was significantly upregulated throughout the course of CREAE (Jee *et al.*, 2002) moreover mice deficient in CCR2 do not develop EAE (Fife *et al.*, 2000). Although the same chemokines are repeatedly reported in various EAE studies, chemokine expression patterns differ in different mouse strains and EAE models (Karpus and Ransohoff, 1998). In EAE, fractalkine expression is reported to be upregulated on microglia and blood vessels (Pan *et al.*, 1997; Jiang *et al.*, 1998), however others report no change in fractalkine mRNA expression levels (Schwaebel *et al.*, 1998).

### 1.9.2.3 Adhesion molecules

ICAM-1 and VCAM-1 are upregulated during the course of EAE development reaching a maximum at peak clinical disability (Selmaj, 2000; Laschinger and Englehardt, 2000; Scott *et al.*, 2004). E-selectin is an adhesion molecule that is associated with activated endothelia in response to inflammatory cytokines including TNF and IL-1 $\beta$  and is proposed to play a role in the rolling stage of leukocyte recruitment (Wagnerova *et al.*, 2002). Increased levels of soluble E-selectin have been reported in MS, corresponding to disease activity (Dore-Duffy *et al.*, 1995), however little is known about E-selectin expression in EAE. L-selectin is mainly expressed on the cell surface of leukocytes and like E-selectin is believed to be involved in the rolling phase of leukocyte transmigration (Archelos *et al.*, 1998). L-selectin positive cells have been demonstrated in the brain and spinal cord during active EAE (Allen *et al.*, 1994; Dopp *et al.*, 1994) (Figure 1.6). Administration of an antibody to L-selectin has been reported to effectively suppress clinical signs, and mononuclear infiltration in an MBP-induced EAE model (Archelos *et al.*, 1998). VLA-4 is the surface receptor for VCAM-1 and its expression is required for T-cell migration into the brain parenchyma (Baron *et al.*, 1993; Laschinger and Englehardt, 2000) (Figure 1.6). Monoclonal antibodies and synthetic antagonists of VLA-4 have been demonstrated to inhibit the initiation of EAE (Brocke *et al.*, 1999; Cannella, *et al.*, 2003). VCAM-1 and ICAM-1 are mostly associated with the endothelial

cells of the microvasculature but are also expressed by astrocytes and cells of microglial lineage (Selmaj, 2000). Treatment with a soluble p55 TNFR significantly reduced VCAM-1 expression in EAE to level comparable to that of non-immunised animals (Selmaj, 2000).

### *1.10 The aims of this thesis*

The overall aim of this thesis is to further elucidate the immunopathological events ongoing in the CNS in MS (Figure 1.9) in particular the integrity of the interendothelial tight junction proteins of the cerebral blood vessels and to characterise the expression of ADAM-17 and TIMP3 within MS autopsy tissue, and to assess their role in MS pathogenesis. Specifically to determine:

- The expression of the TJ associated proteins, occludin and ZO-1, in MS at different stages of lesion development and in control white matter using immunofluorescence and confocal microscopy.
- Expression of ADAM-17 and TIMP3 within MS and control white matter at the protein level by immunofluorescence and western blotting and at the mRNA level by RT-PCR.
- Expression of ADAM-17 and TIMP3 over the disease course of EAE, an experimental model of MS, at the protein level by immunofluorescence and western blotting and at the mRNA level by RT-PCR and real-time PCR.
- Regulation of ADAM-17 and TIMP3 under pro-inflammatory conditions using rat cerebral endothelial cell cultures and analysis at the protein level by immunofluorescence and western blotting.
- Functional activity of ADAM-17 in rat cerebral endothelial cells under pro-inflammatory conditions by measuring soluble TNF using ELISA techniques.

## 1. Introduction

The purpose of this report is to analyze the current market conditions and provide a comprehensive overview of the industry trends. The data presented here is based on a thorough review of recent market reports and industry news.

### 2. Market Overview

The market has shown significant growth over the past year, driven by several key factors. The overall economic environment remains stable, with a steady increase in consumer spending and a strong focus on innovation and technology.

Key trends include a shift towards digital marketing, increased investment in research and development, and a growing emphasis on sustainability and ethical sourcing.

The industry is expected to continue its upward trajectory, with several new entrants and established players alike, all vying for market share.

Overall, the market is in a strong position, with a clear focus on long-term growth and innovation.

The following sections provide a detailed analysis of the market's performance and outlook.

### 3. Financial Performance

The financial performance of the industry has been robust, with a steady increase in revenue and profit margins. This is primarily due to the strong demand for products and services, as well as the effective implementation of cost-cutting measures.

### 4. Conclusion

In conclusion, the market is in a strong position, with a clear focus on long-term growth and innovation. The industry is expected to continue its upward trajectory, with several new entrants and established players alike, all vying for market share.

The following sections provide a detailed analysis of the market's performance and outlook.

Overall, the market is in a strong position, with a clear focus on long-term growth and innovation.

### 5. Future Outlook

The future outlook for the industry is positive, with a strong focus on innovation and technology. The market is expected to continue its upward trajectory, with several new entrants and established players alike, all vying for market share.

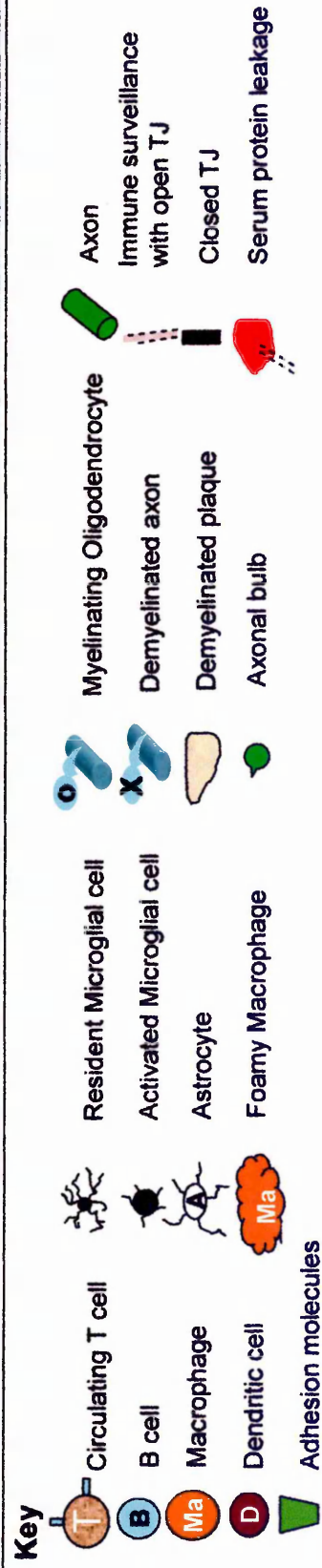
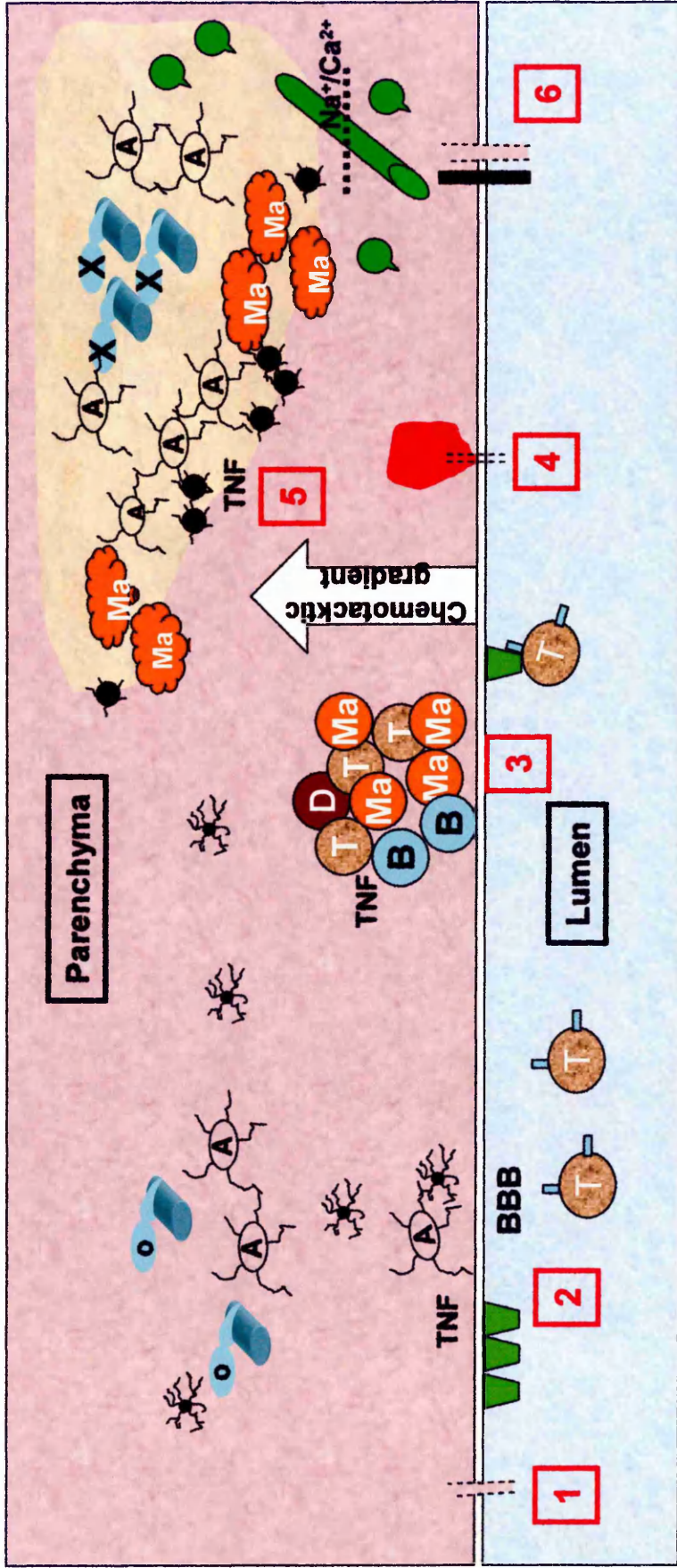
Overall, the market is in a strong position, with a clear focus on long-term growth and innovation.

The following sections provide a detailed analysis of the market's performance and outlook.

Overall, the market is in a strong position, with a clear focus on long-term growth and innovation.

1. The CNS is under constant surveillance by T cells that enter the brain across the BBB and then return to the cervical lymph nodes via the subarachnoid space and the perineuronal spaces of the cranial nerves. Under basal conditions astrocytes are in close contact with the BBB, oligodendrocytes manufacture and maintain myelin, resting microglia are ramified in morphology.
2. Increased expression of adhesion molecules on the luminal surface of the vascular endothelium of the BBB from MS lesions compared to NAVM and control sample white matter
3. Interaction of leukocyte cell adhesion molecules (LFA-1, VLA-4, L-selectin) with the endothelial adhesion molecules (ICAM-1, VCAM-1 and E-selectin) enables the transmigration of cells across the BBB into the Verchow-Rubin space where they accumulate as a perivascular cuff. Close proximity of these cells enables antigen presentation to T cells evoking Th1 and Th2 responses. Chemokines and their receptors have been reported in perivascular cuffs and MS lesion creating a chemotactic gradient to direct cell migration
4. Gd-MRI along with immunocytochemical labelling for fibrinogen has distinguished BBB breakdown with serum protein leakage as one of the pathogenic hallmarks of MS.
5. Demyelination in MS may occur following attack of the oligodendrocyte-myelin sheath complex and can occur either by a direct antibody-mediated attack, cytotoxic cell death of the oligodendrocyte, or secondary as a result of axonal death. Resident microglia become activated increasing MHC class II expression, secrete pro-inflammatory cytokines, chemokines and growth factors and along with macrophages, can phagocytose myelin debris resulting in a foamy morphology. High levels of activated microglia and macrophages are prominent along a clearly demarcated edge of a demyelinating lesion. Astrocytes proliferate and become hypertrophic, replacing myelin, creating an astrocytic glial scar that has been suggested to prevent the recruitment of myelinating oligodendrocytes or oligodendrocyte precursors to plaque centres
6. BBB disruption is suggested to be transient and returns to normal after the attack. Persistent BBB leakage however has been reported in chronic MS lesions and may render the BBB susceptible to further breakdown and may contribute to the relapsing-remitting progression of MS.

Figure 1.9 Schematic Representation of pathological mechanisms in the CNS during MS



## **Chapter 2**

### **Endothelial tight junction-associated proteins of the blood-brain barrier in multiple sclerosis**

## 2.1 Introduction

The existence of a BBB was discovered towards the end of the 19<sup>th</sup> century through the studies of Ehrlich (1885) (De Vries *et al.*, 1997). Ehrlich reported that the brain tissue remained clear following an intravascular injection of a vital dye. However Goldmann (1909) reported that human brain tissue stained when trypan blue was injected directly into the ventricular system, leading to the suggestion of a barrier at the site of the cerebral microvasculature (De Vries *et al.*, 1997).

### 2.1.1 Molecular composition of the BBB tight junction

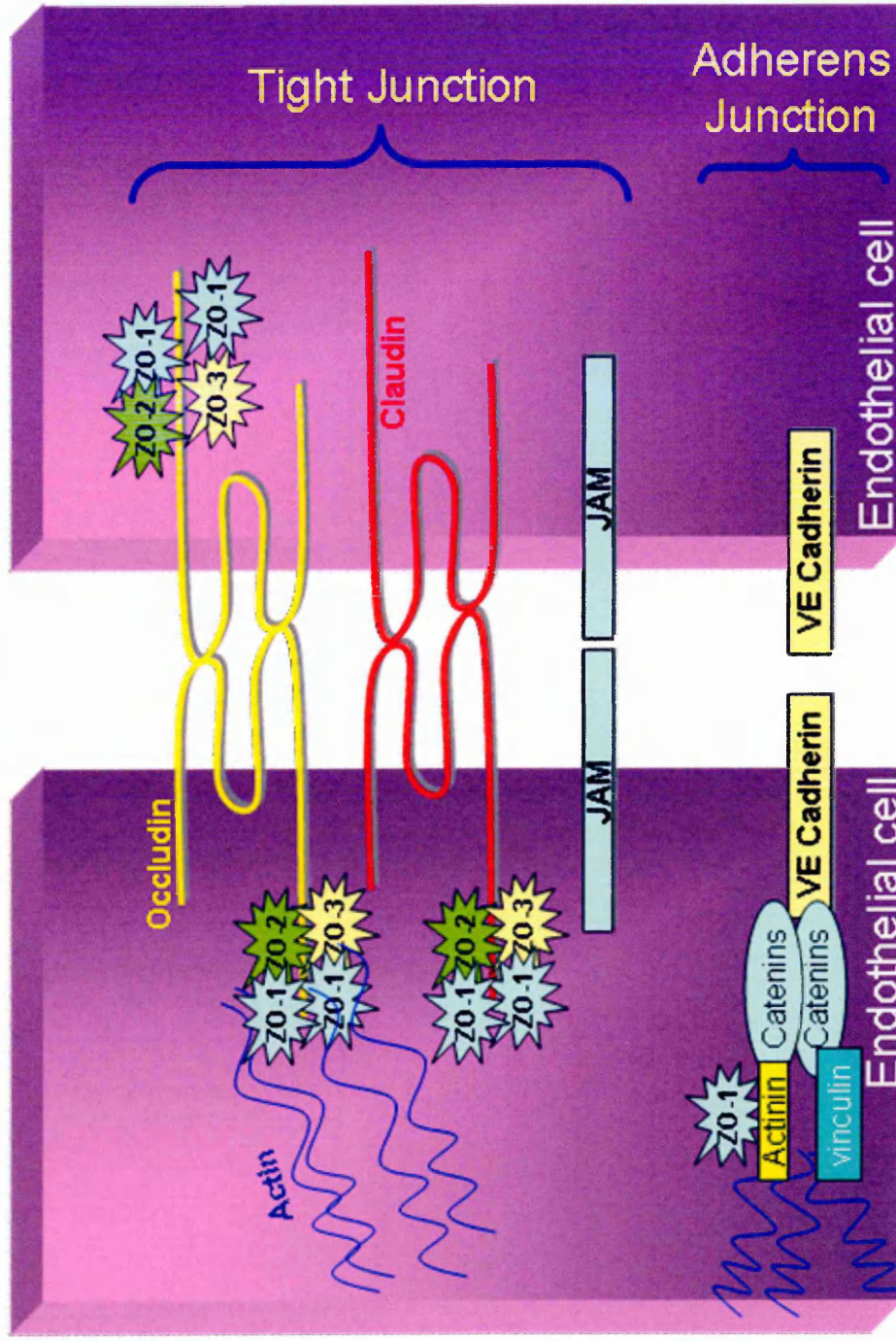
TJ complexes of the BBB are located at the most apical location of the plasma membrane of adjacent endothelial cells (Wittchen *et al.*, 1999). Unlike the case in epithelial junctional complexes however, the adherens component (vascular cadherin) of the endothelial BBB TJ complex is not separate from the TJ components *sensu stricta*, but is intercalated throughout the whole junctional area (Schulze and Firth, 1993). The TJ complex is composed of interactions between transmembrane, cytoplasmic and cytoskeletal proteins (Figure 2.1 adapted from Petty and Lo, 2002).

#### 2.1.1.1 Transmembrane Proteins

Formation of the inter-endothelial TJ involves the integrated function of three types of transmembrane proteins from adjacent cells; occludin, claudin and junctional adhesion molecule (JAM) (Figure 2.1).

Occludin was identified as the first integral transmembrane protein of the TJ (Furuse *et al.*, 1993; Ando-Akatuska *et al.*, 1996). Occludin is a 60-65 kDa phosphoprotein that is composed of four transmembrane domains, three cytoplasmic domains and two extracellular loops. The cytoplasmic domains include a short NH<sub>2</sub>-terminal, a long COOH-terminal and a short intracellular turn (Fanning *et al.*, 1999; Tsukita and Furuse, 1999; Ballabh *et al.*, 2004). The two extracellular loops, which bind with occludin loops on neighbouring cells to form the TJ paracellular barrier (Ballabh *et al.*, 2004), contain a high percentage of tyrosine and glycine residues (~65%) although the significance of this is unclear (Fanning *et al.*, 1999). Occludin is not the only

Figure 2.1 Schematic representation of the molecular components of the TJ at the BBB



The TJ complex is composed of the TJ and the adherens junction. The TJ consists of 3 transmembrane proteins, the zonula occludens cytoplasmic proteins that bind to the transmembrane proteins and the actin cytoskeleton. (Figure adapted from Petty and Lo., 2002)

transmembrane protein of the TJ however and does not appear to be essential for establishing a TJ (Tsukita and Furuse, 1999; Wolburg and Lippoldt, 2002). Thus, transgenic occludin-deficient mice were able to form morphologically normal TJs, which showed no reduction in transendothelial resistance (TER) in comparison to wild-type (Saitou *et al.*, 2000). Other experimental data suggests that mature cells require occludin to regulate and seal rather than to establish the TJ (Wolburg and Lippoldt, 2002).

The second integral transmembrane protein or family of proteins of the TJ is the claudin family (From the Latin *claudere* meaning to close). Claudin-1 and -2 were first described in 1998 and now the family has expanded to consist of at least 24 members following sequence tagged database searches (Furuse *et al* 1998; Morita *et al.*, 1999a; Ballabh *et al.*, 2004). Claudins are 22 kDa phosphoproteins that contain four transmembrane domains with COOH- and NH<sub>2</sub>- cytoplasmic terminals. Despite the topographical similarities, claudins contain no sequence similarity to occludin (Furuse *et al.*, 1998). Claudins form dimers which bind homotypically and heterotypically to claudins from adjacent cells (Huber *et al.*, 2001; Ballabh *et al.*, 2004) to form the primary seal of the TJ. Claudins are differentially expressed throughout the body, depending on the functional requirements of the tissue.

There is contradictory evidence as to which claudins are expressed in the CNS (Morita *et al.*, 1999). The latest evidence suggests that BBB endothelium expresses claudin-5 and claudin-3 and possibly also claudin-12 (Kraus *et al* 2004). Previous reports of the expression of claudin-1 in BBB endothelium may have been due to the cross reaction of a claudin-1 antibody with the claudin-3 molecule (Wolburg *et al.*, 2003; Kraus *et al.*, 2004; Hamm *et al.*, 2004). Outside the vessels but within the CNS parenchyma, claudin-11, also known as oligodendrocyte specific protein (OSP), has been identified as a major component of CNS myelin (Fanning *et al.*, 1999; Ballabh *et al.*, 2004). The importance of claudins as major structural components of the TJ is demonstrated by the finding that claudin-1 and claudin-2 can induce TJs in fibroblast cells initially lacking TJs (Tsukita and Furuse, 1999). The significance of the large number and variety of claudins is hinted at by the fact that TJ strands containing claudin-1 are believed to form tighter junctions

than those containing claudin-2 (Tsukita and Furuse, 1999). Claudins have been shown to be important determinants in TJ regulation of paracellular ionic charge selectivity transcellular conductance (Van Itallie *et al.*, 2003). The direction of charge selectivity conferred by individual claudins may be due to the electrostatic effects of the charged amino acids in their first extracellular loops (Van Itallie *et al.*, 2003).

The third transmembrane protein is the recently identified junction adhesion molecule (JAM) (Martin-Padura *et al.*, 1998) family. JAM family proteins are members of the immunoglobulin superfamily that have one transmembrane domain that binds homotypically to JAM of adjacent cells and also to monocytes to aid transmigration (Fanning *et al.*, 1999; Wolberg and Lippoldt, 2002). JAM-1 is expressed in both endothelial and epithelial cells whereas JAM-2 and -3 are expressed in most vascular endothelial cells (Wolberg and Lippoldt, 2002). These molecules are involved in the organisation of TJs, with JAM-1 responsible for promoting occludin localisation at the TJ (Dejana *et al.*, 2000).

#### *2.1.1.2 Cytoplasmic sub-membranous plaque-associated proteins of the TJ*

The first peripheral TJ protein to be identified was zonula occludens (ZO-1) (Stevenson *et al.*, 1986) which is a 220 kDa peripheral membrane protein from the membrane-associated guanylate kinase (MAGUK) family. To date three MAGUK family members have been associated with TJs, ZO-1, -2, and -3 (Itoh *et al.*, 1999 a&b). The ZO proteins contain three defined core regions that are essential for their interaction with the rest of the TJ structure. They contain three PDZ, one GUK and one SH3 domain (Furuse *et al.*, 1994; Itoh *et al.*, 1999; Wittchen *et al.*, 1999; Wolburg and Lippoldt, 2002). The PDZ domains have been reported to bind ZO proteins to claudin (Itoh *et al.*, 1999b) whereas the GUK domain binds to occludin (Furuse *et al.*, 1994) thus playing a role in organisation of the TJ at the plasma membrane (Ballabh *et al.*, 2004). ZO-1 also forms independent complexes with ZO-2 and ZO-3 via their second PDZ domain however ZO-2 and ZO-3 do not bind together (Wittchen *et al.*, 1999) (Figure 2.1). Following immunoprecipitation experiments, the ZO proteins were also shown to bind to the primary cytoskeletal protein, actin (Blum *et al.*, 1997; Wittchen *et al.*, 1999; Itoh *et al.*,

1999b; Fanning *et al.*, 1999) providing a structural support as well as a possible dynamic linking role between membrane proteins and the cytoskeleton (Fanning *et al.*, 1999; Ballabh *et al.*, 2004).

Other less well characterized components of the TJ include Cingulin a cytoplasmic TJ associated protein that does not have a PDZ domain but forms bonds with the ZO proteins and myosin from the cytoskeleton, suggesting a structural role at the TJ (Petty and Lo, 2002). Another component 7H6 is a 155 kDa phosphoprotein that is found at TJs that are impermeable to ions and macromolecules (Huber *et al.*, 2001, Petty and Lo, 2002).

### 2.1.1.3 *The adherens junction*

The TJ complex includes intercalated adherens junction (AJ) components that are composed of vascular cadherin (v-cadherin) that binds homotypically to extracellular domains of neighbouring v-cadherin. V-cadherin is also connected indirectly to the cytoskeleton through catenin that binds to actin (Ballabh *et al* 2004). AJs also interact with TJs through the binding of catenin to ZO-1 (Petty and Lo, 2002).

### 2.1.2 *Regulation of tight-junctions*

The selectively permeable BBB is rapidly responsive to physiological and pathological stimuli and plays a key role in maintaining the distinctive CNS metabolic and immunoregulatory homeostasis (Huber *et al.*, 2001). As a result, TJ function is strictly regulated, the microenvironment of cerebral capillaries is highly complex with interactions and signals originating from numerous exogenous and endogenous sources (Huber *et al.*, 2001; Wolburg and Lippoldt, 2002). *In vitro* models have been utilised in an attempt to unravel the complexities governing TJ structure and function. Recent *in vitro* studies have investigated the role of astrocytes in regulating TJs (Prat *et al.*, 2001). Evidence has been provided which suggests that humoral factors released from astrocytes, as assessed by the effect of astrocyte conditioned media on BBB characteristics of animal and human brain endothelial cells in culture, are sufficient to establish a functional barrier (Wolburg *et al.*, 1994;

Prat *et al.*, 2001). It was previously reported however that cellular contact between cerebral endothelia and astrocytes is required for an efficient barrier (Tao-Cheng *et al.*, 1987). The glial cell line-derived neurotrophic factor (GDNF) appears to be one of several factors necessary for the induction of the BBB (Wolburg and Lippoldt, 2002).

Although occludin does not appear to be necessary for the formation of the TJ (Tsukita and Furuse, 1999), it does have important regulatory properties (Petty and Lo, 2002). Following TJ disruption, phosphorylation of the TJ associated proteins occludin and ZO-1 correlates with the recovery of the permeability barrier (Petty and Lo, 2002).

Cerebral endothelial cells are sensitive to cAMP levels, with increased levels associated with increased transendothelial resistance (Wolburg and Lippoldt, 2002; Petty and Lo, 2002). *In vitro* studies have suggested that G-proteins play a role in maintaining the barrier integrity (Wolburg and Lippoldt, 2002). Activation of heterotrimeric G-proteins leads to activation of secondary messengers, cAMP and Ca<sup>2+</sup> (Wolburg and Lippoldt, 2002). Precipitation assays have been used to demonstrate the co-localisation of G $\alpha$  subunits with ZO-1 (Petty and Lo, 2002; Wolburg and Lippoldt, 2002), and with the TJ region in rat cerebral endothelial cells *in vivo* (Wolburg and Lippoldt, 2002).

The primary cytoskeletal protein actin, which binds to ZO, occludin and claudin proteins, plays a major role in the regulation of TJ function. Circumferential contraction of the perijunctional actin ring increases paracellular permeability of the TJ (Fanning *et al.*, 1999; Wittchen *et al.*, 1999). Actin disrupting substances, such as cytochalasin D as well as cytokines disrupts the TJ structure and function of endothelial cells *in vitro* (Huber *et al.*, 2001).

### 2.1.3 Aim of study

In view of the MRI and pathological findings on the BBB in MS, this study set out to assess TJ integrity histopathologically by establishing a reproducible protocol for the investigation of the expression of the TJ associated proteins, ZO-1 and occludin, at the microscopic level. Immunofluorescent techniques were applied and a confocal scanning laser

microscope was used to enable the visualisation of the entire TJ by scanning through the vessel. Formalin fixed paraffin embedded (FFPE) and snap-frozen control tissue were used to establish which tissue would allow optimal immunostaining of the endothelial TJs.

Snap-frozen (SF) autopsy MS tissue was used and classified according to macrophage/microglial activation and evidence of recent myelin breakdown, as described previously (van der Valk and de Groot, 2000). A semi-quantitative analysis of ZO-1 expression was applied to establish if any differences in TJ integrity exists between study groups. TJ integrity was also investigated in relation to pathological features of MS, namely leukocyte infiltration, cellular activation and BBB leakage. The major aims addressed were:

- (i) To establish which autopsy material would allow optimal immunostaining of TJs for the study
- (ii) To determine whether there is TJ disruption in MS which is detectable microscopically at the level of its constituent proteins
- (iii) To determine whether such disruption predominates at a particular stage or stages of lesion development
- (iv) To determine whether TJ disruption correlates with BBB leakage
- (v) To determine whether TJ disruption, like BBB leakage is persistent

The major objective was to establish whether alterations in TJs are involved in the pathogenesis of the MS lesion and if so to develop an understanding of the destructive and reparative phases of the process.

## *2.2 Materials and Methods*

All tissues were obtained from the files of the Belfast Brain Bank, Northern Ireland Regional Neuropathology Service, Royal Group of Hospitals Trust, Belfast, Northern Ireland.

A retrospective case selection was carried out on the basis of a confirmed clinical and neuropathological diagnosis of MS and availability of suitable snap-frozen tissue samples containing active or chronic lesions or normal appearing white matter (NAWM). NAWM blocks were selected at the time of initial block preparation from white matter areas which were at least 1cm from macroscopically identified plaque tissue. Tissue was received fresh from autopsy (<24 hours death-autopsy intervals for 13 out of 14 MS cases see Table 2.1). Two of the MS cases had a neuropathologically confirmed clinical diagnosis of acute MS and the other 12 cases had a confirmed diagnosis of secondary progressive MS. Individual tissue blocks were orientated on a cork block, SF in isopentane (cooled in liquid nitrogen) and immediately stored in air-tight containers at -70°C until required. These MS cases included 6 females, mean age 49.5 years (range 22-69) and 8 males with a mean age of 48.75 years (range 18-66). The tissue used had a mean time from death to freezing of 14.7 hours (range 1.5-29 hours). 32 SF control white matter blocks were also available and were obtained from 2 normal (road traffic accident) and 6 other neurological disease (OND) controls (1 head injury, 3 sub-acute sclerosing panencephalitis (SSPE), 1 metastatic carcinoma, 1 transverse myelitis). Informed consent for research for all brain tissues and local ethical committee approval for the conduct of this study was obtained. All tissue blocks were anonymised prior to use.

### *2.2.1 Selection of tissue for TJ study*

Samples from formalin fixed paraffin embedded (FFPE) and snap-frozen control tissue were prepared to determine optimal staining protocols for the immunocytochemical detection of occludin and ZO-1 at the cerebral vascular inter-endothelial tight-junctions.

Table 2.1 Summary of individual details of all the cases used in the TJ study

Case ID	Age	Sex (M/F)	Clinical Diagnosis	Disease Duration (yrs)	DAI (hrs)	No. of Study Blocks			
						Active	NAWM	Chronic Inactive	Control
MS1	24	M	Acute MS	13 months	3.5	2			
MS2	22	F	Acute MS	5 months	10	3	5		
MS3	40	F	SPMS	7	11	1	1	3	
MS4	34	M	SPMS	10	1.5	4		3	
MS5	58	M	SPMS	20	24	2		2	
MS6	33	M	SPMS	9	7.5	7			
MS7	53	F	SPMS	25	19.5	13			
MS8	54	M	SPMS	7	12			3	
MS9	62	M	SPMS	12	23		4	1	
MS10	60	F	SPMS	25	29		1		
MS11	66	M	SPMS	26	4.5		1		
MS12	69	F	SPMS	46	18		4		
MS13	53	F	SPMS	n/a	24			2	
MS14	59	M	SPMS	25	18			4	
ONC1	18	M	Head Injury		10				4
ONC2	74	F	Metastatic Carcinoma	n/a	10				8
ONC3	45	M	Transverse Myelitis	2	8				2
ONC4	20	M	SSPE	n/a	14				3
ONC5	21	M	SSPE	3	10				1
ONC6	16	M	SSPE	7	8				2
NC1	29	F	RTA		4				11
NC2	27	F	RTA		14				3

DAI = Death-autopsy interval  
 NC = Normal control  
 SPMS = Secondary progressive MS  
 n/a = not available  
 SSPE = Subacute sclerosing panencephalitis  
 RTA = Road traffic accident  
 ONC = Other neurological control

### 2.2.1.1 Formalin-fixed paraffin-embedded tissue

6µm microtome paraffin sections of normal brain were dewaxed through two 5 minute changes of xylene then rehydrated through three changes of 64OP (degrees over proof) and placed under running water. Sections were then pre-treated with one of the following methods to establish optimal levels of antigen retrieval.

#### 2.2.1.1.1 Microwave antigen retrieval

Sections were immersed in citrate microwave buffer (see appendix) and microwaved for 20 minutes at maximum power (McQuaid *et al.*, 1995). Sections were allowed to cool in running water then incubated in rabbit polyclonal antibodies to either occludin (1:200, Zymed) or ZO-1 (1:400, Zymed) overnight at 4°C. Following two five minute washes in Tris buffered saline (TBS, see appendix) antibodies were detected by incubating sections in Alexa 488 conjugated goat anti-rabbit IgG (1:500, Molecular Probes) for 1 hour at 37°C. Cell nuclei were counterstained by incubating sections in propidium iodide (Sigma, 2µg/ml) for 30 seconds. Sections were mounted with coverslips in the non-fading mountant citifluor (see appendix). All dilutions were carried out in TBS.

#### 2.2.1.1.2 Proteinase K

Following dewaxing and rehydration, sections were incubated in proteinase-K (Sigma, 0.5mg/ml in phosphate buffered saline (PBS)) for 5 or 10 minutes at RT. Sections were then washed in TBS and primary antibodies applied and detected as described above (2.2.1.1.1).

#### 2.2.1.2 Snap frozen tissue

12µm cryostat sections were either fixed in methanol, 10% formalin, 4% paraformaldehyde (see appendix), 74OP or ice-cold acetone for 10 minutes. Following fixation all sections were washed in PBS (see appendix) with the exception of ice-cold acetone fixed sections that were allowed to air dry for at least 15 minutes prior to the next step. Sections were then incubated in antibodies to occludin (1:200) or ZO-1 (1:400) overnight at 4°C, washed in PBS then incubated in Alexa 488 conjugated goat anti-rabbit IgG

for 1 hour at 37°C. Sections were counter stained and mounted as above (2.2.1.1.1). All dilutions were carried out in PBS.

## *2.2.2 Tissue characterisation*

All MS and control snap-frozen blocks underwent preliminary screening to determine the pathological state of individual blocks. Cryostat sections (12µm) were cut onto glass slides (Superfrost) and routinely stained with haematoxylin and eosin (H&E) and oil red O (ORO, see appendix) to identify and grade lesion activity. ORO positive blocks were classified as active plaque. Plaque-containing blocks that were ORO-negative were classified as chronic inactive, while blocks derived from macroscopically normal white matter that was devoid of ORO and plaques were classified as NAWM.

### *2.2.2.1 Single label immunofluorescence staining*

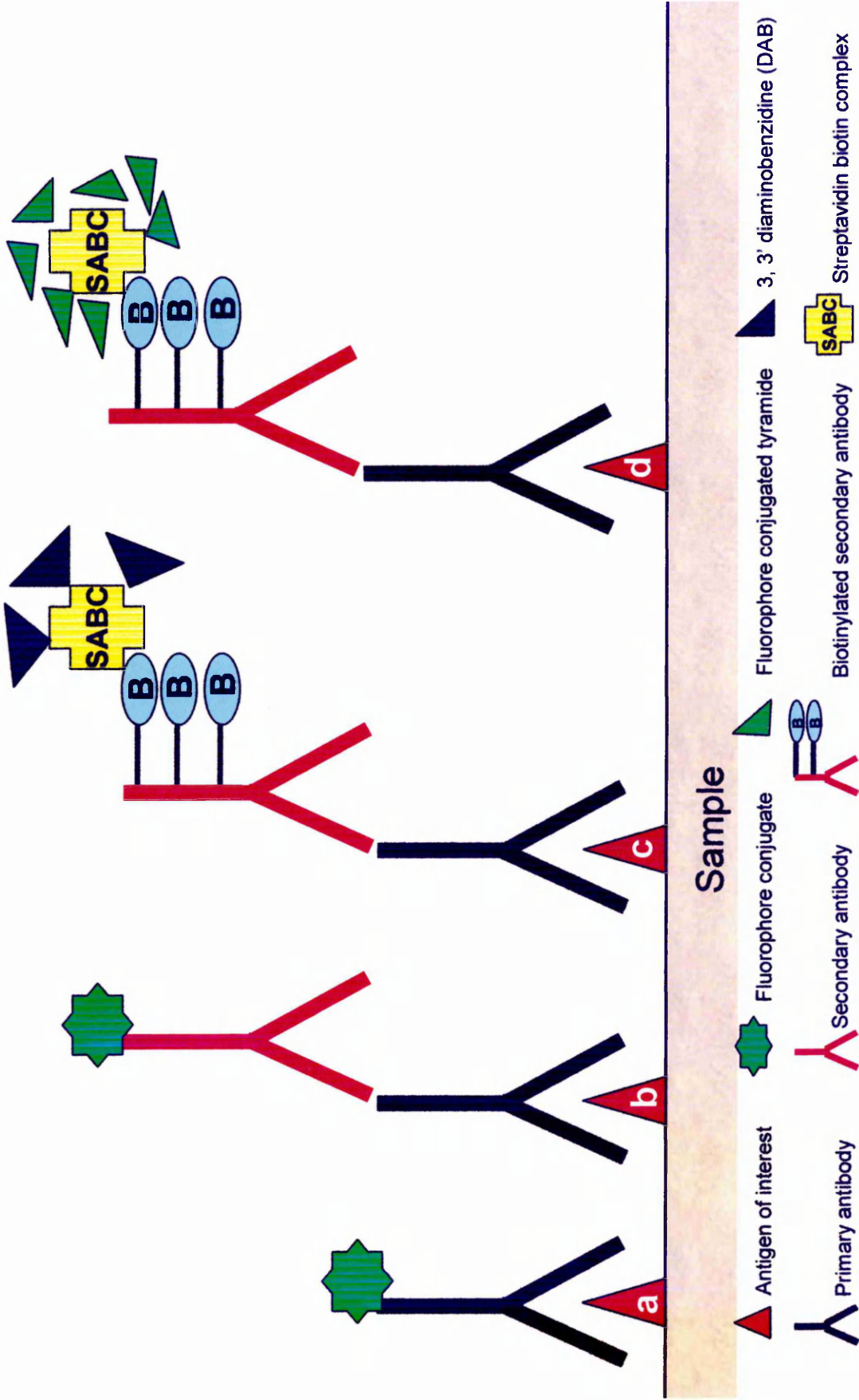
#### *Principle of method*

Immunohistochemistry (IHC) and immunofluorescence combines anatomical, immunological and biochemical principles to identify specific tissue components by specific antigen/antibody reactions. The concept of IHC has been evident since the 1930s, however the first report was not until 1942 when Albert Coons used fluorescent labelled antibodies to detect antigens in tissue sections (Coons, 1942). The principle of IHC is based on the identification of the antigen of interest by binding an antibody specific to that antigen, then visualising the antigen/antibody complex by fluorescent dyes, enzymes or radioactive elements linked to a secondary antibody directed against the primary antibody (Figure 2.2). IHC or immunofluorescence (fluorescent label) can be applied to a wide variety of tissues or cell cultures.

#### *Method*

Cryostat sections (12µm) were cut onto aminopropyltriethoxysilane (APES) coated slides (Starfrost) and fixed in ice-cold acetone for 10 minutes

Figure 2.2 Schematic representation of different antibody detection methods



at room temperature (RT). Indirect immunofluorescence was carried out to examine cerebral vascular endothelium, basement membrane, inter-endothelial tight junction integrity and the extent of macrophage/microglial activation, using the following antibodies and dilutions (in PBS): mouse monoclonal antibodies to laminin (1:1000, Sigma) and HLA-DR (1:100, Novocastra,) and rabbit polyclonal antibodies to occludin (1:200, Zymed) and ZO-1 (1:400, Zymed). A biotinylated Ulex europaeus agglutinin (UEA) (1:500, Vector laboratories) was used as a marker for vascular endothelial cells. Assessment of serum protein leakage was visualised using a FITC conjugated antibody to fibrinogen (1:100, Dako). Primary antibodies, biotinylated UEA and fibrinogen-FITC were incubated on sections overnight at 4°C and detected by incubating in Alexa 488-conjugated rabbit anti-mouse or goat anti-rabbit IgGs (1:500, Molecular Probes) or Z-Avidin FITC (1:50, Zymed; for UEA) for 1 hour at 37°C. Cell nuclei were counter-stained with propidium iodide for 30 seconds then washed in PBS and mounted with coverslips using citifluor.

#### *2.2.2.2 Dual Label Immunofluorescence staining*

In selected samples, sequential dual labelling immunofluorescence was used to illustrate the relationship between TJ abnormalities (ZO-1 or occludin) and HLA-DR activation (HLA-DR), lymphocytic infiltration (leucocyte common antigen (LCA, 1:50, Dako), blood brain barrier disruption (fibrinogen-FITC) and basement membrane integrity (laminin). Acetone fixed sections were incubated in the polyclonal primary antibody overnight at 4°C. After washing in PBS, the sections were incubated in Alexa 568 conjugated goat anti-rabbit IgG (1:500, Molecular Probes) for one hour at 37°C, washed in PBS and then incubated in the monoclonal primary antibody for one hour at 37°C. Detection of the monoclonal antibodies was carried out by incubating in Alexa 488 conjugated rabbit anti-mouse IgG, excluding fibrinogen-FITC as it has a direct fluorescent conjugate, for 1 hour at 37°C. Sections were then washed in PBS and mounted with coverslips in citifluor.

For all single and dual labelling negative control sections, the primary or secondary antibody (dual) was omitted from the protocol.

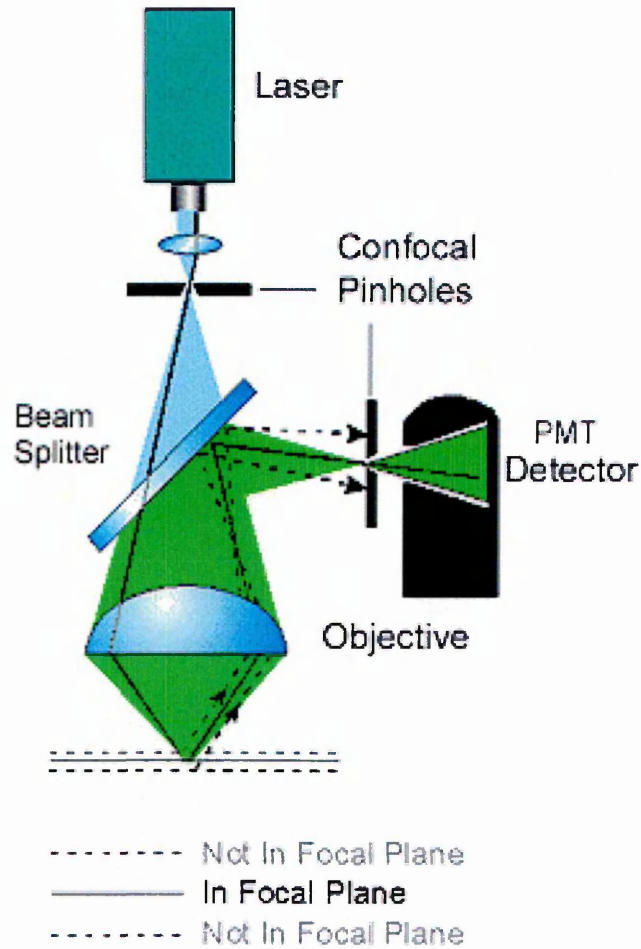
## 2.2.3 Imaging

### 2.2.3.1 Confocal Scanning Laser Microscopy

#### *Principles of method*

The confocal laser scanning microscope (CSLM) is a microscope that scans, uses a laser and produces a confocal image (Figure 2.3). The CSLM is an advancement on the conventional epi-fluorescent microscope that is now commonly being employed in biological research to detect specimens labelled with fluorophores (Amos and White, 2003). The CSLM uses a laser as a light source which unlike the light source of the epi-fluorescent microscope (mixed wavelengths) provides a discrete wavelength band and has a very high intensity. The main difference between the two microscopes is, in the confocal microscope, the presence of small apertures called pinholes which regulate the detection of emitted light. In focus, light converges to a point on the imaging plane whereas out of focus light converges either above or below the imaging plane. A pinhole at the imaging plane prevents the out of focus light being detected allowing an image composed of only in focus light resulting in greater resolution (Figure 2.3). CSLM cannot “see” out of focus objects (Murray, 1992). A specimen viewed by CSLM is irradiated in a point to point fashion therefore to obtain information about an entire specimen the laser must be guided across the specimen or the specimen moved relative to the laser beam along the x-y axis, this process is called scanning. CSLM also allows the processing of information taken from optical slices along the z-axis (optical sectioning), which is beneficial in biological research where a lot of the specimens are thick tissue samples. The CSLM obtains an in focus optical slice from different focal planes through predefined limits of the section forming a z-stack. Z-stacks can be reassembled to create three-dimensional constructs which provides information about the spatial structure and localisation of the antigen of interest within the specimen. Another advantage of the CSLM is the ability to scan the image with different laser wavelengths to detect several different wavelengths of emitted light. This enables the co-localisation of two or three different labels simultaneously.

Figure 2.3 Schematic representation of the detection principles in CSLM



A laser source excites the fluorophore attached to the antigen of interest, resulting in an emitted light. Using a series of pinholes ensures that only emitted light from the focal plane are detected by the photomultiplier tubes (PMT). Removal of the out-of-focus light by the pinholes produces an image of greater resolution than conventional microscopes.

Emitted signals from the specimen are detected by photon multiplier tubes (PMT) which converts the photon into an electron which forms an analogue current which is then digitized by an analogue-digital converter and sent to the digital image processor of the associated CSLM computer. The computer software then allows a variety of processing techniques including co-localisation studies.

To summarise the CSLM system includes a point light source for illumination, a point light focus within the specimen and a pinhole at the image detecting plane. When these three points are optically conjugated together and aligned accurately to each other in the light path of image formation, this is confocal.

Although the CSLM is designed to produce high quality in focus high resolution images there are limitations in obtaining optimal images. The smaller the pinhole the greater the resolution obtained however the smaller pinhole also results in diminished illumination intensity resulting in diminished emitted signals. There is also a limit to how long fluorophores can be excited by the laser. Excessive excitation of the fluorophore by the laser can result in saturation of emission where illumination does not result in more emission which is called photo-bleaching. Normal CSLM scans are carried out to obtain images at 512x512 (pixels scanned per second) and a quick scan speed for higher resolution images, 1024x1024, or higher require a slower scan speed which can result in photo-bleaching of the fluorophore.

### *Method*

Immunofluorescent images were acquired using a Leica TCS/NT confocal scanning laser microscope equipped with a krypton/argon laser as the source for the ion beam. Selection of the FITC/TRITC filter selects a predefined set of parameters for data acquisition. Alexa 488 and FITC labelled antibodies were visualised by excitation at 488nm with a 506-538 band-pass emission filter. Alexa 568 labelled antibodies were imaged by excitation at 568nm with a 564-594 band-pass emission filter. Acquiring 16 optical sections in the Z-plane and running the series-scanning mode from the deepest focus point to the highest focus point, allowed a projected image and data set to be generated from which composite projected images were

saved as tif files in Adobe 5.0 at 300 dpi (dots-per-inch) without further digital manipulation.

### *2.2.3.2 Data Collection*

Only recognizable vessels whose profile was contained within the field of view of the x40 objective lens were imaged. The images of 30-50 cerebral blood vessels were collected from each block for an analysis of TJ integrity, from all MS and control cases. In performing the dual labelled ZO-1 and fibrinogen study, data sets for approximately 20 cerebral blood vessels from each selected block were obtained.

### *2.2.3.3 Data Analysis*

Initial examination of TJ expression (ZO-1 or occludin), resulted in a crude analysis of the TJ associated proteins either being described as normal (continuous, linear expression), as observed from the staining in normal control brains and previous literature reports, or abnormal (definitive evidence of TJ disruption). Stored images used to assess TJ integrity were redisplayed and the diameter of each vessel was measured on screen, using the quantification software in TCS-NT. The incidence of TJ abnormality was plotted for 'all vessels' and individually for vessels in each of the four size classes (diameter < 10 $\mu$ m; >10-30 $\mu$ m; >30-50 $\mu$ m; and >50 $\mu$ m).

When assessing the relationship between TJ abnormalities and the degree of serum protein leakage, a three point grading system was applied for each variable (Table 2.2). TJ abnormality was graded from 0-2 based on an estimated percentage. A grade of 0 was assigned to normal TJ expression, grade 1 if up to 25% of the vessel appeared abnormal, grade 2 if >25% of the vessel appeared abnormal. Similarly, fibrinogen leakage was graded as 0 when there was no evidence of leakage, 1 for moderate leakage and 2 when there was severe, widespread leakage. All assessment of grading was carried out blinded by at least 2 independent observers. For all analyses where the observers result disagreed, a consensus was reached following joint re-examination.

Table 2.2 TJ and fibrinogen scoring grades

<i>TJ score</i>	<i>Extent of abnormality</i>
<b>0</b>	No disruption
<b>1</b>	Up to 25% of the vessel displays TJ abnormality
<b>2</b>	≥ 26 % of the vessel displays TJ abnormality
<i>Fibrinogen score</i>	
<b>0</b>	No leakage
<b>1</b>	Moderate leakage
<b>2</b>	Severe leakage

#### 2.2.3.4 Statistical analysis

The incidence of TJ abnormality in the five tissue categories examined was compared using the non-parametric Kruskal-Wallis test for group differences. A *p-value* below 0.05 was considered as significant. Where significance was observed, Dunn's test was carried out to determine the significance and direction of significance, using the recommended experimental error rate,  $\alpha = 0.15$  (Daniel, 1978). All analyses were performed on the SPSS statistical package (version 11.0, SPSS Inc, Chicago, IL, USA).

#### 2.2.3.5 Digital Photography

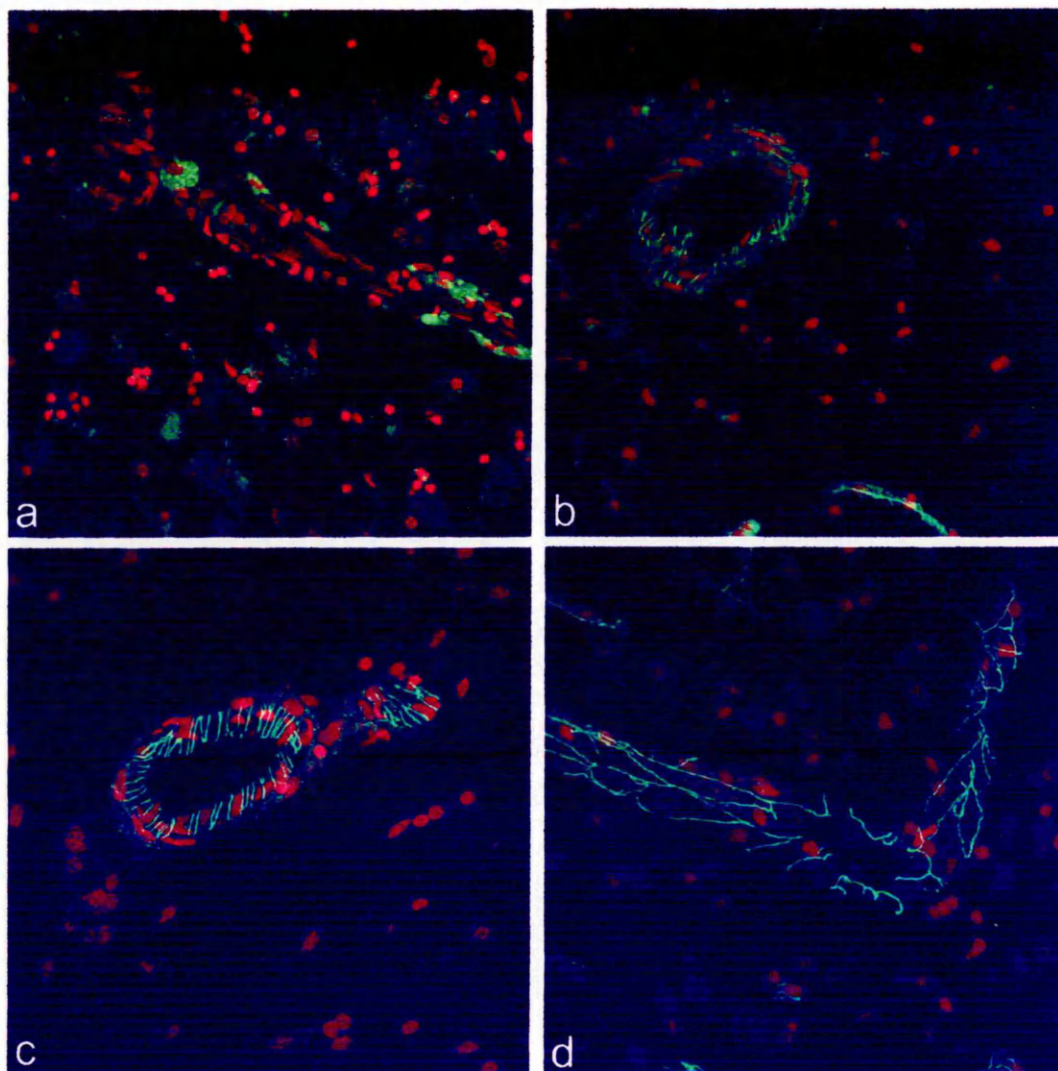
All routine histological images were acquired using a Leitz Dialux 20 light microscope equipped with a Nikon CoolPix 950 digital camera. Images were transferred to Adobe 5.0 and saved as JPEGs at 300dpi.

### 2.3 Results

#### 2.3.1 Optimisation of immunostaining protocols for TJ study

Consideration of which type of tissue samples should be used and optimal fixation and immunostaining protocols were assessed in preliminary experiments. Sections of formalin fixed paraffin embedded (FFPE) and snap frozen tissues from a normal control case were used for ZO-1 and occludin immunostaining optimisation. Sections of FFPE tissue underwent pre-treatments (microwave retrieval, Proteinase K), but yielded very low levels, if any, of ZO-1 staining (Figure 2.4). Comparison of fixatives on snap frozen tissue using methanol, 10% formalin, 4% paraformaldehyde, 99% IMS or ice-cold acetone were undertaken. All fixatives allowed ZO-1 expression to be detected although in the methanol, 99% IMS and formalin fixed sections, ZO-1 expression was fragmented and weak in comparison to the normal intense, linear, continuous expression of ZO-1 in the acetone and paraformaldehyde fixed tissue (Figure 2.4). Ice-cold acetone fixation permitted effective dual labelling experiments with ZO-1 and occludin so was therefore used for all TJ studies on snap frozen tissue.

Figure 2.4 ZO-1 detection using different tissues and fixatives



Indirect immunofluorescence detection of ZO-1(Green) in FFPE (a) and SF tissue (b-d). (a) Proteinase K pre-treated FFPE tissue devoid of ZO-1 expression. (b) 99% IMS fixed SF tissue with fragmented, weak ZO-1 expression. (c) 4% paraformaldehyde fixed SF tissue and (d) ice-cold acetone fixed SF tissue expressing linear, intense and continuous ZO-1 expression. Cell nuclei in all sections were counterstained with propidium iodide. Mag x400.

### 2.3.2 Characterisation of SF tissue

SF blocks from 21 MS autopsy cases from the Belfast Brain Bank, Neuropathology Department, Royal Group of Hospitals Trust, Belfast, were screened by H&E, ORO and HLA-DR to characterise the pathological state of individual blocks and the viability of blocks for use in this study:

- ORO-positive blocks were characterised as containing active plaque,
- ORO negative blocks with plaques present were characterised as chronic inactive plaque,
- ORO-negative blocks without plaque and greater than 1cm from macroscopically visible plaque were characterised as NAWM.

From the initial screening process, 32 blocks from 8 MS cases contained active plaque, 18 blocks from 7 cases were classified as chronic inactive plaque and 16 blocks from 6 cases were classified as NAWM (Table 2.1). 32 blocks from 8 control cases (2 normal and 6 OND) were also obtained from the Belfast Brain Bank.

To assess the extent of recent myelin breakdown and cellular activation within the active blocks a 3 point grading system was applied to the ORO and HLA-DR staining (Figure 2.5, Table 2.3). Of the 32 active blocks, 12 displayed scattered isolated ORO-positive cells (Grade 1), while 12 had in addition, one or more foci or clusters of ORO-positive cells (Grade 2). In 8 blocks however, ORO-positive cells were abundant throughout the entire section (Grade 3) (Table 2.3).

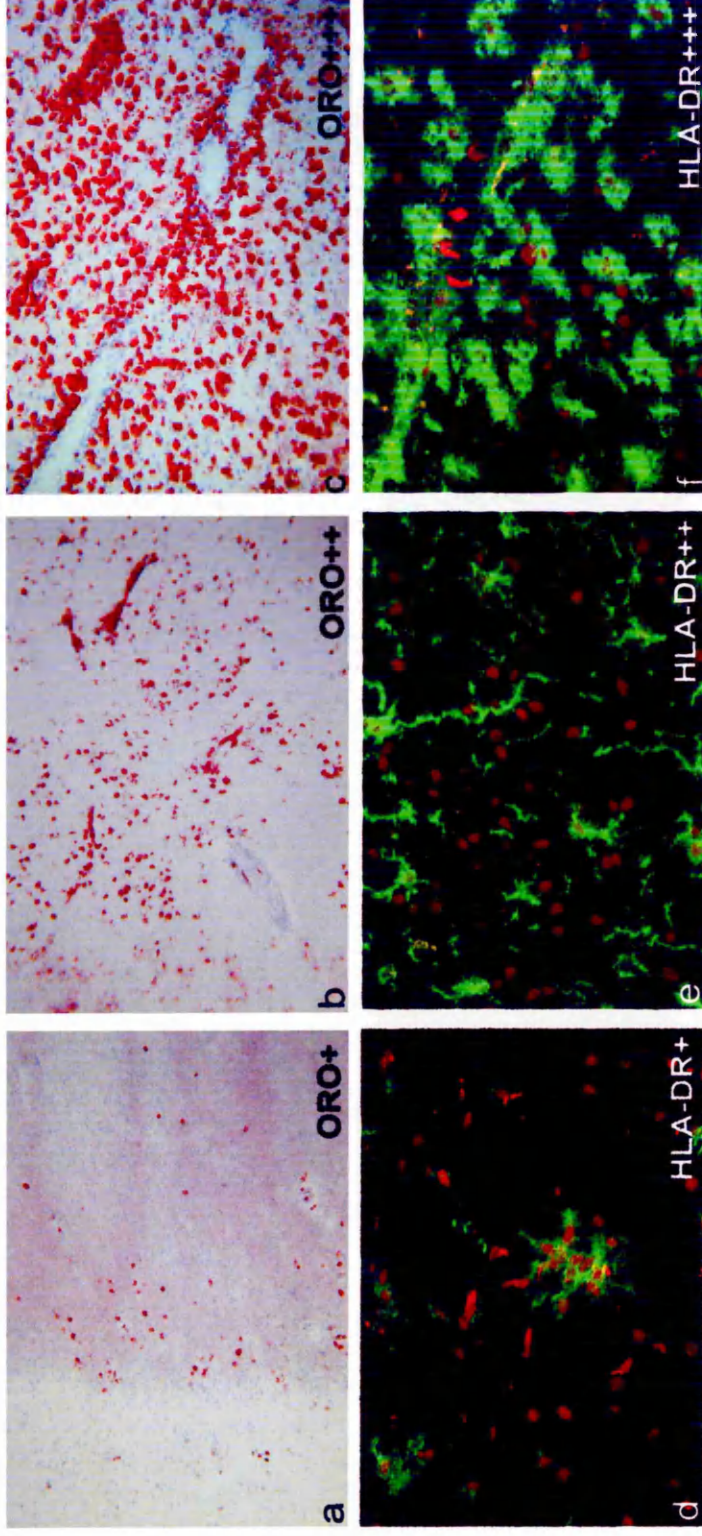
All of the 18 chronic inactive blocks, 5 of the active and 5 blocks from the NAWM displayed anti-HLA-DR staining of scattered, isolated HLA-DR<sup>+</sup> microglia (Grade 1). 15 of the active and 7 of the NAWM blocks displayed HLA-DR immunostaining that was diffuse and widespread (Grade 2), which involved either parenchymal process bearing cells or cells in the distribution of small perivascular infiltrates. An abundance of large HLA-DR positive cells corresponding to foamy macrophages, observed on H&E staining, were detected in both parenchymal and perivascular distributions in 12 of the active and 4 of the NAWM blocks (Grade 3) (Table 2.3).

Table 2.3 Description and distribution of scoring for cellular activation within the MS tissue samples studied.

<i>Stain</i>	<i>Grade</i>	<i>Description</i>	<i>Active</i>	<i>Chronic Inactive</i>	<i>NAWM</i>
<b>ORO</b>	1	Sparse +ve cells	12	0	0
	2	Diffuse small foci +ve cells	12	0	0
	3	Abundance of +ve cells throughout	8	0	0
<b>HLA-DR</b>	1	Sparse single microglia +ve	3*	18	5
	2	Foci of +ve microglia and foamy macrophages	15	0	7
	3	Abundance of +ve cells throughout	12	0	4

\* 2 active blocks displayed no HLA-DR immunoreactivity

Figure 2.5 Grading of MS lesion activity



Grades of lesion activity as indicated by ORO (a-c) and anti-HLA-DR antibody (Green) (d-f). (a) Grade 1 ORO; sparsely distributed single positive cells. (b) Grade 2 ORO; small foci of positive cells throughout the parenchyma. (c) Grade 3 ORO; an abundance of positive cells both perivascular and parenchymal. (d) Grade 1 HLA-DR; single positive microglial cell. (e) Grade 2 HLA-DR; increased numbers and expression of HLA-DR+ macrophage and microglia population. (f) Grade 3 HLA-DR; abundance of foamy macrophages. Cell nuclei are counter stained with Harris's haematoxylin (a-c) and propidium iodide (d-f). Magnification x200 (a-c) and x400 (d-f).

### 2.3.3 Indirect Immunofluorescence

All of the selected MS and control blocks used in this study were stained by indirect immunofluorescence for endothelial (UEA) basement membrane (Laminin) and TJ associated proteins (ZO-1, Occludin). Consistent uniform staining for the endothelial marker and the basement membrane protein laminin indicated that blood vessel integrity remained intact throughout all categories of MS and control tissues.

#### 2.3.3.1 Tight junction expression in normal and OND controls

Immunofluorescent staining of normal and OND control CNS tissues with either antibodies to occludin or ZO-1 resulted in a continuous, linear staining pattern of strong intensity, in a very high percentage of blood vessels (95.54% and 90.52% respectively). In the transverse view, TJ staining revealed short, radial or near-radial, continuous fluorescent band (Figure 2.6a). Within longitudinally sectioned blood vessels the TJ protein staining was predominantly axial and linear with occasional anastomoses/bifurcations (Figure 2.6e). There was no consistent numerical or spatial relationship between the numbers of fluorescent TJ bands seen and the number or disposition of nuclei as revealed by the propidium iodide counterstain.

#### 2.3.3.2 Tight Junction expression in MS

In comparison to the continuous, intense linear expression and regular deposition of ZO-1 and occludin observed in normal control brain, abnormalities in ZO-1 and occludin expression were observed in MS brains. TJ abnormality was heterogeneous, observed as three types (Figure 2.6):

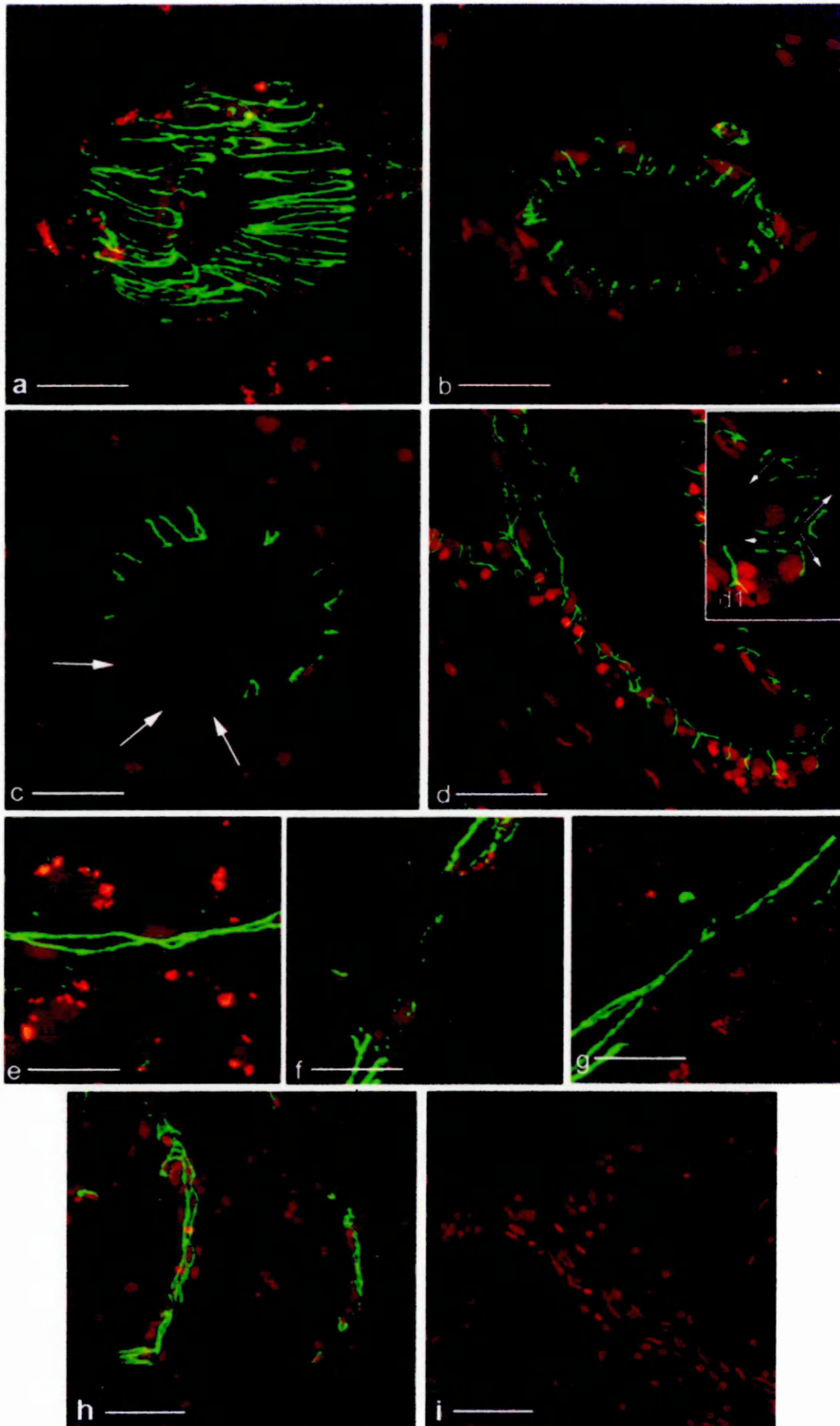
- interruption or beading
- absence
- separation or opening

The abnormality was focal, never affecting all junctions within a single transected vessel. As no differences in the expression levels or distribution of ZO-1 and occludin were observed in control or MS tissues the former was therefore used in the quantitative studies on the basis of 'sharper'

1. DN-nya berinteraksi dengan protein yang mengikat DNA untuk mengontrol ekspresi gen.  
2. DN-nya berinteraksi dengan protein yang mengikat DNA untuk mengontrol ekspresi gen.  
3. DN-nya berinteraksi dengan protein yang mengikat DNA untuk mengontrol ekspresi gen.  
4. DN-nya berinteraksi dengan protein yang mengikat DNA untuk mengontrol ekspresi gen.  
5. DN-nya berinteraksi dengan protein yang mengikat DNA untuk mengontrol ekspresi gen.  
6. DN-nya berinteraksi dengan protein yang mengikat DNA untuk mengontrol ekspresi gen.  
7. DN-nya berinteraksi dengan protein yang mengikat DNA untuk mengontrol ekspresi gen.  
8. DN-nya berinteraksi dengan protein yang mengikat DNA untuk mengontrol ekspresi gen.  
9. DN-nya berinteraksi dengan protein yang mengikat DNA untuk mengontrol ekspresi gen.  
10. DN-nya berinteraksi dengan protein yang mengikat DNA untuk mengontrol ekspresi gen.

Confocal microscopic images from snap-frozen, cryostat sections stained with ZO-1 (Green) / propidium iodide. (a) Continuous, linear and intense appearance of the interendothelial TJ protein ZO-1 as viewed in a transverse section of a cerebral blood vessel from normal control brain. (b-d) Variations in abnormal appearing TJ protein expression in transverse sections of cerebral blood vessels in MS tissue sections, (b) beaded and discontinuous (c) disrupted and absent. On rare occasions TJ proteins were observed as displaying an open junction. Inset d1 displays the apparent gross separation of two neighbouring TJs in a BV from an active plaque. (e) Normal expression of TJ in longitudinally sectioned blood vessel in MS tissue. Beaded and discontinuous (f) and disrupted and absent (g) abnormal expression of TJ in longitudinally sectioned blood vessels in MS tissue. (h) Comparative staining for occludin and a representative of a negative control (i) following omission of the primary antibody. Scale bars = 25 $\mu$ m (a, b, c, e, f, g), 50 $\mu$ m (d, h, i).

Figure 2.6 Normal and abnormal TJ protein expression



immunofluorescence signal. Both ZO-1 and occludin abnormalities were observed in the presence of intact endothelium and basement membrane as detected by dual immunofluorescence for ZO-1 and UEA/laminin (Figure 2.7).

#### 2.3.3.3 *Extent of abnormal ZO-1 expression in MS*

30-50 blood vessels from each control and MS block (dependent on block size) were assessed for TJ abnormality. 3.9% and 8% of the normal and OND (285 and 411 blood vessels respectively) displayed abnormalities in ZO-1 expression. Of the 32 blocks containing active plaques 42.5% of the 622 blood vessels examined displayed definitive ZO-1 abnormalities. 22.76% of the 672 blood vessels examined from the chronic inactive MS blocks contained abnormal expression of ZO-1, whilst 13.09% of the 904 blood vessels from MS NAWM, contained abnormal ZO-1 expression (Figure 2.8a). Statistical analysis of the incidence of TJ abnormality in the five tissue categories was very highly significant ( $p < 0.0005$ ) using Kruskal-Wallis test, indicating that there were differences in the group of means (Figure 2.8a). The subsequent application of Dunn's test ( $\alpha = 0.15$ ) revealed that the incidence of TJ abnormality in the active plaques (42.5%) was significantly higher than in normal control (4.46%) OND controls (9.48%), or NAWM (13.09%) and that TJ abnormality in the inactive plaques (22.76%) was significantly greater than in the normal controls. The differences in TJ abnormality incidence between normal controls and either OND or NAWM did not reach statistical significance.

#### 2.3.3.4 *TJ abnormalities and vessel size*

Using the quantitative software of the Leica CSLM TJ abnormality was assessed against blood vessel diameter. A spectrum of blood vessel sizes was recorded, with the following groups established:

Blood vessels with a diameter of:

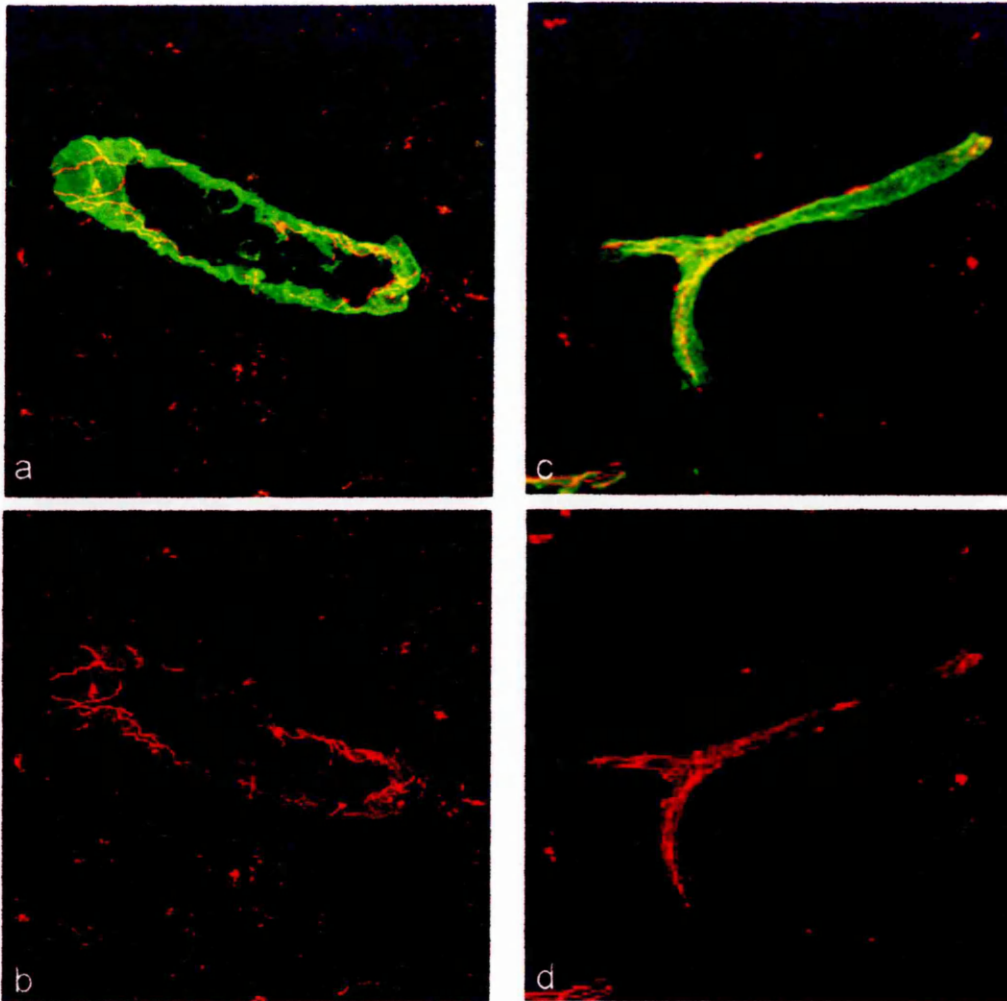
$\leq 10\mu\text{m}$  were capillaries

11-30 $\mu\text{m}$  small-intermediate vessels

31-50 $\mu\text{m}$  large-intermediate vessels

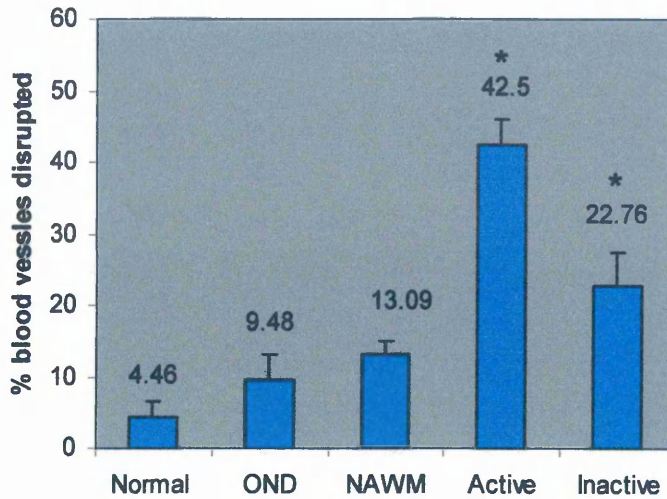
$\geq 51\mu\text{m}$  were classed as large vessels

Figure 2.7 Assessing blood vessel integrity with TJ proteins



CSLM dual immunofluorescent images showing maintained blood vessel integrity (Green) as detected by anti-laminin antibody (a) and UEA (c) in the presence of Grade 3 abnormal ZO-1 (Red) (b) and Grade 1 abnormal ZO-1 (Red) (d). Mag x400

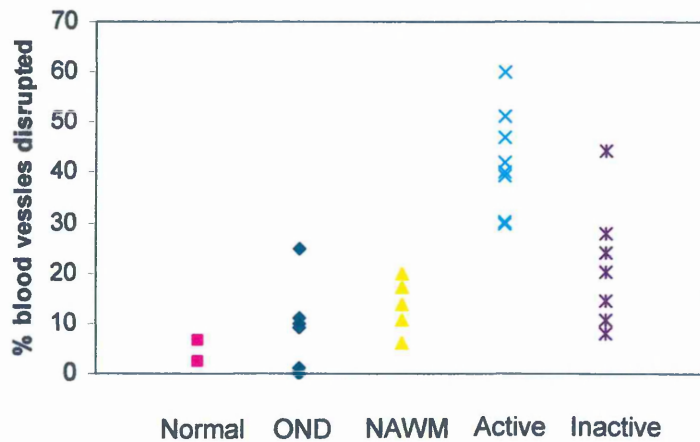
Figure 2.8a Extent of TJ disruption in all tissue categories



No. of BV examined: 313 461 904 622 672  
 No. of Cases examined: 2 6 6 8 7

Extent of disrupted blood vessels across all the tissue groups examined. A significant increase (\*) occurs in the number of disrupted blood vessels in the active and inactive MS tissue group when compared to normal and OND controls, following Kruskal-Wallis non-parametric test (\*).

Figure 2.8b Extent of TJ disruption in all tissue categories from each case



Scatter plot of individual case means for TJ disruption from all of the tissue study groups.

The majority of the vessels examined (88%) were either capillaries or small-intermediate vessels. TJ abnormalities were recorded in all sizes of blood vessel not just confined to this microvasculature. Variation of incidence of TJ abnormality between tissue groups was maintained irrespective of vessel size (Figure 2.9).

#### *2.3.4. Correlation of TJ abnormalities with other aspects of MS pathology*

To determine whether TJ abnormalities occurred in the presence of other MS pathologies dual label immunofluorescence for ZO-1 and occludin was carried out with antibodies to detect macrophage/microglial activation, lymphocytic infiltration and serum protein leakage. The extent of TJ abnormality in blocks containing recent myelin breakdown products, as determined by ORO, was also compared.

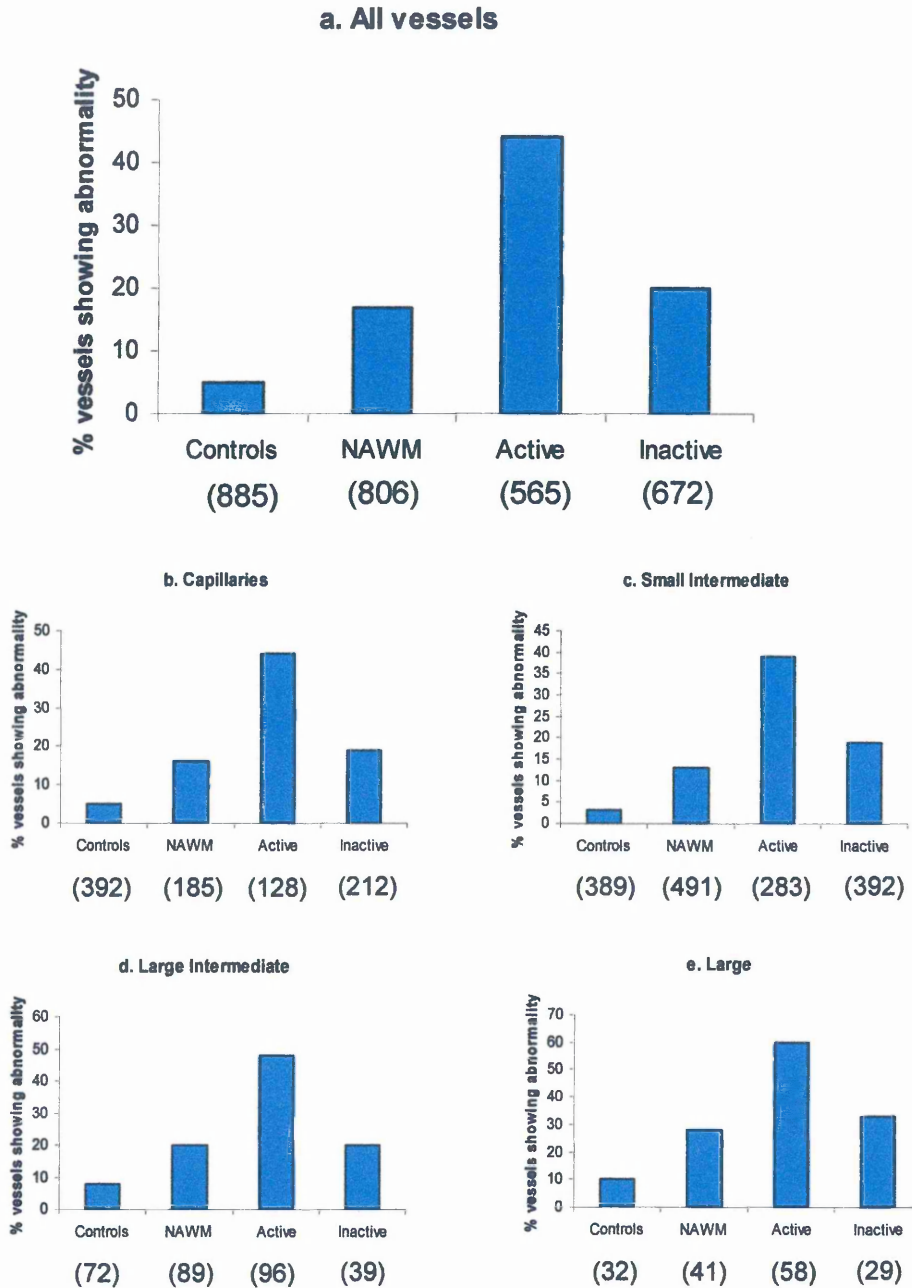
##### *2.3.4.1 TJ abnormality and evidence of recent myelin breakdown*

In the active MS block series it was possible to correlate TJ expression to the grade of ORO. 12 active blocks (ORO-grade 1) had 39.6% of blood vessels displaying clear ZO-1 abnormality. 12 active blocks (ORO-grade 2) had 40.7% with ZO-1 abnormality. 9 active blocks (ORO-grade 3) displayed 44.6% ZO-1 abnormality. A trend for increased ZO-1 abnormality with extent of disease activity is evident although without statistical significance (Figure 2.10).

##### *2.3.4.2 TJ abnormality and macrophage/microglial activation*

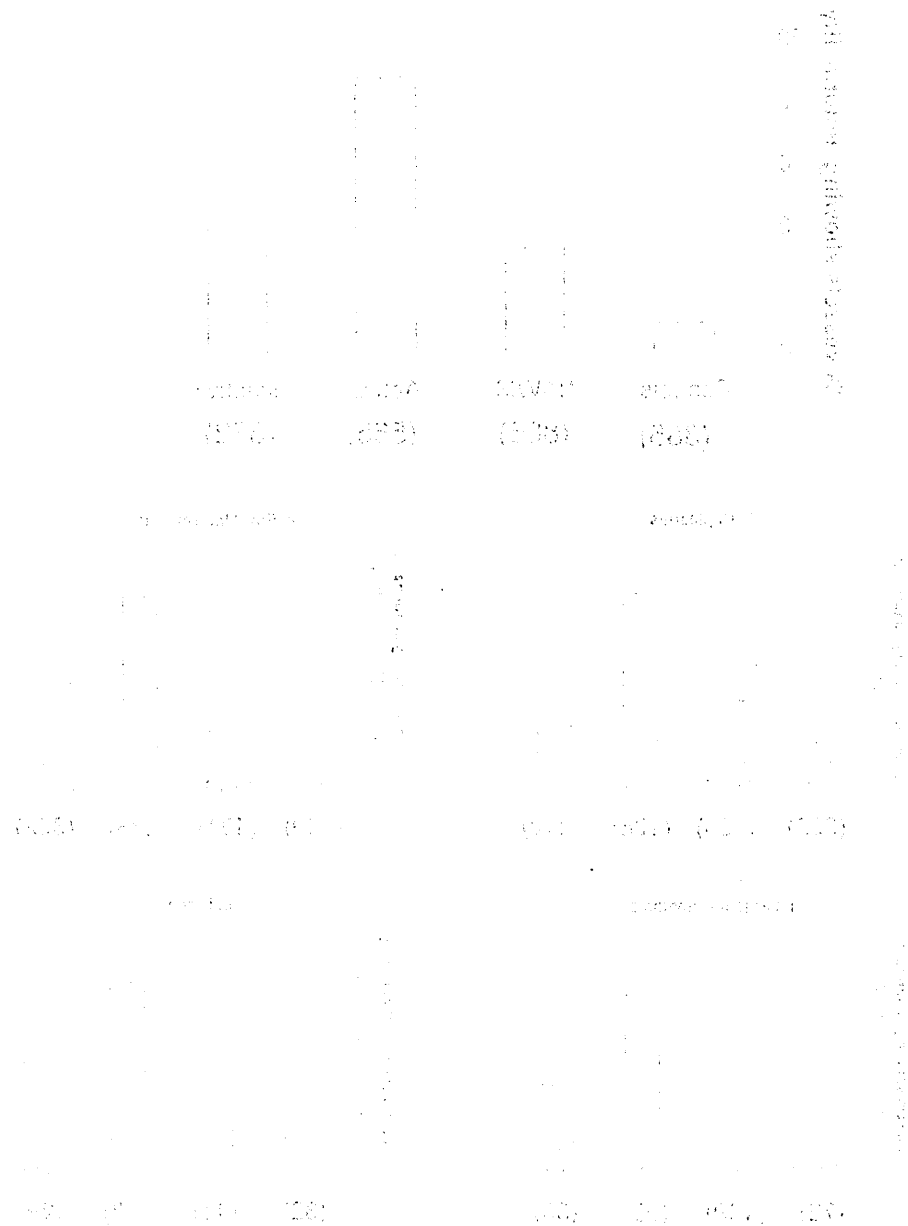
The MHC class II marker HLA-DR detects macrophages and microglial cells in an activated state and has hence been applied as another indicator of lesion activity. Following the trend observed with ORO, areas of higher microglial activation in active plaques had a (marginally) higher frequency of ZO-1 abnormality (Figure 2.10). 45.5% of the blood vessels in highly activated (grade 3) areas displayed abnormal TJ expression, compared with 41.3% in grade 2 areas and 33% in grade 1 areas. Dual labelling provided clear evidence for abnormality coincident with high HLA-DR immunoreactivity on numerous foamy macrophages that were evident in

Figure 2.9 Comparison of TJ abnormality with blood vessel sizes



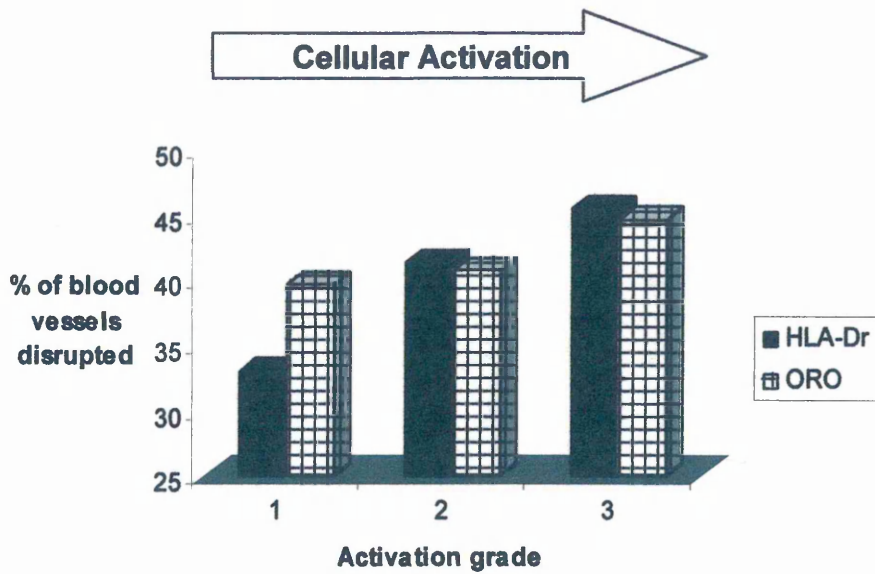
Comparison of the incidence of tight junction abnormality between MS and control tissues in all vessels (a) and in vessels of different sizes (b-e). Normal and neurological controls are grouped in this analysis. Numbers in parentheses indicates the number of individual blood vessels examined.

energy level



low energy level systems with a large number of particles, and a small number of particles with a high energy level. The energy level is generally low for a large number of particles, and high for a small number of particles. The energy level is generally low for a large number of particles, and high for a small number of particles. The energy level is generally low for a large number of particles, and high for a small number of particles.

Figure 2.10 TJ abnormality and cellular activation within active MS lesions



Bar graph illustrating relationship between blood vessel disruption and level of cellular activation in active MS plaques as measured by both HLA-DR and ORO. Although not statistically significant, a definite trend exists in that increased blood vessel disruption occurs with increased cellular activation (3).



perivascular locations and throughout the parenchyma of active plaques (Figure 2.11a).

#### *2.3.4.3 TJ abnormality and lymphocytic infiltration*

Lymphocytic infiltration as observed in perivascular cuffs is a hallmark of MS pathology. Lymphocytic infiltration as detected by immunofluorescence for LCA was observed in many of the MS sections. Dual label immunofluorescence provided clear evidence for ZO-1 abnormality in vessels displaying high concentration of infiltrating lymphocytes within perivascular cuffs (Figure 2.11b)

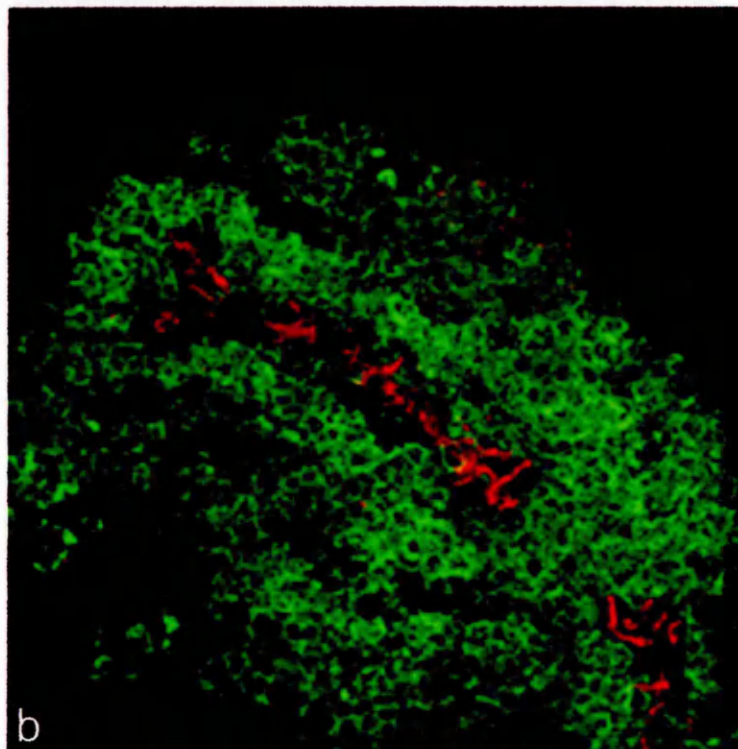
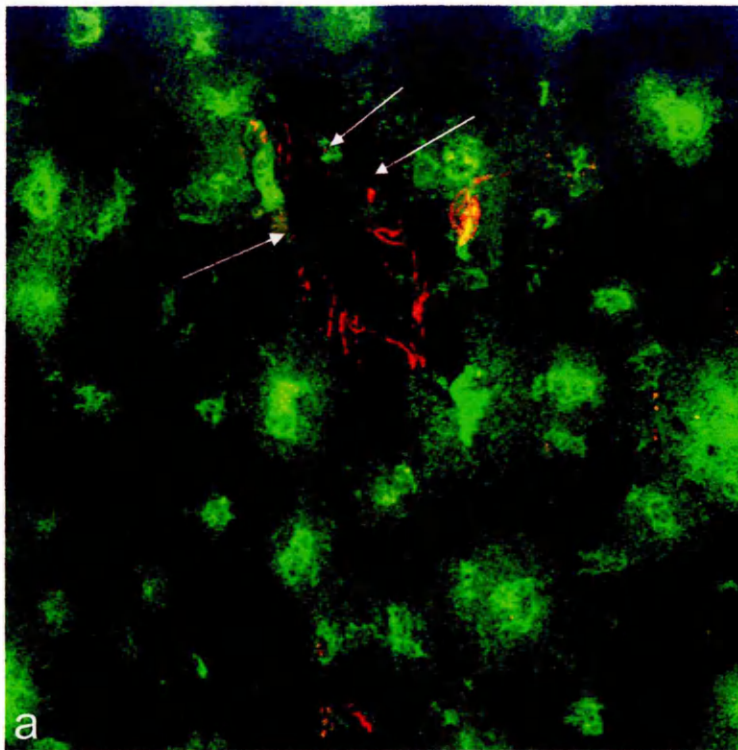
#### *2.3.4.4. TJ abnormality and serum protein leakage*

None of the control blocks examined for TJ proteins displayed extravascular staining for fibrinogen indicating intact BBB. However, fibrinogen leakage was observed in all MS cases to varying extents. In a small proportion of the MS blocks, marked alterations in the intensity and pattern of TJ staining co-incident with moderate to severe perivascular extravasation of fibrinogen and fibrillary immunoreactivity was seen. Dual label immunofluorescence provided clear evidence for ZO-1 abnormality in vessels displaying all levels of fibrinogen leakage (Figure 2.12). Immunostaining for fibrinogen was of a fibrillary nature indicative of astrocytic uptake during the disease course, suggesting pre-mortem leakage (Brown et al., 1999). Dual label for fibrinogen and GFAP commonly revealed an association between extravasted fibrinogen and the processes of astrocytes (Figure 2.12d-f).

In the semi-quantitative dual-labelling study three grades were used for each variable. Thus TJ abnormalities were graded on the following scale:

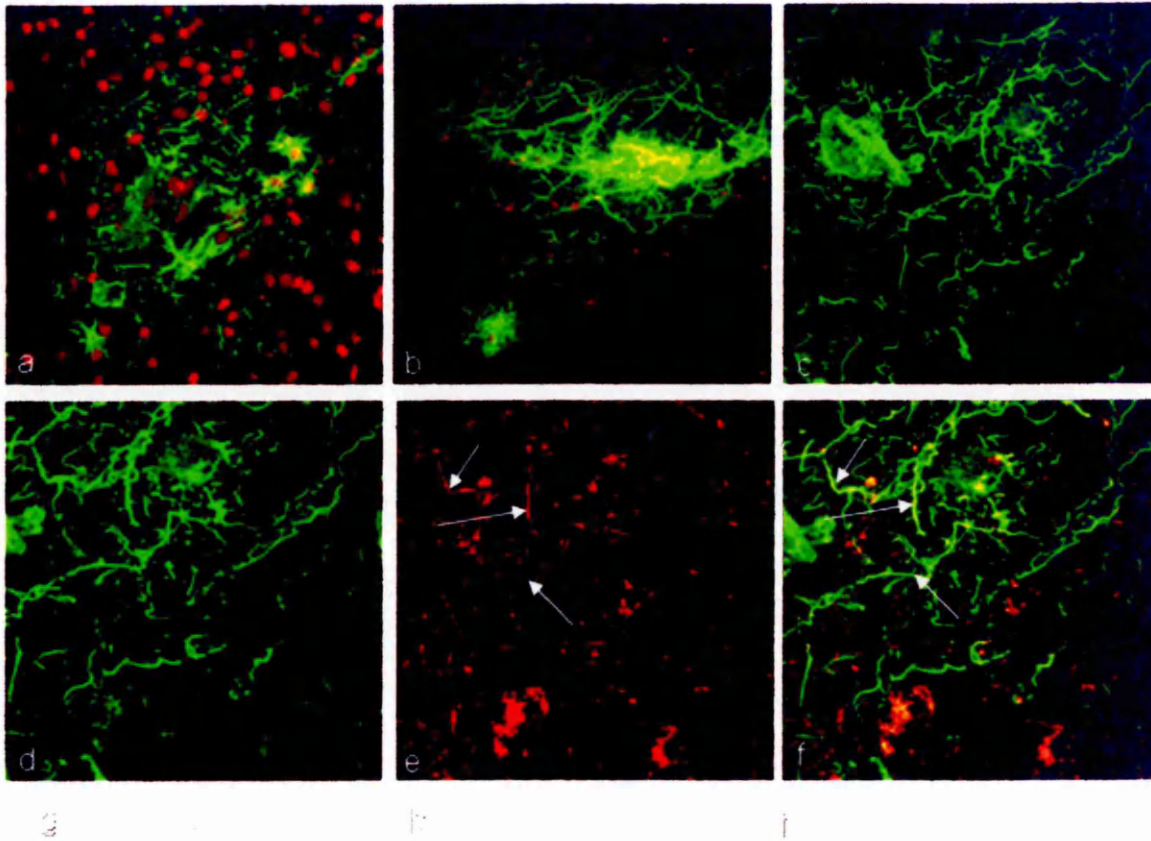
- 0= no clear abnormality
- 1= up to 25% of the vessel wall shows abnormalities in TJ protein expression
- 2= more than 25% of the vessel wall contains abnormal TJs (Figure 2.3.13 a-c)

Figure 2.11 TJ abnormality associated with inflammatory cells



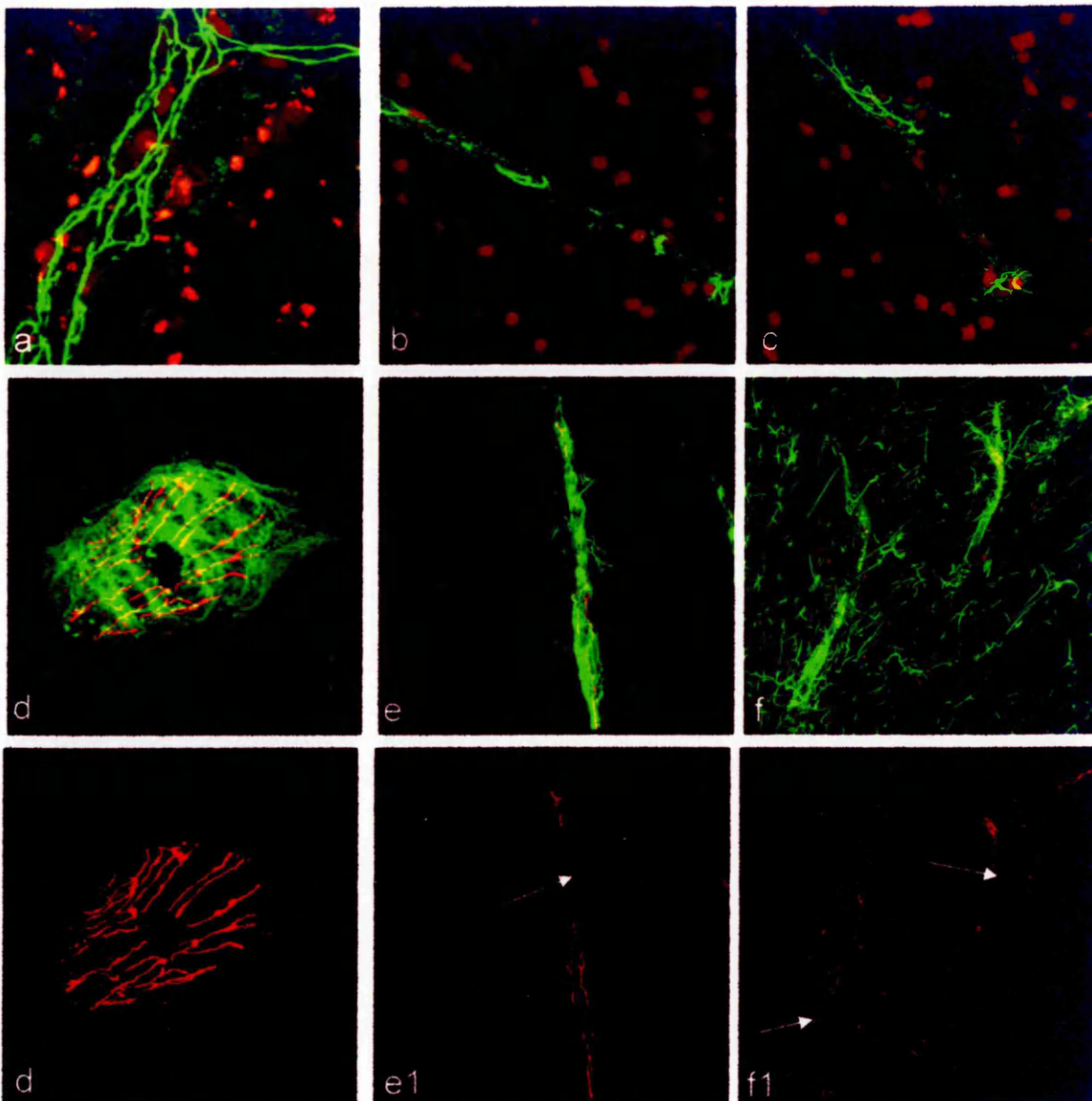
TJ abnormalities in active MS lesions. (a) Foamy macrophages in the perivascular cuff and surrounding parenchyma of a blood vessel expressing abnormal occludin (arrows). HLA-Dr (Green) / Occludin (Red). (b) A lymphocytic infiltrate associated with a collapsed vessel which reveals abnormal expression of occludin. LCA (Green) / Occludin (Red). Mag x400.

Figure 2.12 Serum protein leakage and TJ disruption



Immunolabelling analysis of the characteristics of fibrinogen leakage and tight junction abnormality in MS lesions. A fibrillary (pre-mortem) pattern of serum protein leakage (Green) is shown in vessels (a) from NAWM, (b) from an inactive/chronic lesion, and (c) from an active lesion, nuclei are counterstained with propidium iodide. The relationship between extravascular fibrinogen and astrocyte processes is revealed in the same lesion by dual labelling (d, fibrinogen (FITC; green) and e, GFAP (Alexa 568; Red) f, composite image). The arrows in (e) indicate fibrinogen-positive processes which are also stained for GFAP.

Figure 2.13 TJ abnormality and fibrinogen leakage



TJ (green) integrity was graded as; 0= no abnormality (a), 1= 1-25% abnormal TJ (b), 2= more than 25% TJ abnormality (c). Fibrinogen (green d-f) in a blood vessel with no abnormalities (d, d1). Fibrinogen leakage co-localizes with abnormal tight junctions (ZO-1, red, arrows) in an active lesion (e, e1) and an inactive lesion (f, f1).

Similarly, fibrinogen leakage was graded:

- 0= no leakage
- 1= moderate leakage
- 2= widespread, severe leakage

Anti-fibrinogen antibody labelled leakage was observed in blocks from all 3 categories of MS tissue but not in any blocks from the control cases (Figure 2.14). In many of the MS blocks, a fibrillary pattern of extravascular staining was present, indicative of pre-mortem leakage. Most commonly fibrinogen leakage had a distinct perivascular distribution but on rare occasions was observed more widely throughout the parenchyma. The relationship between TJ protein abnormalities and fibrinogen leakage was assessed at the level of the individual blood vessel, with each vessel being graded both for TJ abnormality and fibrinogen leakage.

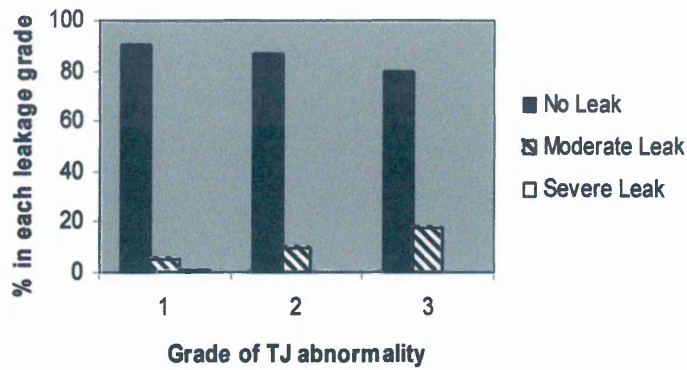
292 blood vessels were analysed from 19 active MS lesions, 243 vessels from 14 areas of NAWM and 291 vessels from 17 chronic inactive MS lesions. Overall there was a trend that with increasing severity of TJ abnormality there was an increase in severity in fibrinogen leakage, which was most evident in the active MS cases. In 26% of the vessels in active lesions with severe TJ abnormality (grade 3) extensive perivascular and parenchymal fibrinogen leakage was observed. In chronic inactive lesions and areas of NAWM, where fibrinogen leakage was not as prominent, the severest fibrinogen leakage was associated with vessels displaying the most TJ abnormality (Figure 2.14).

### *2.3.5 Influence of Death-autopsy interval on TJ abnormalities and serum protein leakage*

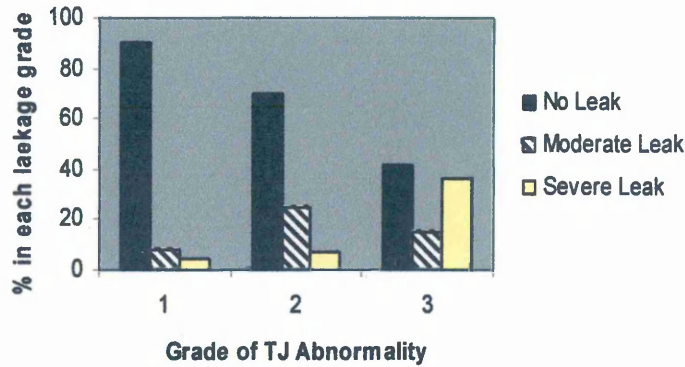
As mentioned previously utmost care was taken in selecting tissue samples with a death-autopsy interval (DAI)  $\leq$  24 hours, however the DAI varied within this group from 1.5-24 hours. The incidence of TJ abnormality and serum protein leakage was examined against DAI to determine whether post-mortem autolysis had an effect on BBB breakdown and leakage. However it was found that there was no correlation between either presence

Figure 2.14 Association of TJ disruption with serum protein leakage in white matter from MS tissue including NAWM, active and inactive lesions

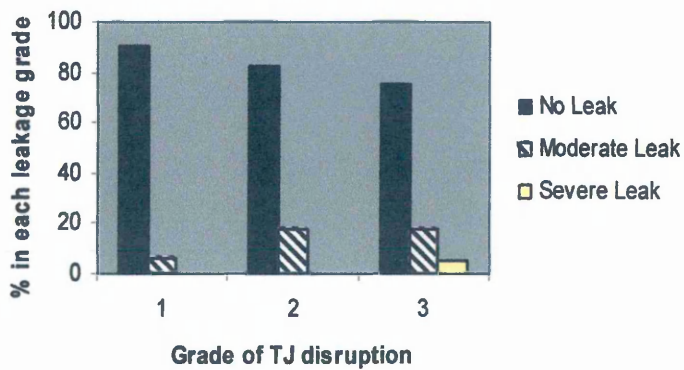
**NAWM**



**Active**

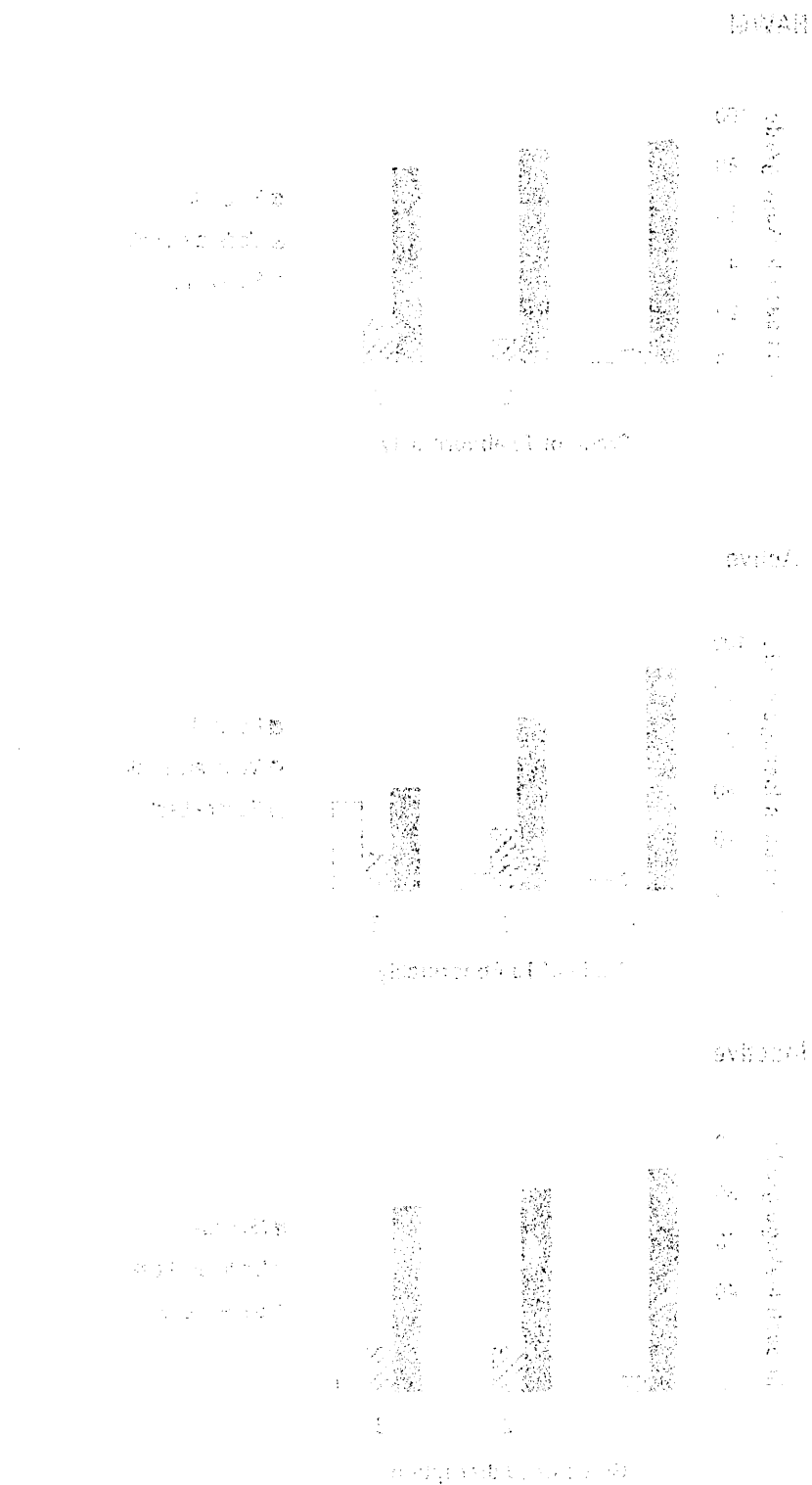


**Inactive**



Analysis of the relationship between the severity of fibrinogen leakage and the extent of TJ abnormality in individual MS blood vessel segments of known TJ status. Individual vessel grades: 0= normal TJs; 1= 1-25% abnormal TJs; 2= 26-100% abnormal TJs.

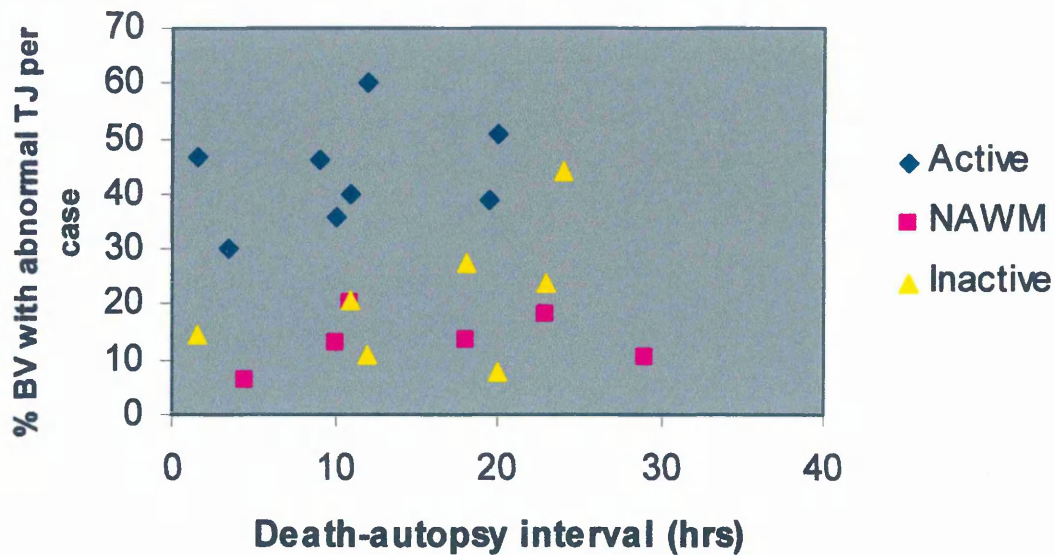
Figure 1. Association of the distribution of the number of children with autism and children with Down syndrome with the number of children with autism.



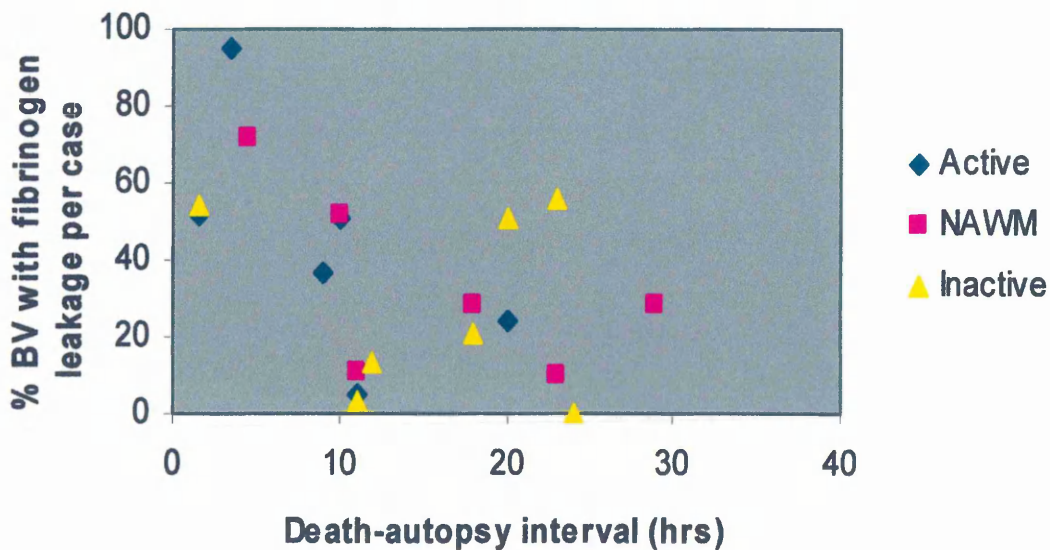
of children with autism and children with Down syndrome. The number of children with autism and children with Down syndrome were both significantly associated with the number of children with autism. The number of children with autism was significantly associated with the number of children with Down syndrome. The number of children with autism was significantly associated with the number of children with Down syndrome.

Figure 2.15 Association of death-Autopsy interval with TJ disruption and serum protein leakage in active and inactive MS lesions and NAWM

**a. DAI and TJ disruption**



**b. DAI and serum protein leakage**



Scatter plots to determine whether death-autopsy interval (DAI) has an influence on the parameters measured in the study, (a) TJ disruption and (b) serum protein leakage. No correlation appears to exist in either plot.

Figure 3. Average (mean  $\pm$  SD) of the number of cells in each phase of the cell cycle in the presence of the anti-CDK2 antibody (A) and the anti-CDK4 antibody (B) in the presence of the anti-CDK2 antibody (A) and the anti-CDK4 antibody (B).



Figure 3. Average (mean  $\pm$  SD) of the number of cells in each phase of the cell cycle in the presence of the anti-CDK2 antibody (A) and the anti-CDK4 antibody (B) in the presence of the anti-CDK2 antibody (A) and the anti-CDK4 antibody (B).

and extent of TJ abnormality with varying DAI times or with the extent of serum protein leakage (Figure 2.15).

## 2.4 Discussion

The results presented here provide evidence for a spectrum of TJ disruption in MS CNS tissue. A semi-quantitative analysis of TJ disruption in active and chronic inactive lesions compared with the NAWM of MS and the white matter of normal control and OND samples was also undertaken. Utilising archival snap frozen autopsy material, the timing of the disease process was established based on evidence of recent myelin breakdown and extent of cellular activation determined by ORO staining and HLA-DR immunoreactivity respectively, parameters used by other authors to assess lesion activity (Sanders *et al.*, 1993; van der Valk and de Groot, 2000). Confocal scanning laser microscopy and immuno-labelling described here provides a reliable method for detecting and visualising the inter-endothelial TJ of the BBB. Using this method the TJ associated proteins ZO-1 and occludin were detected in cerebral vessels of normal control white matter tissue as intense continuous linear bands that extended in a radial (transversely sectioned vessels) or longitudinal (longitudinally sectioned vessels) direction. Alterations in ZO-1 and occludin appearance were observed in cerebral vessels of MS tissue. A spectrum of TJ disruption was observed in MS tissue ranging from either, loss of TJ expression, interruption or beading of expression and even a parting or opening of the TJ.

Quantification of TJ disruption revealed an increased incidence in active MS lesions (42%), however “activity” does not appear to be a prerequisite for TJ disruption, as abnormal TJ expression was recorded in chronic inactive MS lesions (22%) and the NAWM (13%) at a frequency greater than those observed in the white matter of normal controls and OND. Upon examination of individual case-means there is an overlap in the incidence of TJ disruption between the active MS lesions (range 30-60%) and the more variable but lower mean values for abnormalities found in chronic inactive lesions (range 8-44%). This overlap may reflect the

heterogeneity of older lesions and the heterogeneity of MS pathogenesis (Lucchinetti *et al.*, 2000; Wingerchuk *et al.*, 2001). Analysis of normal control white matter revealed a low level (4%) incidence of TJ disruption, which is in keeping with the view that a small degree of barrier opening may occur as a well regulated process under normal physiological conditions (Abbott, 2002). This opening is believed to be transient and strictly controlled by the interactions of the TJ and the cytoskeleton (Abbott, 2002). TJ abnormality is observed here at an increased incidence (13%) in MS NAWM in comparison to the normal white matter of normal control tissue (4%). It has long been considered that the NAWM in MS is not “normal” and indeed forms the basis from which early plaque formation develops (Allen and McKeown, 1979; Filippi *et al.*, 1998; Goodkin *et al.*, 1998). This supports the view that an alteration in the BBB, and hence inflammation, is an early event in the pathogenesis of a new lesion in MS (Kermode *et al.*, 1990a).

The use of ZO-1 as the tight junction marker in this study is consistent with that of other groups (Bolton *et al.*, 1998; Dallasta *et al.*, 1999; Boven *et al.*, 2000; Kuruganti *et al.*, 2002). Its known function is to act as an essential link between the transmembrane TJ proteins and the cytoskeleton. ZO-1 and occludin have however been reported to be expressed in astrocytes and non-endothelial cells (Howarth *et al.*, 1992) but the focus of this study was on the endothelial TJ and as such the protocols were optimised to demonstrate the proteins in this context. Occludin has been successfully utilised as an integral membrane protein marker for TJ in a number of pathological studies (Bolton *et al.*, 1998; Dallasta *et al.*, 1999; Luabeya *et al.*, 2000). In comparing immunostained serial sections of control tissue for ZO-1 and occludin, no detectable differences in the expression levels and distribution were observed, however ZO-1 did produce a sharper immunofluorescent signal, and hence was used for the quantitative aspect of this study. Recognition of a major new transmembrane component of the TJ has emerged with claudin-1, -3, -5 and possibly claudin-12 associated with the TJ of the BBB (Morita *et al.*, 1999; Liebner *et al.*, 2000; Kraus *et al.*, 2004). Claudin expression was not investigated in this study due to poor quality of immunostaining on the available snap-frozen tissue sections with

the commercial antibodies currently available for these proteins. Three claudin-5 antibodies (two monoclonal and one polyclonal) were tested on sections of control white matter however the reaction product proved weak and inconsistent. However, using fresh human tissues which were immersion fixed in 2% paraformaldehyde plus 0.2% glutaraldehyde before vibratome sectioning Virgintino *et al.*, 2004, were able to obtain high resolution immunostaining with anti-claudin-5 antibodies. Recently in an immunostaining study examining CD45 and the TJ associated proteins, occludin and claudin-1, -3 and -5 in SJL/N mice affected with EAE, and their healthy littermates, showed selective loss of only claudin-3 in blood vessels associated with large CD45<sup>+</sup> perivascular cuffs (Wolburg *et al.*, 2003). Contrary to what is observed in MS lesions here it was reported that occludin immunostaining in inflammation associated blood vessels was indistinguishable from those observed in healthy brains (Wolburg *et al.*, 2003). Provision of a wide range of MS and controls blocks prepared in this manner or more suitable anti-claudin antibodies for snap-frozen tissues may provide different, more reliable or more comprehensive data in the range of human disorders examined with antibodies to ZO-1 and occludin in the future.

Investigation of blood vessel integrity was important to ensure TJ alterations were not due to blood vessel distortion during sample processing therefore additional markers were tested in conjunction with ZO-1 and occludin. The lectin *Ulex europaeus agglutinin* (UEA) stains the endothelium of the microvasculature intensely (Prat *et al.*, 2001) whilst laminin was used as an additional marker for the capillary basement membrane, allowing identification of disrupted TJ proteins in the presence of a normal intact basement membrane. The use of fibrinogen as a marker for BBB serum protein leakage has been used in previous human and animal model autopsy tissue studies (Kwon and Prineas, 1994; Claudio *et al.*, 1995; Gay *et al.*, 1997; Dallasta *et al.*, 1999; Brown *et al.*, 1999; Luabeya *et al.*, 2000). Pre-mortem leakage is determined by the fibrillary nature of fibrinogen following uptake by perivascular astrocytes (Gay *et al.*, 1997; Brown *et al.*, 1999). Fibrinogen was observed within the cell bodies and elongated processes of

astrocytes. Thus fibrinogen staining was used to assess the association between TJ disruption and BBB leakage.

It has been reported that the BBB is permanently damaged in many old chronic plaques, at a level undetectable by Gd-DTPA-MRI (Kwon and Prineas, 1994; Claudio *et al.*, 1995). This observation is further confirmed here with the presence of leaking blood vessels in chronic inactive lesions. It is tempting to suggest that such persistent leakage through disrupted junctions with constant destabilization of homeostasis in the parenchymal microenvironment could contribute to the overall inefficiency of remyelination in chronic plaques. Targeted therapy, directed at repair of TJ disruption in these areas may promote a much greater efficiency of remyelination. The highest degree of BBB leakage was observed in the active lesions with the most severe leakage occurring with the most severe TJ disruption, suggesting a possible causal link. Not all blood vessels with disrupted TJs displayed evidence of leakage this could be due to either, a lack of sensitivity in the detection protocol or the existence of a threshold of disruption of the TJ which is required to be reached before fibrinogen, a large serum protein (340 kD), is released and can be detected in the surrounding perivascular astrocytes.

Blood vessels of all sizes displayed the same pattern of TJ disruption between groups of blocks in different phases of disease. This demonstration that all blood vessels are involved in the breakdown of the BBB and that the greatest number of abnormal TJs coincided with the highest levels of microglial activation, may point to the nature of the causal mechanisms. Had the TJ disruption been as a result of local effects arising from transendothelial migration of inflammatory cells, post-capillary venules and veins would have been expected to bear the brunt of the TJ disruption (Boven *et al.*, 2000). The involvement of all vessels and the correlation with perivascular HLA-DR<sup>+</sup> foamy macrophages and activated microglia suggests that TJ disruption may be as a result of the pathophysiological actions of cytokines, MMPs and other mediators of inflammation present in MS lesions. Proinflammatory cytokines, TNF and IFN- $\gamma$ , have been shown to disrupt TJ

function and cause reorganisation of the actin cytoskeleton and redistribution of the ZO-1 and occludin (Blum *et al.*, 1997; Walsh *et al.*, 2000; Prat *et al.*, 2001; Mayhan, 2002; Kuruganti *et al.*, 2002). Treatment of HUVEC cultures with IFN $\beta$ 1b inhibits IFN $\gamma$  induced occludin disruption (Minagar *et al.*, 2003). Transendothelial resistance, the barrier function of the TJ, is reported to be reduced by 50% upon treatment with TNF and IFN $\gamma$ , with a striking fragmentation of ZO-1 appearance (Blum *et al.*, 1997). Treatment with IFN $\beta$  was able to alter ZO-1 distribution with the staining observed along the endothelial cell borders (Kuruganti *et al.*, 2002). MMPs have been implicated in disruption of the BBB in MS (Cossins *et al.*, 1997; Walsh *et al.*, 2000) while another member of the MMP family, TNF $\alpha$ -converting enzyme (TACE, or ADAM-17) has been shown to cleave TNF from its membrane bound form into a soluble form (Black *et al.*, 1997; Moss *et al.*, 1997; Black, 2002;) allowing TNF to diffuse within the CNS parenchyma to trigger further inflammatory responses (Probert and Akassoglou, 2001).

In conjunction with BBB breakdown and serum protein leakage, disruption in ZO-1 and occludin was also associated with an accumulation of perivascular HLA-DR<sup>+</sup> foamy macrophages and LCA<sup>+</sup> perivascular lymphocytes. HLA-DR<sup>+</sup> macrophages have previously been reported to be associated with blood vessels with damaged walls in acute MS lesions (Gay and Esiri, 1991). Similar loss in immunoreactivity of the TJ associated proteins, ZO-1 and occludin, with an accumulation of perivascular HIV-1 infected macrophages and serum protein leakage has been reported in HIVE (Dallasta *et al.*, 1999). The loss of ZO-1 has also been associated with monocyte infiltration and CD68<sup>+</sup> perivascular macrophages in HIV-associated dementia (Boven *et al.*, 2000). Similar observations have been recorded in an animal model study of simian immunodeficiency virus encephalitis (SIVE) (Luabeya *et al.*, 2000). Cerebral vessels from macaques with SIVE displayed fragmentation and decreased immunoreactivity for ZO-1 and occludin, in association with perivascular macrophage accumulation and extravasation of serum protein leakage (Luabeya *et al.*, 2000). The authors report a further association between TJ disruption and the abnormal appearance of glucose transporter isoform-1 (GLUT-1), a metabolic BBB

marker, suggesting an alteration in function with the presence of disrupted TJ (Luabeya *et al.*, 2000). ZO-1 immunoreactivity is also reported to undertake a diffuse expression in the cerebral endothelium of dystrophic mdx mice (Nico *et al.*, 2003).

Death-autopsy intervals were recorded for each case investigated to establish or eliminate autolysis as a cause of the abnormal TJ and serum protein leakage. Most of the DAI were less than 24 hours with the exception of one case which was 29 hours (range 1.5-29 hours). No correlation was observed between the extent of TJ disruption or serum protein leakage and length of DAI. This is in keeping with earlier studies that have shown that extended DAI had no effect on the quality of immunohistochemical characterization and the ability to extract mRNA (DeGroot *et al.*, 1995; Cummings *et al.*, 2001). This suggests that the quantified differences in extent of TJ disruption and BBB leakage between active MS lesions, chronic inactive lesions and NAWM are due to the pathological process. What processes are involved remains unclear, the complex cascade system involving MMPs, cytokines, chemokines and other signalling proteins within the inflammatory milieu that is present in MS lesions remains to be unravelled.

The results indicate that TJ disruption and abnormality is widespread throughout MS white matter, persisting in chronic inactive lesions but most common in active lesions. Further investigation would be required to investigate the functional aspects associated with this TJ disruption. The use of cell culture studies has been well documented and allows the investigator to manipulate the culture conditions to emulate those observed in CNS inflammation. However extrapolating information from culture studies and applying it to MS pathogenesis is fraught with problems. Endothelial cells from the microvasculature of the CNS differ from other vascular endothelial cells. CNS derived endothelial cells are phenotypically unstable in long-term culture (Romero *et al.*, 2003). To overcome this problem well differentiated immortalised cultures can be used, however they lose their ability to maintain functional tight junctions (Romero *et al.*, 2003).

These results further underline the dramatic nature of the events at the BBB during lesion formation in the pathogenesis of MS (Claudio *et al.*, 1995). Although TJ disruption cannot be viewed in isolation from other aspects of lesion formation, it does present a valid area for research as a therapeutic target. The effect of short-term or pulsed glucocorticosteroids, is transient, as indicated by changes in the number of Gd-DTPA-enhancing lesions on MRI imaging (Richert *et al.*, 2001). *In vitro* and *in vivo* studies have demonstrated that TJ abnormality is responsive to IFN- $\beta$  however the clinical benefits of this remain to be established (Richert *et al.*, 2001; Kuruganti *et al.*, 2002). A means of preventing the BBB damage associated with acute inflammation is offered by a new anti-leukocyte trafficking drug, the  $\alpha$ 4 integrin antagonist Natalizumab (Elan Pharmaceuticals, Biogen). This had recently entered phase III clinical trials in the UK and North America (O'Connor *et al.*, 2004). Single dose treatment of Natalizumab has been shown to decrease the Gd-enhancing lesion volume in MS patients in acute relapse (O'Connor *et al.*, 2004). Natalizumab binds to VLA-4 on T cells preventing the coupling of VLA-4 with VCAM-1 on the luminal surface of cerebral endothelium, an integral step in the transendothelial migratory process, thus preventing entry of T cells into the CNS. However following reports of progressive multifocal leukoencephalitis (PML) in two patients receiving dual therapy in the trial, Natalizumab (Tysabri) was withdrawn at the end of February 2005.

The widespread TJ disruption described here clearly has implications in MS prognosis and should be taken into account when planning therapies aimed at repairing established lesions and thereby possibly preventing disease progression. The extent of TJ disruption as shown here within all MS tissue, even in chronic inactive lesions, merits recognition as a third distinct form of tissue injury in MS, alongside demyelination and axonopathy.

## **Chapter 3**

### **Expression of ADAM-17 in the CNS in MS: a pathologic role**

## Chapter 3

### 3.1 Introduction

#### 3.1.1 ADAM-17

ADAM-17 is regarded to be the major physiological TNF convertase (Black *et al.*, 1997; Moss *et al.*, 1997). ADAM-17 was first identified by its ability to cleave membrane bound TNF into a soluble form and was therefore termed **T**NF $\alpha$  **c**onverting **e**nzyme (TACE) (Moss *et al.*, 1997; Black *et al.*, 1997). ADAM-17 was purified from membrane fractions of the TNF producing human macrophage-like cell line, Mono-Mac 6 cells and extracts from pig spleen (Moss *et al.*, 1997; Black *et al.*, 1997). As with other members of the ADAM family, ADAM-17 is a multi-domain type I transmembrane protein, composed of 824 amino acids (Itai *et al.*, 2001; Black, 2002;). A putative furin-cleavage motif lies between the pro-domain and the catalytic domain suggesting that ADAM-17 is produced as a zymogen that becomes active following the removal of the pro-domain (Moss *et al.*, 1997; Schlöndorff *et al.*, 2000; Itai *et al.*, 2001). However arguments in favour of a role for furin in the maturation of ADAM-17 are speculative rather than direct (Peiretti *et al.*, 2003). X-ray crystal structure analysis of ADAM-17 catalytic domain shows that the zinc environment and the placement of the major structural elements are very similar to catalytic domains of the SVMP family members (Maskos *et al.*, 1998).

TNF has been associated with numerous inflammatory diseases including, Crohn's disease, rheumatoid arthritis, and MS, therefore research into the properties of ADAM-17 have been of interest in view of the search for therapeutic targets for these chronic diseases (Hyrich *et al.*, 2004; Dalton *et al.*, 2004; Baker, 2004). ADAM-17 has proved to be a protein with more diverse functions than its role in the cleavage of TNF. Knowledge of ADAM-17 substrates has been derived from studies using genetically modified animals that are devoid of catalytically active ADAM-17 (Peschon *et al.*, 1998; Killar *et al.*, 1999). ADAM-17 knockout in these animals lead to perinatal lethality with the majority of embryos dying between embryonic day 17.5 and one day after birth (Peschon *et al.*, 1998).

ADAM-17 has been demonstrated to mediate the cleavage of other members of the TNF superfamily (Peschon *et al.*, 1998; Lum *et al.*, 1999; Black, 2002; Contin *et al.*, 2003) as well as macrophage colony-stimulating factor receptor, transforming growth factor- $\alpha$  (TGF- $\alpha$ ), epidermal growth factor receptor and IL-6 receptor (Moss *et al.*, 1997; Black *et al.*, 1997; Rovida *et al.*, 2001; Hinkle *et al.*, 2004;). Both p55 and p75 TNFR have been shown to be substrates of ADAM-17 (Peschon *et al.*, 1998; Dri *et al.*, 2000), along with TNF-related activation-induced cytokine (TRANCE) (Lum *et al.*, 1999; Schlondorff *et al.*, 2001) and CD40 (Contin *et al.*, 2003). CD40 is expressed on the surface of antigen presenting cells and is essential for the induction of immune responses (Contin *et al.*, 2003). Interaction between CD40 and CD40 ligand (CD40L) is required for co-stimulatory molecule expression and induction of cytokine synthesis (Shinde *et al.*, 1996; Contin *et al.*, 2003). The shedding of CD40 from APCs, into soluble CD40, is important as it is able to bind to membrane bound CD40L and inhibit CD40/CD40L-mediated antibody production by B cells (Contin *et al.*, 2003). ADAM-17 has also been demonstrated as an effective mediator in the shedding of the adhesion molecules L-selectin and VCAM-1 (Borland *et al.*, 1999; Garton *et al.*, 2003) which are vital for cell adhesion and migration at the BBB.

Recently fractalkine, a new chemokine has been discovered to be a substrate of ADAM-17 activity that exists in both a membrane bound and a soluble form and has adhesive properties (Tsou *et al.*, 2001; Garton *et al.*, 2001; Kastenbauer *et al.*, 2003). Fractalkine (CX3CL1) is a novel member of the chemokine group CX3C that exists as a membrane form on endothelial cells, neurons, astrocytes and epithelial cells that has adhesive properties for cells expressing its receptor CX3CR1 (Imai *et al.*, 1997; Garton *et al.*, 2001; Tsou *et al.*, 2001; Hulshof *et al.*, 2003; Ahn *et al.*, 2004;). CX3CR1 is expressed on monocytes, T-cells, natural killer cells, neurons and microglia (Nishiyori *et al.*, 1998; Garton *et al.*, 2001). Fractalkine can be cleaved from the cell membrane to produce a soluble form that creates a chemotactic gradient for inflammatory cells (Tsou *et al.*, 2001; Garton *et al.*, 2001; Kastenbauer *et al.*, 2003). However soluble fractalkine reduces the potential of CX3CR<sup>+</sup> leukocytes to bind to endothelial membrane bound fractalkine, by

blocking their receptor (Imai *et al.*, 1997), thus reducing leukocyte transmigration. Reported *in vitro* studies have shown soluble fractalkine being unable to induce transendothelial migration in human umbilical vein endothelial and brain microvascular endothelial cells (Ancuta *et al.*, 2004). Increased fractalkine expression has been observed in the CSF and serum of patients with inflammatory diseases, including MS and bacterial meningitis (Kastenbauer *et al.*, 2003). *In vitro* studies have reported that constitutive shedding of fractalkine remained unaltered in unstimulated ADAM-17 null-fibroblast cells suggesting constitutive cleavage is mediated by a metalloproteinase other than ADAM-17 (Tsou *et al.*, 2001; Garton *et al.*, 2001) which has recently been identified as ADAM-10 (Hundhausen *et al.*, 2003).

#### 3.1.1.1 ADAM-17 in disease

ADAM-17 has the potential to participate in a broad range of immune functions and immune-mediated diseases through modulation of shedding of proteins vital to immune responses. The functional activity of ADAM-17, as measured by release of soluble TNF, is reported to be elevated in patients with ulcerative colitis in comparison to controls (Brynskov *et al.*, 2002) suggesting a pathogenic role involving increased TNF release and inducible nitric oxide synthase (iNOS) (Colón *et al.*, 2001). ADAM-17 expression and activity within the synovial tissue of people with rheumatoid arthritis is reported to be increased in comparison with the synovial tissue of people with osteoarthritis and controls (Patel *et al.*, 1998; Ohta *et al.*, 2001;). ADAM-17 has been shown to be up-regulated and associated with prostatic tumor cells and the metastatic capabilities of these cells, while TIMP3, an endogenous inhibitor of ADAM-17, has been reported to be down-regulated in prostate cancer biopsies (Karen *et al.*, 2003).

ADAM-17 has recently been reported to be an  $\alpha$ -secretase of APP and is localised in neurones where it is suggested that it competes with  $\beta$ -secretases for APP cleavage (Skovronsky *et al.*, 2001; Blacker *et al.*, 2002; Asai *et al.*, 2003; Kojro and Fahrenholz, 2005). The neuronal expression of ADAM-17 has been proposed as having neuroprotective properties in rodent models of ischemic stroke by increasing the level of glutamate transporters in

neurons and glia (Cardenas *et al.*, 2002; Romera *et al.*, 2004;) therefore decreasing neurotoxic levels of glutamate within the extracellular space (Romera *et al.*, 2004). Pre-treatment of rat cortical cultures with an ADAM-17 inhibitor, BB3103, prevented oxygen-glucose deprived increase of glutamate transporters suggesting that neuroprotection by glutamate transporters is mediated by an ADAM-17-TNF dependent pathway (Romera *et al.*, 2004). Another study however reports that the selective inhibition of ADAM-17 protects rats from focal ischemic injury, suggesting ADAM-17 plays a deleterious role in stroke (Wang *et al.*, 2004).

### 3.1.1.2 ADAM-17 and MS

The role of ADAM-17 in the pathogenesis of MS has not been extensively studied. Increased expression of ADAM-17 mRNA by peripheral blood mononuclear cells in serum samples from MS patients is reported to correlate with new Gd- DTPA MRI lesions, following a longitudinal study with 11 patients with RRMS (Seifert *et al.*, 2002). ADAM-17 protein has been detected in CSF samples from patients with MS and bacterial meningitis but not in other non-inflammatory neurological controls (Kieseier *et al.*, 2003). ADAM-17 expression in MS autopsy brain has been demonstrated in small rounded CD3<sup>+</sup> lymphocytes, primarily located in the perivascular cuffs associated with acute and chronic active plaques with no astrocytic or endothelial ADAM-17 expression in normal control or MS brain tissue (Keiseier *et al.*, 2003). This contradicts an earlier study however where ADAM-17 immunoreactivity was been demonstrated to be expressed by the astrocytes and endothelial cells of normal control white matter (Goddard *et al.*, 2001).

### 3.1.2 TIMP3

Like MMPs, ADAM-17 is regulated at a transcriptional level, pro-enzyme activation, and inhibition by TIMP3 (Amour *et al.*, 1998; Ozenci *et al.*, 1999). TIMP3 is a 24 kDa protein composed of an amino-terminal domain and a carboxy-terminal domain that are held together by 6 disulphide bonds that hold the protein in a wedge shape resembling the Fab portion of immunoglobulins (Crocker *et al.*, 2004). TIMP3 differs from the other 3

members of the TIMP family in that it is the only one that is bound to the ECM via sulphated glycosaminoglycans (Borland *et al.*, 1999; Yu *et al.*, 2000; Crocker *et al.*, 2004; Visse and Nagase, 2003;).

TIMP3 mRNA has been reported to be expressed in the choroid plexus and dentate gyrus in normal mouse brain and within developing embryonic neural tissues and within astrocytes and neurons of the cerebellum, cerebral cortex, thalamus and the brain parenchyma of postnatal and adult rat brain (Pagenstecher *et al.*, 1998; Vaillant *et al.*, 1999; Jaworski and Fager, 2000).

TIMP3 is directly implicated in disease processes (Weber *et al.*, 1994). Mutations in the TIMP3 gene and not over expression of TIMP3 by retinal pigment epithelial cells leads to Sorby's fundus dystrophy, a rare autosomal-dominant condition that causes blindness due to macular degeneration (Weber *et al.*, 1994; Chong *et al.*, 2003). Addition of recombinant human TIMP3, and not TIMP1 and 2 has been shown to inhibit PMA-induced shedding of L-selectin from human lymphocytes *in vitro* suggesting that ADAM-17 is responsible for the induced proteolytic cleavage of L-selectin (Borland *et al.*, 1999). TIMP3 is reported to have functions that are independent of its role as an MMP inhibitor (Visse and Nagase, 2003). TIMP3 has anti-angiogenic properties and actively inhibits VEGF-mediated angiogenesis by blocking the binding of VEGF to its receptor thus inhibiting a downstream signal for angiogenesis (Qi *et al.*, 2003). TIMP3 is also believed to have pro-apoptotic activity through a Fas-associated apoptotic pathway, which leads to cell death in tumor cells and neurons (Bond *et al.*, 2002; Wallace *et al.*, 2002; Wetzel *et al.*, 2003).

### 3.1.3. Aim of study

The key aim of this study was to establish whether ADAM-17 is involved in the pathogenesis of MS and if so to develop an understanding of its activity, which may then subsequently be exploited therapeutically through the design and application of ADAM-17 inhibitors.

This study set out to establish a reproducible protocol for the investigation of ADAM-17 expression together with phenotypic markers of specific CNS cells. Snap-frozen autopsy MS tissue was used and classified as described

in Chapter 2. A semi-quantitative analysis of ADAM-17 expression by immunofluorescence was applied to establish if any differences in extent of ADAM-17 expression exists between MS and controls. The major objectives addressed were:

- (i) To determine whether ADAM-17 and TIMP3 immunoreactivity is detectable in snap frozen autopsy material.
- (ii) If so, to determine which cells are responsible for ADAM-17 and TIMP3 expression.
- (iii) To establish whether ADAM-17 expression predominates at a particular stage or stages of lesion development.
- (iv) To determine whether there is an imbalance between the expression of the enzyme and its inhibitor at a particular stage of lesion development.

### 3.2 Materials and Methods

42 blocks of snap frozen autopsy CNS tissue from 19 clinically and neuropathologically confirmed MS cases, together with 18 blocks from 5 normal control cases and one case of transverse myelitis, received from the UK Multiple Sclerosis Tissue Bank, Charing Cross Hospital, London and the Netherlands Brain Bank for Multiple Sclerosis, Amsterdam, The Netherlands were used in this study. Informed consent for research for all brain tissues and local ethical approval for the conduct of this study was obtained. These MS cases included 7 females, mean age 58.1 years (range 45-76) and 12 males with a mean age of 56.16 years (range 44-75). The tissue used had a mean time from death to freezing of 18.1 hours (range 8-58 hours). 18 snap-frozen control white matter blocks were obtained from 5 normal controls and 1 other neurological disease (OND). Mean age of the control cases was 75 years (range 45-92). Table 3.1 contains the clinical and demographic details of all cases used in this part of the study.

#### 3.2.1 Tissue characterisation

All MS and control snap-frozen blocks underwent preliminary screening to determine the pathological status of individual blocks. Cryostat sections (12µm) were cut onto polysine glass slides (BDH) and routinely stained with H&E and ORO (see appendix) for presence and grading of lesion activity. ORO positive blocks were classified as described in section 2.2.2.

##### 3.2.1.1 Immunohistochemistry

All MS and control samples were routinely screened for presence and extent of expression of HLA-DR. Sections were fixed in ice-cold acetone for 10 minutes and allowed to air dry for at least 15 minutes prior to use. Endogenous peroxidase was quenched by incubating sections in 0.5% H<sub>2</sub>O<sub>2</sub> in methanol for 10 minutes at room temperature (RT). Following washes in running tap water and PBS, sections were incubated in mouse monoclonal anti-HLA-DR antibody (1:50, Novocastra) overnight at 4°C. Sections were washed 3 x 5 minutes in PBS then incubated in biotinylated rabbit anti-

Table 3.1 Case details of subjects, used in study of ADAM-17 expression within the CNS

<i>Case No</i>	<i>Age (yrs)</i>	<i>Sex (M/F)</i>	<i>DAI (h)</i>	<i>Diagnosis</i>	<i>Cause of death</i>
<b>C1</b>	77	M	27	Normal	Lung Cancer
<b>C2</b>	64	F	18	Normal	Cardiac Failure
<b>C3</b>	82	M	21	Normal	na
<b>C4</b>	92	M	13	Normal	Cardiac failure, old age
<b>C5</b>	90	F	15	Normal	Old age
<b>OND1</b>	45	M	8.5	Transverse Myelitis	na
<b>MS1</b>	57	F	38	SPMS	Pneumonia, MS
<b>MS2</b>	63	M	11	SPMS	Pneumonia, MS
<b>MS3</b>	44	M	16	SPMS	Bronchial Pneumonia
<b>MS4</b>	53	M	12	SPMS	Advanced MS
<b>MS5</b>	60	F	22	SPMS	Myocardial Infarct
<b>MS6</b>	58	F	9	SPMS	na
<b>MS7</b>	58	M	16	SPMS	na
<b>MS8</b>	75	M	8	RPMS	Pneumonia
<b>MS9</b>	76	F	58	PPMS	Pulmonary embolus
<b>MS10</b>	46	M	7	SPMS	Pneumonia
<b>MS11</b>	51	M	21	SPMS	MS/Bronchial Pneumonia
<b>MS12</b>	59	M	18	SPMS	Bronchial Pneumonia
<b>MS13</b>	51	F	12	SPMS	na
<b>MS14</b>	47	M	14	SPMS	na
<b>MS15</b>	53	M	17	SPMS	na
<b>MS16</b>	62	M	22	SPMS	na
<b>MS17</b>	45	F	10	SPMS	na
<b>MS18</b>	60	F	29	SPMS	Bronchial Pneumonia
<b>MS19</b>	63	M	10	SPMS	na

na = Not available

DAI (h) = Death autopsy interval (hours)

SPMS = Secondary progressive MS

PPMS = Primary progressive MS

RRMS = Relapsing Remitting MS

Table 2.1. Case details of subjects used in study of adult ADHD with the OAS

Case	Age	Sex	Diagnosis	ADHD
MS19	23	M	SPMS	AD
MS10	20	F	SPMS	AD
MS17	19	F	SPMS	AD
MS16	18	M	SPMS	AD
MS18	17	M	SPMS	AD
MS14	15	M	SPMS	AD
MS15	14	F	SPMS	AD
MS13	13	F	SPMS	AD
MS20	12	M	SPMS	AD
MS21	11	M	SPMS	AD
MS22	10	M	SPMS	AD
MS23	9	F	SPMS	AD
MS24	8	M	SPMS	AD
MS25	7	F	SPMS	AD
MS26	6	M	SPMS	AD
MS27	5	M	SPMS	AD
MS28	4	F	SPMS	AD
MS29	3	F	SPMS	AD
MS30	2	F	SPMS	AD
MS31	1	F	SPMS	AD
MS32	0	F	SPMS	AD
MS33	0	F	SPMS	AD
MS34	0	F	SPMS	AD
MS35	0	F	SPMS	AD
MS36	0	F	SPMS	AD
MS37	0	F	SPMS	AD
MS38	0	F	SPMS	AD
MS39	0	F	SPMS	AD
MS40	0	F	SPMS	AD
MS41	0	F	SPMS	AD
MS42	0	F	SPMS	AD
MS43	0	F	SPMS	AD
MS44	0	F	SPMS	AD
MS45	0	F	SPMS	AD
MS46	0	F	SPMS	AD
MS47	0	F	SPMS	AD
MS48	0	F	SPMS	AD
MS49	0	F	SPMS	AD
MS50	0	F	SPMS	AD
MS51	0	F	SPMS	AD
MS52	0	F	SPMS	AD
MS53	0	F	SPMS	AD
MS54	0	F	SPMS	AD
MS55	0	F	SPMS	AD
MS56	0	F	SPMS	AD
MS57	0	F	SPMS	AD
MS58	0	F	SPMS	AD
MS59	0	F	SPMS	AD
MS60	0	F	SPMS	AD
MS61	0	F	SPMS	AD
MS62	0	F	SPMS	AD
MS63	0	F	SPMS	AD
MS64	0	F	SPMS	AD
MS65	0	F	SPMS	AD
MS66	0	F	SPMS	AD
MS67	0	F	SPMS	AD
MS68	0	F	SPMS	AD
MS69	0	F	SPMS	AD
MS70	0	F	SPMS	AD
MS71	0	F	SPMS	AD
MS72	0	F	SPMS	AD
MS73	0	F	SPMS	AD
MS74	0	F	SPMS	AD
MS75	0	F	SPMS	AD
MS76	0	F	SPMS	AD
MS77	0	F	SPMS	AD
MS78	0	F	SPMS	AD
MS79	0	F	SPMS	AD
MS80	0	F	SPMS	AD
MS81	0	F	SPMS	AD
MS82	0	F	SPMS	AD
MS83	0	F	SPMS	AD
MS84	0	F	SPMS	AD
MS85	0	F	SPMS	AD
MS86	0	F	SPMS	AD
MS87	0	F	SPMS	AD
MS88	0	F	SPMS	AD
MS89	0	F	SPMS	AD
MS90	0	F	SPMS	AD
MS91	0	F	SPMS	AD
MS92	0	F	SPMS	AD
MS93	0	F	SPMS	AD
MS94	0	F	SPMS	AD
MS95	0	F	SPMS	AD
MS96	0	F	SPMS	AD
MS97	0	F	SPMS	AD
MS98	0	F	SPMS	AD
MS99	0	F	SPMS	AD
MS100	0	F	SPMS	AD

AD = Attention Deficit Disorder  
 SPMS = Specific Phobic Disorder  
 AD/SPMS = Attention Deficit Disorder with Specific Phobic Disorder  
 PMS = Primary Obsessive Compulsive Disorder  
 OAS = Obsessive-Compulsive Anxiety Scale

mouse IgG1 (1:400, Dako) for 30 minutes at RT. Following a further 3 x 5 minute washes in PBS, sections were incubated in a streptavidin-biotin HRP-conjugated complex (SABC-Px, Dako) for 30 minutes at RT. SABC-Px was made 30 minutes prior to use to allow formation of avidin-biotin complex, by adding 45µl each of streptavidin and biotin to 5ml of PBS. Antibody affinity was detected using a commercial diaminobenzidine chromatin substrate (DAB, Dako). Sections were washed in running water and then counterstained for 45 seconds in Harris's haematoxylin, washed for 5 minutes in running tap water then dehydrated through graded ethanol. Sections were then transferred through two changes of xylene and mounted in DPX (BDH).

### *3.2.2 Indirect Immunofluorescence staining*

12µm cryostat sections were cut and mounted onto polysine coated glass slides (BDH), fixed for 10mins in either ice-cold acetone, 4% paraformaldehyde or 70% methanol. After fixation, samples were washed in PBS with the exception of the acetone fixed samples which were allowed to air-dry for 15 minutes prior to further steps. Table 3.2 provides a summary of all the primary antibodies used in this study. Sections were incubated in the primary antibody overnight at 4°C, washed in PBS, and incubated in the appropriate secondary antibody for 90mins at room temperature (RT). Monoclonal mouse 1° antibodies were detected using FITC-conjugated rabbit anti-mouse immunoglobulins (1:50, Dako) and polyclonal 1° rabbit antibodies were detected with Alexa 488 conjugated goat anti-rabbit immunoglobulins (1:500, Molecular Probes).

To determine the cellular origin of ADAM-17 expression, the following sequential dual label immunofluorescence protocol was carried out. Sections were incubated with rabbit polyclonal antibody overnight at 4°C and then detected by incubating in Alexa 568 conjugated goat anti-rabbit immunoglobulins (1:500, Molecular Probes) at RT for 90mins. Following three, 5min washes in PBS, sections were then incubated in the monoclonal antibody overnight at 4°C. Sections were washed in PBS and incubated in rabbit anti-mouse FITC (1:50, Dako) for 90 minutes at RT. Following three

Table 3.2 Summary of primary antibodies used for indirect immunofluorescence staining

Primary Antibody	Species	Target	Working Dilution	Source
HLA-DR	M	activated macrophages & microglia	1 in 100	Novocastra, Newcastle upon Tyne, UK
GFAP	M	astrocytes	1 in 100	Chemicon, Cambridge UK
GFAP	P	astrocytes	1 in 100	Dako, Cambridge, UK
TACE	P	ADAM 17	1 in 50	Abcam, Cambridge, UK
M222	M	ADAM 17	1 in 100	A kind gift from Amgen
TACE (C15)	P	ADAM 17	1 in 20	Santa Cruz, California, USA
VWF	P	endothelial cells	1 in 100	Dako, Cambridge, UK
TIMP3	M	TIMP3	1 in 100	Calbiochem, Nottingham, UK
TIMP3	M	TIMP3	1 in 50	Oncogene, California, USA
TIMP3	P	TIMP3	1 in 50	Abcam, Cambridge, UK

GFAP = glial fibrillary acidic protein  
VWF = Von Willebrand Factor  
M = mouse monoclonal antibody  
P = rabbit polyclonal antibody



5min washes in PBS, sections were mounted in Vectorshield mount with DAPI (Vector labs).

As a control during dual staining, serial sections were single label immunostained for each primary antibody to ensure that no cross reaction was observed when using two secondary antibodies. Omission of either primary antibody from the protocol resulted in no signal detection in the channel used to detect that antigen.

#### *3.2.2.1 Semi quantitative analysis of ADAM-17 immunoreactivity*

All blocks investigated in this study were coded and evaluated for the extent of ADAM-17 immunoreactivity by two blinded investigators. The following scoring system was applied; + when ADAM-17 immunoreactivity was associated to cerebral blood vessels; ++ when blood vessel immunoreactivity was present in the presence of distinct astrocytic immunoreactivity; +++ when there was an abundance of ADAM-17 immunoreactivity throughout the section.

#### *3.2.2.2 Tyramide Signal Amplification*

A tyramide signal amplification kit (Molecular Probes) was used to localise TIMP3 within normal control and MS white matter. Sections were fixed in 4% paraformaldehyde for 20 mins at RT then washed through 2 x 5 minute washes in PBS. Endogenous peroxidase was then quenched by incubating sections in 0.5% H<sub>2</sub>O<sub>2</sub> in methanol for 10 mins at RT. Following 5 minute washes in running tap water and then PBS, sections were incubated in blocking reagent for 1 hour at RT. Sections were then incubated in primary antibodies to TIMP3, diluted in 1% blocking reagent, overnight at 4°C. Following 3 x 5 minute washes in PBS, sections were incubated in HRP conjugate for 45 mins at RT. Following 3 x 5 minute washes in PBS, sections were incubated in Alexa 488-conjugated tyramide working solution for 10 mins at RT. Sections were washed, counterstained in propidium iodide and mounted in citifluor as described in section 2.2.2.1.

### 3.2.3 Imaging

#### 3.2.3.1 Confocal Scanning Laser Microscopy

Immunofluorescent images were acquired using a Zeiss 510 confocal scanning laser microscope equipped with a krypton/argon laser as the source of the ion beam. Acquiring the optimal amount of optical sections in the Z-plane (as gauged by Zeiss 510 CSLM software) and running the series-scanning mode from the deepest focus point to the highest focus point, allowed a projected image and data set to be generated from which composite projected images were exported as high quality JPEGs without further manipulation

#### *Co-localisation*

Analysis of all dual stained sections was carried out using the Zeiss 510 CSLM software. This software examines each individual pixel for emission in each fluorescent channel, where co-localisation occurs that pixel is displayed as white on the composite image and in the upper right quadrant of the spectra graph (See results and appendix).

#### 3.2.3.2 Digital photography

Light microscope images were obtained using a Coolsnap-Pro<sub>cf</sub> digital image camera (Media Cybernetics) attached to an Olympus BX60 upright fluorescent microscope. Images were acquired using the labworks software and saved as high quality JPEGs. The Leica digital camera was utilized to enable capture of comparable fields of view between anti-HLA-DR, ORO and anti-ADAM-17 (fluorescence) stained sections.

#### 3.2.4 Protein and RNA extraction

5 x 30µm cryosections from each of 12 MS and 7 control blocks were collected in pre-cooled Eppendorfs (-20°C). Protein and RNA was extracted using 1ml of Tri Reagent<sup>TM</sup> (Sigma) following the manufacturer's protocol (See Appendix).

#### 3.2.4.1 Bicinchoninic acid (BCA) Assay

The BCA assay was used to determine the amount of protein present in the extracted samples (Smith et al., 1985). Protein samples were resuspended in 200µl of 1% SDS. 20µl duplicates of bovine serum albumin protein standards (ranging from 0.1-2mg/ml) were added to a 96 well plate along with 20µl of each protein sample in triplicate. 200µl of copper II sulphate BCA solution (Sigma, Poole, UK) was added to each well and the plate incubated at RT for 30 minutes. Absorbance spectrophotometry was carried out at 570nm (Wallac). Protein concentrations for each sample were calculated from the trend line of the standard curve using the equation:  $Y=mx + c$  using Microsoft Excel (See appendix).

#### 3.2.5 SDS PAGE and Western blotting

##### *Principles of method*

Sodium dodecyl sulphate (SDS) polyacrylamide gel electrophoresis (PAGE) is a technique used to separate a mixture of proteins by their size using an electrical current. SDS is a detergent that denatures and applies a negative charge to individual proteins. SDS is important as proteins of similar size (molecular weight) but with different tertiary structure would migrate different distances through the gel. Denaturing the proteins allows protein separation based on protein length (number of amino acids). The gel in SDS-PAGE refers to the matrix used to separate the proteins. Gels can be made of different concentrations of acrylamide with a cross linker to form a solid but porous polyacrylamide mesh network. Electrophoresis refers to the electromotive force that pushes or pulls the molecules through the gel matrix. An electrical current is passed across the polyacrylamide gel and the negatively charged samples migrate through the gel towards the positive electrode. SDS binds to proteins in a consistent ratio of 1.4:1 SDS:protein, therefore the amount of bound SDS is relative to the size of the protein. The distance migrated through the gel is directly related to the size of the protein due to the constant mass to charge ratio. The smaller proteins migrate further through the gel with the larger proteins remaining towards the top of the gel. Marker proteins, of known molecular weights, are loaded into a lane

adjacent to the samples to allow calculation of the molecular weights of the samples (See Appendix).

Western blotting is a method of detecting specific proteins in a complex mixture of proteins separated by SDS-PAGE based on the principles described in immunohistochemistry (section 2.2.2.1). Following SDS-PAGE, proteins are transferred or blotted onto a nitrocellulose membrane by applying an electrical current. The nitrocellulose membrane is “sticky” and binds all proteins equally. Blotted membranes must be blocked in 5% non-fat milk solution to saturate any free protein binding sites, in order to prevent any non-specific binding of primary antibody to the membrane. Primary and secondary antibodies are applied to the membrane following the principles described in section 2.2.2.1.

### *Method*

Extracted protein samples were added to sample buffer consisting of 50% 4x concentrate NuPAGE LDS sample buffer, 20% sample reducing agent (Invitrogen) and 30% distilled H<sub>2</sub>O (1:1 v/v) and then denatured by heating at 60°C for 30 minutes. 20µl of each sample were loaded into wells and separated by SDS-polyacrylamide gel electrophoresis on 10% pre-cast bis/tris gels (Invitrogen) at 150V for 1 hour using a Novex Mini-cell gell tank (Invitrogen). SeeBlue Plus2 pre-stained standard (Invitrogen) molecular weight markers (range 191-14 kDa) were included in each run.

Proteins were transferred onto nitrocellulose membranes (Hybond-C, Amersham) at 150V for 1 hour. Membranes were blocked overnight in 5% non-fat milk TBS-tween (Tris-buffered saline containing 0.02% Tween-20) solution at 4°C. Membranes were incubated in primary antibody for 1 hour at RT (polyclonal TACE, 1:500, Abcam, or monoclonal TIMP3, 1:1000, Oncogene). Following 3 washes in TBS-tween, membranes were incubated in either peroxidase-conjugated rabbit anti-mouse (1:1000, Dako,) or goat anti-rabbit (1:80,000, Sigma) immunoglobulins for 90 minutes at RT. All antibodies were diluted in 5% blocking solution.

Immunoreactivity was detected by chemiluminescence by incubating membranes in ECL reagent kit (Amersham) for five minutes at RT. Excess

ECL reagent was removed and membranes were placed in clear plastic envelopes and visualised using a UVP Bioimaging system attached to a computer with Labworks software (Bio-Rad). Membranes were exposed 10 times each over 90 seconds and an image series was obtained.

### 3.2.6 mRNA analysis

#### 3.2.6.1 Reverse transcriptase PCR

##### *Principles of method*

Reverse transcriptase-polymerase chain reaction (RT-PCR) refers to a technique that transcribes RNA into complementary DNA (cDNA) which can then be amplified by the polymerase chain reaction. The original PCR technique was designed by Kay Mullis and patented by the Cetus Corporation in 1986 as a result Kay Mullis was awarded the Nobel Prize for chemistry in 1993. The classical PCR technique can only be applied to DNA strands. Reverse transcriptase is an enzyme from retroviruses that transcribes the genetic information from RNA to DNA. The enzyme works on a single strand of RNA and generates a complementary DNA (cDNA) based on the pairing of RNA bases (A, U, G, C) to their DNA complements (T, A, C, G).

PCR is a method of producing multiple copies (amplifying) of DNA. Amplification of PCR products is exponential with the first cycle producing 2 copies, the next 4, the next 8, then 16 copies and so on. The DNA fragment to be amplified is determined by the use of specific primers. Primers are artificial oligonucleotide strands that match the beginning and end of the DNA fragment to be amplified. Heating double stranded DNA to 96°C breaks the hydrogen bonds separating the two strands. Another enzyme is required to create new copies of DNA, due to the high temperature required to separate the DNA this enzyme must be thermostable. The first thermostable DNA-polymerase was obtained from *Thermus aquaticus* and was named Taq polymerase. Once the DNA strands are separated the temperature is reduced to allow the primers to adhere (anneal) to the beginning and end of the DNA fragment, the Taq polymerase then binds and begins to synthesise copies of the new DNA strand.

### *Primers*

Paired forward and reverse primers are used in each reaction to amplify the double stranded DNA fragment. There are a number of considerations to be taken into account when using primers. The melting temperature ( $T_m$ ) of primers is defined as the temperature below which the primer will anneal to the DNA template and above which the primer will dissociate from the DNA template. The  $T_m$  of individual primers used should not differ by more than  $10^\circ\text{C}$ . Primers are usually small ideally 18-25 base pairs (bp), the  $T_m$  increases with increasing primer size. The annealing temperature of the primers should be approximately  $5^\circ\text{C}$  below the  $T_m$ . The GC content of primers should be approximately 40-60%.

### *Agarose gel electrophoresis*

The DNA PCR products can be identified by loading onto an agarose gel and subjecting them to electrophoresis. An electrical current is passed through the gel, separating DNA products based on size. Unlike proteins, DNA PCR products naturally migrate due to the negative charge carried on their sugar-phosphate backbone. PCR product size can be determined by running a DNA ladder of known size in the gel along side the samples. The agarose gels are normally stained with ethidium bromide, a dye that binds to double stranded DNA and fluoresces under ultraviolet radiation.

### *Method*

RNA was reverse transcribed to cDNA using Superscript II RT (Invitrogen, Paisley, Scotland) with poly-dT primers. The PCR-amplification of the cDNA was achieved using commercially available primer pairs for ADAM-17, TIMP3 and GAPDH (R&D Systems) and the conditions used were according to the manufacturer's protocol (see appendix), using Taq polymerase (Invitrogen) and an annealing temperature of  $55^\circ\text{C}$  using a Biometra trio-thermoblock (Biometra, UK). The amplified PCR products were analyzed on ethidium bromide stained 1% agarose gel. Product size was determined using a 100bp DNA ladder (Invitrogen). Gel images were obtained using a UVP Bioimaging system (Bio-Rad).

### 3.3 Results

#### 3.3.1 Tissue characterisation

To assess the extent of recent myelin breakdown and cellular activation within the active blocks, a 3 point grading system was applied to the ORO and HLA-DR staining (Table 3.3). Characterisation of the 42 MS blocks investigated revealed that 14 contained active lesions, 11 had chronic lesions and 17 were from NAWM. In the active lesion areas, 6 MS blocks displayed scattered isolated ORO-positive cells (Grade +) while 6 had in addition one or more foci or clusters of ORO-positive cells (Grade ++). In 2 blocks however, ORO-positive cells were abundant throughout the entire section (Grade +++), as detailed and illustrated in section 2.3.2 and Figure 2.5a-c.

HLA-DR immunoreactivity was graded as described and illustrated in section 2.3.2 and Figure 2.5d-f. 12 of the MS samples and one of the OND samples displayed a widespread level of HLA-DR immunoreactivity in the presence of foamy macrophages (Grade +++), 21 MS, 2 OND and 1 control samples displayed distinct foci of immunoreactivity (Grade ++), the remainder of the control samples and 8 of the MS samples, displayed a low level of activity associated with individual parenchymal microglia (Grade +). None of the samples used were classified as negative for HLA-DR immunoreactivity. 3 chronic lesion blocks, one of the active and 5 blocks from the NAWM displayed HLA-DR staining of scattered, isolated microglia (Grade +). Five of the active lesions, 6 of the chronic lesions and 10 of the NAWM blocks displayed HLA-DR immunostaining that was diffuse and widespread (Grade ++), which involved either parenchymal process-bearing cells or cells in small perivascular infiltrates. An abundance of large HLA-DR positive cells corresponding to foamy macrophages observed on H&E staining, were detected in both parenchymal and perivascular distributions in 14 of the active lesion, 2 of the chronic lesion and 2 of the NAWM blocks (Grade +++), (Table 3.3).

Table 3.3 Individual block characterisation for lesion activity and ADAM-17 expression

Block ID	ORO	HLA-DR	ADAM-17	Characterisation
MS122 A4E5 lesion	-	+++	++	Chronic
MS18 lesion	-	+	+++	Chronic
MS 18 P2C2	-	+	++	Chronic
MS100 4/B6	-	+++	+++	Chronic
MS 21 NAWM	-	++	++	Chronic
MS 21 Lesion	-	++	+	Chronic
MS 22 Lesion	-	++	+	Chronic
MS 22 A1B3	-	++	+	Chronic
MS3 (104/97 79 94)	-	++	++	Chronic
MS3 (104/97 75 94-009)	-	++	++	Chronic
MS3 (104/97 75 94)	-	+++	++	Chronic
MS104 P2A3	+	++	+++	Active
MS104 12/D7	++	+++	+++	Active
MS 56 P4D3	++	++	+++	Active
MS 22 NAWM	+++	+++	+++	Active
MS 109 1a3c2	+	+	++	Active
MS122 A1D7 lesion	+	+++	++	Active
MS127 L12C8	++	+++	+++	Active
MS2 (103/97 91-307)	++	++	++	Active
MS2 (103/97 93-308)	+	+++	+++	Active
MS3 (104/97 75 92-56)	++	++	++	Active
MS4 (105/97 94-110)	++	++	+++	Active
MS4 (105/97 80 92-187)	+	+++	+	Active
MS 5 (106/97 84B 91.172)	+	+++	+++	Active
MS 6 (107/97 944 cBrBr)	+++	+++	+++	Active
MS104 P2C1	-	+	+	NAWM
MS 45 P2C3	-	+	+++	NAWM
MS 49 P2C2	-	+	+	NAWM
MS 49 P2C4	-	+	+++	NAWM
MS1 (25/01a)	-	++	+	NAWM
MS1 (25/01b)	-	++	+	NAWM
MS1 (25/01c)	-	+	+	NAWM
MS2 (103/97 78 94-256)	-	++	++	NAWM
MS2 (103/97 78 91-230)	-	++	++	NAWM
MS3 (104/97 75 93-288)	-	++	++	NAWM
MS3 (104/97 75 92-187)	-	+++	++	NAWM
MS4 (105/97 80 91-182)	-	++	+++	NAWM
MS7 (10/99a)	-	++	++	NAWM
MS8 (102/97 186 95-339)	-	++	++	NAWM
MS8 (102/97 186 95-549)	-	++	+	NAWM
MS8 (102/97 186A 96-102)	-	+++	++	NAWM
MS8 (102/97 186 96-37)	-	++	++	NAWM



Table 3.4 Description and distribution of scoring for cellular activation within the MS tissue samples studied.

<i>Stain</i>	<i>Grade</i>	<i>Description</i>	<i>Active Lesion</i>	<i>Chronic Lesion</i>	<i>NAWM</i>
<b>ORO</b>	+	Sparse +ve cells	6	0	0
	++	Diffuse small foci +ve cells	6	0	0
	+++	Abundance of +ve cells throughout	2	0	0
<b>HLA-DR</b>	+	Sparse single +ve microglia	1	3	5
	++	Foci of +ve microglia and foamy macrophages	5	6	10
	+++	Abundance of +ve cells throughout	8	2	2

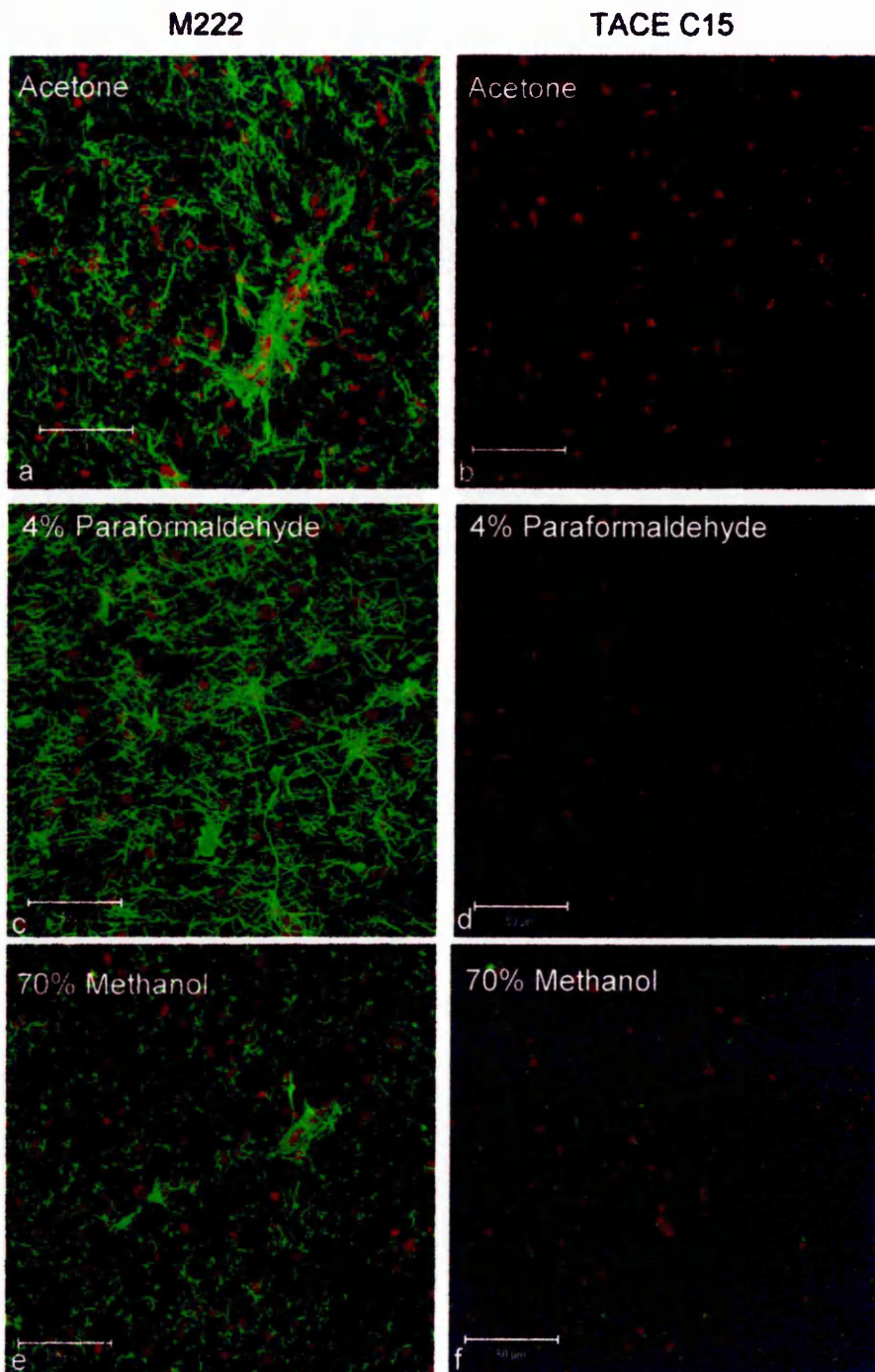


### 3.3.2. ADAM-17 immunoreactivity within control and MS white matter

ADAM-17 immunoreactivity was detected following ice-cold acetone, 4% paraformaldehyde or 70% methanol fixation to assess optimal technique. Fixation of sections with 70% methanol provided a restricted ADAM-17 expression in glial cell processes within the parenchyma. To allow efficient dual label immunofluorescence, acetone fixation was chosen as the optimal fixative for the study of ADAM-17 in snap frozen human autopsy material.

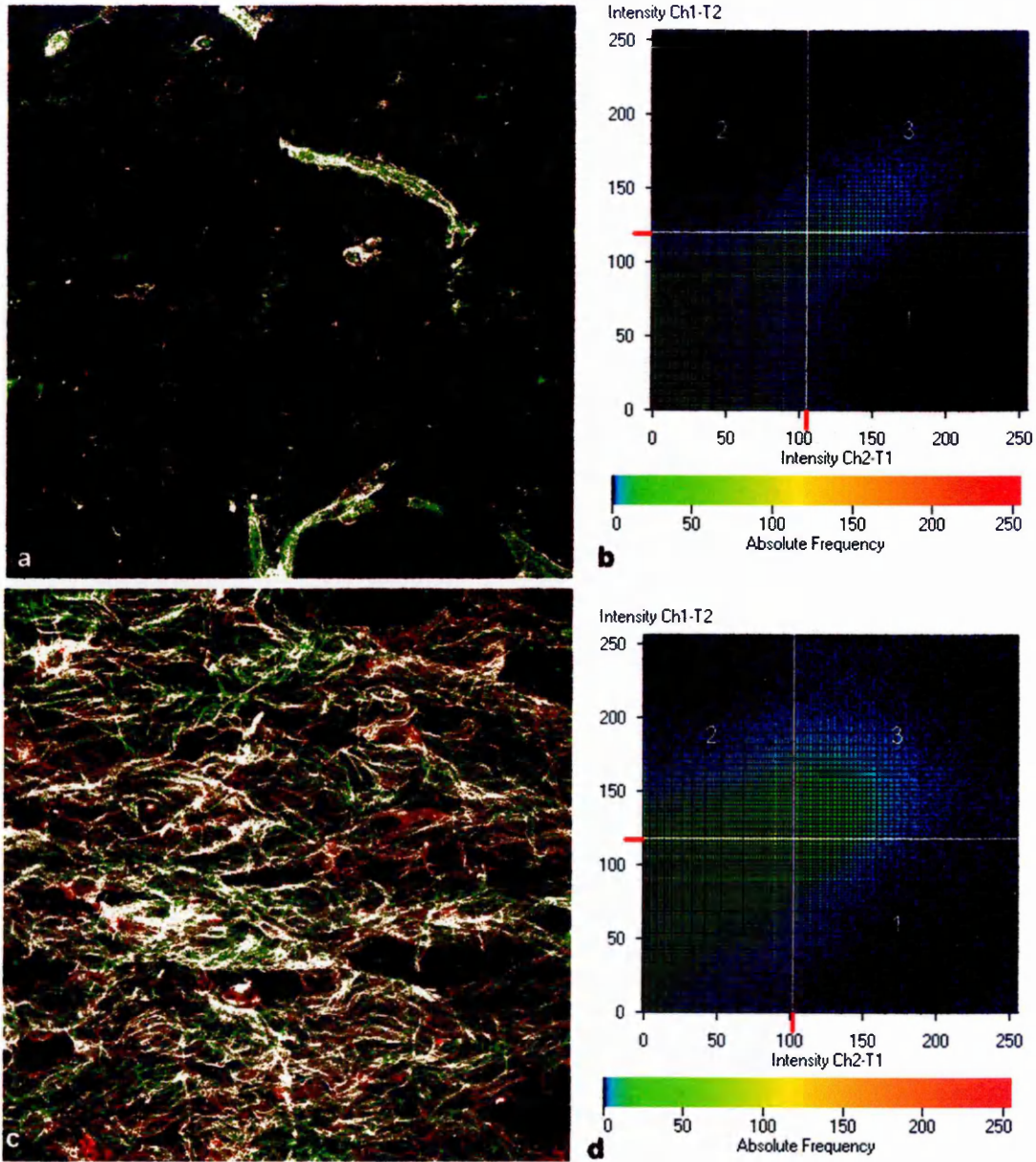
No immunoreactivity was observed for the polyclonal TACE (C15) antibody (Santa Cruz) using indirect immunofluorescence following any of the fixation methods used (Figure 3.1). ADAM-17 immunoreactivity was consistently demonstrated using both monoclonal anti-ADAM-17 (M222, Amgen) and polyclonal anti-TACE (Abcam) antibodies. Dual label immunofluorescence for the polyclonal anti-TACE and the monoclonal anti-ADAM-17 confirmed that these antibodies co-localised (Figure 3.2). ADAM-17 immunoreactivity was detected in all 60 samples of MS, OND and normal control brain tissue studied. ADAM-17 immunostaining appears heterogeneous in its distribution both between samples and within the same sections. ADAM-17 immunoreactivity was detected within normal control and MS white matter associated with the blood vessels and parenchymal glial cells (Figure 3.3). ADAM-17 immunoreactivity was also detected within the grey matter of both MS and controls, which was only associated with vasculature and did not vary between sections (Figure 3.3). ADAM-17 was observed within a few cells in occasional perivascular cuffs within inflammatory MS areas (Figure 3.3). Due to the varying extent of ADAM-17 immunoreactivity within MS and control white matter, blinded scoring of the level of ADAM-17 immunoreactivity (Grade +, ++, +++) was carried out on each sample by two independent observers (Figure 3.4). 60% of the normal control samples displayed ADAM-17 expression only associated with the blood vessels (Grade +) whilst the remaining 40% showed a low level of astrocytic immunoreactivity along with the blood vessel staining (Grade ++). Samples displaying an abundance of parenchymal ADAM-17 staining (Grade +++) were only found in MS samples. Abundant grade +++ ADAM-17 staining was predominantly observed within active lesions (Figure 3.5) where

**Figure 3.1 Comparison of immunostaining for ADAM-17 using different fixatives and antibodies**



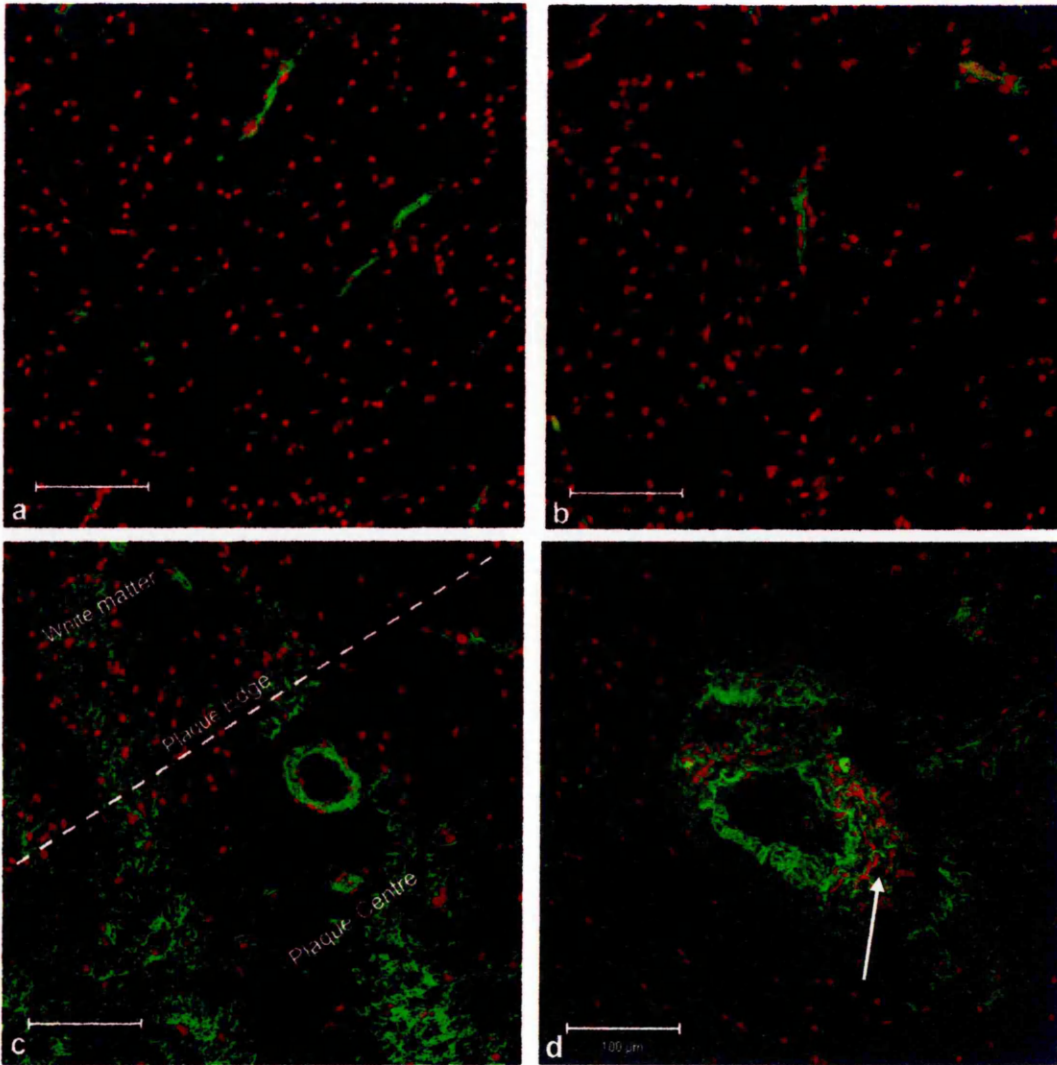
CSLM images comparing immunoreactivity for two ADAM-17 (Green) antibodies M222 (a, c, e) and TACE (C15) (b, d, e) after fixation in acetone (a, b), 4% paraformaldehyde (c, d) and 70% methanol (e, f). Note the reduced expression of M222 after methanol fixation. Nuclei are counter stained with propidium iodide (Red). Scale bar = 50 $\mu$ m.

Figure 3.2 Co-localisation of the monoclonal (Amgen) and polyclonal (Abcam) antibodies to ADAM-17



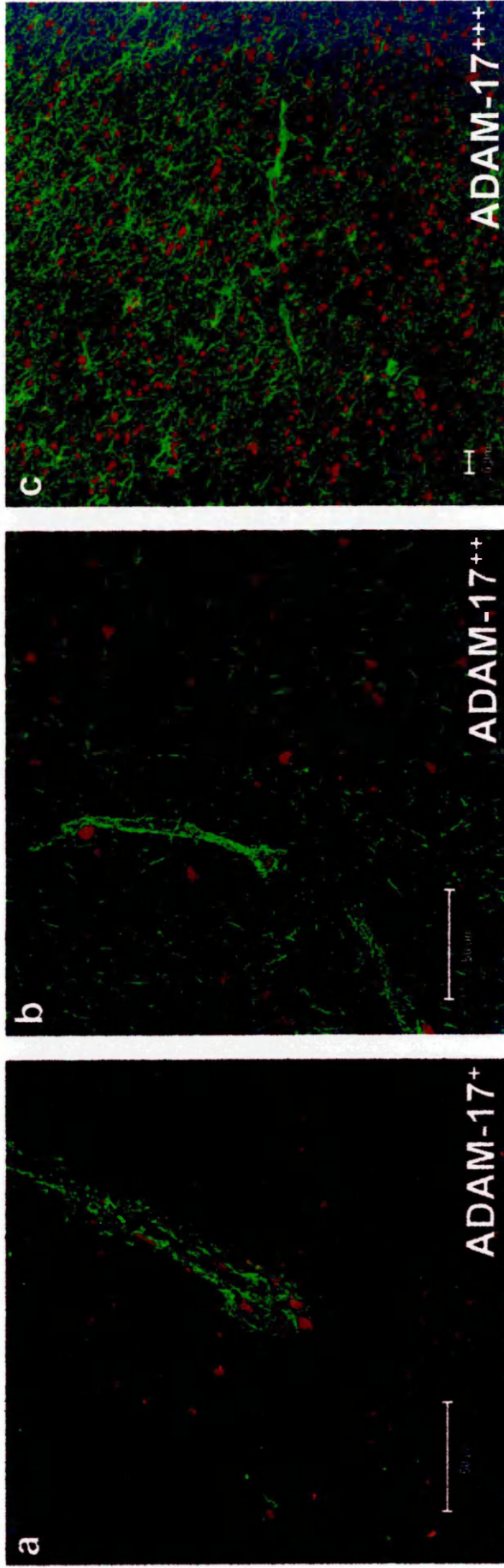
Dual label immunofluorescence for M222 (Green) and TACE (Red) demonstrating an overlap in fluorescent signal in blood vessels (a) and astrocytic processes (c). Co-localisation is demonstrated as white pixels on the composite images (a, c) and represented by the pixels in quadrant 3 (b, d) following Zeiss 510 CSLM software reading of individual pixels for each fluorophore. Mag x400

Figure 3.3 ADAM-17 expression within control and MS CNS tissue



ADAM-17 immunoreactivity (Green), using the M222 anti-ADAM-17 monoclonal antibody, was observed within both control and MS white matter (a, c) to various extents but was only observed consistently in blood vessels within the grey matter (b). ADAM-17 expression was observed within MS lesions (c) and was observed to be expressed by a small number of cells within perivascular cuffs in MS white matter (d). Cell nuclei are counterstained with propidium iodide (Red) Scale bar = 100µm

Figure 3.4 ADAM-17 immunoreactivity grading system



CSLM images of ADAM-17 immunoreactivity (Green) within control (a) and MS white matter (b, c). ADAM-17 immunoreactivity was graded as a. + only associated to the blood vessels, b. ++ associated with blood vessels and surrounding astrocytes, and c. +++ an abundance throughout the tissue. Cell nuclei are counter stained with propidium iodide (Red). Scale bar = 50µm (a, b) 20µm (c).

64.3% of the active lesions in the study were graded +++ for ADAM-17 staining. High levels of ADAM-17 expression were observed in lesional areas that were high in lipid laden activated macrophages (Figure 3.6).

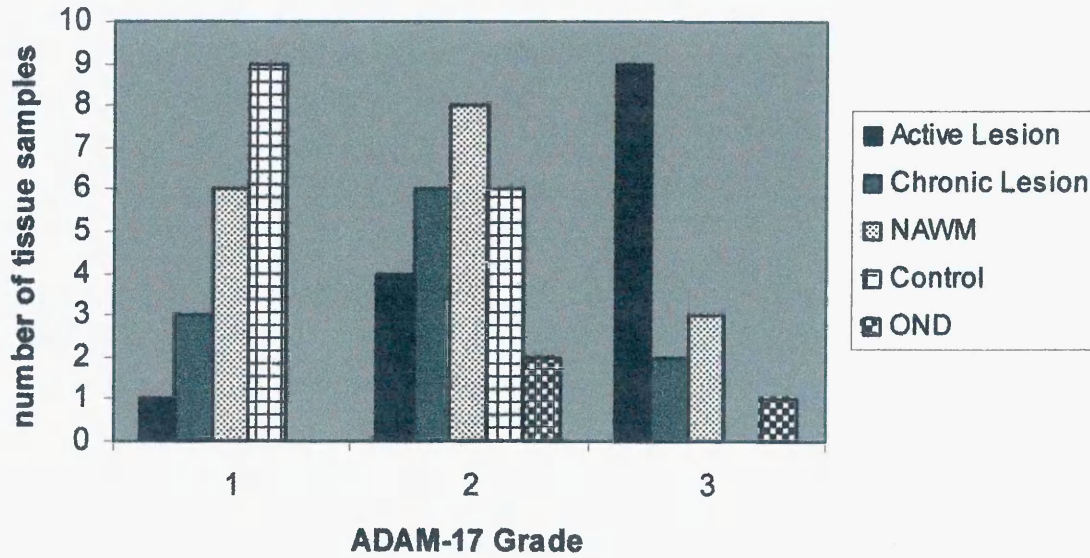
#### *Cellular localisation of ADAM-17 within control white matter and MS tissue*

Upon morphological examination, ADAM-17 expression appeared to be associated with the cell body and the elongated processes of parenchymal astrocytes. There was also a high level of blood vessel associated ADAM-17 expression, which appeared to be both endothelial and astrocytic-end-feet in origin. To determine the exact cellular distribution of ADAM-17, dual label immunofluorescence was carried out with monoclonal mouse anti-ADAM-17 (M222) and rabbit anti-GFAP or rabbit anti-VWF, for identification of astrocytes and endothelial cells respectively. Dual labelling was also carried out with polyclonal anti-TACE antibody and monoclonal anti-HLA-DR to identify activated macrophage/microglia cells. Utilisation of the Zeiss 510 software enabled individual pixels to be scanned and designated a white colour if true co-localisation existed between the two channels of interest. Co-localisation was observed with ADAM-17 and the cerebral vascular endothelium (Figure 3.7) and the surrounding parenchymal astrocytes and end-feet processes (Figure 3.8). Co-localisation was also observed in the foamy macrophages and activated microglia in MS lesions (Figure 3.9). Co-localisation of the endothelial and astrocytic phenotypic markers with M222 and the macrophage/microglia marker with TACE, provides definitive evidence of ADAM-17 expression being produced by astrocytes, endothelial cells and activated macrophage/microglia within MS tissue.

#### *3.3.3 TIMP3 immunoreactivity in control and MS white matter*

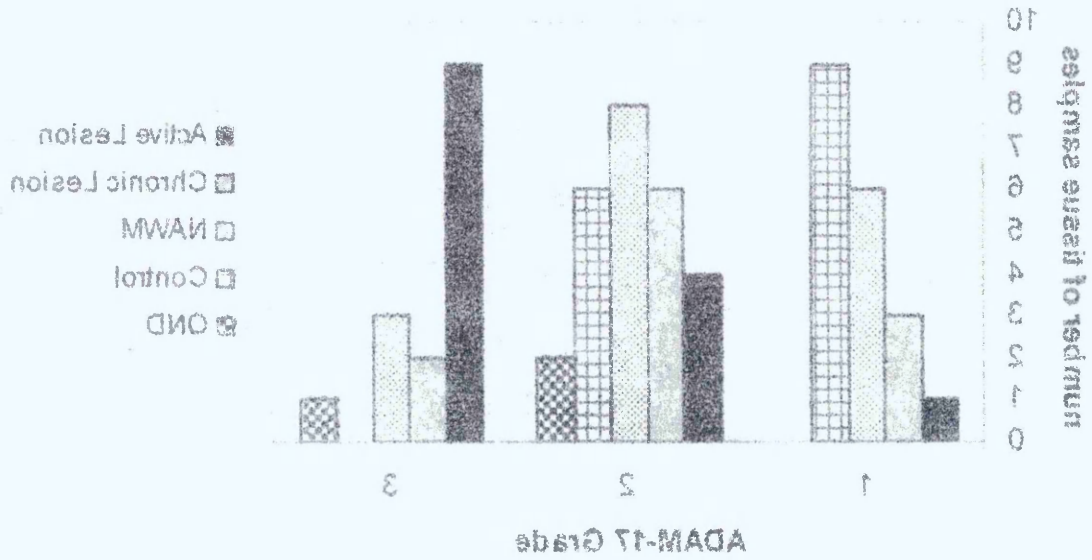
Immunofluorescence was carried out following the application of three different commercially available antibodies to determine the cellular location of TIMP3 protein expression. However TIMP3 immunoreactivity appeared to be at a level that is below the detection threshold of the three techniques

Figure 3.5 Extent of ADAM-17 immunoreactivity in active and chronic MS lesions, MS NAWM and control and OND white matter



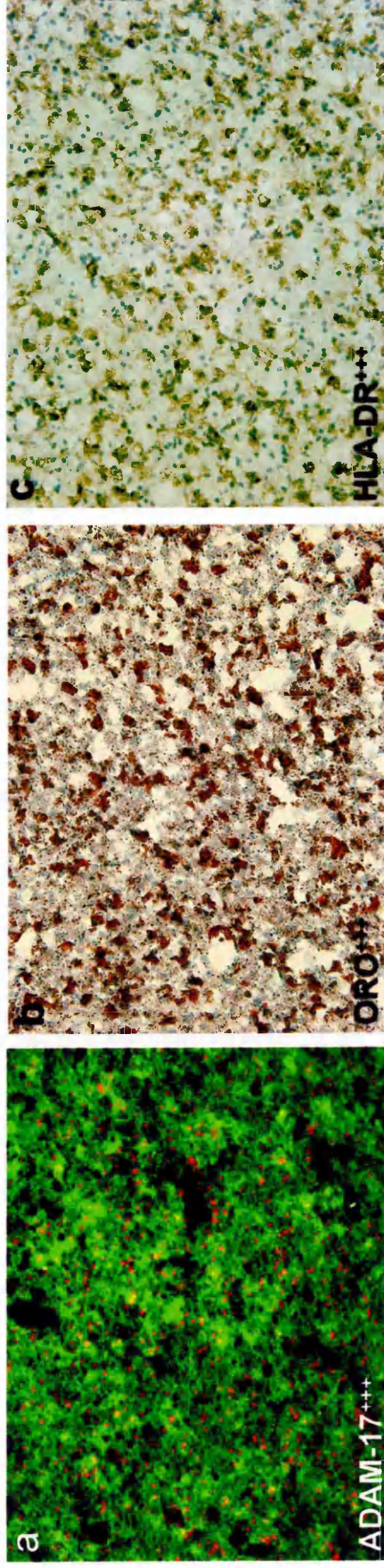
The extent of ADAM-17 immunoreactivity across the 5 categories of tissue investigated within the study. Note highest level of ADAM-17 expression (grade 3) is predominantly observed in the active lesions (9/14 blocks).

Figure 3.5. Extent of ADAM-17 immunoreactivity in active and chronic MS lesions. MS NAWM and control and OND white matter



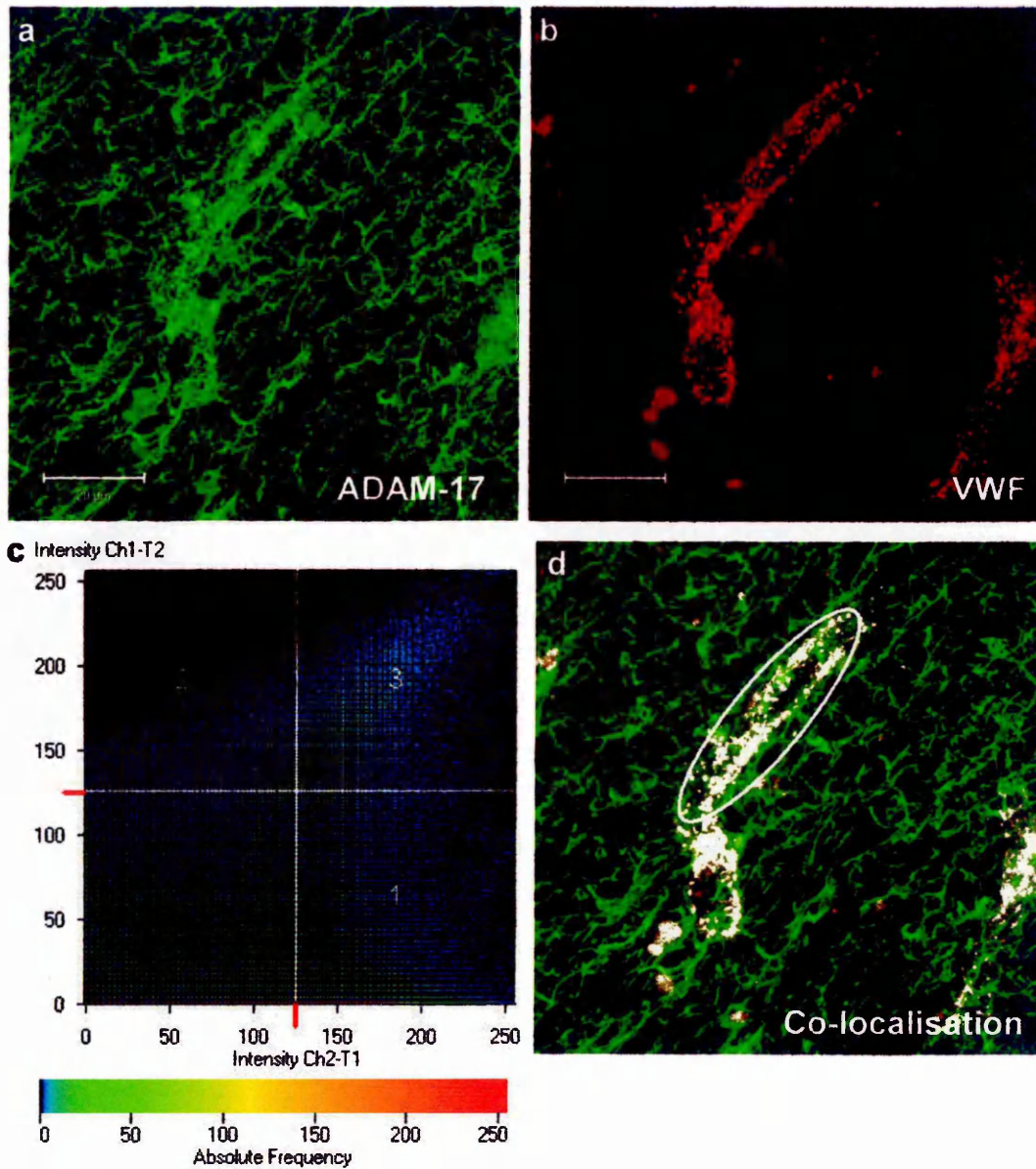
The extent of ADAM-17 immunoreactivity across the 5 categories of tissue investigated within the study. Note highest level of ADAM-17 expression (grade 3) is predominantly observed in the active lesions (9/14 blocks).

Figure 3.6 Expression of ADAM-17 in lesions displaying active disease process



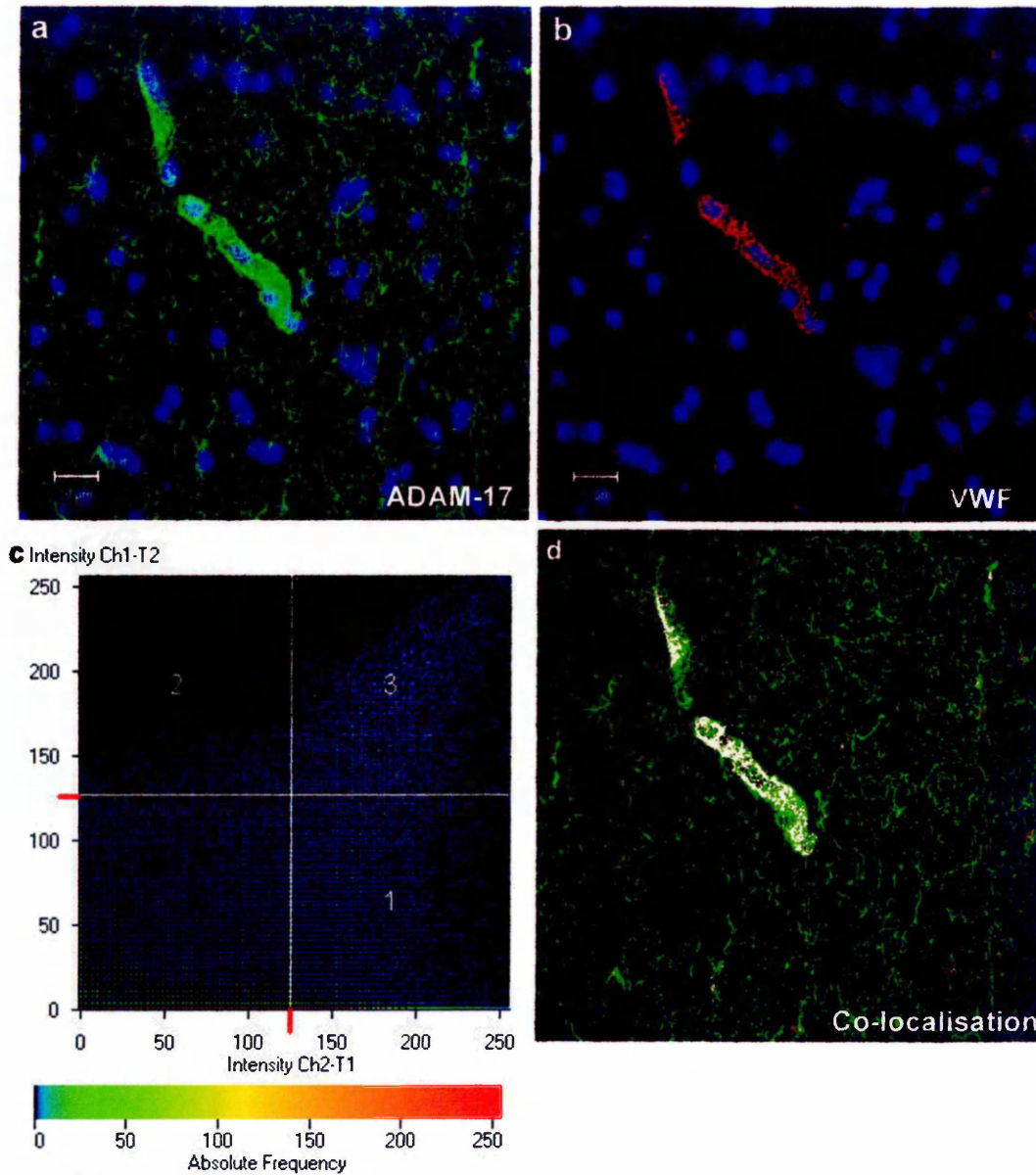
High levels of ADAM-17 immunoreactivity (a) was observed in active lesions with an abundance of ORO (b) and HLA-DR (c) positive macrophages. ADAM-17 immunoreactivity appeared morphologically to be associated with the foamy macrophages of the lesions. Images taken from serial sections. Cell nuclei are counter stained with propidium iodide (a) and haematoxylin (b, c)  
Magnification x200

Figure 3.7a ADAM-17 co-localisation with the endothelial marker, von Willebrand factor



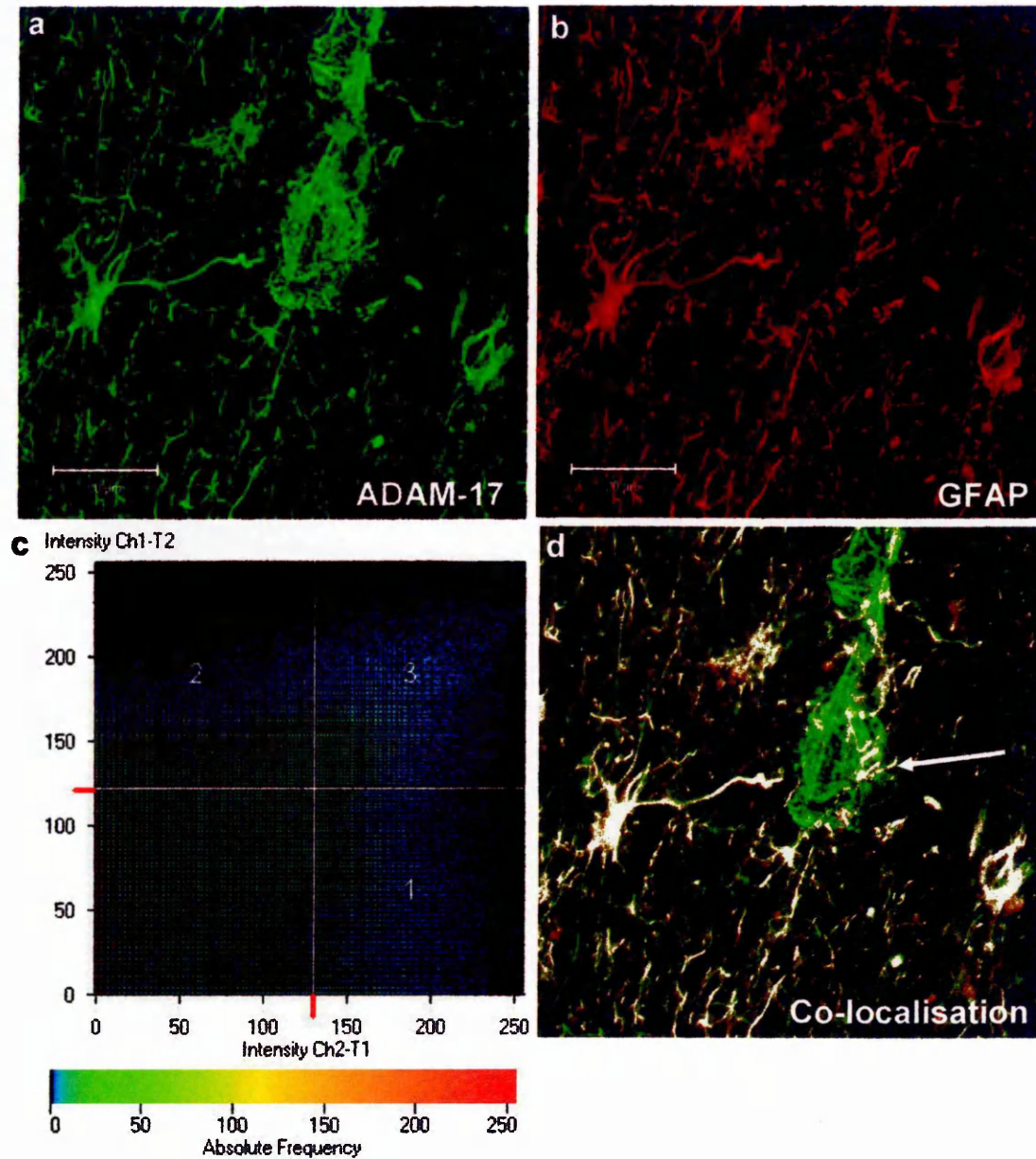
Dual label immunofluorescence for (a) ADAM-17(Green) and (b) von Willebrand factor (Red) in MS white matter with a high level of parenchymal ADAM-17 immunoreactivity. (c) Co-localisation is represented by the pixels in quadrant 3 on graph and is demonstrated as white pixels in the composite image (d) following Zeiss 510 CSLM software reading of individual pixels for each fluorophore. Bar = 20μm

Figure 3.7b ADAM-17 co-localisation with the endothelial marker, von Willebrand factor



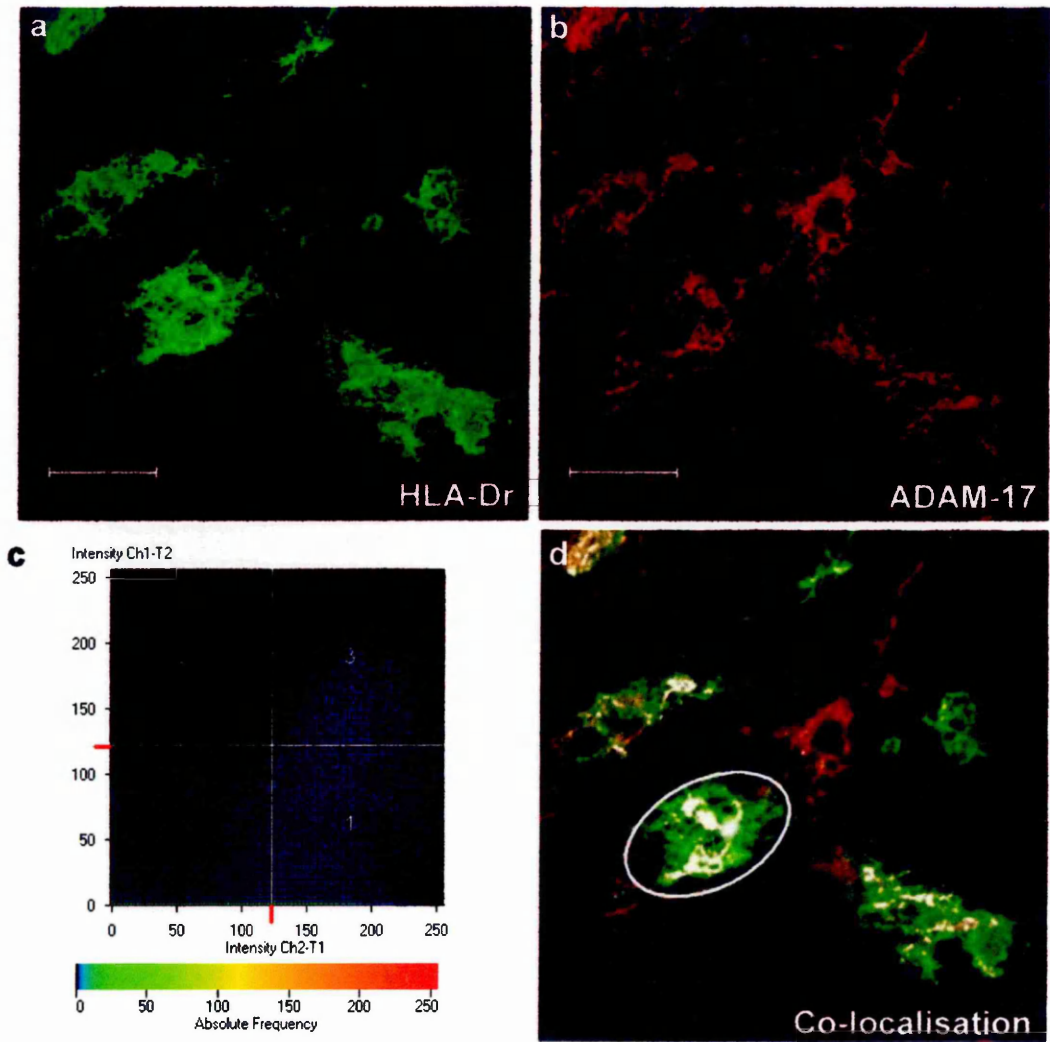
Dual label immunofluorescence for (a) ADAM-17(Green) and (b) von Willebrand factor (Red) in MS white matter with a low level of parenchymal ADAM-17 immunoreactivity. (c) Co-localisation is represented by the pixels in quadrant 3 on graph and is demonstrated as white pixels in the composite image (d) following Zeiss 510 CSLM software reading of individual pixels for each fluorophore. Cell nuclei are counter stained with DAPI (Blue a&b). Bar = 20µm.

Figure 3.8 ADAM-17 co-localisation with the astrocytic marker GFAP



Dual label immunofluorescence for (a) ADAM-17(Green) and (b) GFAP (Red) in MS white matter. (c) Co-localisation is represented by the pixels in quadrant 3 (c) and demonstrated as white pixels on the composite image (d) following Zeiss 510 CSLM software reading of individual pixels for each fluorophore. Note blood vessel associated ADAM-17<sup>+</sup> and GFAP<sup>+</sup> astrocytic end feet (arrow).  
Bar = 20μm

Figure 3.9 ADAM-17 co-localisation with MHC class II expressing microglia and macrophages



Dual label immunofluorescence for (a) HLA-Dr (Green) and (b) ADAM-17 (Red) in MS white matter. (c) Co-localisation is represented by pixels in quadrant 3 and demonstrated as white pixels in the composite image (d) following Zeiss 510 CSLM software reading of individual pixels for each fluorophore. Bar = 20µm.

used, indirect immunofluorescent, SABC immunoperoxidase and tyramide fluorescent amplification techniques as no TIMP3 was detected.

#### *3.3.4 Western blot analysis of ADAM-17 and TIMP3 in CNS tissue from MS and control*

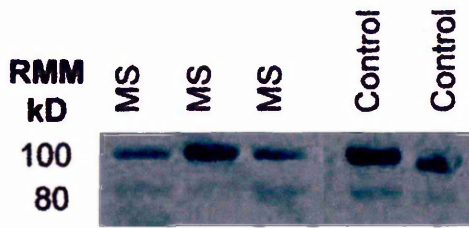
Western blotting of protein samples obtained from CNS tissue homogenates provides evidence that ADAM-17 and its natural inhibitor TIMP-3 are constitutively expressed within MS and normal control CNS tissue (Figure 3.10). M222 antibody stains bands at 80kDa and 100kDa representing the active and pro forms of ADAM-17 respectively (Hurtado *et al.*, 2001, Peiretti *et al.*, 2003), with the proform predominating in both control and MS tissue. Anti-TIMP3 antibody revealed a single band at approximately 48kDa corresponding to either a dimer of the mature form of the protein (Langton *et al.*, 1998) or a stable complex formed between TIMP3 and ECM ligands (Jaworski and Fager 2000). As variations in the extent of ADAM-17 immunoreactivity were detected within the white matter and not the grey matter no quantitation of protein samples were carried out due to the varying amount of grey and white matter in the tissue blocks used.

#### *3.3.5 Identification of ADAM-17 and TIMP3 mRNA in MS and normal control CNS tissue*

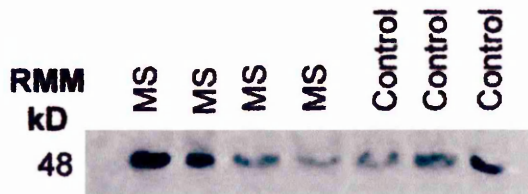
RT-PCR revealed mRNA for ADAM-17 (Figure 3.11) and TIMP3 (Figure 3.12) were present in all MS and control samples tested. ADAM-17 and TIMP3 PCR products were observed at 527bp and 442bp with the positive controls at 380bp and 340bp respectively, as indicated by the manufacturer, in all MS and normal control samples investigated.

Figure 3.10 Western blot analysis of ADAM-17 and TIMP3 protein expression in MS and control white matter

**a. ADAM-17**

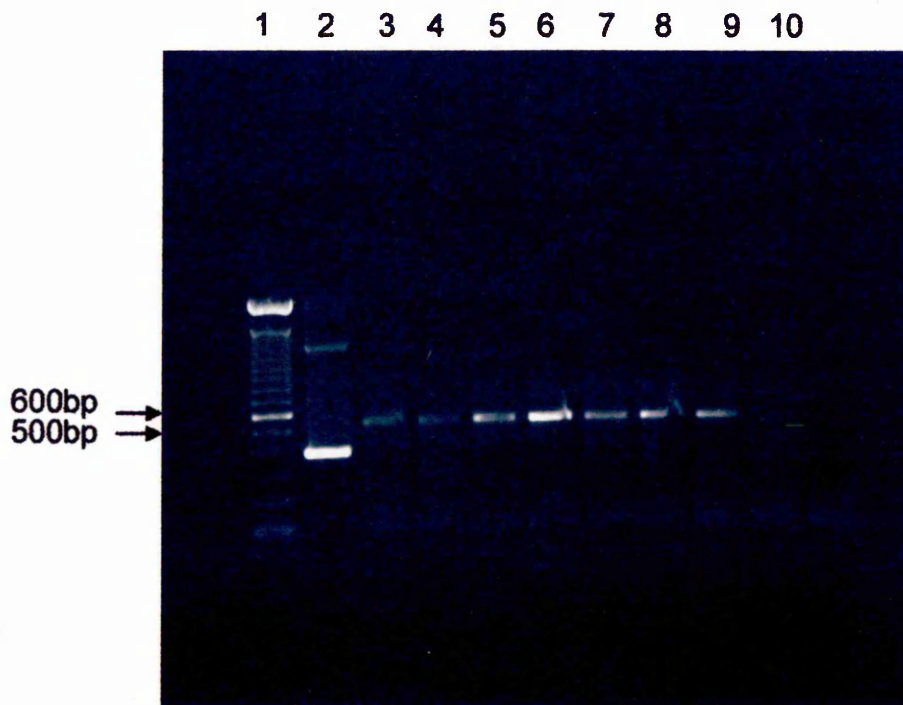


**b. TIMP3**



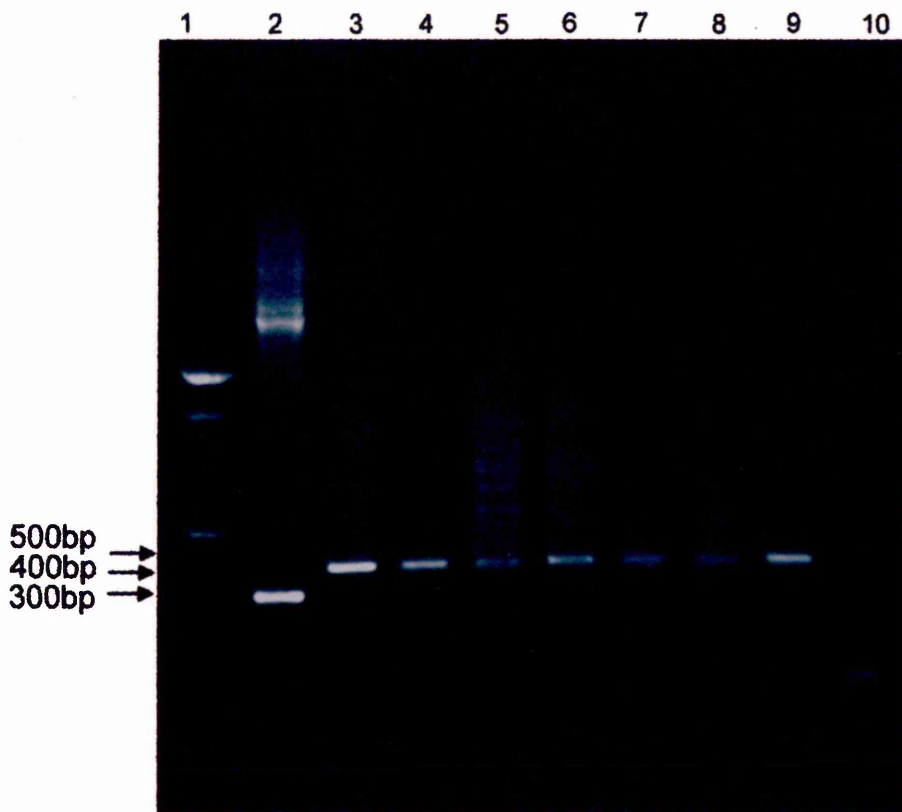
The constitutive expression of both (a) ADAM-17 and (b) TIMP3 protein in tissue homogenates of MS and control white matter.

Figure 3.11 ADAM-17 mRNA expression in MS and normal control white matter using RT-PCR



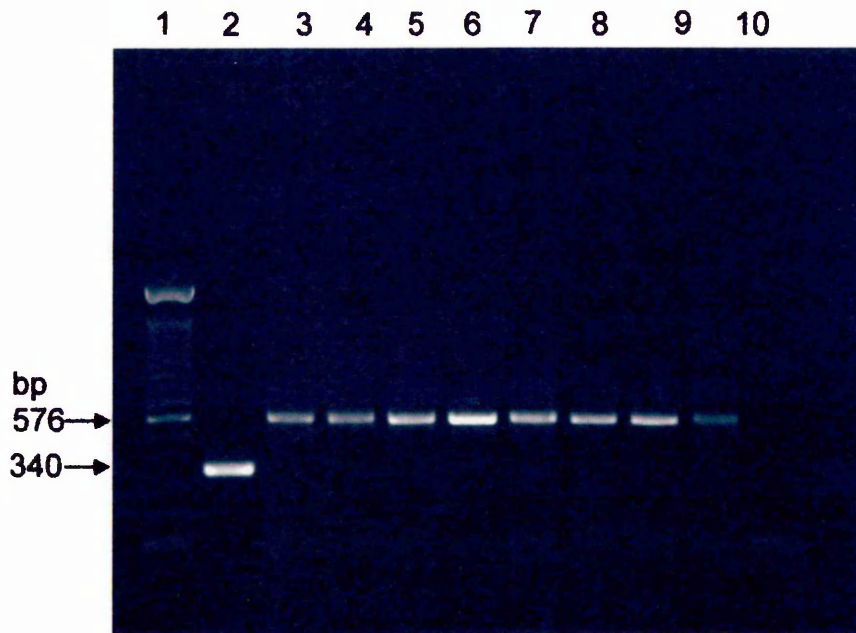
ADAM-17 PCR product expression within samples of normal control white matter (lanes 3, 4), MS NAWM (lane 5), active MS (lanes 6, 7), chronic inactive MS (lanes 8, 9) tissue. No RT negative control is in lane 10. 100bp DNA ladder is shown in lane 1 and an R&D systems positive control in lane 2.

**Figure 3.12 TIMP3 mRNA expression in MS and normal control white matter using RT-PCR**



TIMP3 PCR product expression within samples of normal control white matter (lanes 3, 4), MS NAWM (lane 5), active MS (lanes 6, 7), chronic inactive MS (lanes 8, 9) tissue. No RT negative control is in lane 10. 100bp DNA ladder is shown in lane 1 and an R&D systems positive control in lane 2.

**Figure 3.13 GAPDH mRNA expression in MS and normal control white matter using RT-PCR**



GAPDH PCR product expression within samples of normal control white matter (lanes 3, 4), MS NAWM (lane 5), active MS (lanes 6, 7), chronic inactive MS (lanes 8, 9) tissue. No RT negative control is in lane 10. 100bp DNA ladder is shown in lane 1 and an R&D systems positive control in lane 2. GAPDH results of these samples illustrates the lack of effect postmortem delay has on mRNA for these blocks used.

### 3.4 Discussion

The results presented here demonstrate the spectrum of ADAM-17 distribution in MS CNS tissue, along with a semi-quantitative analysis of the extent of ADAM-17 expression in active and chronic inactive lesions as well as the NAWM of MS and the white matter of normal control and OND cases. Utilising archival, SF autopsy material, tissue was classified based on evidence of recent myelin breakdown and extent of cellular activation as determined by ORO staining and HLA-DR immunoreactivity, classification parameters as described by other authors (Sanders *et al.*, 1993; van der Valk and de Groot, 2000).

The first objective of this study was to determine whether ADAM-17 and TIMP3 were expressed and then to establish a reproducible protocol for the identification of ADAM-17 and its natural inhibitor TIMP3 by immunofluorescence in snap frozen human autopsy brain material. Three antibodies for each protein were used, in conjunction with different fixation and detection methods. Protein expression of ADAM-17 and TIMP3 were further confirmed by western blotting following separation of protein extracts from tissue homogenates by SDS PAGE. Gene transcripts for these proteins were also demonstrated by reverse transcribing sample mRNA into cDNA followed by RT-PCR using commercially available primer pairs.

ADAM-17 and TIMP3 were demonstrated to be expressed in MS, OND and normal control white matter. ADAM-17 expression was associated with the endothelium of the blood vessels and with the cell body and elongated processes of parenchymal astrocytes and the astrocytic endfeet that encompass the cerebral vasculature. Since both ADAM-17 and TIMP3 were expressed in normal control brain this suggests that they play a constitutive role within the CNS. Co-localisation of ADAM-17 with the astrocyte phenotypic marker, GFAP, or the endothelial marker, von Willebrand factor, following dual labelled immunofluorescence, confirmed the morphological observations and clearly demonstrated that these two cell types are responsible for ADAM-17 expression in both MS and normal control white matter. These observations confirm those of ADAM-17

expression within normal control white matter reported previously (Goddard *et al.*, 2001). Furthering these observations here, ADAM-17 was also demonstrated to be expressed by activated macrophage/microglial cells in MS tissue and was upregulated in MS, particularly in active lesions where ADAM-17 immunoreactivity is evident on numerous large foamy macrophages, implicating a possible role in the disease process. Further evidence suggesting a disease association of ADAM-17 with MS was provided when gene transcripts for ADAM-17 in peripheral blood mononuclear cells (PBMCs) were shown to be positively correlated with MS disease progression in RRMS. Increases in ADAM-17 mRNA expression by PBMCs accompanied a higher mean number of new Gd-DTPA enhancing lesions on MRI following PBMC sampling (Seifert *et al.*, 2002).

ADAM-17 may play a role in a number of ways in the development of MS; proteolytic cleavage of fractalkine into its soluble form may create a chemotatic gradient for inflammatory cells to enter the CNS; ADAM-17 is reported to cleave adhesion molecules from the luminal surface of blood vessels, however in MS increased expression of endothelial cell adhesion molecules has been reported suggesting an imbalance in enzyme/inhibitor activity which is investigated *in vitro* in Chapter 5; ADAM-17 expression has been demonstrated to be associated with astrocytes and activated macrophage/microglial cells and expressed at high levels in lesions with high levels of cellular activity as gauged by HLA-DR and ORO expression. ADAM-17 cleaves TNF into its soluble form thereby possibly subjecting oligodendrocytes to its cytotoxic effects; TNF has been reported to alter TJ expression in endothelial cultures possibly resulting in the disrupted TJ expression reported in chapter 2.

In the current study ADAM-17<sup>+</sup> cells have been observed in a few perivascular cuffs within MS lesions in agreement to a previous study, which reported that ADAM-17 immunoreactivity in MS tissue was limited to a small number of CD3<sup>+</sup> lymphocytes primarily located within perivascular cuffs associated with acute and chronic active plaques (Kieseier *et al.*, 2003). In contrast to the present study however no astrocytic or endothelial cell ADAM-17 expression was reported by Kieseier *et al.*, 2003. This difference in

reported expression with the present study may be explained by the use of formalin fixed paraffin embedded tissue by Kieseier *et al* (2003) which may have reduced antigenicity, even following microwave antigen retrieval, whereas in this study snap frozen tissue was used. The differences in staining pattern may also be due to differences in primary antibodies used. Incorporating TACE (C15) with both the monoclonal M222 and another polyclonal TACE (Abcam) antibody to ADAM-17 within the various protocols used in this study on serial sections enabled comparisons to be drawn. Both the monoclonal M222 and polyclonal TACE, anti-ADAM-17 antibodies gave comparable results on the snap frozen tissue and were shown to be co-localised following dual label immunofluorescence. However serial sections stained with the polyclonal anti-TACE antibody from Santa Cruz as used by Kieseier *et al* (2003) were devoid of any ADAM-17 immunoreactivity.

The identification of the cells responsible for the synthesis of ADAM-17 is important when analysing the functional aspects of ADAM-17. It has been shown to be the sheddase responsible not only for cleaving TNF, but also cytokine receptors p75 and p55 TNFR, IL-6R, the growth factor TGF $\alpha$ , growth factor receptor for macrophage colony stimulating factor (M-CSF), and the adhesion molecule L-selectin and the chemokine fractalkine (Black *et al.*, 1997; Moss *et al.*, 1997; Borland *et al.*, 1999; Dri *et al.*, 2000; Rovida *et al.*, 2001; Garton *et al.*, 2001 & 2003). Astrocytes along with microglia and macrophages have been shown to be responsible for synthesising TNF within MS tissue (Hofman *et al.*, 1989). However, it has also been suggested that astrocytes may not actively synthesise TNF but merely take it up from the extracellular space as a consequence of receptor-mediated internalisation of TNF (Aranguiz *et al.*, 1995; Bitsch *et al.*, 2000). It is important to note that immunoreactivity does not necessarily indicate synthesis (Selmaj *et al.*, 1991a). Regardless of synthesis, ADAM-17 expression by astrocytes and activated macrophage/microglia would allow cleavage of TNF releasing proinflammatory soluble TNF (see Chapter 5). ADAM-17 has also been reported to be constitutively expressed by neurons under basal conditions and has been associated with neuroprotective roles in the CNS by modulating the amount of glutamate deposits in the ECM by

regulating the number of glutamate transporters and also by competing with  $\beta$ - and  $\gamma$ -secretases to cleave APP via a non-amyloidogenic pathway (Allinson *et al.*, 2003; Romera *et al.*, 2004; Kojro and Fahenholz, 2005;). Inhibition of ADAM-17 activity by pre-treatment of rat cortical cultures with the ADAM-17 inhibitor BB3103 has been reported to prevent oxygen-glucose deprived increase in glutamate transporters (Romera *et al.*, 2004). As a result it has been suggested that physiological neuroprotection by glutamate transporters is mediated by an ADAM-17-TNF dependent pathway (Romera *et al.*, 2004).

TNF has a host of pro-inflammatory effects including increased leukocyte cell attachment via upregulated adhesion molecules, chemotaxis and migration. TNF has also been shown to disrupt the function of the BBB in *in vitro* models (Dobbie *et al.*, 1999). Conversely TNF induces a beneficial response to immune situations by causing apoptosis of autoreactive T-cells through TNF/p55 TNFR interaction as seen in experiments on EAE (Probert and Akassoglou, 2001; Weishaupt *et al.*, 2004). It has been reported that induction of EAE in TNFR p55 deficient mice resulted in increased and prolonged levels of inflammation during later stages of the disease, with a marked reduction in T cell apoptosis in inflammatory infiltrates, suggesting that TNFR p55 plays a role in the removal of T cells from lesions and disease resolution (Probert and Akassoglou, 2001). It has been reported that membrane bound TNF is more effective than soluble TNF at binding with p75 TNFR (Grell *et al.*, 1995). Levels of TNF and TNFp75 have been positively correlated with relapses in MS (Martino *et al.*, 1997). TNF/TNFR p75 interaction on cerebral endothelial cells has been reported to lead to increased ICAM-1 expression (Akassoglou *et al.*, 2003). ADAM-17 cleavage of TNF may therefore play a protective role by reducing the efficacy of TNF/p75 TNFR binding thus resulting in less T-cell infiltration and possibly facilitating in disease resolution.

Immunohistochemical studies of endothelial cell associated adhesion molecules have shown an increase in adhesion molecules on the cell surface of the vascular endothelial cells from MS lesions compared to NAWM and

control sample white matter (Sobel *et al.*, 1990; Washington *et al.*, 1994; Dobbie *et al.*, 1999; Etienne-Manneville *et al.*, 2000). This increase in adhesion molecule expression is reported to be mediated by TNF (Wong and Dorovini-Zis, 1992 & 1995). Interaction of membrane bound TNF with p75 TNFR on endothelial cells is reported to lead to an increase in expression of ICAM-1, which potentially allows increased infiltration across the BBB via interactions of endothelial ICAM-1 with LFA-1 on the surface of T-cells (Wong and Dorovini-Zis, 1992). ADAM-17 expression by the vascular endothelium in normal control brains, as shown here, may regulate adhesion molecule expression through their cleavage from the cell surface, thus ensuring a low level of entry of inflammatory cells under normal conditions (Hickey, 2001). However it is proposed that high levels of ICAM-1 substrate for ADAM-17 on endothelial cells in MS may saturate the enzyme, eventually leading to an increased number of membrane-bound adhesion molecules available for leukocyte infiltration.

People with MS treated with IFN- $\beta$  have been reported to have higher serum and CSF levels of soluble VCAM-1 (Calabresi *et al.*, 1997; Rieckmann *et al.*, 1998). VCAM-1 has been shown to be proteolytically cleaved from the surface of murine endothelial and N1H3T3 cells in an MMP dependent mechanism under basal conditions and an ADAM-17-dependent mechanism following PMA stimulation (Garton *et al.*, 2003) similar to those observed during L-selectin shedding from leukocytes (Faveeuw *et al.*, 2001). PMA induced shedding of VCAM-1 was reported to be inhibited in ADAM-17 deficient cells and following treatment with an ADAM-17 inhibitor (Garton *et al.*, 2003). Cleavage of VCAM-1 may play a role in regulating cellular infiltration by limiting the amount of VCAM-1 available at the cell surface (Garton *et al.*, 2003). Serum samples from patients with MS having IFN- $\beta$  treatment are reported to contain CD4<sup>+</sup> and CD8<sup>+</sup> T cells with decreased levels of VLA-4 and increased amounts of soluble VCAM-1 (Jensen *et al.*, 2005). It may be possible that IFN- $\beta$  stimulates ADAM-17 mediated cleavage of adhesion molecules resulting in the reported increased amounts of soluble adhesion molecules within the serum and CSF however this requires further investigations *in vitro* (Calabresi *et al.*, 1997; Rieckmann *et al.*, 1998; Jensen *et al.*, 2005). Production of soluble VCAM-1 may represent a further

protective role if it maintains adhesive function and binds to VLA-4 expressed on lymphocytes preventing them adhering to the vessel wall and subsequent transmigration.

The presence of ADAM-17 and TIMP3 protein and mRNA were analysed by western blotting and RT-PCR using protein and RNA extracted from 12 MS and 7 control tissue samples. TIMP3 protein was detected as a single band at approximately 48 kDa. ADAM-17 was detected in all samples by bands at 100kDa and 80kDa, probably corresponding to immature and mature forms of the protein (Skovronski *et al.*, 2001; Hurtado *et al.*, 2001; Peiretti *et al.*, 2003). It is important to note that no quantitative analyses were carried out on whole tissue lysates due to the inter-sample variability in grey matter/white matter content. Western blot analysis has been used here to determine the presence of TIMP3 protein in both MS and control tissue, as commercial antibodies for TIMP3 have proved ineffective in detecting TIMP3 protein by immunofluorescence. The RT-PCR results are in agreement with those of other workers, demonstrating ADAM-17 and TIMP3 mRNA is expressed in both MS and control samples (Lindberg *et al.*, 2001).

TIMP3 is expressed in both normal control and MS brain at the transcriptional and protein level, but to date the attempts to elucidate the cellular origins of this protein have proved inconclusive. Difficulty in identifying the cellular localisation of TIMP3 may be due to the poor quality of commercial antibodies currently available. TIMPs interact with a 1:1 stoichiometry with MMPs to inhibit their activity (Kossakowska *et al.*, 1998; Crocker *et al.*, 2004). It has been suggested that normally a balance is maintained between ADAM-17 and TIMP3. However, in inflammatory conditions, this balance may be disturbed allowing an overproduction of soluble TNF. Whether the imbalance is due to excess of the sheddase or a reduction in its inhibitor is unclear at present. TNF increases the adhesion molecule expression by endothelial cells and ADAM-17 cleaves TNF from the cell surface, whether TNF from parenchymal astrocytes and microglia cause this apparent increase in adhesion molecules remains to be clarified.

In summary, the results indicate that ADAM-17 expression occurs throughout MS white matter, persisting in chronic inactive lesions but highest expression is seen in active lesions. Further investigation would be required to investigate the functional aspects associated with this increased ADAM-17 expression in active lesions. To determine the role of ADAM-17 expression by the cerebral endothelium in both normal control white matter and MS lesion and the influence TIMP3 exerts during inflammatory conditions requires *in vitro* studies (See chapter 5).

TNF has long been associated with a pathological role in MS (Brosnan *et al.*, 1988) and as such development of TNF inhibitors is an active area of drug discovery (Duan *et al.*, 2003; Cherney *et al.*, 2003). However recent trials using anti-TNF treatment were unsuccessful in MS as this treatment exacerbated disease rather than ameliorating the disease course (Lenercept study 1999; Sicotte and Voskuhl, 2001). ADAM-17 may be a potential alternative therapeutic target to TNF for the treatment of MS.

## **Chapter 4**

**ADAM-17 expression within rat spinal cords of experimental autoimmune encephalitis, an experimental model of MS**

## 4.1 Introduction

A major problem in investigating the pathogenesis of neuroinflammatory disorders in humans is the inaccessibility of the affected tissue or organ. As a result human tissue for research can only be obtained from end stage autopsy material that may present results that do not have any bearing on the initiation processes of the disease ('t Hart and Amor, 2003; 't Hart *et al.*, 2004 ). To address these issues, experimental autoimmune (allergic) encephalomyelitis (EAE), a T-cell mediated autoimmune disease of the CNS is widely used in laboratories as an experimental model of MS (Genain and Hauser, 1997; 't Hart *et al.*, 2004; Behi *et al.*, 2005). EAE was first developed in an effort to gain an understanding of the initiation of the encephalomyelitis which develops after inoculation of subjects with Pasteur rabies vaccine (Behi *et al.*, 2005). The Pasteur rabies vaccine was produced from virally infected neural tissue, so animals were either inoculated with the infected neural tissue or with uninfected neural tissue for control subjects. It was during these experiments when it was noticed that some of the controls subjects receiving uninfected neural tissue also developed encephalomyelitis (Behi *et al.*, 2005). Although EAE was first described in macaque monkeys, most forms of EAE are produced in inbred laboratory rodents (Rivers *et al.*, 1933; Rivers and Schwenkter, 1935; Genain and Hauser, 1997; Brok *et al.*, 2001).

### 4.1.1 The use of EAE as a therapeutic model for MS treatment

EAE, as well as being readily inducible in susceptible animals is also readily treated. Many successful treatments in EAE have failed when transferred to treatment of humans. A prime example of this comes from the exciting findings in the treatment of EAE with soluble p55 TNFR which lead to a large clinical trial in people with MS, with disappointing results. Indeed the phase II randomised trial resulted in increased exacerbations in a dose dependent manner in comparison to placebo (Lenercept study 1999). Species differences appear to be an obvious reason for this. The majority of drugs or therapeutic tests are applied to and rely upon the rodent models as 'preclinical' tests, these findings are then applied directly to humans in clinical trials. However rats and mice appear too distant from man to fulfil this

(t'Hart *et al.*, 2004). In transplantation research a non-human primate model is required for preclinical tests to bridge the gap between human and rodents, however for autoimmune disease research this does not appear to be the case (t'Hart *et al.*, 2004). Encouraging results taken from the anti-VLA-4 MAb treatment of EAE also came from the natalizumab clinical trial in relapsing remitting MS, where decreased numbers of enhancing MRI lesions and relapses have been reported with few side effects (Miller *et al.*, 2003). However following reports of progressive multifocal leukoencephalitis (PML) in two patients receiving dual therapy in the trial, Tysabri (natalizumab) was withdrawn at the end of February 2005 (Kleinschmidt-DeMasters and Tyler, 2005).

#### 4.1.2 Aim of study

The aim of this study was to establish whether ADAM-17 is involved in the pathogenesis of EAE and if so to develop an understanding of its functional role so that the potential for therapeutic intervention targeting ADAM-17 could be exploited.

The known pathological role of TNF and adhesion molecules in EAE together with ADAM-17's known involvement with their shedding, lead this study to establish the expression profile of ADAM-17 and its natural inhibitor TIMP3 at the protein and mRNA level during initiation, peak disease and recovery from rats with EAE. Snap-frozen spinal cord tissue from EAE rats was used. A semi-quantitative analysis of ADAM-17 protein and mRNA expression was applied to establish if any differences exist between study groups. ADAM-17 immunoreactivity was also investigated in relation to phenotypic markers for cells from the CNS, namely astrocytes, cerebral endothelium and activated macrophages and microglia. The major objectives addressed were:

- (i) To determine whether ADAM-17 and TIMP3 immunoreactivity and mRNA was detectable in naïve and EAE rat spinal cord and whether there were any differences in expression levels between the different disease stages

- (ii) To determine which cells are responsible for ADAM-17 and TIMP3 expression within the spinal cord

## 4.2 Materials and methods

### 4.2.1 Experimental autoimmune encephalomyelitis tissue

EAE was induced in 15 Lewis rats by immunisation with spinal cord homogenate plus adjuvant, as previously described (Ohgoh *et al.*, 2002, see appendix). The animal work was carried out at Eisai London Research Laboratories Ltd, University College London by Dr T Smith. Clinical disability was scored: 0, no detectable change in muscle tone and motor behaviour; 1, flaccid tail; 2, impairment of righting reflex and/or loss of muscle tone in hindlimbs; 3, complete hindlimb paralysis; 4, paraplegia; and 5, death (Ohgoh *et al.*, 2002). At three time points during the disease course, 5 rats were sacrificed. Pre-disease rats were sacrificed 10 days post immunisation (dpi) with a clinical disability score of 0. Peak-disease rats were sacrificed 12 dpi with a score of 3.25. Recovered rats were sacrificed 4 days after their score had returned to 0 (see appendix). Spinal cords from 5 naïve rats were also obtained. Spinal cords were removed by insufflation with ice cold saline, placed onto foil and rapidly frozen on dry ice, serial 12 $\mu$ m cryostat sections were obtained for immunohistochemistry.

### 4.2.2 Immunohistochemistry

12 $\mu$ m cryostat sections were cut and mounted on to polylysine coated glass slides (BDH). Sections were fixed in ice cold acetone for 10 minutes then allowed to air dry for at least 15 minutes at RT prior to use or storage at -20°C. Endogenous peroxidase was quenched by incubating the sections in 0.5% H<sub>2</sub>O<sub>2</sub> in methanol for 10 minutes at RT. Following 5 minute washes in running water and PBS, non specific binding was eliminated by incubating the sections in 5% normal rabbit serum for 10 minutes at RT. Sections were incubated in mouse anti-rat monoclonal ED1 (1:50, Serotec) antibody overnight at 4°C. ED1 immunoreactivity was detected using the SABC immunoperoxidase method as described in section 3.2.1.1.

#### 4.2.3 Indirect Immunofluorescence staining

12µm cryostat sections were either fixed in 70% methanol, 4% paraformaldehyde (see appendix), or ice-cold acetone for 10 minutes. Following fixation all sections were washed in PBS with the exception of ice-cold acetone fixed sections, which were allowed to air dry for at least 15 minutes prior to the next step.

##### 4.2.3.1 Single label immunofluorescence

Following fixation, sections were incubated in polyclonal TACE antibody (1:100, Abcam) overnight at 4°C, washed in PBS then incubated in goat anti-rabbit IgG Alexa 488 (1:500, Molecular Probes) for 90 minutes at RT. Cell nuclei were counterstained by incubating sections in propidium iodide (Sigma, 2µg/ml) for 30 seconds. Sections were mounted with coverslips in the non-fading mountant, citifluor (see appendix). All dilutions were performed in PBS except antibodies that were used on paraformaldehyde fixed sections, which were diluted in PBS with 0.5% Triton X-100. Table 3.2.2 provides the details of all the antibodies used in this study.

##### 4.2.3.2 Dual label immunofluorescence

To determine the cellular origin of ADAM-17 expression, the sequential dual label immunofluorescence protocol, as described in section 3.2.2, was carried out. Dual staining was performed with polyclonal antibodies to either the astrocytic marker, GFAP (1:100, Dako) or the endothelial marker von Willebrand Factor (1:100, Dako,) with the monoclonal antibody to ADAM-17, human anti-mouse M222 (1:100, Amgen). Rabbit polyclonal TACE was used in dual staining with the inflammatory macrophage marker, mouse anti-rat ED1 (1:50, Serotec) or a mouse monoclonal anti-GFAP (1:1000, Chemicon) antibody. All dilutions were carried out with PBS.

As a control during dual staining, serial sections were single label immunostained for each primary antibody to ensure that no cross reaction was observed when using two secondary antibodies. Sections with primary antibody omitted from the protocol showed no immunoreactivity.

#### 4.2.4 Imaging

All imaging was obtained using the Zeiss 510 confocal scanning laser microscope and Leica upright light microscope as described previously in section 3.2.3.

#### 4.2.5 Quantification

Semi quantitative analysis was carried out to assess the extent of ED1 and ADAM-17 immunoreactivity, following observation through the x20 objective lens of the upright Leica microscope.

##### 4.2.5.1 ADAM-17 and ED1 grading

All sections within this study were single label immunostained for ED1 and ADAM-17 as described previously (Chapter 4.2.2 and 4.2.3.1 respectively). Analyses of the staining was carried out by two independent observers, and a 4 point grading scale (-ve, +, ++, +++) was applied;

- 0 = no immunoreactivity observed;
- + = sections with only blood vessel associated immunoreactivity;
- ++ = sections where there is blood vessel immunoreactivity together with distinct white matter glial cell expression;
- +++ = sections which displayed an abundance of immunoreactivity throughout the spinal cord white matter.

Where observers scores differed a consensus score was obtained following joint re-examination.

##### 4.2.5.2 Co-localisation

Analysis of all dual stained sections was carried out using the Zeiss 510 CSLM software as described in section 3.2.3.1.

#### 4.2.6 Protein and RNA extraction

From each of the 20 rat spinal cords, white matter was excised from the grey matter (at -20°C) and collected in pre-cooled Eppendorfs (-20°C). Protein and RNA were extracted by application of 1ml of Tri Reagent™ (Sigma) following the manufacturer's protocol (See appendix). Sample

protein concentrations were determined using the BCA assay as previously described in section 3.2.4.1.

#### *4.2.7 Western blotting for ADAM-17 and TIMP3*

Extracted protein samples (6 $\mu$ g) were loaded into wells and separated by SDS-polyacrylamide gel electrophoresis on 10% pre-cast bis/tris gels (Invitrogen) at 150V for 1hour and proteins transferred onto nitrocellulose membrane for western blotting as described (section 3.2.5). Omission of primary antibody during the first stage of western blotting was carried out as a control. Quantitative analysis was carried out by comparing the integrated optical density (IOD) using densitometric software of the UVP Bioimaging system. Group means of IODs were obtained and any significant differences determined using the two-tailed Mann-Whitney U-test ( $p < 0.05$ ).

#### *4.2.8 RNA analysis for ADAM-17 and TIMP3*

##### *4.2.8.1 Reverse transcriptase PCR*

RNA was reverse transcribed to cDNA using Superscript II RT (Invitrogen, Paisley, Scotland) with poly-dT primers. The PCR-amplification of the cDNA was achieved using rat specific ADAM-17 real time PCR primer pair (MWG Biotech, Ebbersberg, Germany, Table 4.1) and a rat specific TIMP3 primer pair (R&D Systems) using Taq polymerase (Invitrogen) and an annealing temperature of 60°C and 55°C respectively. The amplified PCR products were analyzed on ethidium bromide stained 4% and 1% agarose gels. Product size was determined using 10bp and 100bp DNA ladders (Invitrogen). Gel images were obtained using a UVP Bioimaging system (Bio-Rad).

##### *4.2.8.2 Real time PCR*

###### *Principle of method*

RT-PCR is a semi-quantitative method for analysis of gene expression. Real-time quantitative PCR (qRT-PCR) provides a more sensitive analysis that enables quantification of gene expression (Wilheim

Table 4.1 Rat specific primer sequences as used during qRT-PCR to assess mRNA in EAE.

<i>Primer</i>	<i>Accession</i>	<i>Sequence</i>	<i>Position</i>	<i>Product</i>
	<i>No.</i>			<i>size (bp)</i>
<b>ADAM-17</b>	NM020306	5'ATG GGA AAG AGG AAA GCG AGT AC 3' 5' CCC TAG AGT CAG GCT CAC CAA 3'	540-620	80
<b>TIMP-3</b>	U27201	5' GAA CGG AAG CGT GCA CAT G 3' 5' CAG CTT CTT TCC CAC CAC TTT G 3'	62-156	94
<b>GAPDH</b>	M17701	5' TGA TTC TAC CCA CGG CAA GT 3' 5' AGC ATC ACC CCA TTT GAT GT 3'	171-295	124

Table 4.1 Rat specific primer sequences as used during RT-PCR to assess mRNA in SAE

Gene	Accession	Forward	Reverse
ADAM-17	U050306	5'-GCA TGA GCG AAA GCG GAA GCG GTAC-3'	5'-GCG TAG AGT CAG GCT CAG CAA-3'
IL-6	U05138	5'-GAA GCG GAG CCG CAT G-3'	5'-CAG GTC CTT TCC CAG CAC TTT G-3'
IL-1	U05137	5'-TGA TTC TAC CCA GCG GAA GT-3'	5'-AGC GTA ACC GCA TTT CAT GT-3'

and Pingould 2003; Arya *et al.*, 2005). The principle of qRT-PCR was first put forward by Higuchi and colleagues in 1993 and relies upon the detection of a fluorescent signal that is proportional to the amount of PCR product generated during the reaction. Fluorescent dyes are used that bind specifically to double stranded DNA allowing the amount of PCR product being produced to be analysed after every cycle in real-time using a fluorimeter. One of the major fluorescent dyes used in qRT-PCR is SYBR Green 1. SYBR Green 1 binds to the minor groove of double stranded DNA and is reported to have a binding affinity that is over 100 times higher than that of ethidium bromide (Wilhelm and Pingould, 2003; Ponchel *et al.*, 2003). During the initial phase of qRT-PCR the fluorescent signal is below that detected as background, once the signal rises above this baseline (cycle threshold (CT)) the signal increases exponentially until it reaches a plateau phase (Ponchel *et al.*, 2003). The CT value is proportional to the logarithm of the initial amount of target in the sample. The relative concentration of a target with respect to another is determined as the difference in cycle number to achieve the same level of fluorescence ( $\Delta$ CT). Experimental comparisons usually involve comparing  $\Delta$ CT values of the target against those of an internal reference or housekeeping gene that remains constant during experimental conditions. Glyceraldehyde-3-phosphate dehydrogenase (GAPDH) is a common housekeeping gene used in qRT-PCR.

### *Method*

The real time PCR analysis was carried out by Dr A Cross, Sheffield Hallam University, Sheffield. cDNA was used as a template for qRT-PCR using the ABI PRISM 7900 sequence detection system and 2xSYBR Green mastermix (Applied Biosystems, Warrington, UK). PCR primers were designed using Primer Express software (Applied Biosystems) and obtained from MWG Biotech (Ebbersberg, Germany). In order to preclude the amplification of nuclear DNA, all primers crossed an exon-exon boundary. Primer sequences and accession numbers are shown in Table 4.1. Expression of ADAM-17 and TIMP3 were analysed, as well as the housekeeping gene GAPDH to normalise expression between different

samples. Sequences were confirmed as unique by a BLAST search ([www.ncbi.nlm.nih.gov/BLAST](http://www.ncbi.nlm.nih.gov/BLAST)).

Each primer pair generated a single product of the appropriate size when visualised by agarose gel electrophoresis, and by melt curve analysis following qRT-PCR (not shown). Relative mRNA levels of ADAM-17 and TIMP3 were determined using the formula  $2^{-\Delta CT}$  where  $\Delta CT = CT$  (target gene) – CT (GAPDH).

Differences in mRNA levels were determined using the two-tailed Mann Whitney U test ( $p > 0.001$ ).

### 4.3 Results

20 Lewis rats used in this study were designated into 4 categories dependant on EAE disease course and clinical disability score: non-inoculated rats were naïve; inoculated rats with a clinical score of 0 were pre-disease; rats with a clinical score  $>3$  were peak disease; whereas rats whose clinical course had been  $>3$  but had returned to 0 were in the recovered group (Table 4.2).

#### 4.3.1 Characterisation of rat spinal cord histopathology

The cervical spinal cord was cryo-sectioned from 20 rat spinal cords (5 naïve, 5 pre-disease, 5 peak disease and 5 recovered) and screened by H&E and for ED1<sup>+</sup> macrophages to characterise the pathological state of individual cords used. No histological difference was observed between the spinal cords from the naïve and pre-disease rats. Examination of H&E sections demonstrated large areas of hypercellular perivascular infiltrates within the white matter of peak-disease and recovered spinal cords. ED1 immunoreactivity, a marker for inflammatory macrophages and microglia, was graded (Table 4.2) and revealed the highest level of immunoreactivity on microglial and perivascular cells at peak disease (2/5 rats) (Grade +++). Grade ++ level of ED1 immunoreactivity, was observed in the remaining peak disease rats and 3/5 recovered rats. Cells within the perivascular infiltrates were ED1<sup>+</sup> as were other cells of microglial and macrophage morphology, throughout the parenchymal white matter of the spinal cords

Table 4.2 ADAM-17 and ED1 immunoreactivity grades EAE rats.

<b>Group</b>	<b>Clinical score</b>	<b>ADAM-17</b>	<b>ED1</b>
<b>Naïve</b>	0	+	0
<b>Naïve</b>	0	+	0
<b>Naïve</b>	0	+	0
<b>Naïve</b>	0	+	0
<b>Naïve</b>	0	+	0
<b>Pre</b>	0	+	+
<b>Pre</b>	0	+	0
<b>Pre</b>	0	+	0
<b>Pre</b>	0	+	+
<b>Pre</b>	0	+	0
<b>Peak</b>	3	+++	++
<b>Peak</b>	3.25	+++	+++
<b>Peak</b>	3.25	+++	+++
<b>Peak</b>	3.25	+++	++
<b>Peak</b>	3.25	+++	++
<b>Rec</b>	0	++	++
<b>Rec</b>	0	++	++
<b>Rec</b>	0	+++	+
<b>Rec</b>	0	+++	+
<b>Rec</b>	0	++	++

Clinical disability scores were assigned by Dr T Smith (Eisai). The extent of ED1 and ADAM-17 immunoreactivity were graded as:

0 = no immunoreactivity observed;

+ = sections with only blood vessel associated immunoreactivity;

++ = sections where there is blood vessel immunoreactivity together with distinct white matter glial cell expression;

+++ = sections which displayed an abundance of immunoreactivity throughout the spinal cord white matter.

The animal's clinical disability score was assigned at Eisai laboratories where a score of 3 represented complete hindlimb paralysis and 4 paraplegia.

Table 1.3 ADAM-17 and ED1 immunoreactivity grades (EAE rat)

0	+	0	Naive
0	+	0	Naive
0	+	0	Naive
0	+	0	Naive
0	+	0	Naive
+	++	0	Pre
0	+	0	Pre
0	+	0	Pre
+	++	0	Pre
0	+	0	Pre
++	+++	3	Peak
+++	+++	3.5	Peak
+++	+++	3.5	Peak
++	+++	3.5	Peak
++	+++	3.5	Peak
++	++	0	Pre
++	++	0	Pre
+	+++	0	Pre
+	+++	0	Pre
++	++	0	Pre

In order to (1) (2) (3) (4) (5) (6) (7) (8) (9) (10) (11) (12) (13) (14) (15) (16) (17) (18) (19) (20) (21) (22) (23) (24) (25) (26) (27) (28) (29) (30) (31) (32) (33) (34) (35) (36) (37) (38) (39) (40) (41) (42) (43) (44) (45) (46) (47) (48) (49) (50) (51) (52) (53) (54) (55) (56) (57) (58) (59) (60) (61) (62) (63) (64) (65) (66) (67) (68) (69) (70) (71) (72) (73) (74) (75) (76) (77) (78) (79) (80) (81) (82) (83) (84) (85) (86) (87) (88) (89) (90) (91) (92) (93) (94) (95) (96) (97) (98) (99) (100) (101) (102) (103) (104) (105) (106) (107) (108) (109) (110) (111) (112) (113) (114) (115) (116) (117) (118) (119) (120) (121) (122) (123) (124) (125) (126) (127) (128) (129) (130) (131) (132) (133) (134) (135) (136) (137) (138) (139) (140) (141) (142) (143) (144) (145) (146) (147) (148) (149) (150) (151) (152) (153) (154) (155) (156) (157) (158) (159) (160) (161) (162) (163) (164) (165) (166) (167) (168) (169) (170) (171) (172) (173) (174) (175) (176) (177) (178) (179) (180) (181) (182) (183) (184) (185) (186) (187) (188) (189) (190) (191) (192) (193) (194) (195) (196) (197) (198) (199) (200) (201) (202) (203) (204) (205) (206) (207) (208) (209) (210) (211) (212) (213) (214) (215) (216) (217) (218) (219) (220) (221) (222) (223) (224) (225) (226) (227) (228) (229) (230) (231) (232) (233) (234) (235) (236) (237) (238) (239) (240) (241) (242) (243) (244) (245) (246) (247) (248) (249) (250) (251) (252) (253) (254) (255) (256) (257) (258) (259) (260) (261) (262) (263) (264) (265) (266) (267) (268) (269) (270) (271) (272) (273) (274) (275) (276) (277) (278) (279) (280) (281) (282) (283) (284) (285) (286) (287) (288) (289) (290) (291) (292) (293) (294) (295) (296) (297) (298) (299) (300) (301) (302) (303) (304) (305) (306) (307) (308) (309) (310) (311) (312) (313) (314) (315) (316) (317) (318) (319) (320) (321) (322) (323) (324) (325) (326) (327) (328) (329) (330) (331) (332) (333) (334) (335) (336) (337) (338) (339) (340) (341) (342) (343) (344) (345) (346) (347) (348) (349) (350) (351) (352) (353) (354) (355) (356) (357) (358) (359) (360) (361) (362) (363) (364) (365) (366) (367) (368) (369) (370) (371) (372) (373) (374) (375) (376) (377) (378) (379) (380) (381) (382) (383) (384) (385) (386) (387) (388) (389) (390) (391) (392) (393) (394) (395) (396) (397) (398) (399) (400) (401) (402) (403) (404) (405) (406) (407) (408) (409) (410) (411) (412) (413) (414) (415) (416) (417) (418) (419) (420) (421) (422) (423) (424) (425) (426) (427) (428) (429) (430) (431) (432) (433) (434) (435) (436) (437) (438) (439) (440) (441) (442) (443) (444) (445) (446) (447) (448) (449) (450) (451) (452) (453) (454) (455) (456) (457) (458) (459) (460) (461) (462) (463) (464) (465) (466) (467) (468) (469) (470) (471) (472) (473) (474) (475) (476) (477) (478) (479) (480) (481) (482) (483) (484) (485) (486) (487) (488) (489) (490) (491) (492) (493) (494) (495) (496) (497) (498) (499) (500) (501) (502) (503) (504) (505) (506) (507) (508) (509) (510) (511) (512) (513) (514) (515) (516) (517) (518) (519) (520) (521) (522) (523) (524) (525) (526) (527) (528) (529) (530) (531) (532) (533) (534) (535) (536) (537) (538) (539) (540) (541) (542) (543) (544) (545) (546) (547) (548) (549) (550) (551) (552) (553) (554) (555) (556) (557) (558) (559) (560) (561) (562) (563) (564) (565) (566) (567) (568) (569) (570) (571) (572) (573) (574) (575) (576) (577) (578) (579) (580) (581) (582) (583) (584) (585) (586) (587) (588) (589) (590) (591) (592) (593) (594) (595) (596) (597) (598) (599) (600) (601) (602) (603) (604) (605) (606) (607) (608) (609) (610) (611) (612) (613) (614) (615) (616) (617) (618) (619) (620) (621) (622) (623) (624) (625) (626) (627) (628) (629) (630) (631) (632) (633) (634) (635) (636) (637) (638) (639) (640) (641) (642) (643) (644) (645) (646) (647) (648) (649) (650) (651) (652) (653) (654) (655) (656) (657) (658) (659) (660) (661) (662) (663) (664) (665) (666) (667) (668) (669) (670) (671) (672) (673) (674) (675) (676) (677) (678) (679) (680) (681) (682) (683) (684) (685) (686) (687) (688) (689) (690) (691) (692) (693) (694) (695) (696) (697) (698) (699) (700) (701) (702) (703) (704) (705) (706) (707) (708) (709) (710) (711) (712) (713) (714) (715) (716) (717) (718) (719) (720) (721) (722) (723) (724) (725) (726) (727) (728) (729) (730) (731) (732) (733) (734) (735) (736) (737) (738) (739) (740) (741) (742) (743) (744) (745) (746) (747) (748) (749) (750) (751) (752) (753) (754) (755) (756) (757) (758) (759) (760) (761) (762) (763) (764) (765) (766) (767) (768) (769) (770) (771) (772) (773) (774) (775) (776) (777) (778) (779) (780) (781) (782) (783) (784) (785) (786) (787) (788) (789) (790) (791) (792) (793) (794) (795) (796) (797) (798) (799) (800) (801) (802) (803) (804) (805) (806) (807) (808) (809) (810) (811) (812) (813) (814) (815) (816) (817) (818) (819) (820) (821) (822) (823) (824) (825) (826) (827) (828) (829) (830) (831) (832) (833) (834) (835) (836) (837) (838) (839) (840) (841) (842) (843) (844) (845) (846) (847) (848) (849) (850) (851) (852) (853) (854) (855) (856) (857) (858) (859) (860) (861) (862) (863) (864) (865) (866) (867) (868) (869) (870) (871) (872) (873) (874) (875) (876) (877) (878) (879) (880) (881) (882) (883) (884) (885) (886) (887) (888) (889) (890) (891) (892) (893) (894) (895) (896) (897) (898) (899) (900) (901) (902) (903) (904) (905) (906) (907) (908) (909) (910) (911) (912) (913) (914) (915) (916) (917) (918) (919) (920) (921) (922) (923) (924) (925) (926) (927) (928) (929) (930) (931) (932) (933) (934) (935) (936) (937) (938) (939) (940) (941) (942) (943) (944) (945) (946) (947) (948) (949) (950) (951) (952) (953) (954) (955) (956) (957) (958) (959) (960) (961) (962) (963) (964) (965) (966) (967) (968) (969) (970) (971) (972) (973) (974) (975) (976) (977) (978) (979) (980) (981) (982) (983) (984) (985) (986) (987) (988) (989) (990) (991) (992) (993) (994) (995) (996) (997) (998) (999) (1000)

0 = no immunoreactivity observed

++ = sections with only blood vessel associated immunoreactivity

+++ = sections where there is blood vessel immunoreactivity together with

distinct white matter cell expression

+++ = sections which display an abundance of immunoreactivity

throughout the spinal cord white matter

The animal's clinical disability score was assigned as EAE latencies

where a score of 0 represented complete hindlimb paralysis and 4

represented

(Figure 4.1). A low level of ED1 immunoreactivity (Grade +) was observed in two pre-disease spinal cords and two spinal cords from rats in recovery and was only associated with the vasculature. The remaining pre-disease naïve spinal cords (3/5) were devoid of any ED1 immunoreactivity (Figure 4.1).

#### *4.3.2 Indirect immunofluorescence*

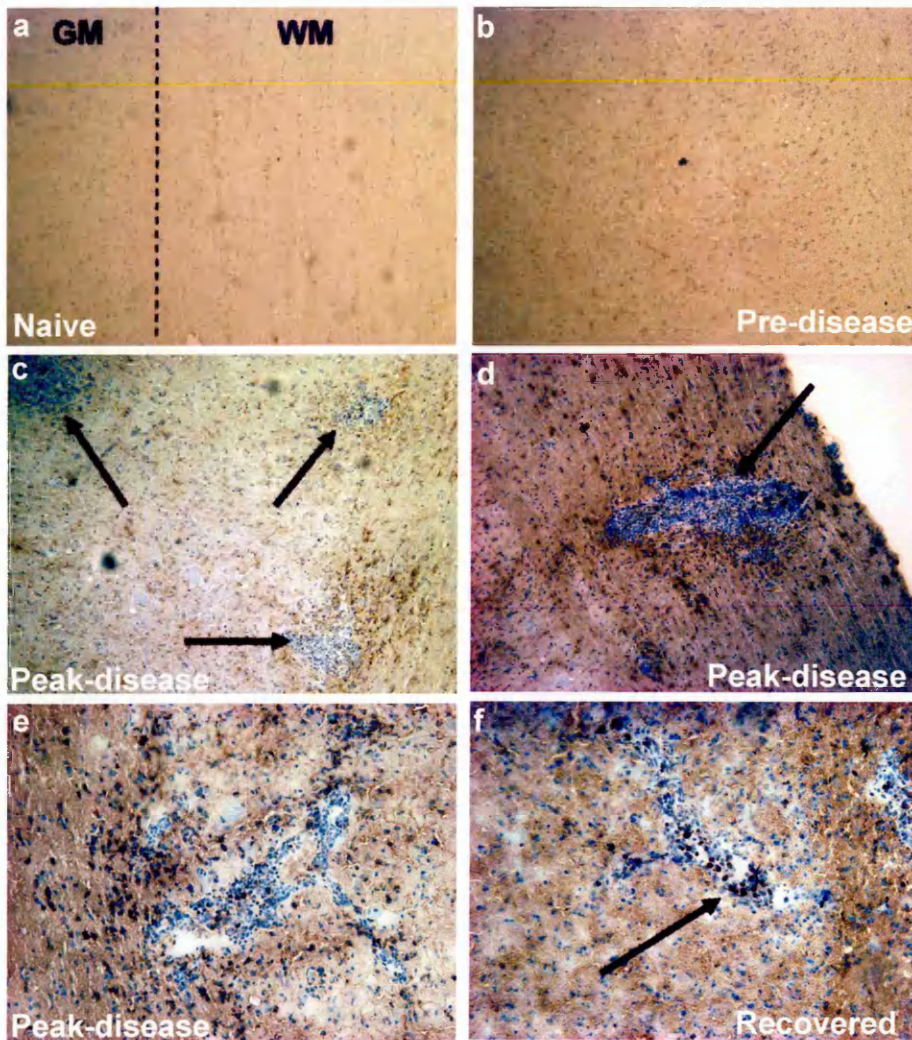
Sections of rat spinal cord were fixed either in ice-cold acetone, 4% paraformaldehyde or 70% methanol to determine the optimal protocol for ADAM-17 and TIMP3 staining by indirect immunofluorescence. All fixatives permitted ADAM-17 immunoreactivity, however where parenchymal staining was evident, 70% methanol fixed sections provided a truncated expression upon glial cell processes within the parenchyma, as seen in human tissue (Figure 3.1e). Also under consideration was the efficacy of each fixative to permit optimal dual labelled immunofluorescence. 4% paraformaldehyde did not allow sufficient staining of ED1 and as such ice-cold acetone fixation was adopted as the fixative of choice for this study, since it enabled optimal staining for ED1, GFAP and VWF.

##### *4.3.2.1 ADAM-17 expression in EAE and control rat spinal*

All samples were stained with polyclonal anti-TACE to detect presence and extent of ADAM-17 within rat spinal cords (Figure 4.2). ADAM-17 immunoreactivity was constitutively expressed in all spinal cords assessed. All naïve (5/5) and pre-disease (5/5) rat spinal cords were graded as ADAM-17+, with ADAM-17 expression associated with the vasculature. All peak disease animals (5/5) displayed abundant ADAM-17 immunoreactivity (graded +++) with an abundance of ADAM-17 staining throughout the spinal cord white matter, perivascular infiltrate and vasculature. Rats in the recovery phase maintained a high level of ADAM-17 (scores of ++/+++ for 3/5 and 2/5 animals respectively).

Upon morphological examination, ADAM-17 immunoreactivity within both the naïve and pre-disease spinal cords was only associated with the vascular endothelium, which was intensely stained (Figure 4.2a & b). Upon examination of the peak-disease spinal cords and those from rats in recovery, ADAM-17 expression associated with blood vessels appears to be both endothelial and

Figure 4.1 ED1 expression within naïve and EAE spinal cords



ED1 expression within spinal cord of naïve (a) and Lewis rats with EAE (b-f). Naïve spinal cords were devoid of any inflammatory cells and ED1 immunoreactivity (a). Numerous inflammatory cuffs were detectably within the white matter of the spinal cords from peak disease (c, arrows) and animals in recovery (f). ED1+ cells are evident within these perivascular inflammatory infiltrate (d-f). Cell nuclei are counter stained with haematoxylin. Mag x200.

astrocyte end-feet in origin. Within peak disease and rats in recovery phase, ADAM-17 immunoreactivity was also associated with the cell body and the elongated processes of parenchymal astrocytes and the perivascular infiltrate (Figure 4.2c & d). Upon examination of the spinal cord, grey matter displayed ADAM-17 immunoreactivity associated with the vasculature that was consistent between sample groups. Sections where the primary antibody was omitted from the protocol displayed no immunoreactivity.

#### *4.3.2.2 TIMP3 expression in EAE and control rat spinal*

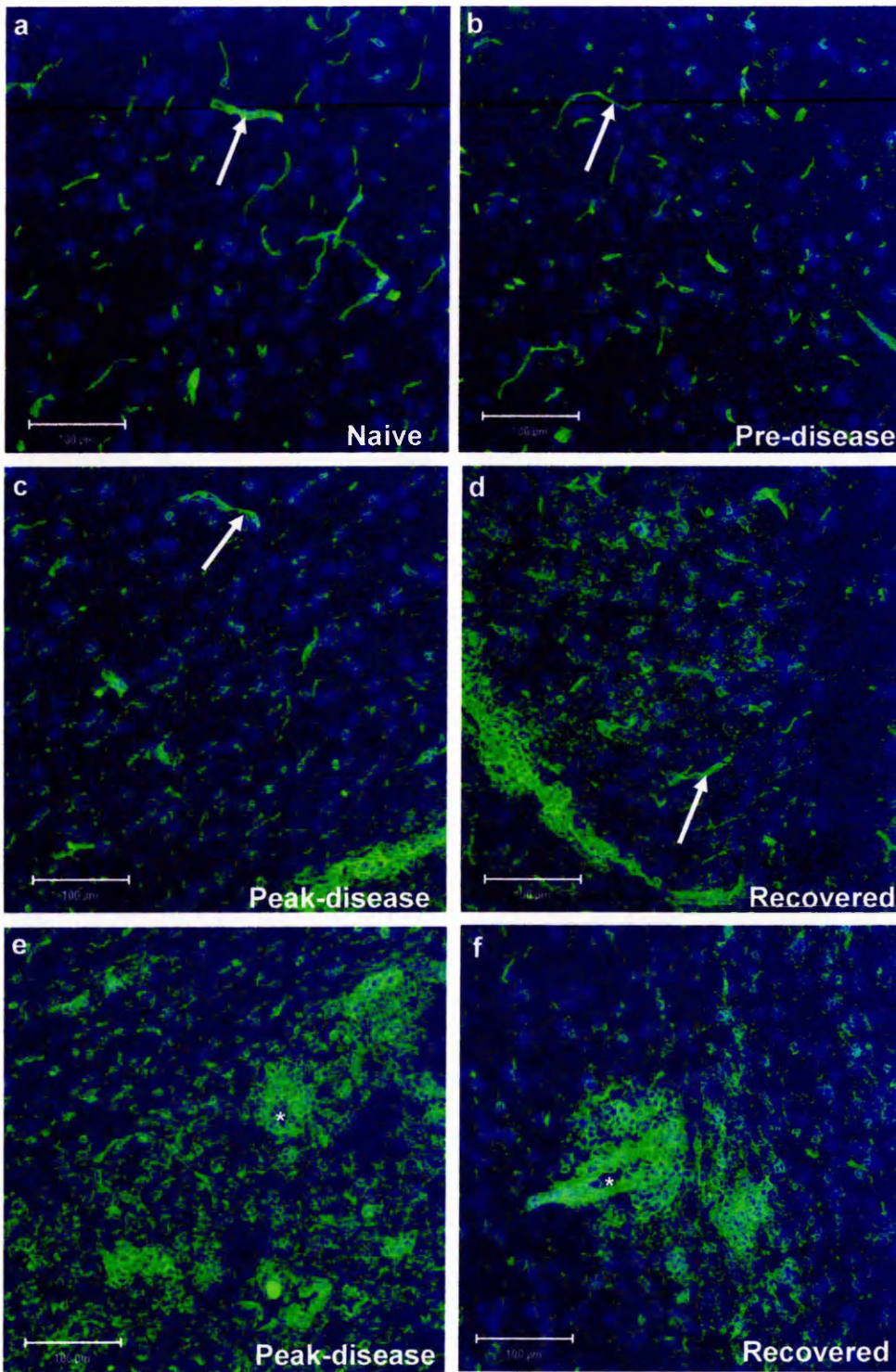
TIMP3 immunoreactivity detection was assessed by both the indirect immunofluorescence and streptavidin/biotin methods using three commercially available primary antibodies to TIMP3. TIMP3 immunoreactivity however was not detectable due to the expression being below that of the detection thresholds of the techniques carried out.

#### *4.3.2.3 Cellular localisation of ADAM-17*

To determine the specific cellular localisation of ADAM-17, dual labelled immunofluorescence was carried out with monoclonal mouse anti-ADAM-17 (M222) and rabbit anti-GFAP or rabbit anti-VWF, for identification of astrocytes and endothelial cells respectively. Dual labelling with polyclonal rabbit anti-TACE antibody and anti- ED1 was used to identify the inflammatory macrophage expression of ADAM-17.

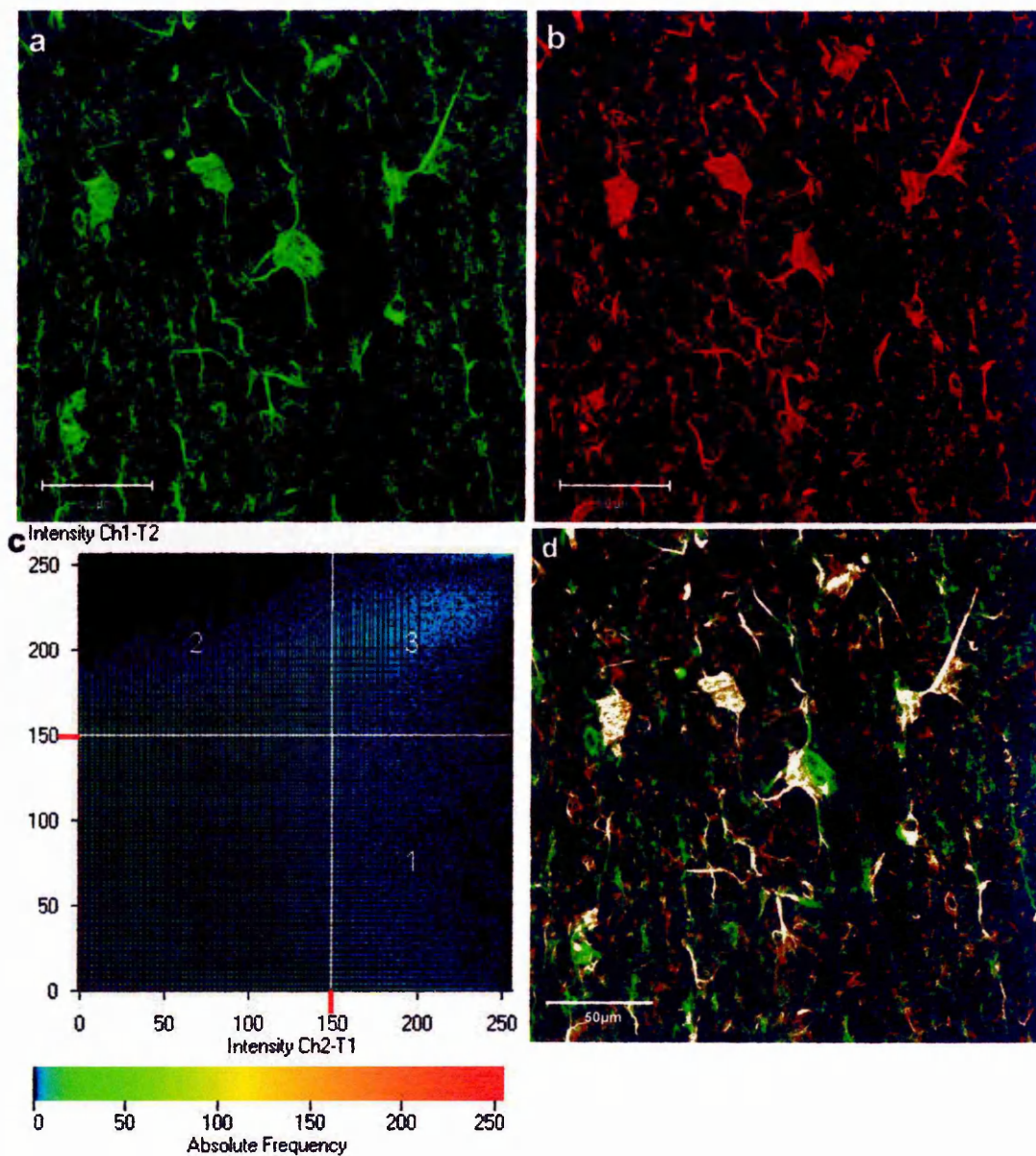
In EAE samples where parenchymal ADAM-17 expression was prevalent, GFAP and ADAM-17 immunoreactivity were co-expressed in astrocyte cell bodies and along their processes (Figure 4.3). ADAM-17 expression was also in cells of the perivascular infiltrate. ED1 and ADAM-17 immunoreactivity were co-expressed on the inflammatory cells in spinal cords of peak EAE and rats in recovery (Figure 4.4). VWF and ADAM-17 immunoreactivity were observed at the vascular endothelium of all blood vessels from all four study groups (Figure 4.5).

Figure 4.2 ADAM-17 expression within naïve and EAE spinal cord



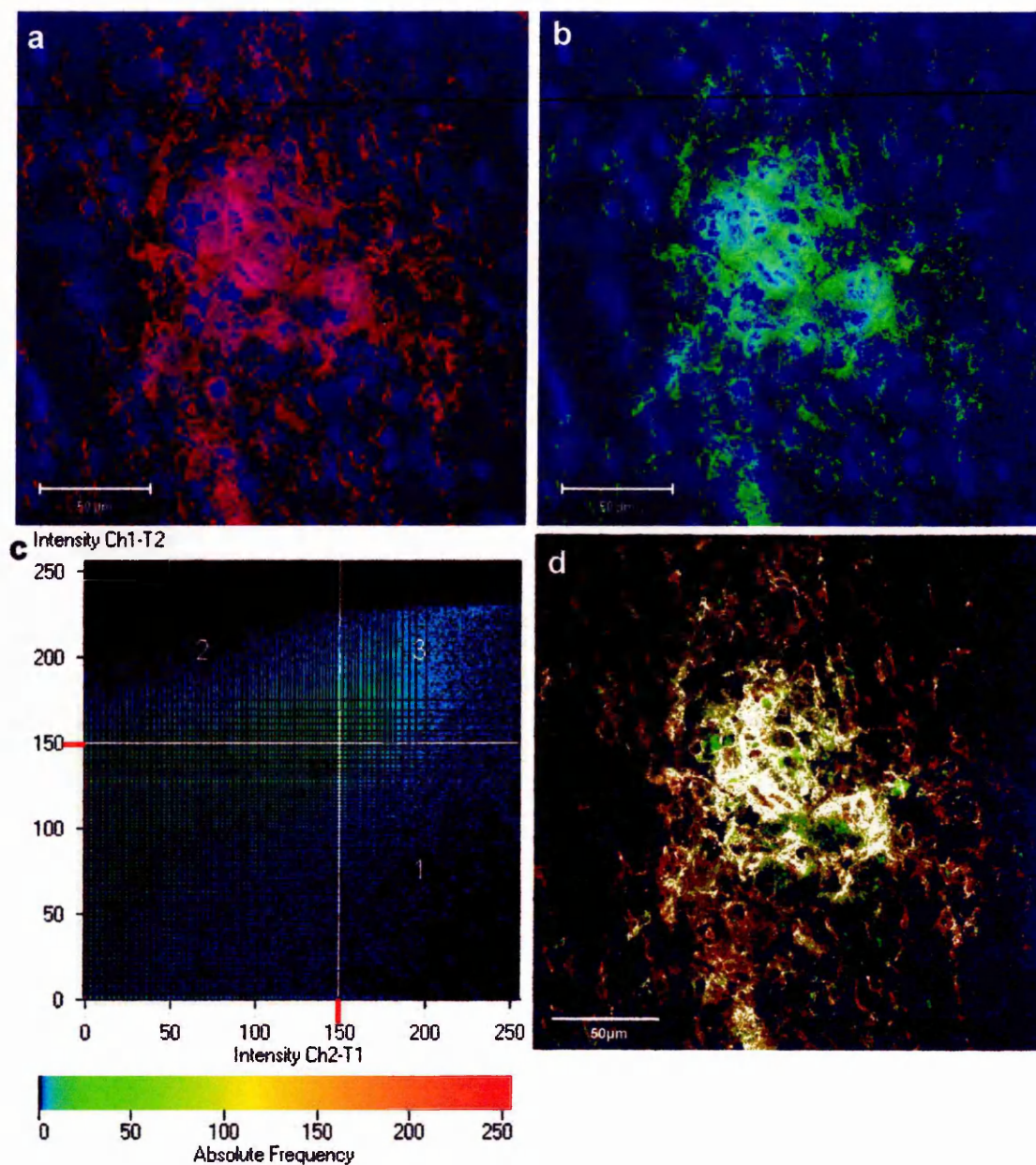
Single label immunofluorescent images of ADAM-17 expression (Green) within naïve (a) and EAE spinal cord white matter (b-d). ADAM-17 expression is associated with blood vessels in all naïve and EAE samples (a-d arrows). At peak-EAE and in animals in recovery there is an abundance of ADAM-17 cells throughout the white matter and in the perivascular infiltrate indicated by \* (e, f). All cell nuclei are counter stained with DAPI (Blue). Bar = 100µm.

Figure 4.3 ADAM-17 co-localisation with the astrocytic marker GFAP in EAE spinal cords



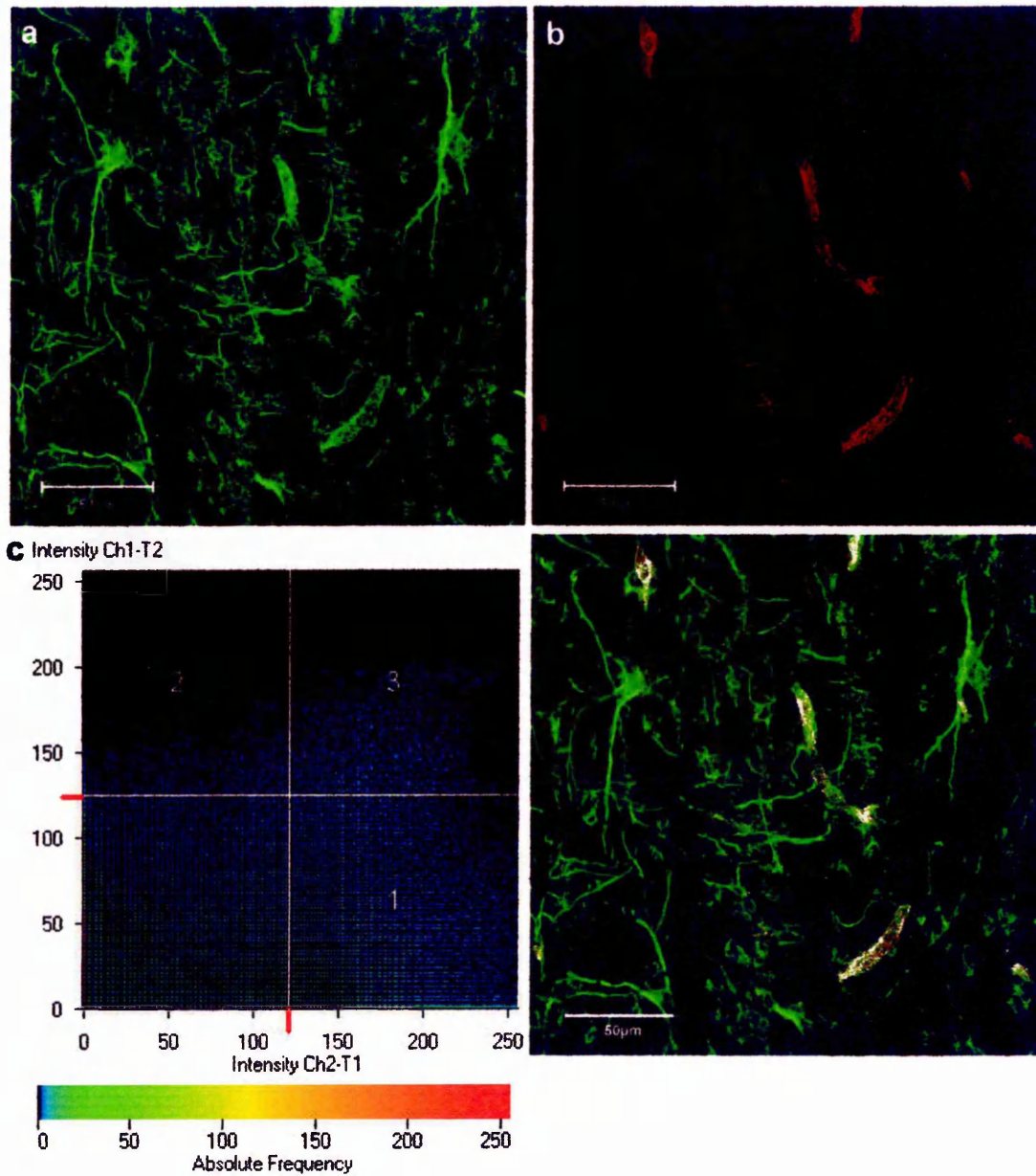
Dual label immunofluorescence for (a) ADAM-17(Green) and (b) GFAP (Red) in EAE spinal cord white matter. (c) Co-localisation is represented by the pixels in quadrant 3 on graph and is demonstrated as white pixels in the composite image (d) following Zeiss 510 CSLM software reading of individual pixels for each fluorophore. Bar = 50µm.

Figure 4.4 ADAM-17 co-localises with the macrophage marker ED1 in EAE



Dual label immunofluorescence for (a) ADAM-17(Red) and (b) ED1 (Green) in EAE spinal cord white matter. Co-localisation is represented by the pixels in quadrant 3 on graph (c) and is demonstrated as white pixels in the composite image (d) following Zeiss 510 CSLM software reading of individual pixels for each fluorophore. Nuclei in a&b are counterstained with DAPI (Blue). Bar = 50µm.

Figure 4.5 ADAM-17 co-localises with the endothelial marker von Willebrand factor in EAE



Dual label immunofluorescence for (a) ADAM-17(Green) and (b) von Willebrand factor (Red) in EAE spinal cord white matter. Co-localisation is represented by the pixels in quadrant 3 on graph (c) and is demonstrated as white pixels in the composite image (d) following Zeiss 510 CSLM software reading of individual pixels for each fluorophore. Bar = 50µm.

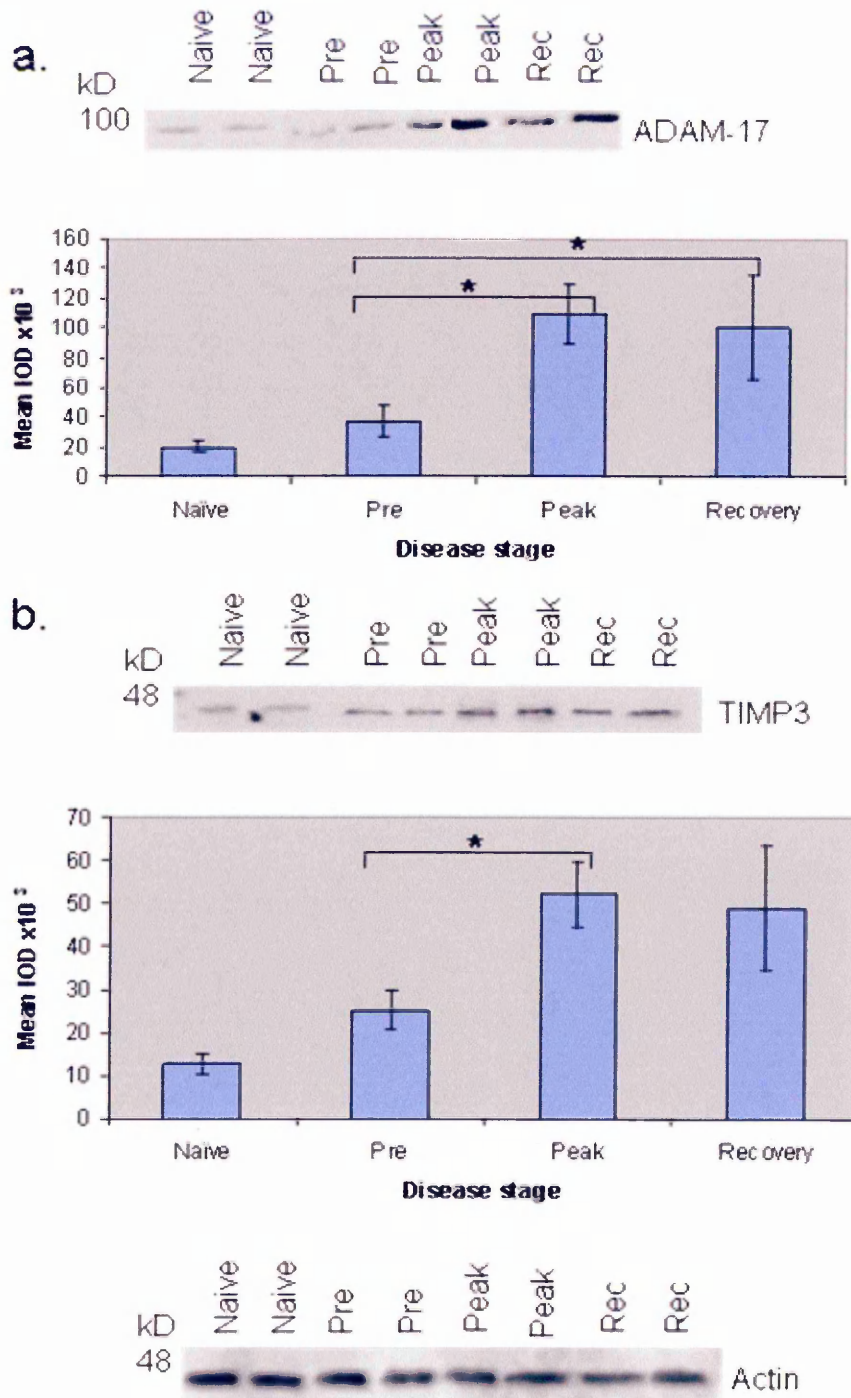
#### 4.3.3 ADAM-17 and TIMP3 protein levels in EAE and control rat spinal cord white matter

To confirm the indirect immunofluorescence findings for ADAM-17 and to assess TIMP3 expression in EAE CNS white matter SDS PAGE and western blot analysis was carried out upon extracted protein (6µg). ADAM-17 and its natural inhibitor TIMP3 are co-expressed constitutively within both naïve and EAE rat spinal cord white matter. Polyclonal TACE antibody produced a band at a molecular weight of 110 kDa whilst anti-TIMP3 was revealed a band at 46 kDa (Figure 4.6). Densitometric analysis of the western blots for ADAM-17 and TIMP3 expression in each group of 5 rats, shows a significant increase in integrated optical density (IOD) at peak-disease ( $p=0.016$ ,  $p=0.028$  respectively) compared with pre-disease. A significant increase was also observed in ADAM-17 ( $p=0.028$ ) in recovery. However the increase in TIMP3 at this time point was not significant ( $p=0.27$ ). The ratio of ADAM-17:TIMP3 was calculated from the mean IODs from each group and are given in table 4.3.

Table 4.3 Ratio of ADAM-17 and TIMP3 protein levels at four stages of EAE, as determined by western blotting.

EAE Disease Stage	Ratio of ADAM-17:TIMP3
Naïve	1.58:1
Pre-disease	1.48:1
Peak-disease	2.10:1
Recovered	2.05:1

Figure 4.6 Western blot analyses of ADAM-17 and TIMP3 expression during the disease course of EAE



Western Blot analysis of proteins extracted from rat spinal cord white matter homogenate for (a) ADAM-17 and (b) TIMP3 in naive (N) pre-disease (Pre), peak-disease (Peak) and rats in recovery (Rec). Two representative samples from each group are shown. Graph shows the mean integrated optical density (IOD)  $\pm$  SEM for each group of 5 animals. \* Indicates statistical significant differences ( $p < 0.05$ ). Western blotting for Actin (c) were performed as controls for sample loading.

#### *4.3.4 Detection of ADAM-17 and TIMP3 mRNA at various stages of EAE disease course*

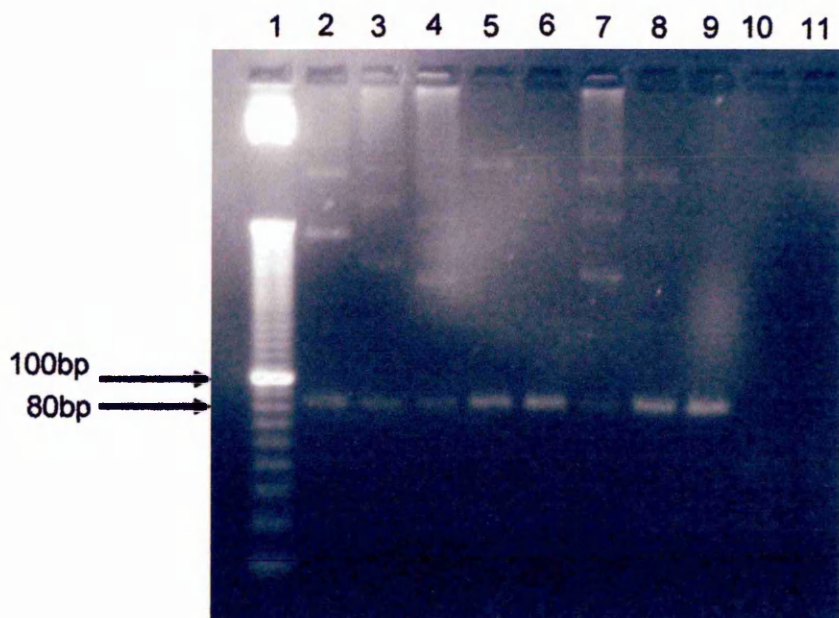
##### *4.3.4.1 RT-PCR*

cDNA was reverse transcribed from RNA extracted from white matter from all of the 20 rat samples. PCR products were obtained from real-time PCR primers designed for ADAM-17 and commercially available primer pairs for TIMP3. The size of the PCR products was determined by agarose gel electrophoresis and found to correspond to predicted sizes. An 80bp fragment was produced by the ADAM-17 real-time PCR primer pair and a 442bp fragment was produced by the TIMP3 primer pair (Figure 4.7 and 4.8).

##### *4.3.4.2 qRT-PCR*

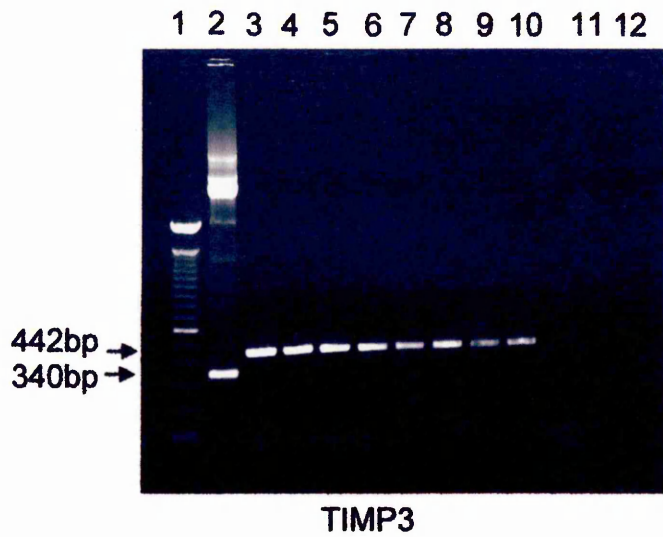
Initially primer pair efficiency was determined by plotting log (cDNA dilution) against cycle threshold (CT), the slope of which was  $-3.3 \pm 0.1$  for each primer pair, indicating maximal efficiency. qRT-PCR amplification of RNA from homogenates of EAE and normal control rat spinal cord white matter revealed that ADAM-17 and its natural inhibitor TIMP3 are constitutively and concurrently expressed at the mRNA level (Figure 4.9). ADAM-17 mRNA levels were shown to be significantly increased at peak-disease, compared with control samples, while TIMP3 mRNA levels were shown to be significantly decreased at peak-disease. ADAM-17 mRNA remained elevated in samples from rats in recovery and TIMP3 mRNA levels were also increased.

**Figure 4.7 RT-PCR products for ADAM-17 mRNA in naïve and EAE spinal cords at different stages of disease**



RT-PCR products of 80bp for rat specific ADAM-17 real-time primer pairs on an ethidium bromide stained 1% agarose gel. 100bp DNA ladder was run in lane 1. Naïve (lanes 2, 3) pre-disease (lane 4, 5), peak-disease (lanes 6, 7) and rats in recovery (lanes 8, 9). A negative control and a sample with no RT are in lanes 10 and 11 respectively.

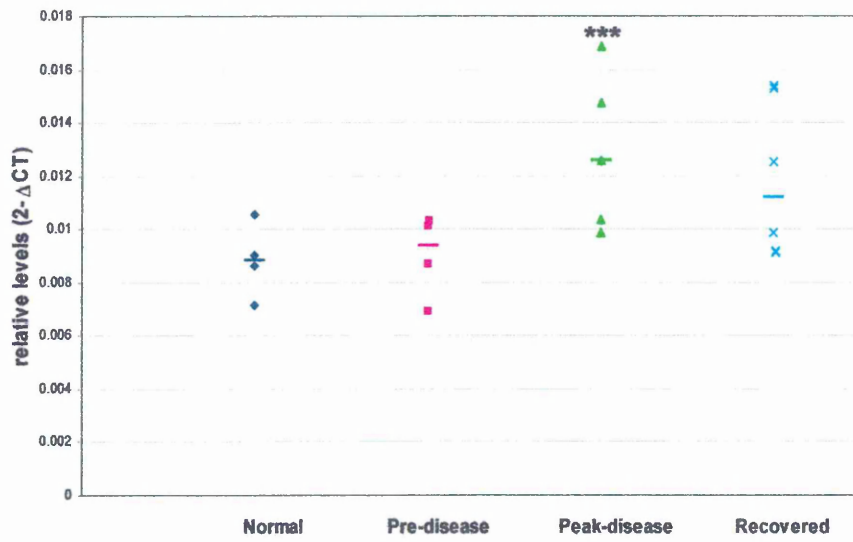
Figure 4.8 RT-PCR products for TIMP3 mRNA in naïve and EAE spinal cords at different stages of disease



RT-PCR products of 442bp for rat specific TIMP3 primer pairs on an ethidium bromide stained 1% agarose gel. 100bp DNA ladder was run in lane 1 and a positive control in lane 2. Naïve (lanes 3, 4) pre-disease (lane 5, 6), peak-disease (lanes 7, 8) and rats in recovery (lanes 9, 10). A negative control and a sample with no RT are in lanes 11 and 12 respectively.

Figure 4.9 qRT-PCR analysis of ADAM-17 and TIMP3 mRNA expression in naïve and EAE rat spinal cords at different stages

a. ADAM-17



b. TIMP3

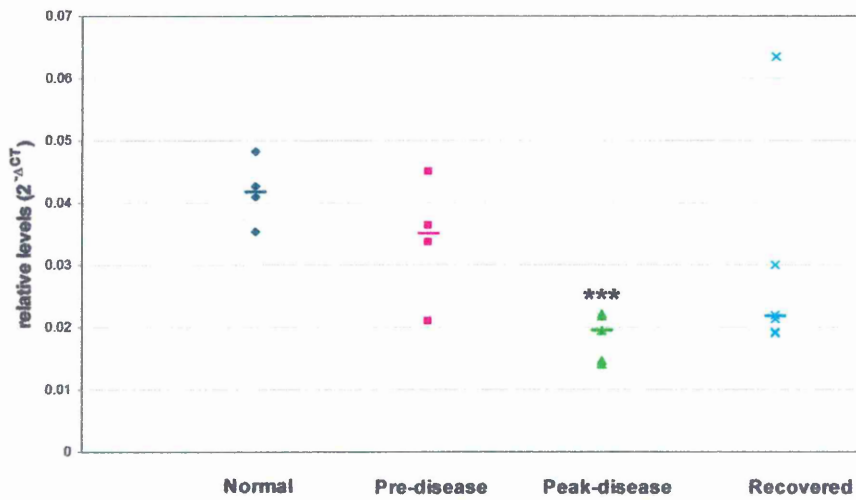
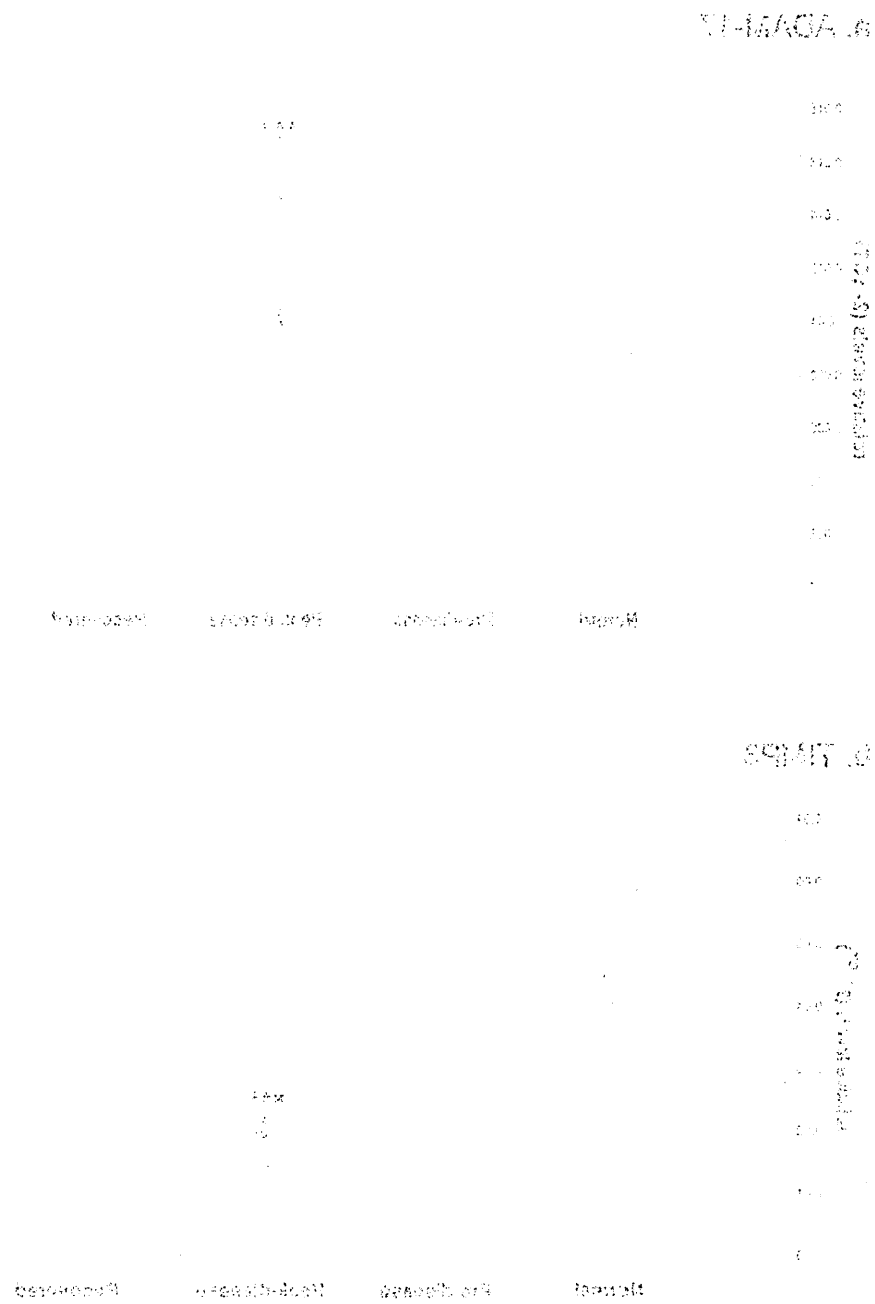


Figure 4.9. qPCR analysis of ADAM-17 and TIMP3 mRNA expression in naive and EA-treated splenic T cells.



#### 4.4 Discussion

The results presented here are the first to demonstrate the spectrum of distribution of ADAM-17 expression in EAE, along with a semi-quantitative analysis of the extent of ADAM-17 and TIMP3 protein and mRNA expression within the spinal cord white matter from pre-disease, peak disease and animals in recovery, compared with naïve animals. The utilisation of a well documented experimental model for MS has allowed the comparison of ADAM-17 and TIMP3 expression at various time points throughout the disease course. The model used in this study was an acute EAE model in Lewis rats. Though it does not exhibit extensive demyelination, it does produce an inflammatory disorder of the CNS that leads to a decline in motor functions, not dissimilar to MS, allowing the mechanisms of which to be studied. Stages of disease progression were determined by the extent of clinical disability and weight loss as described previously (Ohgoh *et al.*, 2002) as well as using the extent of expression of the inflammatory macrophage marker ED1. The first objective of this study was to establish a reproducible protocol for the identification of ADAM-17 and its natural inhibitor TIMP3 by immunofluorescence in snap frozen rat spinal cord material. The spinal cord was analysed instead of the brain as it is the most susceptible region of the CNS to inflammation in EAE (Villarroya *et al.*, 1997). Five antibodies (4 commercial and 1 a gift) were used in conjunction with different fixation and detection methods. Protein expression levels of ADAM-17 and TIMP3 were analysed by western blotting following separation of protein extracts from tissue homogenates by SDS PAGE. Increased expression of ADAM-17 protein was observed at peak stage of disease. Gene transcripts for these proteins were also demonstrated by reverse transcribing sample cDNA with commercially available rat specific primer pairs with semi-quantitative analysis achieved by qRT-PCR. Increased ADAM-17 mRNA was observed to coincide with a decrease in TIMP3 mRNA at peak disease suggesting an imbalance, between the enzyme and its inhibitor, in favour of ADAM-17 enzymatic activity.

ADAM-17 is involved in the proteolytic cleavage of various cytokines, cytokine receptors, chemokines and adhesion molecules suggesting possible immunological and pathological roles in inflammatory CNS diseases like EAE. ADAM-17 is considered to be the major proteinase responsible for the proteolytic processing of TNF into its soluble form (Black *et al.*, 1997). TNF has been shown to be involved in the pathological events in EAE (Kassiotis *et al.*, 1999) and has been reported to be present at sites of inflammatory reactions in EAE and MS (Selmaj *et al.*, 1991; Villarroya *et al.*, 1997). However due to the pleiotropic nature of TNF it has also been reported to have a protective effect in EAE (Liu *et al.*, 1998). In this present study, ADAM-17 immunoreactivity and mRNA levels were detected and reached a maximum at the peak-disease phase of EAE, which coincides with reported peak levels of CSF and serum TNF (Villarroya *et al.*, 1996).

ADAM-17 immunoreactivity is constitutively expressed during the disease course of EAE as demonstrated by indirect immunofluorescence. Morphologically, ADAM-17 immunoreactivity appeared associated with the microvasculature, within the spinal cord white matter of naïve and disease animals. Additionally, ADAM-17 immunoreactivity in the spinal cords of rats at peak disease and in recovery was associated with white matter cells with astrocyte and macrophage morphology. Co-localisation of ADAM-17 immunoreactivity with the astrocyte phenotypic marker, GFAP, the endothelial marker, von Willebrand factor and the inflammatory macrophage marker, ED1, following dual labelled immunofluorescence, clearly demonstrates that these cell types are responsible for ADAM-17 expression in EAE spinal cord white matter. These findings are in agreement with earlier studies on normal human CNS white matter (Goddard *et al.*, 2001) and the results on MS white matter presented here (Chapter 3). The presence of ADAM-17<sup>+</sup> inflammatory cells within the perivascular cuffs is also in agreement with an earlier study on MS lesions (Kieseier *et al.*, 2003) and the results on MS white matter presented here (Chapter 3). Astrocytes along with macrophage/microglial cells have been shown to be responsible for producing TNF in EAE and MS by immunocytochemistry (Hofman *et al.*, 1989; Probert and Akassoglou, 2001). ADAM-17 expression by astrocytes

and inflammatory macrophages would allow cleavage of TNF, releasing pro-inflammatory soluble TNF. TNF is reported to be toxic to myelin and oligodendrocytes therefore the release of membrane bound TNF could diffuse within the CNS parenchyma and mediate demyelination (Hohlfeld, 1997; Bitsch *et al.*, 2000a; Probert and Akassoglou, 2001). Over-expression of TNF in transgenic mice has been shown to trigger CNS inflammation and demyelination (Akassoglou *et al.*, 1998; Probert and Akassoglou, 2001). Further transgenic studies have demonstrated that TNFR p55 plays an exclusive role in mediating TNF-mediated oligodendrocyte apoptosis and primary demyelination in mice (Akassoglou *et al.*, 2003). TNF has also been shown to disrupt the function of the blood brain barrier (BBB) in EAE and in *in vitro* models, as measured by an increase in surface expression of ICAM-1 and a decrease in TER (Mayhan 2002; Dobbie *et al.*, 1999). Thus it is proposed that increased ADAM-17 expression may lead to an increase in soluble TNF leading to subsequent BBB disruption, cellular infiltration and disease progression.

Cerebral endothelial cells are reported to express TNF mRNA *in vitro* and upon bacterial infection release soluble TNF into the culture media as measured by ELISA (Freyer *et al.*, 1999). It is proposed that ADAM-17 expression by glial cells in EAE and MS leads to an increase in soluble TNF which in turn increases the amount of membrane-bound vascular adhesion molecules. The increase in adhesion molecules may provide an increase in substrate availability for endothelial cell ADAM-17. ADAM-17 immunoreactivity is evident at the cerebral endothelia in naïve rats and during all the stages of EAE investigated. As it has been reported that adhesion molecules are increased on cerebral endothelial cells during EAE (Selmaj, 2000) it is suggested that either ADAM-17 is no longer functionally cleaving these molecules, as would occur in basal conditions, possibly due to an increase in TIMP3, as seen at peak disease or that the TNF induced increase in adhesion molecules causes saturation in the ability of ADAM-17 to cleave these molecules.

ADAM-17 activity is dependant on the presence of its natural inhibitor TIMP3, with TIMPs reported to interact with a 1:1 stoichiometry with MMPs to inhibit their activity (Kossakowska *et al.*, 1998, Crocker *et al.*, 2004). The levels of ADAM-17 and TIMP3 were assessed at the protein and mRNA level by western blotting and qRT-PCR, which demonstrated ADAM-17 and TIMP3 protein expression at all stages of disease. Highest levels of ADAM-17 protein and mRNA were observed at peak disease when inflammatory activity, as gauged by ED1 immunoreactivity, was also at its highest. This increase in ADAM-17 is in agreement with immunocytochemistry results which showed an abundance of ADAM-17 immunoreactive cells throughout the white matter and inflammatory cuffs. ADAM-17 was significantly increased at peak disease suggesting a role in the disease process. TIMP3 protein expression was also increased at peak disease and in recovery however the extent of this increase was less than the increase recorded in ADAM-17. The amount of TIMP3: ADAM-17 shows a higher ratio of ADAM-17 at peak disease (2.01:1) compared with naïve rats (1.5:1), suggesting a balance in favour of an inflammatory response when clinical scores are at the highest (Table 4.3). This appears to be the case as mRNA levels of ADAM-17 are increased by almost 50% at peak-disease coupled with a 50% decrease in TIMP3 mRNA levels. However why decreased TIMP3 mRNA levels coexist with increased protein TIMP3 levels at peak disease is unclear. If the reduction of mRNA was due to a negative feed back loop to reduce the production of TIMP3 you would expect there to be an increase in TIMP3 protein prior to the reduction in mRNA, however this doesn't appear to be the case. Examining TIMP3 protein and mRNA at shorter time differences between pre and peak disease may however reveal otherwise.

Increased ADAM-17 activity, release of TNF and lymphocytic infiltration has been observed in TIMP3<sup>-/-</sup> mice (Mohammed *et al.*, 2004). TIMP3<sup>-/-</sup> mice spontaneously develop inflammation of the liver, similar to that observed in chronic hepatitis in humans, which corresponded with increased ADAM-17 activity in liver homogenates compared to wild-type. Soluble TNF is readily detected within the TIMP3<sup>-/-</sup> homogenates but not in wild-type (Mohammed *et al.*, 2004). TIMP3<sup>-/-</sup> mice that were also devoid of TNFR p55 showed no signs of inflammation while treatment of TIMP3<sup>-/-</sup> mice with

TIMP3 prevented inflammation, suggesting that the inflammatory damage was due to ADAM-17/TNF activity (Mohammad *et al.*, 2004). TIMP3 is suggested to be an important innate negative modulator of TNF in both tissue homeostasis and tissue response to injury (Black, 2004; Mohammed *et al.*, 2004). However, how TIMP3 reaches its target remains unclear, as TIMP3 binds to the ECM components (Yu *et al.*, 2000; Woessner, 2001; Black, 2004).

TIMP3 has been reported to be present in the choroid plexus and expressed by neurons and astrocytes in the parenchyma of normal mouse and rat brain (Pagenstecher *et al.*, 1998; Vaillant *et al.*, 1999; Jaworski and Fager, 2000; Crocker *et al.*, 2004). We have shown that TIMP3 is expressed within both naïve and EAE spinal cord white matter at the protein and mRNA level, but to date our attempts to elucidate the cellular origins of this protein in EAE have proved inconclusive. However *in vitro* studies using cerebral brain endothelial cell lines and primary human astrocytes (Chapter 5) have demonstrated TIMP3 to be expressed by these cell types.

Numerous TNF blockade studies, achieved via administration of anti-TNF monoclonal antibodies (MAb) or by soluble TNFRs, have been reported to efficiently inhibit EAE development, by neutralizing the pro-inflammatory properties of TNF (Baker *et al.*, 1994; Selmaj *et al.*, 1995; Selmaj and Raine, 1995; Selmaj, 2000; Glabinski, *et al.*, 2004). Subcutaneous administration of soluble TNFR p55 has been shown to prevent onset of EAE or a shorter and less severe disease course if administered upon clinical presentation of disease (Selmaj *et al.*, 1995; Selmaj, 2000). Intraperitoneal injection of TNFR p75 has been reported to reduce the number of relapses and clinical score in a CREAE model (Glabinski *et al.*, 2004). Treatment with soluble TNFR p55 is reported to be more potent inhibitor of TNF than TNFR p75 (Selmaj, 2000). TNF inhibition has proved highly successful in treating EAE however clinical trials of anti-TNF treatment in relapsing remitting MS proved ineffective and indeed exacerbated the disease (Van Oosten *et al.*, 1996; Lenercept Study, 1999; Sicotte and Voskuhl 2001).

Blockade of cell adhesion and transendothelial migration using anti-adhesion molecule MAbs and glucocorticoids have been investigated with promising results (Cannella *et al.*, 1995; Kent *et al.*, 1995; Engelhardt, 2000;

Theien *et al.*, 2001; van der Laan *et al.*, 2002; Pitzalis *et al.*, 2002; Myers *et al.*, 2005). Glucocorticoids are routinely administered as a treatment in MS and have been shown to modulate EAE disease course by regulating endothelial cellular adhesion molecule expression at the transcription level (Engelhardt, 2000; Pitzalis *et al.*, 2002; Dietrich, 2004). MAbs to VLA-4 have been reported to reverse BBB changes, as gauged by MRI, in an acute EAE model in guinea pigs (Kent *et al.*, 1995). Encouraging results taken from the anti-VLA-4 MAb treatment of EAE have been successfully applied to humans. The Natalizumab clinical trial in relapsing remitting MS was effective in reducing the relapse rate (Miller *et al.*, 2003). However following reports of progressive multifocal leukoencephalitis (PML) in two patients receiving dual therapy in the trial, Tysabri (Natalizumab) was withdrawn at the end of February 2005 (Kleinschmidt-DeMasters and Tyler, 2005; Berger and Korolnik, 2005). Care needs to be taken by researchers when extrapolating EAE data with respect to MS, as EAE is a well characterised disease that can be readily induced, monitored and controlled in inbred animals. MS however, has multiple disease courses and possibly multiple etiologies that occurs in out bred populations. Despite this, studies using EAE models may indicate mechanisms occurring in the pathogenesis of MS. The work here points to a possible role for ADAM-17 in the pathogenesis of EAE especially influencing the inflammatory reactions at the BBB. As such ADAM-17 may be a potential alternative therapeutic target for the treatment of MS.

## **Chapter 5**

**Expression and regulation of ADAM-17 and TIMP3 in  
endothelial cells *in vitro***

## 5.1 Introduction

### 5.1.1. *In vitro* cultures of cerebral endothelial cells

Ethical issues and constraints in access to tissue, means that *in vitro* models of primary cells are predominantly either bovine, porcine or rat (Rubin *et al.*, 1991; Franke *et al.*, 2000; Demeuse *et al.*, 2002). Primary brain capillary endothelial cells can be cultured on collagen coated culture flasks and after approximately 9 days are ready for experimental use (Franke *et al.*, 2000; Gumbleton and Audus, 2001). Primary cultures contain many similarities with the *in vivo* BBB endothelial cells, with the presence of endothelial antigens, adhesion molecules, TJ associated proteins and drug transporter systems. Functionally however, *in vitro* primary cells have a far lower TEER (160-200 $\Omega\text{cm}^2$ ) in comparison to *in vivo* (1000-5000 $\Omega\text{cm}^2$ ) and show an approximately 100 fold increase in sucrose permeability (Gumbleton and Audus, 2001). The use of co-cultures and conditioned media systems using primary porcine and rat astrocytes, astrogloma cells (C6) and brain pericyte cells and cell lines have been investigated as a means of establishing a more appropriate BBB model (Rubin *et al.*, 1991; Rauh *et al.*, 1992; Wolburg *et al.* 1994; Cecchelli *et al.*, 1999; Gumbleton and Audus, 2001; Jeliaskova-Mecheva and Bobilya, 2003; Terasaki *et al.*, 2003; Kraus *et al.*, 2004). These systems show an increase in TEER with a decrease in the paracellular permeability of sucrose. Removal of astrocytes from bovine brain capillary endothelial cell co-cultures returns the paracellular permeability to the high level recorded prior to co-culture (Kraus *et al.*, 2004). However treatment with IFN- $\beta$  enables the endothelial cells to maintain the low permeability even after removal of the astrocytes (Kraus *et al.*, 2004). It is reported however that the intra- and inter- batch reproducibility of results, poor life span of the cells plus the genetic differences across species, does not make these ideal BBB models (Gumbleton and Audus, 2001).

GP8 cells are a cerebral endothelial cell line that has been derived from Lewis rats (Greenwood *et al.*, 1996). GP8 cells have been shown to retain their phenotypic and immunological characteristics *in vitro* (Greenwood, *et al.*, 1996; Harkness *et al.*, 2000; 2003). GP8 cells are reported to express von Willebrand factor, P-glycoprotein and platelet endothelial cell adhesion

molecule. ICAM-1 expression can be up-regulated as can VCAM-1 and MCP1 expression following cytokine stimulation (Greenwood *et al.*, 1996; Etienne-Manneville *et al.*, 2000; Harkness *et al.*, 2003).

ADAM-17 is constitutively expressed by the cerebral endothelium and astrocytes in normal control and MS white matter and also in the spinal cord white matter of Lewis rats with EAE, as described in chapters 3 and 4. As described in chapter 1, cytokines are critical components of the immune inflammatory process and have been implicated in the disease onset and progression in MS and models of EAE (Brosnan, *et al.*, 1995; Imitola, *et al.*, 2005). To confirm the type of cells expressing ADAM-17 and to determine whether pro-inflammatory cytokines regulate expression levels of ADAM-17, and TIMP3, GP8 cells were stimulated with IFN $\gamma$ , TNF, TNF/IFN $\gamma$  combined and LPS *in vitro*.

### 5.1.2 Aim of study

Endothelial cells and astrocytes have been shown to express ADAM-17 in normal control white matter and in the spinal cord white matter of Lewis rats. During the disease processes of MS and EAE, ADAM-17 is upregulated (Chapters 3 and 4) therefore it is important to elucidate the significance of ADAM-17 modulation with respect to inflammatory conditions. The aim of this study was to confirm that both astrocytes and GP8 cells express ADAM-17 *in vitro* and to determine the sub-cellular localisation of the protein and to assess whether pro-inflammatory cytokines can increase the expression of ADAM-17. Any functional consequences of increased ADAM-17 expression on TNF shedding were also examined. ADAM-17 activity may also be affected by changes in TIMP3 thus the expression of this natural inhibitor was also examined.

The major objectives addressed were:

- (i.) To confirm the *in vivo* observation that astrocytes and endothelial cells express ADAM-17 *in vitro*.
- (ii.) To determine whether these cells express TIMP3 *in vitro*.
- (iii.) To examine the effect of pro-inflammatory conditions on ADAM-17, and TIMP3 protein expression in GP8 cells.

- (iv.) To determine whether GP8 cells release TNF under pro-inflammatory conditions.

## 5.2 Materials and methods

All cell culture reagents were obtained from Invitrogen unless stated otherwise. GP8 cells were a kind gift from Prof J Greenwood (University College London, London, UK). Primary human astrocytes were isolated from adult temporal lobe resections carried out at King's College Hospital, London (Flynn *et al.*, 2003) and were obtained with ethical approval from Dr I Romero (Open University, Milton Keynes, UK).

### 5.2.1 Cell cultures

Rat cerebral endothelial cell line (GP8) and primary human astrocyte cultures were grown at 37°C in a 5% CO<sub>2</sub>/95% air, humidified atmosphere. GP8 cells were maintained in MEM/Ham's F10 medium (1:1 v/v) supplemented with 10% heat inactivated fetal calf serum, penicillin (100U/ml) and streptomycin (100µg/ml) (PenStrep) and geneticin (200µg/ml). GP8 cells were grown on collagen coated cell cultureware (see below). Primary human astrocytes were maintained in MEM/Ham's F10 medium supplemented with 10% fetal calf serum, L-glutamine (2mM), fungizone (2.5µg/ml) and PenStrep. Culture media were changed every three days until cells became confluent, at which time they were then subcultured for experimental use or to maintain growth and stock levels. All cultures were grown with plasmocin (5µg/ml) to prevent mycoplasma contamination.

#### 5.2.1.1 Collagen coating

It was essential to grow GP8 cells on collagen coated cellculture ware. Cultureware (flasks, coverslips or well plates) were incubated in 0.1% collagen solution from calf skin (Sigma), diluted 1:20 in Hank's balanced salt solution (HBSS), for 2 hours at room temperature (RT). Excess collagen was removed by sterile aspiration and the culture ware was washed three times in sterile HBSS. Once coated the culture ware was maintained in HBSS at 4°C until ready for use, for up to 7 days.

### *5.2.1.2 Subculture*

Upon reaching confluence, cultures were subcultured using trypsin EDTA solution (1mM EDTA and 2.5g/L of trypsin). 5mls of trypsin-EDTA solution was added to culture flasks where the cells were incubated at 37°C for five minutes until cells detached from the flasks. Cells were centrifuged for 10 minutes at 1000rpm (Sorvall RT7 plus) at RT. The resulting cell pellets were resuspended in the appropriate growth media and plated at a 1:10 split ratio. Growth media was changed the day after subculture and every three days thereafter.

### *5.2.1.3 Culture on coverslips*

To enable immunocytochemical analyses, cells were grown on 13mm diameter glass coverslips (BDH) in the wells of sterile 6 well plates (3 coverslips per well). Coverslips were stored in 70% ethanol until required. Coverslips were removed from the ethanol and allowed to air dry for 20 minutes prior to collagen coating and introduction of the cells.

### *5.2.2 Indirect immunofluorescence staining*

Cells on coverslips were removed from the media and washed through two changes of PBS and were then fixed in either ice-cold acetone or 4% paraformaldehyde at RT for 5 minutes. Acetone fixed cells were allowed to air dry for at least 15 minutes prior to use or storage at -20°C. Following paraformaldehyde fixation, cells were washed and stored in PBS. To enable permeabilisation of the cells for intracellular staining following paraformaldehyde fixation, all antibodies were diluted in 0.5% Triton X-100 (Sigma) in PBS.

The GP8 endothelial cells and primary human astrocytes were labelled for specific phenotypic markers by indirect immunofluorescence. GP8 cells were labelled for VWF and primary human astrocytes for GFAP using polyclonal rabbit anti-human VWF (1:50) and rabbit anti-cow GFAP (1:100) respectively. Cells were incubated in primary antibody for 1 hour at 37°C and then washed three times, 5 mins each, in PBS. Cells were then incubated in Alexa 488 conjugated goat anti-rabbit IgG (1:500, Molecular Probes) for 1 hour at 37°C. Following a further 3 x 5 minutes washes in PBS,

cell nuclei were counterstained by mounting in a Vectashield mounting medium containing DAPI (Vector Labs). Alternatively cell nuclei were counterstained by incubating in propidium iodide in PBS (1:30,000, Sigma) for 15 seconds. Cells were then washed in PBS and mounted in the non-fading mountant, citifluor (See appendix).

Ice cold acetone and 4% paraformaldehyde fixed cells were labelled for ADAM-17 using monoclonal human anti-mouse M222 (1:100, Amgen, USA), and the polyclonal antibodies goat anti-rabbit TACE (1:50, Abcam) and goat anti-rabbit TACE C15 (1:20, Santa Cruz) using the indirect detection method described above. Monoclonal M222 was detected by incubating the cells in FITC-conjugated rabbit anti-mouse IgG (1:50, Dako) for 1 hour at 37°C. Cells were labelled for the cytoskeletal markers  $\beta$ -tubulin, vimentin, and actin as well as the Golgi apparatus, Table 5.1 provides the details of the primary antibodies used in this study and the secondary antibodies used were the same as above for either monoclonal or polyclonal antibodies.

#### *5.2.2.1 Dual label immunofluorescence to determine the sub-cellular localisation of ADAM-17 in GP8 endothelial cells*

Dual label immunofluorescence was performed on cells to determine the sub-cellular localisation of ADAM-17 following the protocol described previously in section 3.2.2. GP8 endothelial cells were dual labelled with monoclonal anti-ADAM-17 antibody (M222) together with polyclonal anti-tubulin and anti-vimentin antibodies and Alexa 568 conjugated phalloidin. Furthermore the polyclonal goat anti-rabbit TACE (Abcam) antibody was dual labelled with a monoclonal anti-Golgi antibody.

#### *5.2.2.2 Imaging*

All images were obtained using the Zeiss 510 confocal scanning laser microscope as described previously in section 3.2.3.

Table 5.1 Primary antibodies used for immunocytochemistry in the cell culture study

Primary Antibody	Species	Target	Working Dilution	Source
Tubulin	M	$\beta$ -Tubulin cytoskeleton, human/rat/mouse	1 in 50	Pharmingen
Phalloidin 568*	Conjugated	Actin cytoskeleton	1 in 40	Molecular Probes
Vimentin	M	Vimentin cytoskeleton, human/rat	1 in 50	Dako
Golgi	M	Golgi apparatus, human/rat/mouse	1 in 50	Abcam
TACE	P	ADAM-17, human	1 in 50	Abcam
M222	M	ADAM-17, human	1 in 100	Amgen
TIMP3	M	TIMP3, human	1 in 100	Calbiochem
TIMP3	M	TIMP3, human	1 in 50	Oncogene
TIMP3	P	TIMP3, human	1 in 50	Abcam
VWF	P	Endothelial cells human/rat	1 in 50	Dako
GFAP	P	Astrocyte, human/rat/mouse	1 in 100	Dako

GFAP = glial fibrillary acidic protein

VWF = Von Willebrand Factor

M = mouse monoclonal antibody

P = rabbit polyclonal antibody

\* = Phalloidin is a phallotoxin isolated from the deadly *Amanita phalloides* mushroom that efficiently labels F-actin (Small *et al.*, 1999).

Table 5.1 Primary antibodies used for immunocytochemistry in the cell culture study

Antibody	Concentration	Species	Isotype	Target
Phalloidin	1 in 50	Human	M	F-actin
Phalloidin	1 in 40	Human	M	F-actin
Phalloidin	1 in 50	Human	M	F-actin
Phalloidin	1 in 50	Human	M	F-actin
Phalloidin	1 in 50	Human	M	F-actin
Phalloidin	1 in 100	Human	M	F-actin
Phalloidin	1 in 100	Human	M	F-actin
Phalloidin	1 in 50	Human	M	F-actin
Phalloidin	1 in 50	Human	M	F-actin
Phalloidin	1 in 50	Human	M	F-actin
Phalloidin	1 in 50	Human	M	F-actin
Phalloidin	1 in 100	Human	M	F-actin
Phalloidin	1 in 100	Human	M	F-actin

GFAP = glial fibrillary acidic protein  
 VWF = Von Willebrand factor  
 M = mouse monoclonal antibody  
 P = rabbit polyclonal antibody  
 \* = Phalloidin is a phalloidin isolated from the deadly Amanita phalloides mushroom that efficiently labels F-actin (Small et al., 1999).

### 5.2.3 Cytokine stimulation of GP8 endothelial cells

GP8 cells were grown in collagen coated T-25 culture flasks. Upon reaching approximately 90% confluence, the cells were incubated in serum free media for 24 hours containing TNF, IFN $\gamma$  and combined TNF/IFN $\gamma$  rat specific recombinant cytokines (Peprotech, London, UK) at concentrations of 1ng/ml, 10ng/ml and 100ng/ml. After 24 hours, the supernatant was removed and stored at -20°C and the protein and RNA were extracted from the cell lysates as described below in section 5.2.4. As a control, cells were also grown in serum free media without any stimulation from cytokines. All stimulation experiments were performed in triplicate.

### 5.2.4 Protein extraction

Following the removal of the cell culture supernatant, 500 $\mu$ l of an extraction buffer (5mM Tris-base, 26mM Tris-HCL, 1.25mM EDTA, pH 7.5) containing a cocktail of protease inhibitors (Roche) was applied to a T-25 flask of cells and a cell suspension was obtained using a cell scraper. The cell suspension was homogenised by repeat pipetting and incubated on ice for 1 hour. Cell homogenates were vortexed every 10 minutes. After the 1 hour incubation on ice, cell homogenates were centrifuged at 12000rpm (Sorvall RT7 plus) for 10 minutes at 4°C and the supernatant containing cell lysate was removed from the pellet and protein estimation was carried out using the BCA assay as described previously in section 3.2.6.1.

#### 5.2.4.1 Western Blot

Extracted protein was added to sample buffer 1:1 (v/v) and the protein was denatured at 60°C for 30 minutes. 6 $\mu$ g of each protein sample was loaded onto pre-cast 10% BisTris gels (Invitrogen) and subjected to SDS PAGE and western blotting as described previously in section 3.2.7. Quantitative analysis was carried out by comparing the IOD using densitometric software of the UVP Bioimaging system. Group means of IODs were obtained, with control samples being the baseline of 100% and any significant differences determined using the two-tailed t test ( $p < 0.05$ ). The statistical analysis was carried out using Microsoft Excel.

### 5.2.5 TNF enzyme linked-immuno-sorbent assay

#### *Principle of method*

The enzyme linked-immuno-sorbent assay (ELISA) used in this study is a solid phase sandwich ELISA. A rat specific TNF antibody is pre-coated onto the wells of the microtiter strips. Any rat specific TNF antigen within the test sample binds to the bound TNF antibody and is then labelled with a biotinylated antibody against TNF. A streptavidin-peroxidase solution binds to the biotinylated antibody completing a four-member sandwich. A substrate solution is added, which is acted upon by the bound enzyme to produce a colour that is directly proportional to the concentration of rat TNF present within the test sample, detected at 450nm in a plate reader. TNF standards of known concentrations are run on the same plate to produce a standard curve from which levels of TNF in cell culture supernatants can be determined.

#### *Method*

Supernatants, removed prior to protein and RNA extractions, were concentrated using a 10MW centricon centrifugal filtering device (Millipore). The original 7ml of supernatant was reduced 14 fold to 500µl prior to measurement of TNF by ELISA (Biosource), by centrifuging samples at 2000g (Sorvall Legend RT) for 5 hours at 4°C. All samples were run in duplicate. All solutions used in the ELISA protocol were supplied within the kit unless otherwise stated.

Briefly, 50µl of incubation buffer was added to each well. 100µl of TNF standards were added to designated wells in duplicate, while 50µl of sample and 50µl standard diluent buffer were added into test wells. 50µl of a biotinylated anti-TNF antibody solution was added to each well and incubated for 90 minutes at RT. Solutions were removed from all wells which were then washed for 4 x 30sec in 400µl wash buffer. Excess wash buffer was removed by firm tapping of the wells onto paper towel. Wells were then incubated in 100µl of Streptavidin-HRP for 45mins followed by a further 4 x 30sec washes with 400µl wash buffer. Wells were incubated in 100µl of

stabilized chromogen (Tetramethylbenzidine) for 30mins at RT in the dark, which resulted in the formation of a blue product. To stop the reaction, 100µl of stop solution was added to each well resulting in a yellow colour.

Absorbance of each well at 450nm was recorded using a Wallac Victor<sup>2</sup> 1420 multilabel counter plate reader.

To distinguish between added and synthesised TNF, media containing TNF was examined along with supernatants from cells treated with TNF.

### *5.3 Results*

#### *5.3.1 Characterisation of cell cultures*

GP8 cells were morphologically homogeneous and appeared as long thin spindle like cells (Figure 5.1a). The primary human astrocytes displayed a more heterogeneous morphology from bipolar to process bearing cells. Upon reaching confluence the primary human astrocytes formed a tightly packed population with few processes (Figure 5.1.c). GP8 cells expressed immunoreactivity for von Willebrand factor, a phenotypic marker for endothelial cells (Figure 5.1 b). The primary human astrocytes were immunoreactive for the intermediate filament protein, GFAP, which is a phenotypic marker for astrocytes (Figure 5.1d).

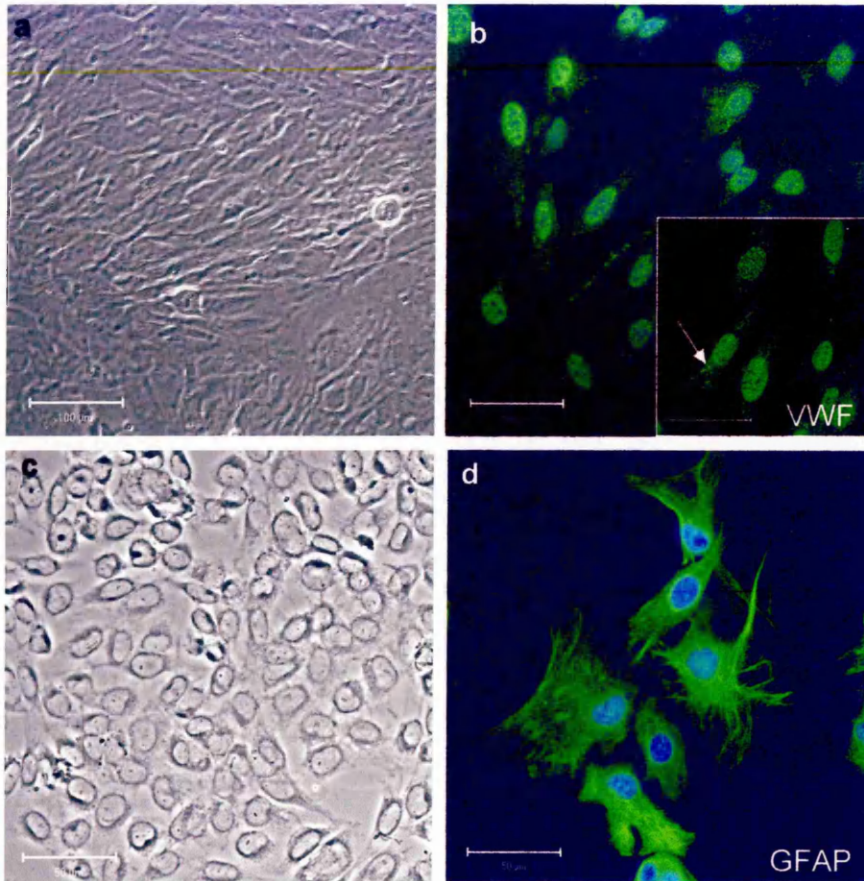
#### *5.3.2 ADAM-17 and TIMP3 expression within cell cultures*

The presence of ADAM-17 and TIMP3 within both cell types was investigated using immunocytochemistry and western blotting.

##### *5.3.2.1 ADAM-17 expression in cell cultures*

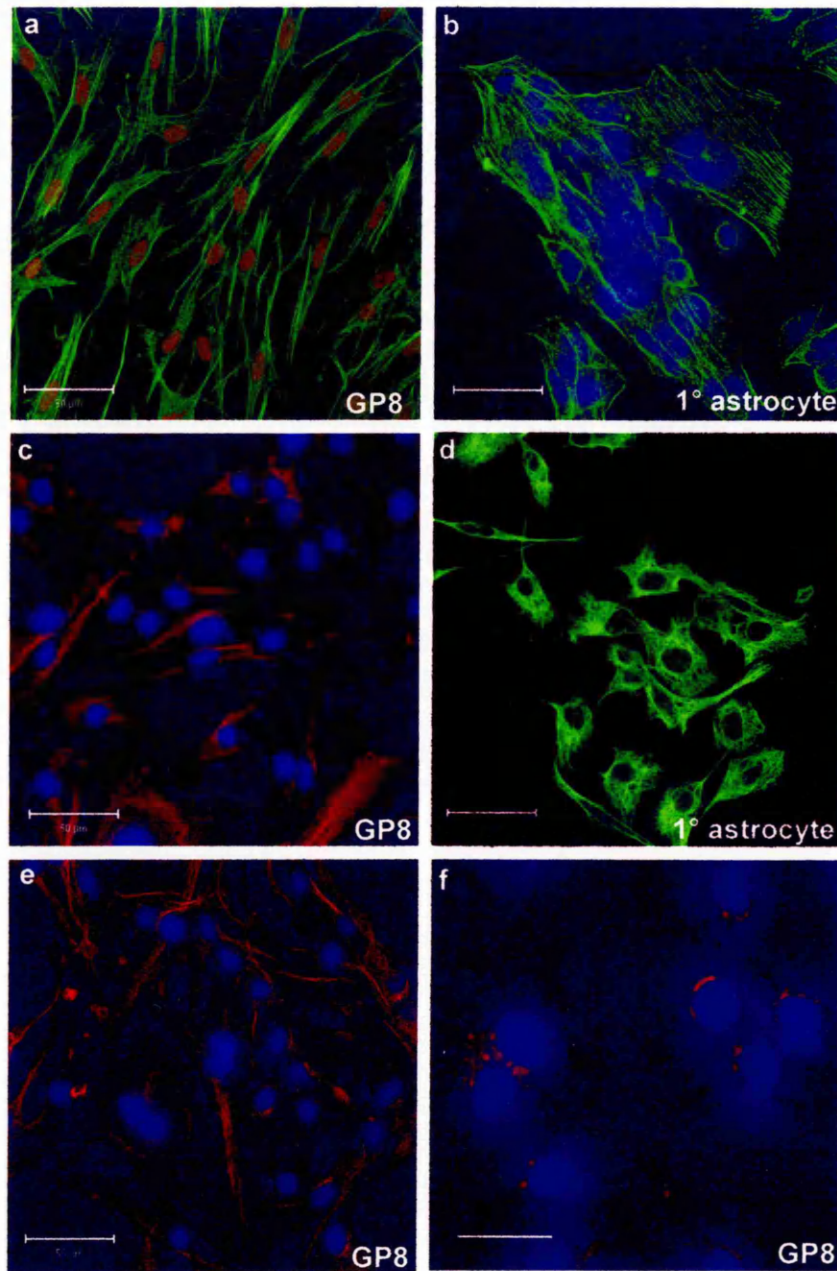
ADAM-17 immunoreactivity was expressed by both the cerebral endothelial cells and primary astrocytes following both acetone or paraformaldehyde fixation and detection by indirect immunofluorescence. The distribution of ADAM-17 immunoreactivity was consistent when comparing staining with the monoclonal anti-ADAM-17 and the polyclonal antibody (TACE from Abcam) for both cell types (Figure 5.2 a & b).

**Figure 5.1 Characterisation of GP8 endothelial and primary human astrocyte cell cultures**



Phase contrast (a, c) and single label immunofluorescent images (b, d) showing the morphology and phenotypic makers of GP8 (a, b) and primary human astrocyte cells (c, d). Note the vesicular staining pattern of VWF (arrows b insert). Cell nuclei are counter stained with DAPI (b, d). Bar = 100µm (a) and 50µm (b-d).

Figure 5.2 Single label immunofluorescence for ADAM-17 and cytoskeletal markers in GP8 endothelial cells and 1° human astrocytes



Single label immunofluorescence on GP8 cells (a, c, e, f) and primary human astrocytes (b, d) for ADAM-17 (a, b), and the cytoskeletal markers phalloidin (c), vimentin (d) and tubulin (e) and the Golgi apparatus (e). Cell nuclei are counterstained with propidium iodide (a, Red) and DAPI (b, c, e, f, Blue). Bar = 50 $\mu$ m (a-e) 25 $\mu$ m (f).

Examination of CSLM z-stacks by the deconvolution software, Velocity 3.0, displayed cell surface ADAM-17 expression (Figure 5.3b) along with intracellular ADAM-17 expression throughout the thickness of the z-stack (Figure 5.3.c). ADAM-17 immunoreactivity appeared fibrillary with a cytoskeletal morphology thus dual label immunofluorescence was performed with Alexa 568 conjugated phalloidin and antibodies to tubulin and vimentin, to determine the specific cytoskeletal localisation of the ADAM-17 expression (Figure 5.4 and 5.5). Using the co-localisation software of the Zeiss 510 CSLM revealed ADAM-17 expression was associated with the actin filaments (Figure 5.4). Dual label immunofluorescence was also carried out with ADAM-17 and antibodies to detect beta tubulin and the Golgi apparatus however no co-localisation was detected by this method (Figure 5.5).

Further evidence for the presence of ADAM-17 protein in both cerebral endothelial cell and primary human astrocytes was obtained using SDS PAGE and western blotting of cell lysates. Western blotting using the monoclonal ADAM-17 antibody consistently gave bands at 80 kDa (Figure 5.6).

#### 5.3.2.2 *TIMP3 expression in cell cultures*

Attempts to identify the cellular localisation of TIMP3 by immunocytochemistry have proved inconclusive as no immunoreactivity was identified using three commercially available antibodies and detection by the indirect and biotin-avidin methods. TIMP3 protein expression as observed following SDS PAGE and western blotting suggests that TIMP3 immunoreactivity may be at a level below the detection threshold of these methods or that the epitope is not accessible or is destroyed following acetone and 4% paraformaldehyde fixation. TIMP3 protein expression however is constitutive in both cell cultures investigated by western blotting. TIMP3 was represented by a band at 46 kDa using the monoclonal antibody from Oncogene (Figure 5.6).

ADAM-17 immunoreactivity (green) in 4% paraformaldehyde fixed GP8 endothelial cells a-c. CSLM z-stacks were deconvolved using Velocity software to enable 3D manipulation of the z-stacks in the x, y and z planes (green, red and blue arrows b & c). ADAM-17 immunoreactivity is detected along the surface over the nuclei of the cells (white arrow d). Cross-section of cells demonstrates ADAM-17 immunoreactivity throughout the thickness of the cell (white arrow c). Cell nuclei are counterstained with propidium iodide (Red). Scale bar = 50µm. One white box unit = 53.1µm.

ADAM-17 immunoreactivity (Green) in 4% paraformaldehyde fixed GP8 endothelial cells a-c. CSLM z-stacks were deconvoluted using Velocity software to enable 3D manipulation of the z-stacks in the x, y and z planes (green, red and blue arrows b & c). ADAM-17 immunoreactivity is detected along the cell surface over the nuclei of the cells (white arrow b). Cross-section of cells demonstrates ADAM-17 immunoreactivity throughout the thickness of the cell (white arrow c). Cell nuclei are counterstained with propidium iodide (Red). Scale bar = 50 $\mu$ m. One white grid unit = 23.1 $\mu$ m.

Figure 5.3 Cellular localisation of ADAM-17 in GP8 endothelial cell cultures

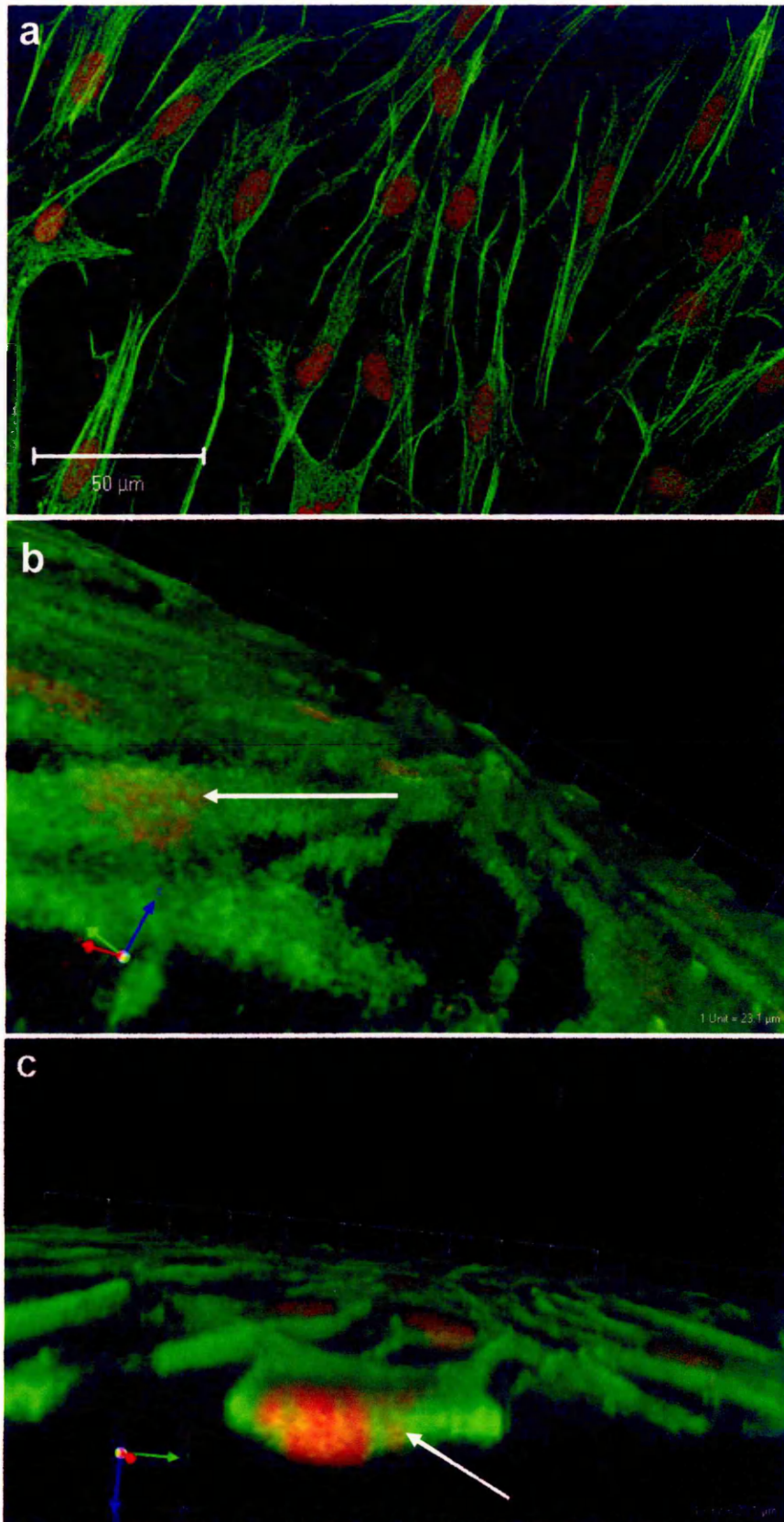
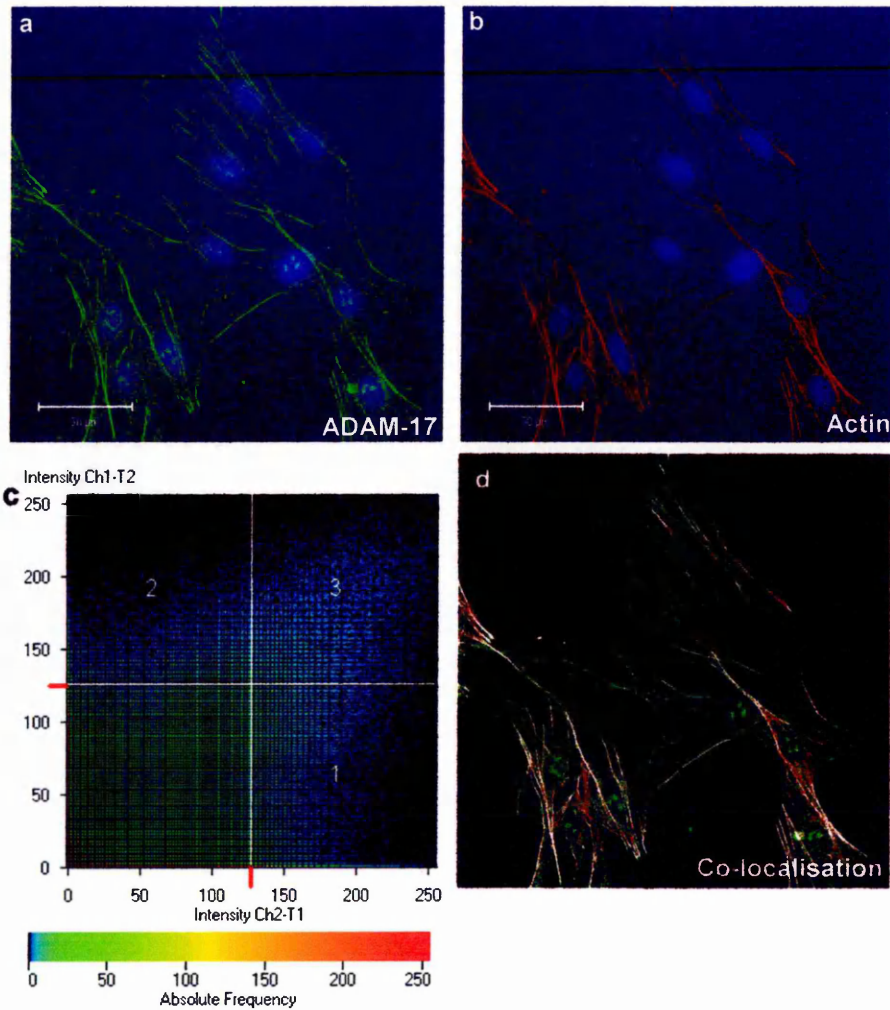
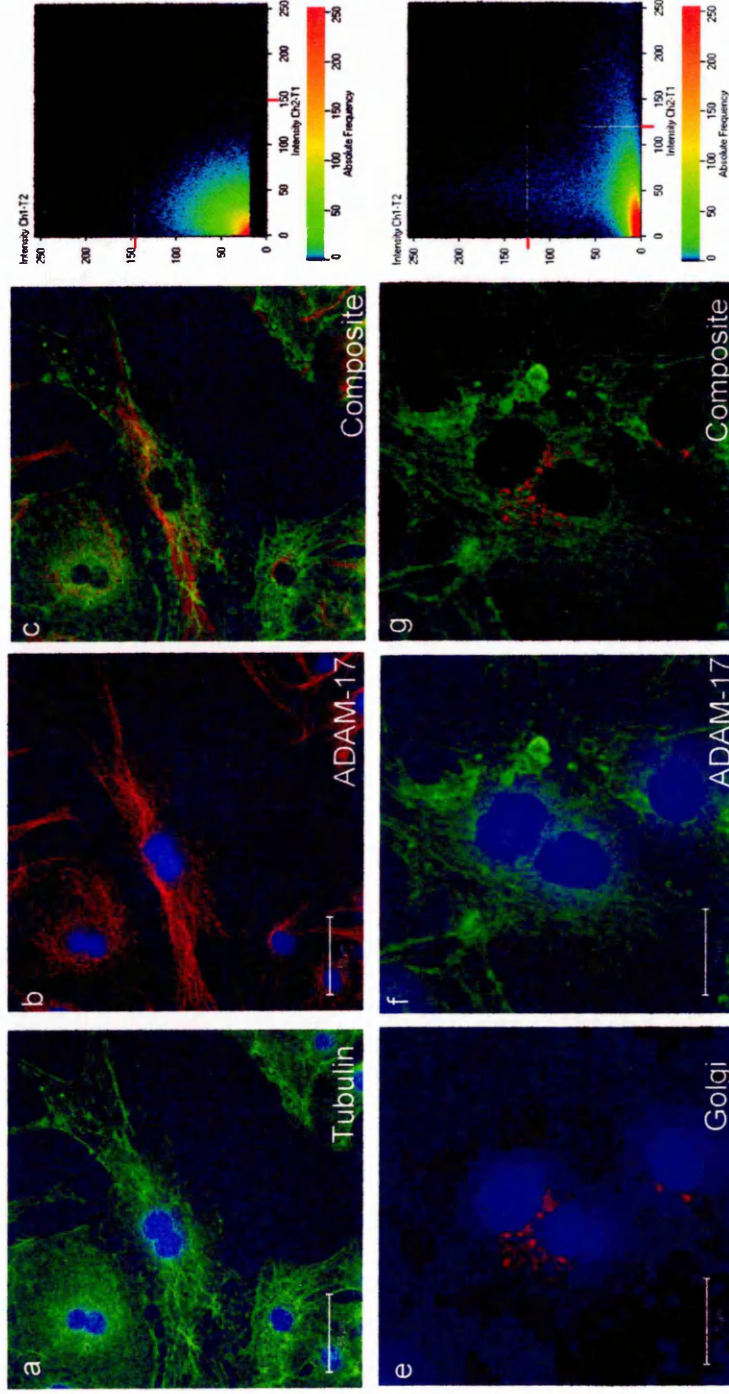


Figure 5.4 ADAM-17 co-localises with actin filaments in GP8 endothelial cells



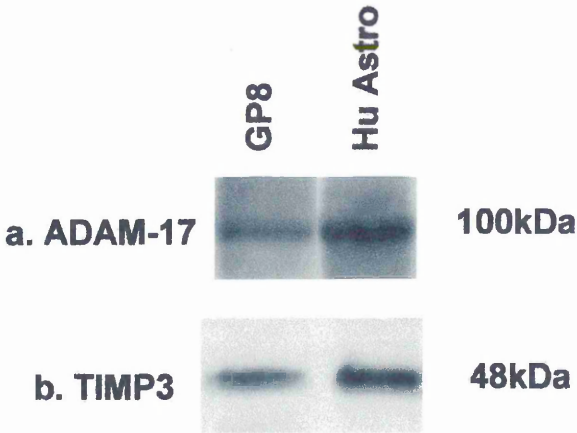
CSLM image of GP8 cells dual labelled for ADAM-17 (a) and actin (b) with the cell nuclei counterstained with DAPI (Blue). Co-localisation analysis shows co-localised pixels in quadrant 3 (c) and ADAM-17 expression co-localising with the actin filaments as white pixels in the composite image (d). Bar = 50 μm

**Figure 5.5 Dual label immunofluorescence for ADAM-17 and markers for Golgi apparatus and tubulin in GP8 endothelial cells**



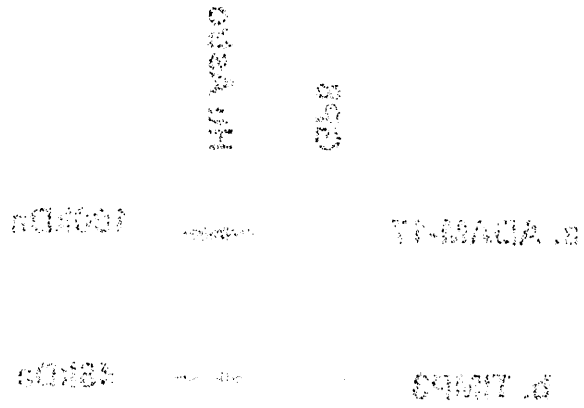
Dual label immunofluorescence for ADAM-17 with antibodies against beta-tubulin (a-c) and the Golgi apparatus (e-h). Using the co-localisation software of the Zeiss 510 CSLM ADAM-17 is shown not to be associated with the beta-tubulin cytoskeleton or the Golgi apparatus. No pixels are represented in quadrant 3 of the spectral scatter graphs (d, h). Bar = 50µm (a & b) 20µm (e & f)

Figure 5.6 ADAM-17 and TIMP3 protein expression in GP8 endothelial and primary human astrocyte cell cultures



Western blots showing constitutive expression of (a) ADAM-17 and (b) TIMP3 in GP8 endothelial cell cultures and primary human astrocytes.

Isiirtoobta B92 ni noqaaqaxa niidooq B910Y baa YI-MACIA 3 3 aagaq  
 ee-kubaa laa-asiyoobaa namuri yarmiq baa



(d) baa YI-MACIA (a) ni noqaaqaxa ee-kubaaqaxa qriwarka afaaf maaqaa  
 .asiyoobaa namuri yarmiq baa ee-kubaaqaxa laa-kubaaqaxa B92 ni B910Y

### *5.3.3 Cytokine regulation of ADAM-17 and TIMP3 expression in GP8 endothelial cells*

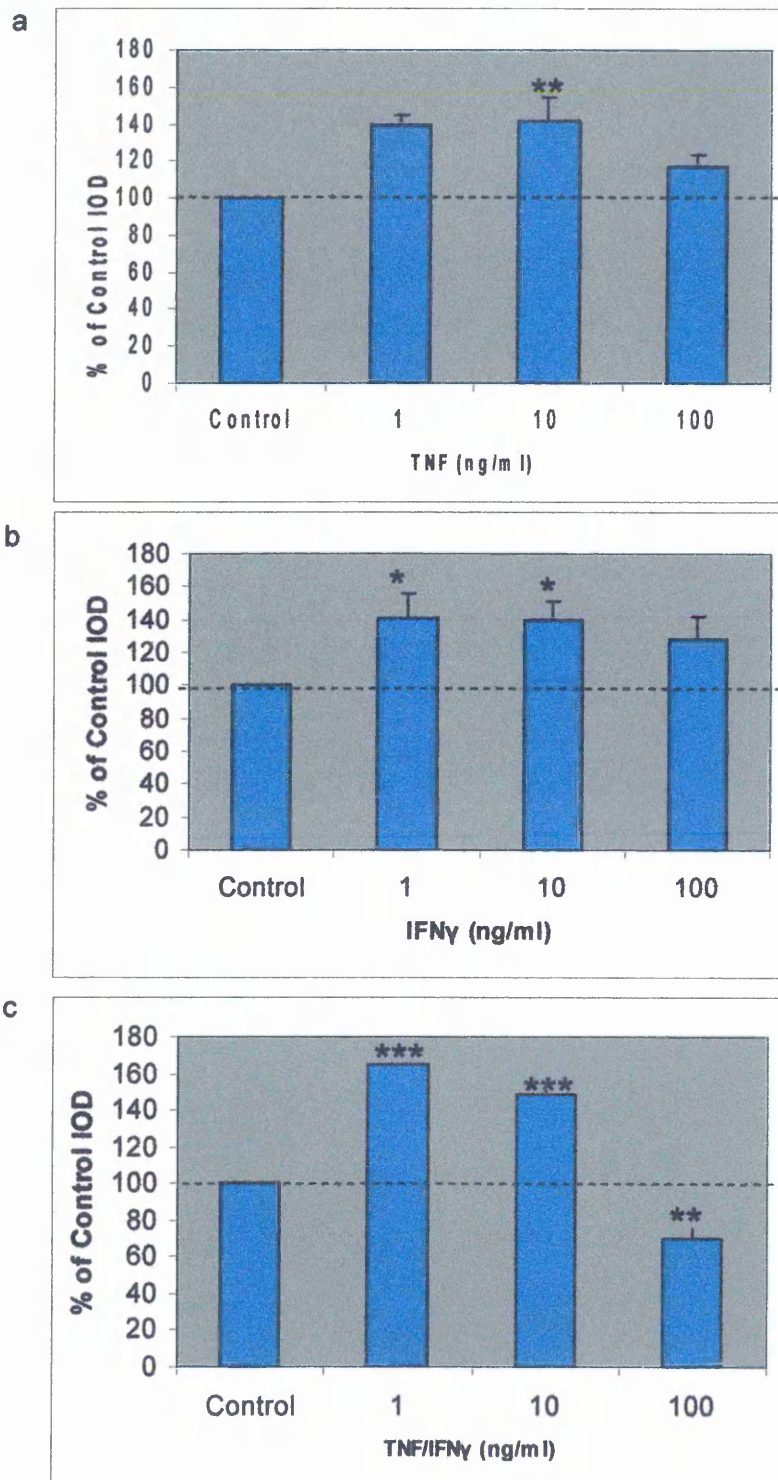
GP8 cells were stimulated for 24hrs in serum free culture media that contained the pro-inflammatory cytokines IFN $\gamma$  and TNF. TNF and IFN $\gamma$  stimulation of GP8 cells resulted in a small significant increase in ADAM-17 protein expression ( $p \leq 0.05$ ) when assessed by western blotting (Figure 5.7). When GP8 cells were incubated simultaneously in both IFN $\gamma$  and TNF, a marked increase was observed following 1ng/ml and 10ng/ml ( $p \leq 0.0001$ ), however a reduction in ADAM-17 expression was observed following concentrations of 100ng/ml compared with control ( $p \leq 0.01$ ) (Figure 5.7). Immunoreactivity for ADAM-17 in GP8 cells no longer appeared associated with the actin cytoskeleton following 24 hour stimulation in pro-inflammatory conditions and showed a diffuse cytoplasmic distribution (Figure 5.8).

Following stimulation by pro-inflammatory cytokines TIMP3 protein expression levels were reduced compared to unstimulated controls when assessed by western blotting (Figure 5.9). Reduction of TIMP3 protein levels were only significant following treatment with TNF at 1ng/ml and IFN $\gamma$  at 10ng/ml ( $p \leq 0.05$ ).

### *5.3.4 Cytokine regulation of TNF release by GP8 cells*

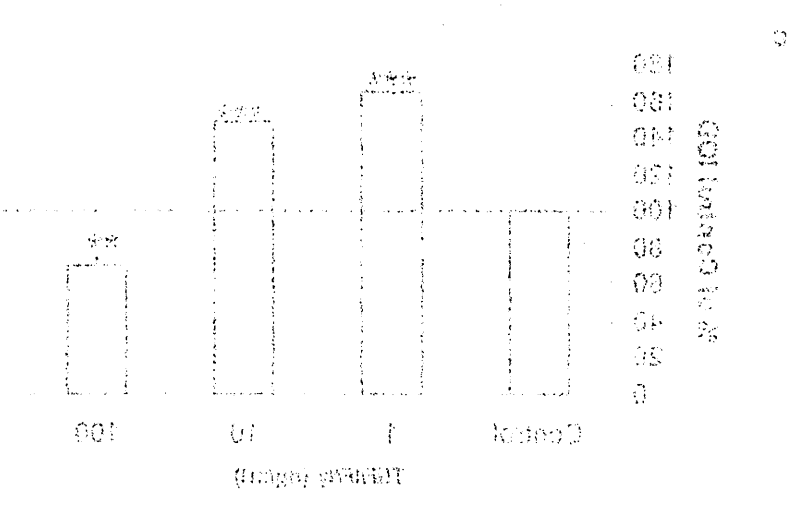
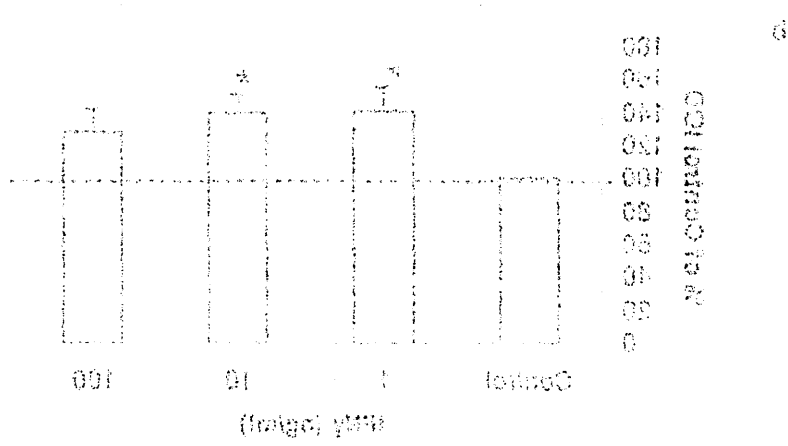
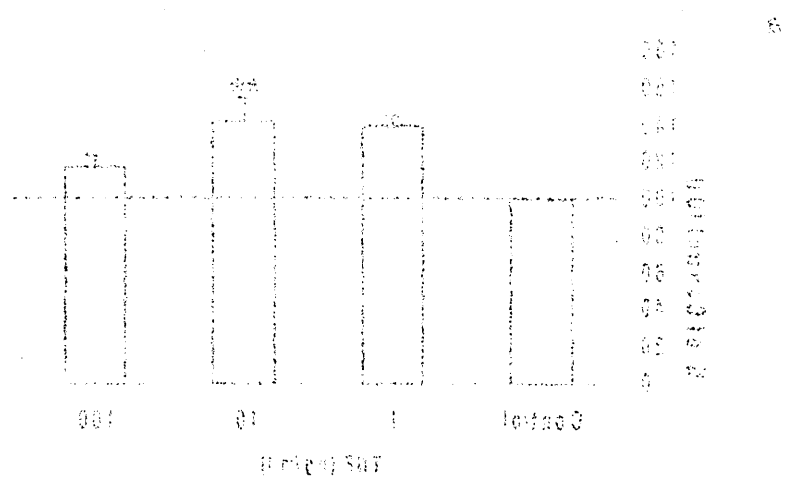
The release of soluble TNF by GP8 endothelial cells was analysed by ELISA to determine ADAM-17 activity by GP8 cells following cytokine and LPS stimulation. Supernatant from GP8 cells incubated in serum free media for 24 hours was devoid of any soluble TNF. TNF was also not detected within the supernatant from cells stimulated with IFN $\gamma$  for 24 hours. Stimulation of GP8 cells with LPS produced soluble TNF within the supernatant in a dose dependent manner, up to a maximum of 250pg/ml. Stimulation of GP8 endothelial cells with TNF induced TNF shedding that was not influenced by simultaneous stimulation with TNF and IFN $\gamma$  (Figure 5.10). To differentiate between added TNF and GP8 synthesized TNF, media with TNF that was incubated in T-25 flasks devoid of cells for 24 hours, were also analysed by ELISA. The amount of TNF within these control samples were more than 50% less than those recorded for the GP8 TNF stimulated samples (Figure 5.10).

Figure 5.7 ADAM-17 expression in GP8 cells following pro-inflammatory stimulation



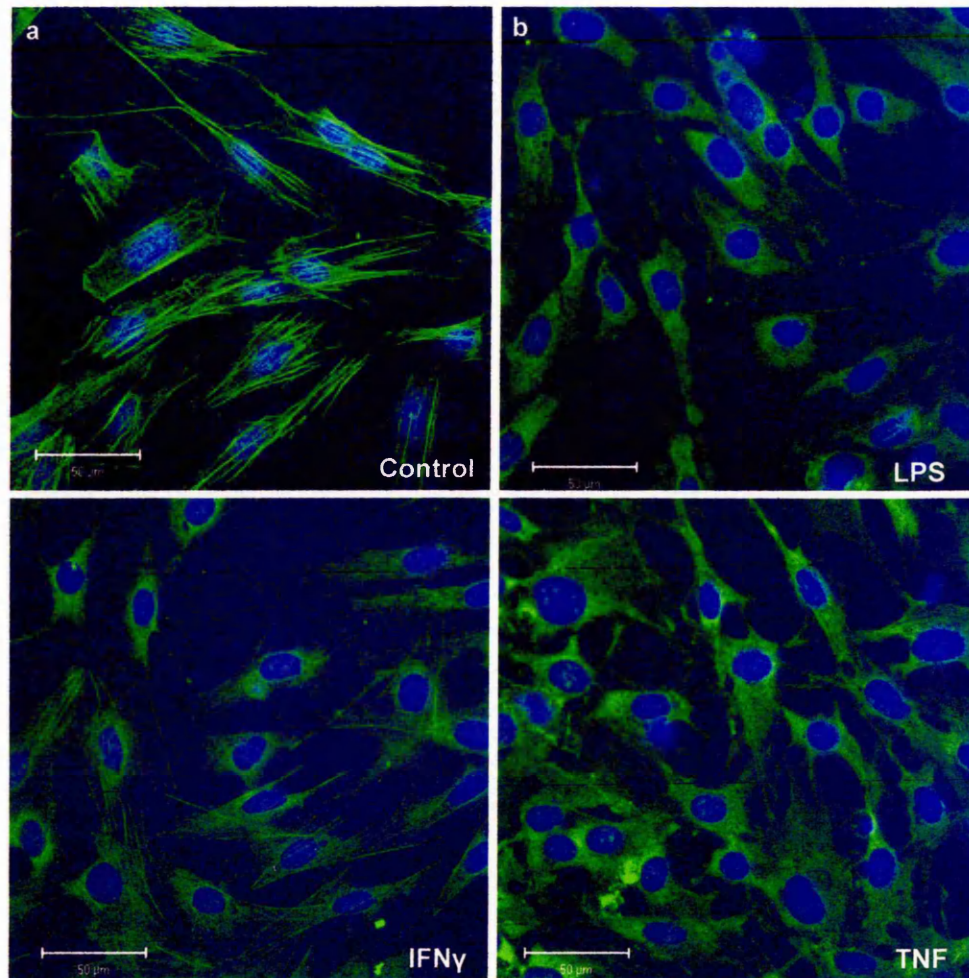
Bar graphs illustrating the extent of ADAM-17 expression in GP8 cells following incubation for 24hrs in a. TNF, b. IFN $\gamma$  and c. TNF/IFN $\gamma$ . Amount of ADAM-17 protein is expressed as a percentage of the unstimulated control IOD +SD. \* indicates significant difference between the means using student t-test  $p \leq 0.05$ .

Figure 2. ADAM-17 expression in BMD of osteoporosis T1-T4 and T5-T6 vertebrae



Bar graphs illustrating the extent of ADAM-17 expression in BMD cells following treatment for 24 weeks in a TMR, a TFR, and a TFR+V. Amount of ADAM-17 protein is expressed as a percentage of the uninjured control. T1-T4 and T5-T6 vertebrae are indicated. Significant differences between the means using Student's *t*-test  $p < 0.05$ .

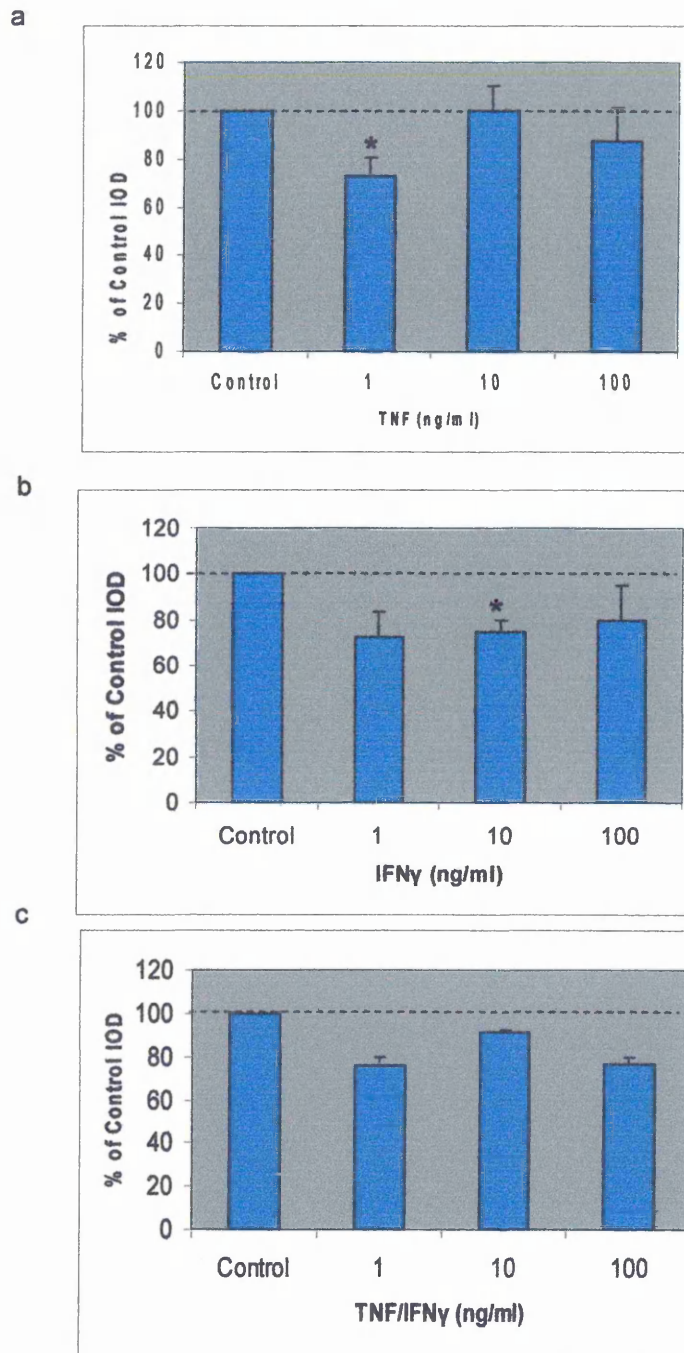
**Figure 5.8 ADAM-17 expression by GP8 endothelial cells under control and inflammatory conditions**



**ADAM-17 expression (Green) in GP8 endothelial cultures under basal control conditions and after 24hr stimulation with b. LPS, c. IFN $\gamma$  and d. TNF. Note that ADAM-17 expression relocates from the cytoskeleton under control conditions to a more perinuclear location under inflammatory conditions. Cell nuclei are counter stained with DAPI (Blue).**

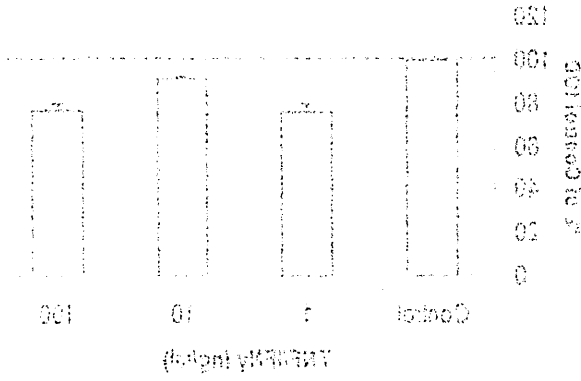
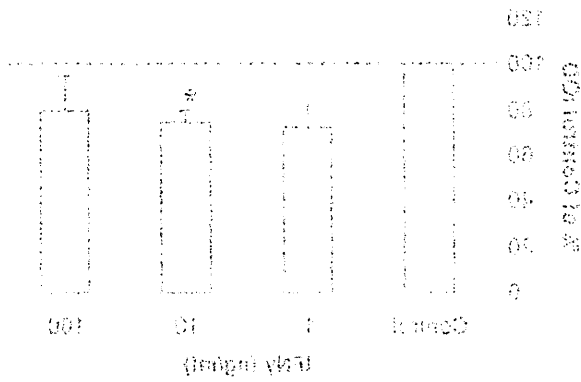
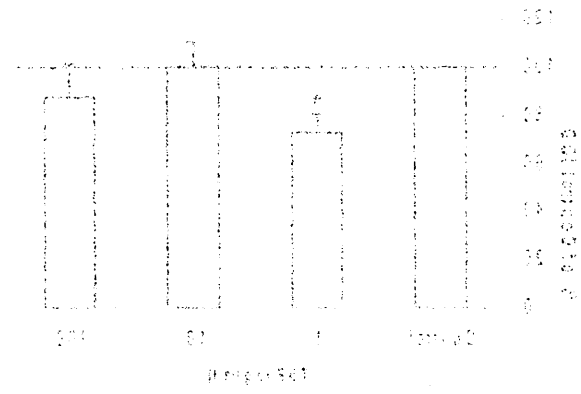
**Bar = 50 $\mu\text{m}$**

Figure 5.9 TIMP3 expression in GP8 cells following pro-inflammatory stimulation



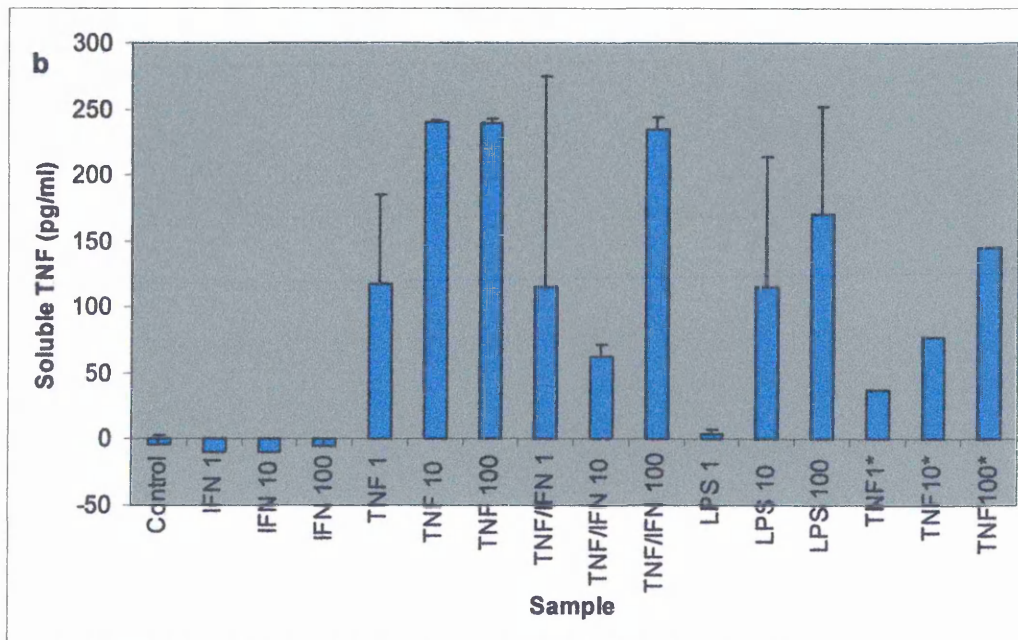
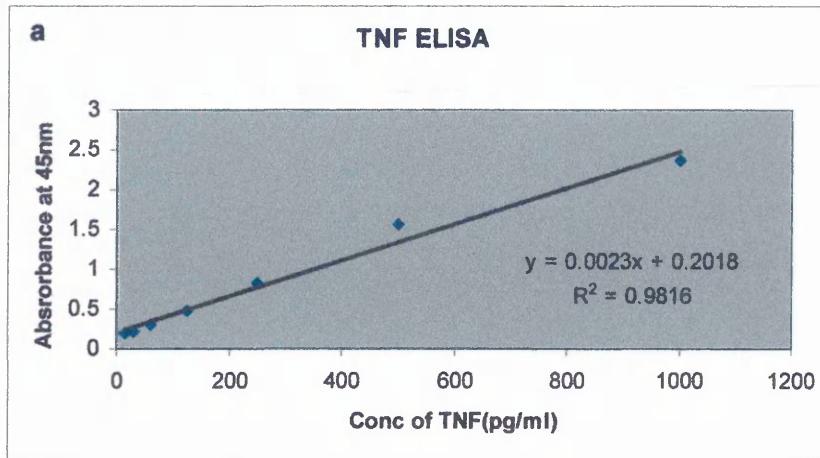
Bar graphs illustrating the extent of TIMP3 expression in GP8 cells following incubation for 24hrs in a. TNF, b. IFN $\gamma$  and c. TNF/IFN $\gamma$ . Amount of TIMP3 protein is expressed as a percentage of the unstimulated control IOD +SD.

\* indicates significant difference between the means using student t-test  $p \leq 0.05$ .



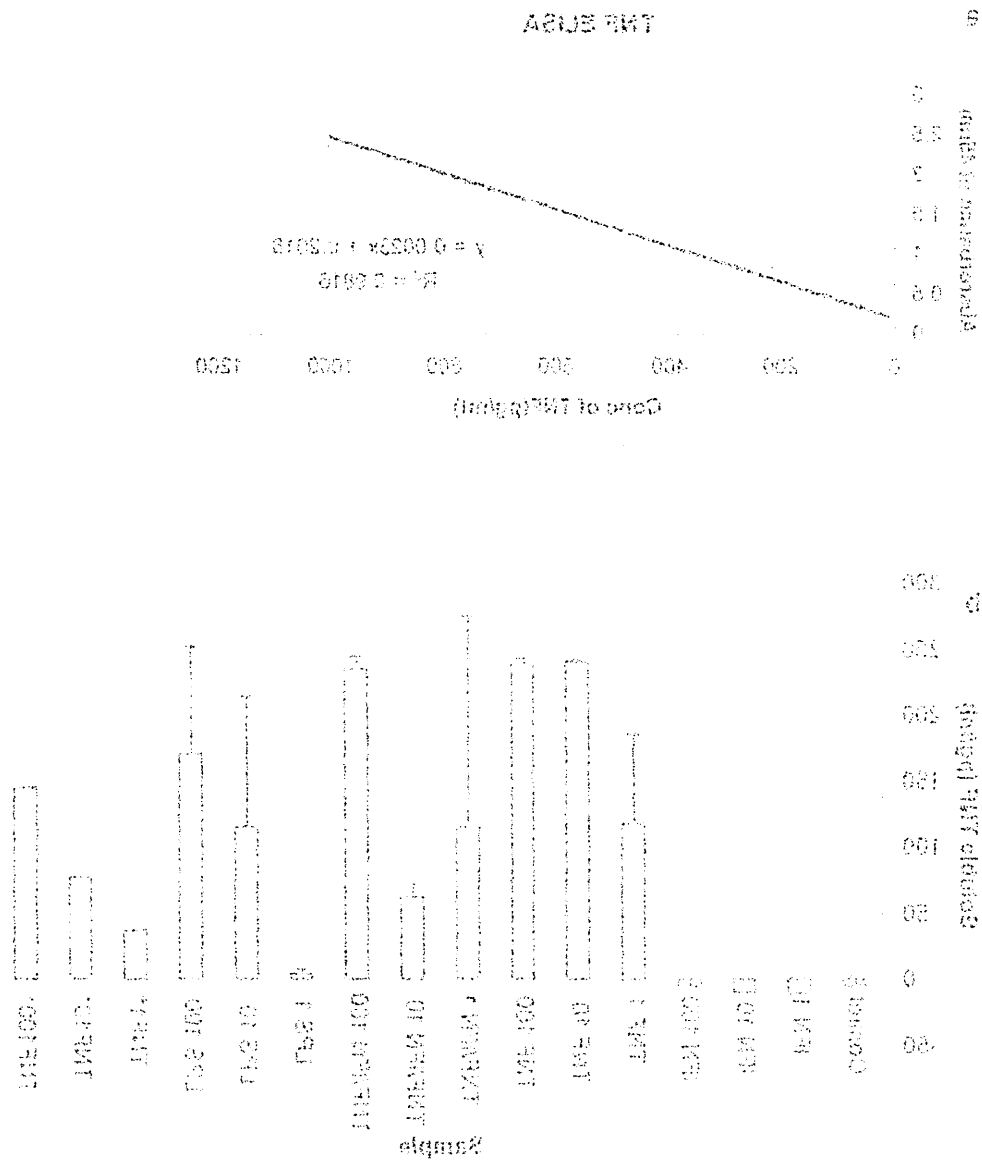
Bar graphs illustrating the extent of TIMP3 expression in GFB cells following stimulation for 24h in a. TNF, b. IFN $\gamma$  and c. TNF/IFN $\gamma$ . Amount of TIMP3 protein is expressed as a percentage of the unstimulated control (0+GFB). \* indicates significant difference between the means using student's t-test at a 0.05 level.

Figure 5.10 Release of soluble TNF from GP8 endothelial cells following pro-inflammatory stimulation



Stimulated release of soluble TNF from GP8 endothelial cells as detected using an ELISA. The absorbance of samples and TNF standards (15.6pg/ml to 1000pg/ml) were read at 450nm and sample TNF concentrations were calculated from the standard curve (a). Samples of media containing TNF that was never introduced to GP8 cells(\*) were also analysed to differentiate between synthesized TNF and added TNF.

Figure 2.10 Release of soluble TRP from GPC endothelial cells following pro-inflammatory stimulation



Standard release of soluble TRP from GPC endothelial cells as detected using an ELISA. The amount of samples and TRP standards (100 ng/ml) were added to 480 nm and used to generate TRP concentrations were calculated from the standard curve. (a) Samples of media containing TRP that were introduced to GPC cells (1000 ng/ml) were also analyzed to differentiate TRP levels and TRP particles received

#### 5.4 Discussion

In human control and MS autopsy material (Chapter 3) and within the spinal cords of Lewis rats with EAE (Chapter 4) ADAM-17 immunoreactivity was shown to be associated with the endothelium of the CNS vasculature as well as white matter astrocytes. In this chapter, *in vitro* studies were performed to assess constitutive ADAM-17 expression following pro-inflammatory cytokine treatment in an attempt to mimic the environment seen in the CNS during MS to support the *in vivo* findings. ADAM-17 was expressed by primary human astrocytes and rat cerebral endothelial cells (GP8) as determined by immunofluorescence and western blotting. The *in vivo* observation that TIMP3 was constitutively expressed within human control white matter and the spinal cord white matter of naïve Lewis rats, was confirmed *in vitro* as TIMP3 was shown to be expressed by both primary human astrocytes and GP8 endothelial cells, suggesting the source of TIMP3 in the CNS is astrocytes and endothelial cells however other cell types may also produce TIMP3.

GP8 cells are an immortalised endothelial cell line derived from the brains of Lewis rats (Greenwood *et al.*, 1996) and therefore provided a suitable resource for the investigation of possible cytokine regulation of ADAM-17 and TIMP3 that may have occurred in EAE and by inference in MS. Other *in vitro* studies have investigated ADAM-17 expression within a human monocyte cell line (THP-1), human acute T leukaemia cells (Jurkat) and a kidney cell line from the African green monkey (COS-7) (Schlöndorff *et al.*, 2000; Peiretti *et al.*, 2003; Srour *et al.*, 2003). Mature and immature ADAM-17 have been reported to coexist on the surface of THP-1 COS-7 and Jurkat cell cultures (Doedens and Black, 2000; Schlöndorff *et al.*, 2000; Endres *et al.*, 2003; Doedens *et al.*, 2003; Peiretti *et al.*, 2003) following immunoprecipitation. Examination of ADAM-17 expression by immunofluorescence has reported diffuse staining, consistent with surface and endoplasmic reticulum staining, with the majority of ADAM-17 immunoreactivity reported to be localised within an intracellular perinuclear compartment (Schlöndorff *et al.*, 2000). This is in contrast to what was observed following immunofluorescence detection of ADAM-17 in GP8 endothelial cell cultures under basal conditions, as reported here. ADAM-17

localisation within these cells appeared to be cytoskeletal as well as diffuse cytoplasmic and on the cell surface. Deconvolution of confocal z-stacks, indicated ADAM-17 immunoreactivity associated with the cell surface of GP8 cells. Following stimulation with PMA and LPS, ADAM-17 expression is reported to disappear from the cell surface of THP-1 cells and become internalised, as evidenced by immunofluorescence (Doedens and Black, 2000; Endres *et al.*, 2003; Doedens *et al.*, 2003; Robertshaw and Brennan, 2005). This relocation of ADAM-17 to the cytoplasm was observed here after stimulation of GP8 cells with LPS, TNF and IFN $\gamma$  (all at 10ng/ml) with a loss of the cytoskeletal ADAM-17 staining. Whether or not there is some functional importance to this sub-cellular location of ADAM-17 remains unclear, however the transmembrane domains of the adhesion molecules, E-selectin and ICAM-1 are reported to be associated with actin filaments and may point towards a possible intracellular function for ADAM-17 (Amos *et al.*, 2001; Vandenberg *et al.*, 2004).

Relocalizing of ADAM-17 to the trans-Golgi is of functional importance as it is here that it is needed to process substrates such as TNF (Moss *et al.*, 2001). ADAM-17 has been reported to mature within the late Golgi apparatus by furin or furin-like cleavage of the prodomain (Endres *et al.*, 2003; Srour *et al.*, 2003), however co-localisation of antibodies to ADAM-17 and the Golgi apparatus was not observed in GP8 cells. ADAM-17 membrane expression by monocytes is at its maximum in basal conditions, however it is rapidly lost from the surface when enzymatic activity is maximal (Robertshaw and Brennan, 2005). In contrast to these findings LPS is reported to have no effect on the ADAM-17 surface expression on THP-1 cells in culture (Doedens and Black, 2000).

TIMP3 is an endogenous inhibitor of MMPs and is the only TIMP that is able to inhibit ADAM-17 (Black, 2004). TIMP3 has been demonstrated to inhibit the release of TNF *in vitro* (Lee *et al.*, 2002b). TIMP3 has been previously reported to be expressed by cultured rat brain microvascular endothelial cells and astrocyte cultures *in vitro* (Bugno *et al.*, 1999; Muir *et al.*, 2002) which is in agreement with the observation of TIMP3 protein

expression by GP8 endothelial cells and primary human astrocytes found in the present study.

Following incubation of GP8 endothelial cells in a pro-inflammatory environment for 24 hours *in vitro*, TIMP3 protein expression was shown here to be reduced by approximately 20% by both TNF and IFN $\gamma$ . This is in concordance with a previous *in vitro* study that demonstrated TIMP3 to be reduced following treatment of cultured microvasculature endothelial cells with TNF and IFN $\gamma$  stimulation (Bugno *et al.*, 1999). A decrease in TIMP3 expression by the cerebral endothelium may result in a balance in favour of ADAM-17 enzymatic activity, which may have a detrimental effect in MS disease progression. TIMP3 expression by endothelial cells may also play a role in BBB breakdown due to its role in ECM remodelling (Crocker *et al.*, 2004). TIMP3 regulates the activities of MMP9 and MMP2 which have been associated with BBB breakdown, therefore a reduction in cerebral endothelium TIMP3 expression could lead to BBB breakdown (Rosenberg *et al.*, 1998).

Both TNF and IFN $\gamma$  have been shown to play a role in the pathogenesis of MS and EAE (Raine, 1995; Glabinski *et al.*, 2003). *In vitro* studies have demonstrated that TNF potentiates the toxicity of IFN $\gamma$  (Andrews *et al.*, 1998). Treatment of GP8 cells here with TNF and IFN $\gamma$  resulted in approximately a 40% increase in ADAM-17 protein expression compared to basal levels of unstimulated cells. This is in concordance with a recent *in vitro* study that reported TNF, IFN $\gamma$  and IL-1 $\beta$  being able to up-regulate the transcription of ADAM-17 and also the expression of ADAM-17 protein in murine brain and human microvascular endothelial cell cultures (Bzowska *et al.*, 2004). This TNF-induced increase in ADAM-17 was also reported to be accompanied by an increase in ADAM-17 enzymatic activity as measured by the shedding of TNFRp55 from the endothelial cell surface (Bzowska *et al.*, 2004). The increase in ADAM-17 protein expression *in vitro* coupled with the decrease in TIMP3 further suggests a balance in favour of ADAM-17 enzymatic activity under inflammatory conditions that was observed during the peak phase of EAE (Chapter 4). However ADAM-17 mRNA expression levels in HUVECs did not alter following treatment with

LPS and IL-1 $\alpha$  (Imaizumi *et al.*, 2000). ADAM-17 is also reported to remain unchanged following TNF stimulation in human colonic epithelial cell lines (Kirkegaard *et al.*, 2004).

TNF, produced mainly by macrophages but also by microglial cells and astrocytes, is a powerful activator of endothelial cells (Franzen *et al.*, 2003). Characteristics of endothelial cells as a target for the actions of TNF have been well described however endothelial cells as a source of TNF is less definitive (Freyer *et al.*, 1999; Imaizumi *et al.*, 2000). Cerebral endothelial cells have shown immunoreactivity for TNF in MS (Cannella and Raine, 1995; Brosnan *et al.*, 1995). TNF has been shown to be released from primary cultures of BMEC from Wistar rats, while its expression, protein and mRNA, is induced in HUVEC by treatment with LPS and IL-1 $\alpha$  (Freyer *et al.*, 1999, Imaizumi *et al.*, 2000). ADAM-17 is responsible for the proteolytic release of TNF by endothelial cell cultures *in vitro*, following treatment of cultures with an ADAM-17 inhibitor decreased levels of TNF secreted by HUVEC was reported (Imaizumi *et al.*, 2000). GP8 cells are shown here to release TNF following stimulation with TNF and LPS however treatment with IFN $\gamma$  did not induce TNF release by GP8 cells, as detected by ELISA. Following these initial experiments TNF release by GP8 cells however cannot be definitively attributed to the actions of ADAM-17. TNF is reported to be manufactured as a membrane bound protein that becomes soluble upon proteolytic cleavage from the cell membrane. Although ADAM-17 is reported to be the main proteolytic convertase of TNF, ADAM-10 is also biologically capable of cleaving TNF (Black *et al.*, 1997, Moss *et al.*, 1997). To determine whether the soluble TNF observed within the current ELISA experiments is due to ADAM-17, repeated experiments pretreating the GP8 cells with anti-ADAM-17 MAb or with a specific ADAM-17 protease inhibitor, would allow comparisons to be drawn and to elucidate whether ADAM-17 is responsible for TNF release in GP8 endothelial cells.

The importance of ADAM-17 in the control of TNF is not only in the production of soluble TNF but also in the removal of membrane bound TNF which has its own biological activities (Robertshaw and Brennan, 2005). TNF

is manufactured as a membrane bound form (mTNF) that is biologically active and has been reported as being capable of mediating cellular responses such as proliferation, apoptosis and some inflammatory responses (Grell *et al.*, 1995; Gerspach *et al.*, 2000). Also important is the ADAM-17-dependant cleavage of TNFR p55 which when released is able to neutralise the effects of soluble TNF (Robertshaw and Brennan, 2005). However, cells expressing mTNF co-express TNFR making experimental data hard to distinguish between mTNF and soluble TNF bound to TNFR (Gerspach *et al.*, 2000).

ADAM-17 and TIMP3 are clearly produced and expressed by GP8 rat cerebral endothelial cells with a balance in favour of enzymatic activity under pro-inflammatory conditions, as observed in active MS plaques and at peak phase of EAE (Chapters 3 and 4). The importance of the relocation of ADAM-17 from the actin cytoskeleton to the cytoplasm following treatment with LPS, TNF and IFN requires further investigation.

The cerebral endothelium of the BBB constitutes a physical and metabolic barrier between the CNS and the periphery (Wolka *et al.*, 2003). The cerebral endothelium expresses an elaborate system of transport proteins on both their luminal and abluminal surfaces, which in conjunction with the TJs ensure nutrient delivery and active regulation of brain extracellular fluid, whilst preventing entrance of harmful exogenous substances (Vorbrodt and Dobrogowska, 2003; Engelhardt, 2003; Ge *et al.*, 2005; McQuaid and Kirk, 2005). The endothelial barrier is supplemented with vascular pericytes and the astrocytic end-feet that encompass approximately 95% of the endothelial abluminal surface, and are in constant communication with the each other (Vorbrodt and Dobrogowski, 2003; Ballabh *et al.*, 2004). As technology and methodologies have evolved it has become evident that the BBB is pathologically affected in numerous diseases including stroke, bacterial infection, HIV encephalitis and MS (McQuaid and Kirk, 2005) and is associated with infiltration of activated monocytes, lymphocytes or neutrophils into the CNS compartment (Kwon and Prineas, 1994; Bolton *et al.*, 1998; Boven *et al.*, 2000).

The TJ of the BBB is comprised of three major transmembrane proteins, claudin, occludin and JAM that are connected to the cytoskeleton via ZO-1 (Vorbrodt and Dobrogowska, 2003). Several groups have demonstrated abnormalities in expression in these TJ-associated proteins in MS (Gay and Esiri, 1991), HIV and SIV encephalitis (Dallasta *et al.*, 1999; Luabeya *et al.*, 2000) and also in human brain endothelial cultures subjected to inflammatory conditions (Blum *et al.*, 1997; Kuruganti *et al.*, 2002; Romero *et al.*, 2003). TJ properties have been reported to be altered as a consequence of TNF and MMP activities in endothelial cultures and animal models of MS (Cossins *et al.*, 1997; Harkness *et al.*, 2000; Minagar *et al.*, 2003; Avolio *et al.*, 2003; Lohmann *et al.*, 2004). The purpose of this study was to investigate the extent of occludin and ZO-1 TJ expression in MS CNS autopsy material, to determine whether any TJ abnormalities were detectable via immunofluorescent techniques and to correlate any findings with specific stages of lesion development.

Histopathological studies of MS and EAE CNS tissues reveal large perivascular inflammatory foci of T cells, B cells, and macrophages.

Formation of the inflammatory foci requires the transendothelial migration of inflammatory cells which involves the interaction of endothelial adhesion molecules and their corresponding integrins on the surface of circulating cells. ICAM-1 and VCAM-1 are reported to be upregulated on the luminal surface of endothelial cells in MS and EAE (Laschinger and Englehardt, 2000; Scott *et al.*, 2004). A member of the ADAM family of metalloproteinases, ADAM-17, has been implicated in the proteolytic cleavage of both membrane-bound VCAM-1 and ICAM-1 from their cell surface.

ADAM-17 was first distinguished as TNF- $\alpha$  converting enzyme, responsible for the shedding of membrane bound TNF into its soluble form (Moss *et al.*, 1997; Black *et al.*, 1997). Soluble TNF has been reported to be implicated in the pathogenesis of MS and EAE. A further purpose of this study was to determine ADAM-17 expression within normal control white matter and MS white matter to assess whether expression levels correspond to different stages of lesion development. The expression of ADAM-17 and TIMP3 was further investigated in the animal model of MS, EAE, to determine any association with the clinical and pathological course of the disease. Pro-inflammatory cytokine effects on ADAM-17, TIMP3 and TNF expression by rat endothelial cell line GP8 was also investigated to elucidate the *in vivo* mechanisms involved in controlling their expression.

*In vivo* occludin and ZO-1 TJ associated protein expression has been described as forming linear continuous lines that form the outline of the blood vessel (Bolton *et al.*, 1998; Brown *et al.*, 1999). These findings are confirmed in the present study which also demonstrates that both occludin and ZO-1 form linear radial bands in transversely transected blood vessels. Examination of ZO-1 and occludin TJ protein expression in MS autopsy material from RRMS and SPMS in the present study has revealed abnormalities in their expression. ZO-1 and occludin expression abnormalities included an interruption or discontinuity of the normally linear bands, redistribution of the fluorescent signal from the cell membrane to the cytoplasm and what appears to be an apparent separation or opening of the fluorescent bands into two adjacent bands. Similar TJ abnormalities have

been reported in autopsy material from HIV encephalitis, SIV encephalitis and cerebral malaria and also in vascular endothelial cells under inflammatory conditions in culture (Bolton *et al.*, 1998; Dallasta *et al.*, 1999; Brown *et al.*, 1999; Boven *et al.*, 2000; Kuruganti *et al.*, 2002).

Quantitatively, the present study indicates that TJ disruption remains a constant feature in MS white matter with significantly increased incidence of TJ disruption in active lesions (42%) and inactive lesions (23%). A recent study using Affymetrix gene microanalysis has indicated lower gene expression of ZO-1 and occludin in active MS lesions compared with normal controls (McQuaid and Kirk, 2005) which would agree with the present study. TJ disruption observed in the present study was also associated with perivascular lymphocytic infiltrates. Leukocyte migration has been shown to trigger signal transduction cascades that lead to increased phosphotyrosine expression and loss of ZO-1 and occludin, and BBB breakdown (Bolton *et al.*, 1998, Ballabh *et al.*, 2004, Song and Pachter 2004) possibly suggesting a role for the TNF/ADAM-17 pathway in TJ disruption via a TNF dependent increase in vascular adhesion molecules. A close relationship between TNF serum and CSF levels and BBB damage has been reported in patients with active MS (Sharief and Thompson, 1992) while several studies have reported an increase in TJ permeability and TJ protein abnormality *in vitro* after exposure to TNF and IFN $\gamma$  (Blum *et al.*, 1997; Kuruganti *et al.*, 2002; Mayhan, 2002; Lohmann *et al.*, 2004) possibly implicating ADAM-17 indirectly in BBB breakdown, through the release of TNF. Thus the present study demonstrates that astrocytic and endothelial cell expression of ADAM-17 would indicate that the enzyme is well placed to release TNF at the BBB.

Abnormalities in TJ protein expression were accompanied by evidence of serum protein leakage. Immunostaining with a FITC-conjugated antibody to fibrinogen revealed serum protein within the perivascular parenchyma, with the serum leakage extending further into NAWM in tissue with active lesions with severely disrupted TJ. This description of serum protein leakage correlates well with previous pathological studies which described the extent, severity and persistence of serum leakage in acute and chronic lesions (Gay and Esiri, 1991; Kwon and Prineas, 1994; Claudio *et al.*, 1995). Fibrinogen leakage in chronic lesions as described in this study

confirms other studies that report the BBB being permanently damaged in many old chronic plaques, at a level undetectable by Gd-DTPA-MRI (Kwon and Prineas, 1994; Claudio *et al.*, 1995). Although TJ disruption and serum protein leakage are described here as pathological features of MS, these features alone do not appear to be capable of inducing the demyelination observed in MS. TJ disruption and BBB breakdown have been reported in other CNS diseases, such as ischemia, HIVE and cerebral malaria where demyelination is not a pathological feature (Perry *et al.*, 1997; Dallasta *et al.*, 1999; Boven *et al.*, 2000).

Chemokines have been associated with regulating leukocyte trafficking into the CNS during MS (Simpson *et al.*, 2000; Mahad *et al.*, 2002; 2003 & 2004). CCL2 has been associated with hypertrophic astrocytes and inflammatory cells within acute and chronic MS lesions whereas its receptor CCR2 has been identified on endothelial cells (McManus *et al.*, 1998; Van der Voorn *et al.*, 1999). *In vitro*, CCL2 is reported to disrupt ZO-1 and occludin in BMEC (Song and Pachter, 2004) whereby it may establish its chemotactic properties from behind the BBB by altering the TJ integrity. However whether TJ disruption is a prerequisite for inflammatory cell transmigration into the CNS is unclear. A recent electron microscopic study of an animal model of MS has suggested that mononuclear cells can cross the BBB via diapedesis leaving the TJs intact (Wolburg *et al.*, 2005).

The NAWM in MS has been reported to be far from normal when assessed by MRI (Goodkin *et al.*, 1998; Fillipi *et al.*, 1998) and histopathological studies (Allen and McKeown, 1979). The present study further demonstrates that there is increased cellular activity and evidence of disease processes occurring within the NAWM. TJ abnormalities were observed in 13% of the blood vessels examined in the NAWM with evidence of moderate serum protein leakage, compared with vessels from normal control matter that displayed no serum protein leakage and TJ disruption in only 4% of the blood vessels examined. This low incidence of TJ abnormality in normal control white matter is in keeping with the view that a small degree of barrier opening may occur as a well regulated process under normal physiological conditions (Abbott, 2002). High levels of HLA-DR immunoreactivity was also observed in six NAWM sections as well as

moderate levels of ADAM-17 immunoreactivity, confirming that the MS NAWM is far from “normal” and may represent pre-lesion disease tissue.

ADAM-17 and its endogenous inhibitor TIMP3 have been demonstrated in the present study as being constitutively expressed in normal control white matter and naïve rat spinal cord white matter, suggesting a possible regulatory role for ADAM-17. Constitutive ADAM-17 expression by cerebral endothelial cells under basal conditions suggests that ADAM-17 may play a regulatory role at the BBB by the proteolytic cleavage of adhesion molecules, TNF and TNFR p75. ADAM-17 cleavage of TNF may play a protective role by reducing the efficacy of TNF/p75 TNFR binding as it has been reported that membrane bound TNF (mTNF) is more effective than soluble TNF at binding with p75 TNFR (Grell *et al.*, 1995). However, serum levels of TNF and p75 TNF have been positively correlated with relapses in people with RRMS (Martino *et al.*, 1997). TNF/ p75 TNFR interaction on cerebral endothelial cells has also been reported to lead to increased ICAM-1 expression and levels of cellular accumulation at the vasculature in experimental cerebral malaria (Akassoglou *et al.*, 2003).

ADAM-17 is reported in the present study to be expressed by endothelial cells, astrocytes, activated microglia/macrophages and by cells of the perivascular infiltrate in both active MS lesions and spinal cords of rats in the peak phase of EAE, suggesting a possible deleterious role in both diseases. *In vitro* results from this study confirmed that ADAM-17 and TIMP3 are expressed by cerebral endothelial cells and astrocytes. The identification of the cell types responsible for ADAM-17 expression within the CNS suggests that ADAM-17 is in a position to be involved in many of the pathogenic mechanisms in MS (Figure 6.1).

ADAM-17 is reported to play a pathological role in stroke however others have reported ADAM-17 as having a beneficial neuroprotective role (Romera *et al.*, 2004; Wang *et al.*, 2004). These contradictory observations are possibly due to the pleiotropic nature of TNF in ischemic stroke although different forms of ADAM-17, in neurons and astrocytes, have been reported (Romera *et al.*, 2004) possibly suggesting different activities of ADAM-17 in different cells. Under hypoxic conditions, astrocytes release inflammatory

abljani ZM to aasengortaq sñi ni TT-MAQDA to ašlu ašiasoq

forderso to goasnu lammiñ sñi moñ F-MAOV bne F-MAOI bnuod enridnem avsalo of nwole nead sñi TT-MAQDA (e)

ZM ni uolhngimann inuvsadu bne nannodis ayokuañ to yillidaseoq sñi gñiulbar ydarsñi ašeo lešidobne ni eonšedini ne gñiasegñe banoqer nead sñi ašlusion noiasñe šeo lešidobne to noiasoqñe bressonñi nevnonñi yivbos toñidihšemyans

šani moñ ašluso a souboq of anñšionñi to gñiibne bəouñi sñi toñ ašidanoqer ad of bəroqer nead sñi TT-MAQDA (d)  
ašeo yolemmšini toñ inabšy aššionerñi s aššaro

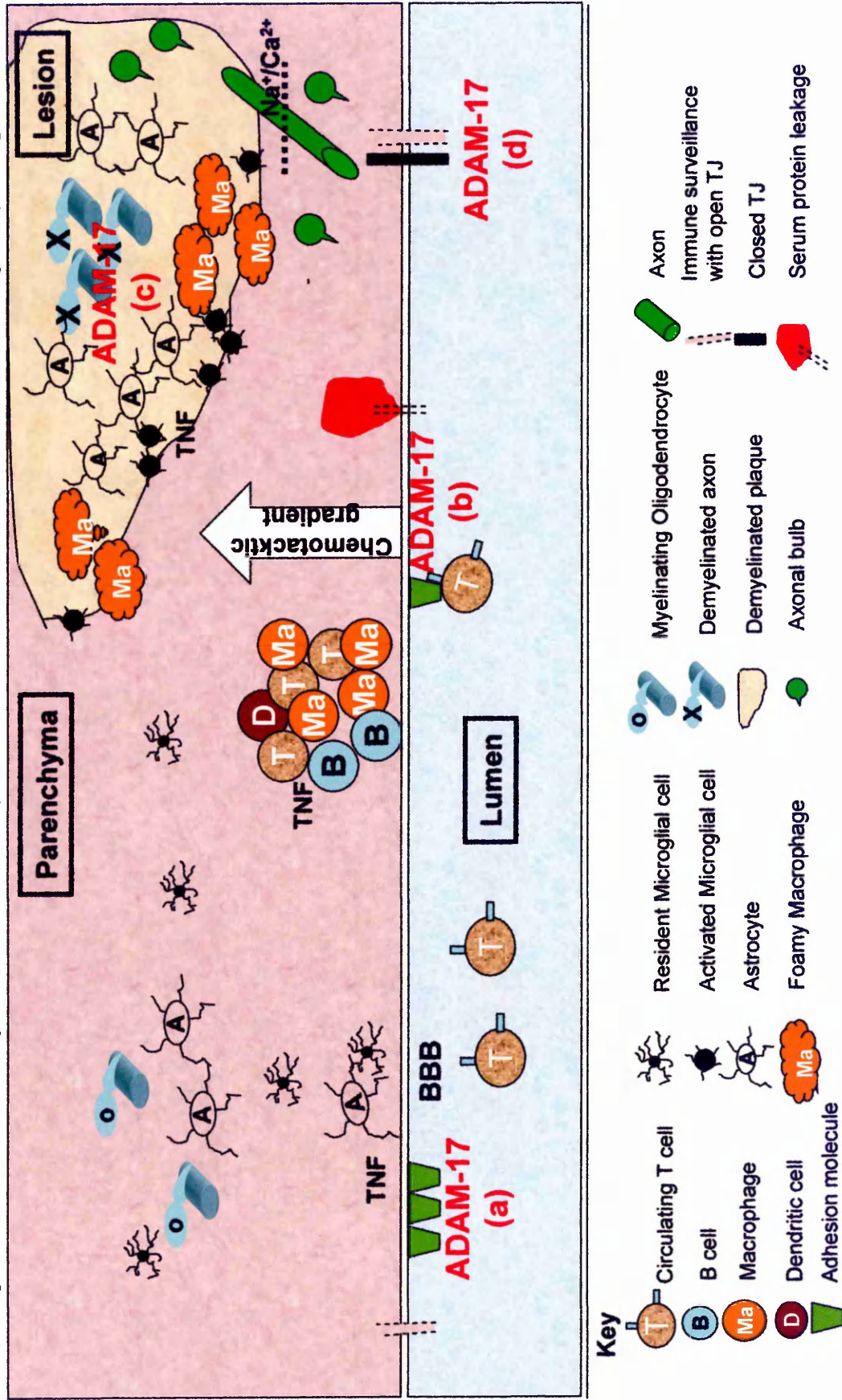
bəloviñ bns ašyooñis niñv bəššosas ad of bəššionerñu nead sñi noiasoqñe TT-MAQDA yvñi sñi ni (c)  
yđ bəgñe ad yivbos ššulo to aševl niñi niñv ašošel ni aševl niñi š bəššerñe bne ašeo lešidomšegñerñosom  
sñi of gñiulbar ydarsñi moñ ašluso sñi omñ FMT ašvəlo TT-MAQDA (š rəšqš) noiasoqñe ORO bne RQ-AMH  
ašokotoy aš of ašyooñibnošio gñiasegñe bns ašyooñis ni nošeršilong a gñiuso ,əbššosə ənikoys yolemmšini  
aššəšš

nead sñi FMT ašyooñis ššusəviñe bns ašeo lešidobne ššardeso to əoññe ad moñ FMT ašvəlo TT-MAQDA (b)  
ni bəroqer noiasoqñe LT bəqñušñi sñi ni gñiulbar ydaseoq aəvñuñ lešidobne ni noiasoqñe LT rəšš of bəroqer  
š rəšqš

Possible roles of ADAM-17 in the pathogenesis of MS include:

- (a) ADAM-17 has been shown to cleave membrane bound ICAM-1 and VCAM-1 from the luminal surface of cerebral endothelial cells thereby reducing the possibility of leukocyte attachment and subsequent transmigration. In MS however increased expression of endothelial cell adhesion molecules has been reported suggesting an imbalance in enzyme/inhibitor activity.
- (b) ADAM-17 has been reported to be responsible for the induced shedding of fractalkine to produce a soluble form that creates a chemotactic gradient for inflammatory cells.
- (c) In this study ADAM-17 expression has been demonstrated to be associated with astrocytes and activated macrophage/microglial cells and expressed at high levels in lesions with high levels of cellular activity as gauged by HLA-DR and ORO expression (Chapter 3). ADAM-17 cleaves TNF into its soluble form thereby leading to the inflammatory cytokine cascade, causing a proliferation in astrocytes and subjecting oligodendrocytes to its cytotoxic effects.
- (d) ADAM-17 cleaves TNF from the surface of cerebral endothelial cells and perivascular astrocytes, TNF has been reported to alter TJ expression in endothelial cultures possibly resulting in the disrupted TJ expression reported in chapter 2.

Figure 6.1 Schematic representation of the possible roles for ADAM-17 in the CNS during MS pathogenesis



mediators that are capable of up-regulating IL-8, ICAM-1, E-selectin, TNF, IL-1 and MCP-1 gene expression in human cerebrovascular cells (Zhang *et al.*, 2000), key proteins in inflammatory cell recruitment and TJ disruption.

ADAM-17 is reported to be responsible for the release of soluble TNF in human colonic epithelial cell lines following TNF stimulation. However, ADAM-17 expression levels remained unchanged following TNF stimulation (Kirkegaard *et al.*, 2004). TIMP3 has been shown to inhibit ADAM-17 activity *in vitro* (Lee *et al.*, 2002). Treatment of cultured microvasculature endothelial cells and astrocytes with the pro-inflammatory cytokines, IL-1 $\beta$ , TNF and IFN $\gamma$  are reported to decrease TIMP3 expression (Bugno *et al.*, 1999; Muir *et al.*, 2002) suggesting a balance in favour of enzymatic activity under inflammatory conditions, in agreement with this study at peak disease in EAE. TIMP3 expression by endothelial cells may also influence BBB breakdown *in vivo* due to its role in regulating ECM remodelling (Crocker *et al.*, 2004) suggesting that the pro-inflammatory environment within the CNS in MS could result in decreased TIMP3 expression with the associated BBB breakdown as reported at the mRNA level in the present study in EAE white matter (Chapter 4).

At the protein level there appears to be discrepancies between the level of TIMP3 at peak EAE, that is increased compared to naive rats and the pro-inflammatory *in vitro* studies of GP8 cells where TIMP3 is reduced following stimulation. The EAE analysis involved examining the homogenate from rat spinal cords composed of various cell types including large foci of inflammatory cells. TIMP3 has been demonstrated here to be expressed by the cerebral endothelia and astrocytes and in neurons by other investigators (Pagenstecher *et al.*, 1998; Vaillant *et al.*, 1999; Jaworski and Fager, 2000). It is reasonable to presume that TIMP3 may mediate different functions by different cell types at different anatomical locations, indeed increased TIMP3 has been associated with neuronal cell death in reperfusion injury (Wallace *et al.*, 2002). Therefore analysing whole white matter spinal cord, TIMP3 protein may be increased, but locally at the cerebral endothelium it may be reduced favouring a balance in favour of ADAM-17 activity.

Successful treatment of EAE and inflammatory diseases such as rheumatoid arthritis, Crohn's disease and psoriasis with monoclonal antibodies (MAbs) and soluble receptors to TNF, lead to a high level of anticipation for their successful application in the treatment of MS (Baker, 2004; Glabinski *et al.*, 2004; Roberts and McColl, 2004; Tobin and Kirby, 2005). Although inhibition of ADAM-17 might be useful in diseases where TNF antagonism has been validated, activation of ADAM-17 might also prove effective in the treatment for Alzheimer's disease, as ADAM-17 cleaves APP by a non-amyloidogenic mechanism, preventing the formation of amyloid plaques (Moss *et al.*, 2001; Skovronsky *et al.*, 2001; Kojro and Fahrenholz, 2005). Targeting of the TJ and ADAM-17 represent plausible therapeutic strategies, however administration of treatment to the CNS is problematic. Recent findings from claudin-5 (Cl-5) knock out mice have demonstrated size selective diffusion into the brain may be manipulated to allow therapeutic access to the brain. Tracer experiments and MRI on these Cl-5<sup>-/-</sup> mice revealed that the BBB permeability was increased for small molecules ( $\leq 800D$ ) but not larger molecules (Nitta *et al.*, 2003). These point towards the potential of targeting Cl-5 to enable access of small molecule therapies across the BBB and into the parenchyma.

#### *Future direction for MS treatments*

The aetiology of MS involves the complex combination of genetics, environmental factors and immune responses that result in a disease that is heterogeneous in both disease course and lesion type. Many of the current treatments for MS, IFN- $\beta$ , Glatiramer acetate and Mitoxantrone, are only effective in some MS patients, suggesting further heterogeneity in MS.

The area of leukocyte cell adhesion presents an array of potential targets for treatment of MS and other inflammatory and autoimmune diseases (Simmons, 2005). MAbs have been applied to disrupt the integrin-ligand interaction that allows leukocytes to strongly adhere to the vascular endothelium that ultimately leads to transmigration across the BBB. MAbs act by binding to the integrin competitively, inhibiting binding to the ligand. Antibodies may also bind in a way that produces an inactive conformation

preventing formation of the activation epitopes and therefore preventing binding to ICAM-1 (Simmons, 2005). MAbs to VLA-4 have been reported to reverse BBB changes, as gauged by MRI, in an acute EAE model in guinea pigs (Kent *et al.*, 1995). Encouraging results from the anti-VLA-4 MAb treatment of EAE has been successfully applied in clinical trials in RRMS (Miller *et al.*, 2003). Tysabri (Natalizumab), approved for treatment of RRMS in November 2004, however it was withdrawn from the market in February 2005 following reports of two cases of PML, one fatal, in MS patients taking Tysabri in conjunction with IFN- $\beta$  (Kleinschmidt-DeMasters and Tyler, 2005) and one fatality in a patient receiving Tysabri for treating Crohn's disease (Van Assche *et al.*, 2005). PML is a demyelinating disease of the CNS caused by the reactivation of latent JC polyomavirus, which usually manifest in people with profoundly impaired cell-mediated immunity for example in patients with AIDS, leukaemia or organ transplant patients (Berger and Koralnik, 2005) thus the impairment of cell recruitment into the CNS via blocking VLA-4 prevented immune cell entry and thus allowed the JC virus to be activated. Although a major setback in the treatment of MS, search for a safe and effective anti-VLA-4 treatment for MS remains ongoing. The companies responsible for Tysabri are actively carrying out comprehensive safety evaluation of patients treated with Tysabri and PML, while GlaxoSmithKline are reported to have a small molecule antagonist of VLA-4 that has entered phase IIb clinical trial (Simmons, 2005). The fact that there was a major improvement in MS patients treated with Tysabri indicates the value in therapeutic targeting of cell trafficking to the CNS and the need to develop antigen-specific inhibitors of migration.

### *Future work*

To extend the current study the following experimental approach would provide further understanding of the complex activities that occur at the BBB in MS.

### *In vitro*

The use of a human cerebral endothelial BBB model would be more relevant due to species differences in the rodent and porcine cerebral endothelial cell culture most commonly used. Establishing a working human model of the BBB would enable the analyses of TJ integrity and ADAM-17 activity in response to cytokines and MMPs. The suggestion of a viral infection being an environmental factor in the aetiology of MS is long standing. Various CNS cells have been shown to be susceptible to viral infection and discovering whether a human model of the BBB could further elucidate the mechanisms and effects of virus entry into the BBB should be assessed. A human model of the BBB would also allow the study of the effects of BBB/TJ strengthening compounds, such as flavanoids, that may provide a way of closing the BBB in pathological conditions, thus ameliorating oedema formation and the severe pathological effects of neuroinflammation.

Further investigation is required to determine whether, under basal conditions, ADAM-17 expression being associated with the actin filaments of the cytoskeleton is due to protein transport or whether or not there is some functional importance to its sub-cellular location. The transmembrane domains of the adhesion molecules, E-selectin and ICAM-1 are reported to be associated with actin filaments and may point towards a possible intracellular function for ADAM-17.

Fractalkine exists as a membrane bound form on endothelial cells, neurons, astrocytes and epithelial cells that has adhesive properties for cells expressing its receptor CX<sub>3</sub>CR1 (Garton *et al.*, 2001; Hulshof *et al.*, 2003). CX<sub>3</sub>CR1 is expressed on monocytes, T-cells, natural killer cells, neurons and microglia (Nishiyori *et al.*, 1998; Garton *et al.*, 2001). Fractalkine can be cleaved from the cell membrane, by ADAM-17, to produce a soluble form that creates a chemotatic gradient for inflammatory cells (Tsou *et al.*, 2001; Garton *et al.*, 2001; Kastenbauer *et al.*, 2003). Increased fractalkine expression has been observed in the CSF and serum of patients with inflammatory diseases, including MS and bacterial meningitis (Kastenbauer *et al.*, 2003). Proteolytic release of fractalkine from activated cerebral endothelial cells might be the source of soluble fractalkine in the circulation. Using flow cytometry and ELISA techniques would help confirm the shedding

of fractalkine by cerebral endothelial cells. Further *in vitro* studies involving the interaction of ADAM-17 and fractalkine may further elucidate whether this interaction is detrimental or beneficial. Small interfering RNAs (siRNAs) specifically knock-down a gene's message, and subsequently the protein level of the targeted gene. Using siRNAs for ADAM-17 would allow cellular-based assays to be conducted in the absence and presence ADAM-17 to clarify its shedding activity under pro-inflammatory conditions.

### *Animal model*

Having demonstrated an increase in ADAM-17 at peak disease in EAE, further studies using EAE would enable the examination of TIMP3 or anti-ADAM-17 treatments on disease progression and pathology. Employing a chronic-relapsing EAE (CREAE) model would enable the investigation of ADAM-17 and TIMP3 expression in a model with a demyelinating pathology. CREAE would also allow the investigation of ADAM-17 and TIMP3 expression during remission and relapses to distinguish whether the increase in ADAM-17 expression observed in the current study is involved during later relapses. The use of ADAM-17, TIMP3 and fractalkine knockout animals could also shed light on the functions of ADAM-17, TIMP3 and fractalkine in disease progression.

### *Summary*

Breakdown of the BBB in MS has been well documented and evidenced by MRI. Here it has been shown that the BBB is disrupted in MS at the microscopic level of the inter-endothelial TJ. TJ disruption is not only prevalent in active MS lesions but is also seen in the NAWM and is persistent in chronic lesions. TNF is known to have immunomodulatory effects on the BBB that lead to increased permeability and adhesion molecule expression on the vascular endothelial surface. ADAM-17, the enzyme responsible for the proteolytic cleavage of TNF, has been shown to be expressed by the vascular endothelium and astrocytes of the CNS in MS and EAE. Increased ADAM-17 expression is also shown to be associated with active lesions in MS and at peak disease stage in EAE. *In vitro*, ADAM-17 expression by endothelial cell cultures is increased under pro-

inflammatory conditions, whereas expression levels of its endogenous inhibitor TIMP3 are decreased. This suggests an imbalance in favour of the enzymatic activity of ADAM-17 under pro-inflammatory conditions, like those observed in EAE. The functional consequence of this activity requires further research, which may lead to greater understanding of the pathological process in MS and to new therapeutic targets for MS being identified.

## A1 Buffers and solutions

### A1.1 Phosphate buffered saline (PBS 10mM)

Weigh out 80g NaCl, 2g KCL, 14.4g Na<sub>2</sub>HPO<sub>4</sub> and 2g KH<sub>2</sub>PO<sub>4</sub>.  
Dissolve the above buffer constituents in 1000ml of distilled H<sub>2</sub>O and pH 7.2.  
This buffer is x10 concentrate and should be diluted 1:10 prior to use.

### A1.2 Phosphate buffer 0.2M

Weigh out 11.36g Na<sub>2</sub>HPO<sub>4</sub> and dissolve in 400ml of distilled H<sub>2</sub>O  
(Solution A).

Weigh out 3.2g NaH<sub>2</sub>PO<sub>4</sub>·2H<sub>2</sub>O and dissolve in 100ml of distilled H<sub>2</sub>O  
(Solution B).

Mix solutions A&B and pH to 7.2.

### A1.3 Paraformaldehyde 4%

Add 16g of paraformaldehyde to 100ml of distilled H<sub>2</sub>O and heat to 60°C then add 2M NaOH to dissolve. Add distilled H<sub>2</sub>O to make a total volume of 200ml. Add 200ml of 0.2M phosphate buffer and pH to 7.2.  
NB Carry out the above procedure in a fume cupboard.

### A1.4 Citifluor

Weigh out 2.5g 1,4-diazobicyclo-2,2,2-octane (Sigma) and add 50mls PBS and 50mls glycerol. Mix well and store in the dark at 4°C.  
NB Carry out the above procedure in a fume cupboard.

### A1.5 Citrate Buffer

10.5g of Trisodium citrate dissolved in 500mls distilled water.  
Add 10mls of 1M HCL and pH to 6.3

#### A1.5.1 Microwave Buffer

50mls of citrate buffer added to 450mls of distilled water and pH 6.0.

#### A1.6 TBS

Weigh out 80g NaCl and 6.05g Tris (hydroxyl-methyl). Add to 44mls of 1M HCL and 10L of distilled water and pH 7.4.

#### A1.7 Oil Red O

Oil Red O solution is prepared by adding 1g of Oil Red O to 60mls Triethyl Phosphate and 40mls of distilled water. The mixture is heated to 100°C for 5 minutes and constantly stirred. The mixture is filtered when hot then again when it cools. This is a stock solution and must be filtered prior to use.

Tissue for ORO staining is post fixed in 10% formalin at 4°C for 1hour.

- Sections are placed in 70% ethanol for 2 minutes
- Sections are incubated in ORO for 20 minutes at RT
- Sections are washed in 70% ethanol until all excess stain is removed
- Sections are washed in distilled water
- Cell nuclei are counter stained by immersion in Harris's haematoxylin for 30 seconds
- Nuclei are "blue up" dipping sections in ammonia water
- Sections are then washed in distilled water
- Sections are mounted in glycerin jelly (Stored at 37°C).

#### A1.8 Protein Sample Buffer

25µl of sample buffer (Invitrogen), 10µl sample reducing buffer (Invitrogen) and 15µl distilled water. Added to extracted protein sample 1:1.

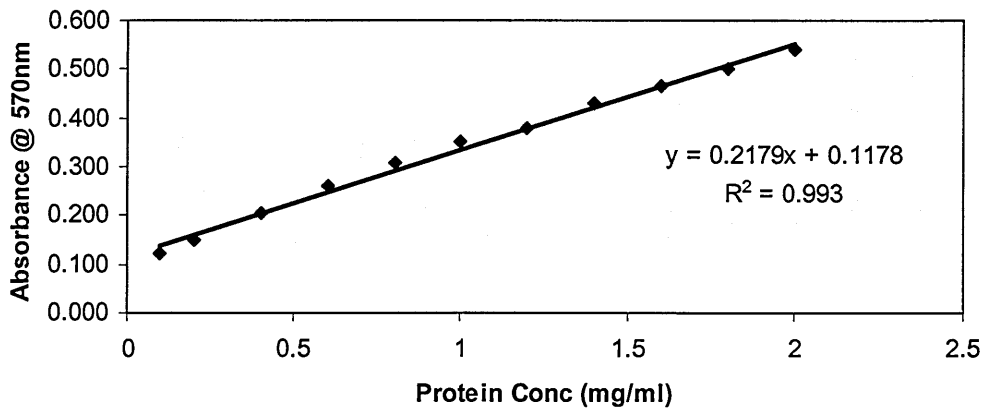
## B1 Extra experimental details

### B1.1 Example of BCA and standard curve

BCA standards were made using bovine serum albumin as shown in table below and analysed in duplicate.

Standards Conc (mg/ml)	Absorbance @ 570nm Reading 1	Absorbance @ 570nm Reading 2	Ave	SD
0.1	0.122	0.120	0.121	0.001509
0.2	0.148	0.152	0.150	0.002697
0.4	0.199	0.214	0.206	0.010596
0.6	0.262	0.259	0.261	0.002237
0.8	0.312	0.305	0.308	0.004847
1	0.350	0.353	0.352	0.002419
1.2	0.372	0.383	0.378	0.007709
1.4	0.428	0.432	0.430	0.00307
1.6	0.467	0.466	0.467	0.000427
1.8	0.500	0.501	0.500	0.000874
2	0.537	0.546	0.542	0.005932

### EAE WM only BCA



Following BCA assay described in 3.2.4.1 sample absorbance at 570nm were read and plotted as illustrated in the graph above. Equation of chart line and R squared value of the chart were displayed.

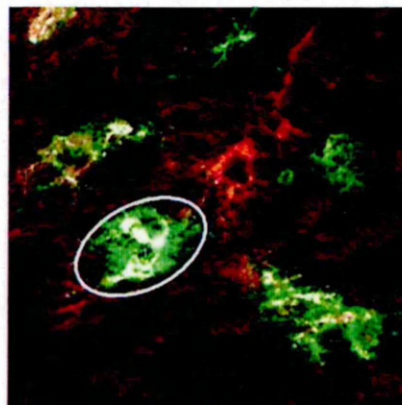
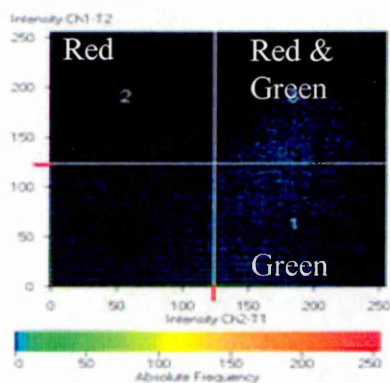
EAE Sample	Reading 1	Reading 2	Reading 3	Ave	Conc (mg/ml)
3	0.311	0.286	0.298	0.298	0.828360212
8	0.340	0.348	0.328	0.339	1.013863396
10	0.283	0.270	0.263	0.272	0.707038932
14	0.274	0.267	0.283	0.275	0.720139407
21	0.341	0.319	0.338	0.333	0.985644255
23	0.199	0.207	0.206	0.204	0.395641899
26	0.189	0.194	0.211	0.198	0.368107919
36	0.363	0.349	0.340	0.351	1.067937039
38	0.276	0.280	0.280	0.279	0.737950208
42	0.190	0.190	0.199	0.193	0.34499101
44	0.362	0.367	0.313	0.347	1.053017008
46	0.346	0.338	0.332	0.339	1.014493036
49	0.216	0.220	0.225	0.220	0.470940544
50	0.262	0.280	0.272	0.271	0.704778807
51	0.252	0.249	0.251	0.251	0.610394305
52	0.342	0.261	0.268	0.290	0.792526756

Test samples were analysed in triplicate and protein concentrations of samples were calculated using the equation  $y = mx + c$  where  $y$  is the absorbance at 570nm and  $x$  is the protein concentration in mg/ml.

$$X = (y-c)/m$$

### B1.2 Co-localisation spectra graphs

Co-localisation software of the Zeiss 510 CSLM was utilised to determine whether or not individual pixels were truly co-localised for the proteins of interest. The software produces a spectra dot plot that displays channel 1<sup>+</sup> pixels in quadrant 2, channel 2<sup>+</sup> pixels in quadrant 1 and pixels that are both channel 1<sup>+</sup> + 2<sup>+</sup> in quadrant 3



### B1.3 EAE induction and copy of clinical data from Eisai

Animal housing and all procedures were carried out according to the guideline laid down by the Animal Care and Use Committee of Eisai. Lewis rats (180–200 g in body weight, 7–9 weeks, Charles River Japan, Tokyo, Japan) were immunized subcutaneously in each hind foot pad with a 50- $\mu$ l inoculum containing 50- $\mu$ g guinea pig myelin basic protein, prepared according to a published method (Dunkley and Carnegie), and emulsified in Freund's complete adjuvant containing 5.5 mg/ml *Mycobacterium tuberculosis* H37Ra (Difco, Detroit, MI).

Dunkley and Carnegie, 1974. P.R. Dunkley and P.R. Carnegie, Amino acid sequence of the smaller basic protein from rat brain myelin. *Biochem. J.* 141 (1974), pp. 243–255.

Carnegie et al., 1974. P.R. Carnegie, P.R. Dunkley, B.E. Kemp and A.W. Murray, Phosphorylation of selected serine and threonine residues in myelin basic protein by endogenous and exogenous protein kinases. *Nature* 249 (1974), pp. 147–150.

### B1.4 Tri reagent method (Sigma protocol)

#### I. Sample Preparation

##### 1A. Tissue:

Homogenize tissue samples in TRI REAGENT (1 ml per 50-100 mg of tissue) in a Polytron or other appropriate homogenizer. Note: If minimal shearing of the DNA is desired, use a loosely fitting homogenizer, not a Polytron (see also Note b. under Step 3 of the DNA Isolation procedure). The volume of the tissue should not exceed 10% of the volume of the TRI REAGENT.

### 1B. Monolayer cells:

Lyse cells directly on the culture dish. Use 1 ml of the TRI REAGENT per 10 cm<sup>2</sup> of glass culture plate surface area. After addition of the reagent, the cell lysate should be passed several times through a pipette to form a homogenous lysate.

### 1C. Suspension cells:

Isolate cells by centrifugation and then lyse in TRI REAGENT by repeated pipeting. One ml of the reagent is sufficient to lyse 5-10 x 10<sup>6</sup> animal, plant or yeast cells or 10<sup>7</sup> bacterial cells.

### Notes:

- a. Some yeast and bacterial cells may require a homogenizer.
- b. After the cells have been homogenized or lysed in TRI REAGENT, samples can be stored at -70 °C for up to 1 month.
- c. If samples have a high content of fat, protein, polysaccharides or extracellular material such as muscle, fat tissue and tuberous parts of plants an additional step may be needed. After homogenization, centrifuge the homogenate at 12,000 x g for 10 minutes at 4 °C to remove the insoluble material (extracellular membranes, polysaccharides, and high molecular weight DNA). The supernatant contains RNA and protein. If the sample had a high fat content there will be a layer of fatty material on the surface of the aqueous phase that should be removed. Transfer the clear supernatant to a fresh tube and proceed with step 2. Recover the high molecular weight DNA from the pellet by following steps 2 and 3 under DNA Isolation.

2. To ensure complete dissociation of nucleoprotein complexes, allow samples to stand for 5 minutes at room temperature. Add 0.2 ml of chloroform (see note below) per ml of TRI REAGENT used. Cover the sample tightly, shake vigorously for 15 seconds and allow to stand for 2-15 minutes at room temperature. Centrifuge the resulting mixture at 12,000 x g for 15 minutes at 4 °C. Centrifugation separates the mixture into 3 phases: a red organic phase (containing protein), an interphase (containing DNA), and a colorless upper aqueous phase (containing RNA).

Note: The chloroform used for phase separation should not contain isoamyl alcohol or other additives.

## II. RNA Isolation

1. Transfer the aqueous phase to a fresh tube and add 0.5 ml of isopropanol per ml of TRI REAGENT used in Sample Preparation, Step 1 and mix. Allow the sample to stand for 5-10 minutes at room temperature. Centrifuge at 12,000 g for 10 minutes at 4 °C. The RNA precipitate will form a pellet on the side and bottom of the tube.

Note: Store the interphase and organic phase at 4 °C for subsequent isolation of the DNA and proteins.

2. Remove the supernatant and wash the RNA pellet by adding 1 ml (minimum) of 75% ethanol per 1 ml of TRI REAGENT used in Sample Preparation,

Step 1. Vortex the sample and then centrifuge at 7,500 x g for 5 minutes at 4°C.

Notes:

- a. If the RNA pellets float, perform the wash in 75% ethanol at 12,000 x g.
- b. Samples can be stored in ethanol at 4 °C for at least 1 week and up to 1 year at -20 °C.

3. Briefly dry the RNA pellet for 5-10 minutes by airdrying or under a vacuum. Do not let the RNA pellet dry completely, as this will greatly decrease its solubility. Do not dry the RNA pellet by centrifugation under vacuum (Speed-Vac). Add an appropriate volume of formamide, water or a 0.5% SDS solution to the RNA pellet. To facilitate dissolution, mix by repeated pipetting with a micropipette at 55-60 °C for 10-15 minutes.

Notes:

- a. Final preparation of RNA is free of DNA and proteins. It should have a 260/280 ratio of  $\geq 1.7$ .

- b. Typical yields from tissues ( $\mu\text{g}$  RNA/mg tissue): liver, spleen, 6-10  $\mu\text{g}$ ; kidney, 3-4  $\mu\text{g}$ ; skeletal muscle, brain, 1-1.5  $\mu\text{g}$ ; placenta, 1-4  $\mu\text{g}$ .
- c. Typical yields from cultured cells ( $\mu\text{g}$  RNA/10<sup>6</sup> cells): epithelial cells, 8-15  $\mu\text{g}$ ; fibroblasts, 5-7  $\mu\text{g}$ .

### III. DNA Isolation

1. Carefully remove the remaining aqueous phase overlaying the interphase and discard. To precipitate the DNA from the interphase and organic phase, add 0.3 ml of 100% ethanol per 1 ml of TRI REAGENT used in Sample Preparation, Step 1. Mix by inversion and allow to stand for 2-3 minutes at room temperature. Centrifuge at 2,000 x g for 5 minutes at 4 °C.

Note: Removal of the remaining aqueous phase before DNA precipitation is a critical step for the quality of the isolated DNA.

2. Remove the supernatant and save at 4 °C for protein isolation. Wash the DNA pellet twice in 0.1 M sodium citrate, 10% ethanol solution. Use 1 ml of wash solution for every 1 ml of TRI REAGENT used in Sample Preparation, Step 1. During each wash, allow the DNA pellet to stand (with occasional mixing) for at least 30 minutes. Centrifuge at 2,000 x g for 5 minutes at 4 °C. Resuspend the DNA pellet in 75% ethanol (1.5-2 ml for each ml TRI REAGENT) and allow to stand for 10-20 minutes at room temperature.

#### Notes:

- a. Important: Do not to reduce the time samples remain in the washing solution. Thirty minutes is the absolute minimum time for efficient removal of phenol from the DNA.
- b. If pellet contains >200  $\mu\text{g}$  of DNA or large amounts of non-DNA material, an additional wash in 0.1 M sodium citrate, 10% ethanol solution is required.
- c. Samples suspended in 75% ethanol can be stored at 4 °C for several months.

3. Dry the DNA pellet for 5-10 minutes under a vacuum and dissolve in 8 mM NaOH and dissolve by repeated slow pipetting with a micropipette. Add

sufficient 8 mM NaOH for a final DNA concentration of 0.2-0.3  $\mu\text{g}/\mu\text{l}$  (typically 0.3-0.6 ml to the DNA isolated from 50-70 mg of tissue or 107 cells). This mild alkaline solution assures complete dissolution of the DNA pellet. Centrifuge at 12,000 x g for 10 minutes to remove any insoluble material and transfer the supernatant to a new tube.

Notes:

- a. A viscous supernatant indicates the presence of high molecular weight DNA.
- b. The size of the DNA will depend on the force exerted during homogenization. Avoid using a Polytron homogenizer.
- c. Samples dissolved in 8 mM NaOH can be stored at 4 °C overnight. For long term storage, adjust the pH value to between 7 and 8 and supplement with EDTA (final concentration 1 mM).
- d. To determine DNA concentration, remove an aliquot, dilute with water and measure the A260. For double stranded DNA, 1 A260 unit/ml = 50  $\mu\text{g}/\text{ml}$ .
- e. To calculate cell number, assume the amount of DNA for 106 diploid cells of human, rat and mouse equals 7.1  $\mu\text{g}$ , 6.5  $\mu\text{g}$  and 5.8  $\mu\text{g}$ , respectively.
- f. Typical yields from tissues ( $\mu\text{g}$  DNA/mg tissue): liver, kidney, 3-4  $\mu\text{g}$ ; skeletal muscle, brain and placenta, 2-3  $\mu\text{g}$ .
- g. Typical yields from cultured human, rat and mouse cells: 5-7  $\mu\text{g}$  DNA/106 cells.

To Amplify DNA by PCR: After dissolving in 8 mM NaOH, adjust to pH 8.4 using HEPES (add 66  $\mu\text{l}$  of 0.1 M HEPES, free acid/ml DNA solution). Add sample (generally 0.1-1  $\mu\text{g}$ ) to PCR mix and follow PCR protocol.

To Digest DNA with Restriction Enzymes:

Adjust the pH of the DNA solution to that needed for the restriction enzyme digestion using HEPES, or dialyze samples against 1 mM EDTA, pH 7-8. Allow the restriction enzyme digestion to continue for 3-24 hours under optimal conditions. It is recommended that 3-5 units of enzyme be used per 1  $\mu\text{g}$  of DNA. Typically, 80-90% of the DNA is digested.

#### IV. Protein Isolation

1. Precipitate proteins (see note below) from the phenol-ethanol supernatant (DNA Isolation, Step 2) with 1.5 ml of isopropanol per 1 ml of TRI REAGENT<sup>®</sup> used in Sample Preparation, Step 1. Allow samples to stand for at least 10 minutes at room temperature. Centrifuge at 12,000 x g for 10 minutes at 4 °C.

Note: For some samples, the protein pellet may be difficult to dissolve in 1% SDS (step 3 below).

Use this alternate procedure to correct the problem:

- a. Dialyze the phenol-ethanol supernatant against 3 changes of 0.1% SDS at 4 °C.
- b. Centrifuge the dialysate at 10,000 x g for 10 minutes at 4 °C.
- c. The clear supernatant contains protein that is suitable for use in western blotting procedures.

2. Discard supernatant and wash pellet 3 times in 0.3 M guanidine hydrochloride/95% ethanol solution, using 2 ml per 1 ml of TRI REAGENT<sup>®</sup> used in Sample Preparation, Step 1. During each wash, store samples in wash solution for 20 minutes at room temperature. Centrifuge at 7,500 x g for 5 minutes at 4 °C. After the 3 washes, add 2 ml of 100% ethanol and vortex the protein pellet. Allow to stand for 20 minutes at room temperature. Centrifuge at 7,500 x g for 5 minutes at 4 °C.

Note: Protein samples suspended in 0.3 M guanidine hydrochloride/95% ethanol solution or 100% ethanol can be stored for 1 month at 4 °C or 1 year at -20 °C.

3. Dry protein pellet under a vacuum for 5-10 minutes. Dissolve pellet in 1% SDS aided by working the plunger of micropipette with tip in the solution. Remove any insoluble material by centrifugation at 10,000 x g for 10 minutes

at 4 °C. Transfer supernatant to a new tube. The protein solution should be used immediately for western blotting or stored at –20 °C.

- Abbott, N.J. 2002. Astrocyte-endothelial interactions and blood-brain barrier permeability. *J Anat* 200:629-638.
- Abbruscato, T.J., Davis, T.P. 1999. Protein expression of brain endothelial cell E-cadherin after hypoxia/aglycemia: influence of astrocyte contact. *Brain Res* 842:277-286.
- Ahmed, Z., Gveric, D., Pryce, G., Baker, D., Leonard, JP., Cuzner, L. 2001. Myelin/axonal pathology in interleukin-12 induced serial relapses of experimental allergic encephalomyelitis in the Lewis rat. *Am J Pathol* 158: 2127-2138.
- Ahn, SY., Cho, CH., Park, KG., Lee, HJ., Lee, S., Park, SK., Lee, IK., Koh, GY. 2004. Tumor necrosis factor- $\alpha$  induces fractalkine expression preferentially in arterial endothelial cells and Mithramycin A suppresses TNF- $\alpha$ -induced fractalkine expression. *Am J Pathol* 164: 1663-1672.
- Akassoglou, K., Bauer, J., Kassiotis, G., Pasparakis, M., Lassmann, H., Kollias, G., Probert, L. 1998. Oligodendrocyte apoptosis and primary demyelination induced by local TNF/p55TNF receptor signalling in the central nervous systems of transgenic mice: Models for multiple sclerosis with primary oligodendroglialopathy. *Am J Pathol* 153: 801-813.
- Akassoglou, K., Douni, E., Bauer, J., Lassmann, H., Kollias, G., Probert, L. 2003. Exclusive tumor necrosis factor (TNF) signalling by the p75TNF receptor triggers inflammatory ischemia in the CNS of transgenic mice. *Proc Nat Acad sci USA* 100: 709-714.
- Allen, I.V., McKeown, S.R. 1979. A histological and biochemical study of the macroscopically normal white matter in multiple sclerosis. *J Neurol Sci* 41:81-91.
- Allen, SJ., Baker, D., O'Neill, JK., Davison, AN., Turk, JL. 1993. Isolation and characterization of cells infiltrating the spinal cord during the course of chronic relapsing experimental allergic encephalomyelitis in Biozzi AB/H mouse. *Cell Immunol* 146: 335-350.
- Allinson, TMJ., Parkin, ET., Turner, AJ., Hooper, NM. 2003. ADAMs family members as amyloid precursor protein  $\alpha$ -secretases. *J Neurosci Res* 74: 342-352.
- Aloisi, F. 2001. Immune function of microglia. *Glia* 36: 165-179.
- Amos, C., Romero, IA., Schultze, C., Rousell, J., Pearson, JD., Greenwood, J., Adamson, P. 2001. Cross-linking of brain endothelial intercellular adhesion molecule (ICAM)-1 induces association of ICAM-1 with detergent-insoluble cytoskeletal fraction. *Arterioscler Thromb Vasc Biol* 21: 810-816.
- Amos, WB., White, JG. 2003. How the confocal laser scanning microscope entered biological research. *Biol Cell* 95: 335-342.

Amour, A., Slocombe, PM., Webster, A., Butler, M., Knight, CG., Smith, BJ., Stephens, PE., Shelley, C., Hutton, M., Knauper, V., Docherty, AJP., Murphy, G. 1998. TNF-alpha converting enzyme (TACE) is inhibited by TIMP-3. *FEBS Lett* 435: 39-44.

Ancuta, P., Moses, A., Gabuzda, D. 2004. Transendothelial migration of CD16+ monocytes in response to fractalkine under constitutive and inflammatory conditions. *Immunobiol* 209: 11-20.

Anders, A., Gilbert, S., Garten, W., Postina, R., Fahrenholz, F. 2001. Regulation of the  $\alpha$ -secretase ADAM10 by its prodomain and proprotein convertases. *FASEB J* 15: 1837-1839

Andrews, T., Zhang, P., Bhat, NR. 1998. TNF $\alpha$  potentiates IFN $\gamma$ -induced cell death in oligodendrocyte progenitors. *J Neurosci Res* 54: 574-583.

Ando-Akastuka, Y., Saitou, M., Hirase, T., Kishi, M., Sakakibara, A., Itoh, M., Yonemura, S., Furuse, M., Tsukita, S. 1996. Interspecies diversity of the occludin sequence: cDNA cloning of human, mouse, dog and rat-kangaroo homologues. *J Cell Biology* 133:43-47.

Agnello, D., Bigini, P., Villa, P., Mennini, T., Cerami, A., Brines, ML., Ghezzi, P. 2002. Erythropoietin exerts an anti-inflammatory effect on the CNS in a model of experimental autoimmune encephalomyelitis. *Brain Res* 952: 128-134.

Aranguiz, I., Torres, C., Rubio, N. 1995. The receptor for tumor necrosis factor on murine astrocytes: characterization, intracellular degradation, and regulation by cytokines and Theiler's murine encephalomyelitis virus. *Glia* 13: 185-194.

Archelos, JJ., Jung, S., Rinner, W., Lassmann, H., Miyasaka, M., Hartung, HP. 1998. Role of the leukocyte-adhesion molecule L-selectin in experimental autoimmune encephalomyelitis. *J Neurological Sci* 159: 127-134.

Archelos JJ., Storch MK., Hartung HP. 2000. The role of B cells and autoantibodies in multiple sclerosis. *Ann Neurol* 47: 694-706.

Armstrong, RC., Dorn, HH., Kufta, CV., Friedman, E., Dubois-Dalq, ME. 1992. Pre-oligodendrocytes from adult human CNS. *J Neurosci* 12: 1538-1547.

Arya, M., Shergill, IS., Williamson, M., Gommersall, L., Arya, N., Patel, HR. 2005. Basic principles of real-time quantitative PCR. *Expert Rev Mol Diagn* 5: 209-219.

- Asai, M., Hattori, C., Szabo, B., Sasagawa, N., Maruyama, K., Tanuma, S-I, Ishiura, S. 2003. Putative formation of ADAM9, ADAM10, and ADAM17 as APP  $\alpha$ -secretase. *Biochem Biophys Res Com* 301: 231-235.
- Avolio C, Giuliani F, Liuzzi GM, Ruggieri M, Paolicelli D, Riccio P, Livrea P, Trojano M. 2003. Adhesion molecules and matrix metalloproteinases in Multiple Sclerosis: effects induced by Interferon-beta. *Brain Res Bull* 61:357-364.
- Ayers, MM., Hazelwood, LJ., Catmull, DV., Wang, D., McKormack, Q., Bernard, CCA., Orian, JM. 2004. Early glial responses in murine models of multiple sclerosis. *Neurochem Int* 45: 409-419.
- Badovinac, V., Mostarica-Stojkovic, M., dinarello, CA., Stosic-Grujicic, S. 1998. Interleukin-1 receptor antagonist suppresses experimental autoimmune encephalomyelitis (EAE) in rats by influencing the activation and proliferation of encephalitogenic cells. *J Neuroimmunol* 85: 87-95.
- Baker, DE. 2004. Adalimumab: Human recombinant immunoglobulin G1 anti-tumor necrosis factor monoclonal antibody. *Rev Gastroenterol Disord* 4: 196-210.
- Baker, D., O'Neill, JK., Gschmeissner, SE., Wilcox, CE., Butter, C., Turk, JL. 1990. Induction of chronic relapsing experimental allergic encephalomyelitis in Biozzi mice. *J Neuroimmunol* 28: 261-270.
- Baker, D., Butler, D., Scallon, BJ., O'Neill, JK., Turk, JL., Feldmann, M. 1994. Control of established experimental allergic encephalomyelitis by inhibition of tumor necrosis factor (TNF) activity within the central nervous system using monoclonal antibodies and TNF receptor-immunoglobulin fusion proteins. *Eur J Immunology* 24: 2040-2048.
- Balashov, KE., Comabella, M., Ohashi, T., Khoury, SJ., Weiner, HL. 2000. Defective regulation of IFN $\gamma$  and IL-12 by endogenous IL-10 in progressive MS. *Neurology* 55: 192-198.
- Ballabh, P., Braun, A., Nedergaard, M. 2004. The blood-brain barrier: an overview structure, regulation, and clinical implications. *Neurobiology of disease* 16:1-13
- Bajetto, A., Bonavia, R., Barbero, Florio, T., Schetti, G. 2001. Chemokines and their receptors in the central nervous system. *Front Neuroendocrinol* 22:147-84.
- Barcellos, LF., Thomson, G. 2003. Genetic analysis of multiple sclerosis. *J Neuroimmunol* 143: 1-6.
- Barnett, MH., Prineas, JW. 2004. Relapsing and remitting multiple sclerosis: pathology of the newly forming lesion. *Ann Neurol* 55: 458-468.

- Baron, JL., Madri, JA., Ruddle, NH., Hashim, G., Janeway, CA. 1993. Surface expression of  $\alpha 4$  integrin by CD4 T cells is required for their entry into the brain parenchyma. *J Exp Med* 177: 57-68.
- Bar-Or, A., Oliveira, EML., Anderson, DE., Hafler, DA. 1999. Molecular pathogenesis of multiple sclerosis. *J Neuroimmunol* 100: 252-259.
- Bechtold, DA., Smith, KJ. 2005. Sodium-mediated axonal degeneration in inflammatory demyelinating disease. *J Neurol Sci* 233: 27-35.
- Begolka, SW., Vanderlugt, CL., Rahbe, SM., Miller, SD. 1998. Differential expression of inflammatory cytokines parallels progression of central nervous system pathology in two clinically distinct models of multiple sclerosis. *J Immunol* 161: 4437-4446
- Behi, EM., Dubucquoi, S., Lefranc, D., Zephir, H., De Seze, J., Vermersch, P., Prin, L. 2005. New insights into cell responses involved in experimental autoimmune encephalomyelitis and multiple sclerosis. *Immunol Lett* 96: 11-26.
- Berger, JR., Koralnik, IJ. 2005. Progressive multifocal leukoencephalopathy and Natalizumab – Unforeseen consequences. *New Eng J Med* 353: 414-416.
- Bitsch, A., Kuhlmann, T., Da Costa, C., Bunkowski, S., Polak, T., Brück, W. 2000a. Tumour necrosis factor alpha mRNA expression in early multiple sclerosis lesions: correlation with demyelinating activity and oligodendrocyte pathology. *Glia* 29: 366-375
- Bitsch, A., Schuchardt, J., Bunkowski, S., Kuhlmann, T., Bruck, W. 2000b. Acute axonal injury in multiple sclerosis correlation with demyelination and inflammation. *Brain* 123: 1174-1183.
- Bjartmar, C., Kidd, G., Mörk, S., Rudick, R., Trapp, BD. 2000. Neurological disability correlates with spinal cord axonal loss and reduced N-acetyl aspartate in chronic multiple sclerosis patients. *Ann Neurol* 48: 893-901.
- Bjartmar, C., Trapp, BD. 2001. Axonal and neuronal degeneration in multiple sclerosis: mechanisms and functional consequences. *Curr Opin Neurol* 14: 271-278.
- Bjartmar, C., Wujek, JR., Trapp, BD. 2003. Axonal loss in the pathology of MS: consequences for understanding the progressive phase of the disease. *J Neurol Sci* 206: 165-171.
- Black, RA., Rauch, CT., Kozlosky, CJ., Peschon, JJ., Slack, JL., Wolfson, MF., Castner, BJ., Stocking, KL., Reddy, P., Srinivasan, S., et al. 1997. A metalloproteinase disintegrin that releases tumour necrosis factor- $\alpha$  from cells. *Nature* 385: 729-733.

Black, RA. 2002. Molecules in focus: Tumor necrosis factor- $\alpha$  converting enzyme. *Int J Biochem Cell Biol* 34: 1-5.

Black, RA. 2004. TIMP3 checks inflammation. *Nat Gen* 36: 934-935.

Blacker, M., Noe, MC., Carty, T.J., Goodyer, CG., LeBlanc, AC. 2002. Effect of tumor necrosis factor- $\alpha$  converting enzyme (TACE) and metalloprotease inhibitor on amyloid precursor protein metabolism in human neurons. *J Neurochem* 83: 1349-1357.

Blakemore, WF., Keirstead, HS. 1999. The origin of remyelinating cells in the central nervous system. *J Neuroimmunol* 98: 69-76.

Blum, M.S., Toninelli, E., Anderson, J.M., Balda, M.S., Zhou, J., O'Donnell, L., Pardi, R., Bender, J.R. 1997. Cytoskeletal rearrangement mediates human microvascular endothelial tight junction modulation by cytokines. *Am J Physiol* 273:H286-284.

Bo, L., Peterson, JW., Mork, S., Hoffman, PA., Gallatin, WM., Ransohoff, RM., Trapp, BD. 1996. Distribution of immunoglobulin superfamily members ICAM-1, -2, -3 and the  $\beta$ 2 integrin LFA-1 in multiple sclerosis lesions. *J Neurol Exp Neuropathol* 55: 1060-1072.

Bolton SJ., Anthony DC., Perry VH. 1998. Loss of the tight junction proteins occludin and zonula occludens-1 from cerebral vascular endothelium during neutrophil-induced blood-brain barrier breakdown in vivo. *Neuroscience* 86: 1245-1257.

Bond, M., Murphy, G., Bennett, MR., Newby, AC., Baker, AH. 2002. Tissue inhibitor of metalloproteinase-3 induces a Fas-associated death domain-dependant type II apoptotic pathway. *J Biol Chem* 277: 13787-13795.

Borland G, Murphy G, Ager A. 1999. Tissue inhibitor of metalloproteinases-3 inhibits shedding of L-selectin from leukocytes. *J Biol Chem* 274:2810-5

Boven, L.A., Middel, J., Verhoef, J., De Groot, C.J., Nottet, H.S. 2000. Monocyte infiltration is highly associated with loss of the tight junction protein zonula occludens in HIV-1-associated dementia. *Neuropathol Appl Neurobiol* 26:356-360.

Brand-Schieber, E., Werner, P. 2004. Calcium channel blockers ameliorate disease in a mouse model of multiple sclerosis. *Exp Neurol* 189: 5-9.

Brok, HPM., Bauer, J., Jonker, M., Blezer, E., Amor, S., Bontrop, RE., Laman, JD., 't Hart, BA. 2001. Non-human primate models of multiple sclerosis. *Immunol, Rev* 183: 173-185.

Brocke, S., Piercy, C., Steinmann, L., Weissman, IL., Veromaa, T. 1999. Antibodies to CD44 and integrin  $\alpha$ 4, but not L-selectin, prevent central nervous system inflammation and experimental encephalomyelitis by

blocking secondary leukocyte recruitment. *Proc Natl Acad Sci USA* 96: 6896-6901.

Brosnan, CF., Raine, CS. 1996. Mechanisms of immune injury in multiple sclerosis. *Brain Pathol* 6: 243-257.

Brosnan, CF., Selmaj, K., Raine, CS. 1988. Hypothesis: a role for tumor necrosis factor in immune-mediated demyelination and its relevance to multiple sclerosis. *J Neuroimmunol* 18: 87-94.

Brosnan, CF., Cannella, B., Battistini, L., Raine, CS. 1995. Cytokine localization in multiple sclerosis lesions: correlation with adhesion molecule expression and reactive nitrogen species. *Neurology* 45: S16-S21.

Brown, H., Hien, TT., Day, N., Mai, NT., Chuong, LV., Chau, TT., Loc, PP., Phu, NH., Bethell, D., Farrar, J., Gatter, K., White, N., Turner, G. 1999. Evidence of blood-brain barrier dysfunction in human cerebral malaria. *Neuropathol Appl Neurobiol* 25: 331-340.

Bruck W., Bitsch A., Kolenda H., Bruck Y., Stiefel M., Lassmann H. 1997. Inflammatory central nervous system demyelination: correlation of magnetic resonance imaging findings with lesion pathology. *Ann Neurol* 42: 783-793.

Brunner, T., Mogil, RJ., LaFace, D., Yoo, NJ., Mahboubi, A., Echeverri, F., Martin, SJ., Force, WR, Lynch, DH., Ware, CF., Green, DR. 1995. Cell-autonomous Fas (CD95)/Fas-ligand interaction mediates activation-induced apoptosis in T-cell hybridomas. *Nature* 373: 441-444.

Brynskov, J., Foegh, P., Pederson, G., Ellervik, C., Kirkgaard, T., Bingham, A., Saermark, T. 2002. Tumour necrosis factor  $\alpha$  converting enzyme (TACE) activity in the colonic mucosa of patients with inflammatory bowel disease. *Gut* 51: 37-43.

Bugno, M., Witek, B., Bereta, J., Bereta, M., Edwards, DR., Kordula, T. 1999. Reprogramming of TIMP-1 and TIMP-3 expression profiles in brain microvascular endothelial cells and astrocytes in response to proinflammatory cytokines. *FEBS Lett* 448: 9-14.

Buntinx, M., Moreels, M., Vandenabeele, F., Lambrichts, I., Raus, J., Steels, P., Stinissen, P., Ameloot, M. 2004a. Cytokine-induced cell death in human oligodendroglial cell lines: I. Synergistic effects of IFN- $\gamma$  and TNF- $\alpha$  on apoptosis. *J Neurosci Res* 76:834-845.

Buntinx, M., Gielen, E., Van Hummelen, P., Raus, J., Ameloot, M., Steels, P., Stinissen, P. 2004b. Cytokine induced cell death in human oligodendroglial cell lines. II. Alterations in gene expression induced by interferon- $\gamma$  and tumor necrosis factor- $\alpha$ . *J Neurosci Res* 76: 846-861.

Burns, A.R., Bowden, R.A., MacDonell, S.D., Walker, D.C., Odebunmi, T.O., Donnachie, E.M., Simon, S.I., Entman, M.L., Smith, C.W. 2000. Analysis of

tight junctions during neutrophil transendothelial migration. *J Cell Science* 113:45-57.

Bzowska, M., Jura, N., Lassak, A., Black, RA., Bereta, J. 2004. Tumor necrosis factor-alpha stimulates expression of TNF-alpha converting enzyme in endothelial cells. *Eur J Biochem.* 271: 2808-2820.

Calabresi, PA., Tranquill, LR., Dambrosia, JM., Stone, LA., Maloni, H., Bash, CN., Frank, JA., McFarland, HF. 1997. Increases in soluble VCAM-1 correlate with a decrease in MRI lesions in multiple sclerosis treated with interferon beta-1b. *Ann Neurol* 41: 669-674.

Cannella, B., Cross, AH., Raine, CS. 1995. Anti-adhesion molecule therapy in experimental autoimmune encephalomyelitis. *J Neuroimmunol* 46: 43-55.

Cannella, B., Gaupp, S., Tilton, RG., Raine, CS. 2003. Differential efficacy of a synthetic antagonist of VLA-4 during the course of chronic relapsing experimental autoimmune encephalomyelitis. *J Neurosci Res* 71: 407-416.

Cannella, B., Raine, CS. 1995. The adhesion molecule and cytokine profile of multiple sclerosis lesions. *Ann Neurol* 37: 424-435.

Cannella, B., Raine, CS. 2004. Multiple sclerosis: cytokine receptors on oligodendrocytes predict innate regulation. *Ann Neurol* 55: 46-57.

Cardenas, A., Moro, MA., Leza, JC., O'Shea, E., Davalos, A., Castillo, J., Lorenzo, P., Lizasoain, I. 2002. Upregulation of TACE/ADAM17 after ischemic preconditioning is involved in brain tolerance. *J Cereb Blood Flow Metab* 22:1297-1302.

Carson, MJ. 2002. Microglia as liaisons between the immune and central nervous systems: functional implications for multiple sclerosis. *Glia* 40: 218-231.

Cartier, L., Hartley, O., Dubois-Dauphin, M., Krause, KH. 2005. Chemokine receptors in the central nervous system: role in brain inflammation and neurodegenerative disease. *Brain Res Rev* 48: 16-42.

Cecchelli, R., Dehouck, B., Descamps, L., Fenart, L., Buee-Scherrer, V., Duhem, C., Lundquist, S., Rentfel, M., Torpier, G., dehouck, M.P. 1999. In vitro model for evaluating drug transport across the blood-brain barrier. *Ad Drug Del Rev* 36:165-178.

Chabot, S., Yong, FP., Le, DM., Metz, LM., Myles, T., Yong, VW. 2002. Cytokine production in T lymphocyte-microglia interaction is attenuated by glatiramer acetate: a mechanism for therapeutic efficacy in multiple sclerosis. *Mult Scler* 8: 299-306.

- Chandler, S., Miller, KM., Clements, JM., Lury, J., Corkill, D., Anthony, DCC., Adams, SE. 1997. Matrix metalloproteinases, tumor necrosis factor and multiple sclerosis: an overview. *J Neuroimmunol* 72: 155-161.
- Chang, A., Tourtellotte, WW., Rudick, R., Trapp, BD. 2002. Premyelinating oligodendrocytes in chronic lesions of multiple sclerosis. *N Eng J Med* 346: 165-173.
- Cherney, RJ., Duan, JJ., Voss, ME., Chen, L., Wang, L., Meyer, DT., Wasserman, ZR., Hardman, KD., Liu, RQ., Covington, MB., Qian, M., Mandlekar, S., Christ, DD., Trzaskos, JM., Newton, RC., Magolda, RL., Wexler, RR., Decicco, CP. 2003. Design, synthesis, and evaluation of benzothiadiazepine hydroxamates as selective tumor necrosis factor- $\alpha$  converting enzyme inhibitors. *J Med Chem* 46:1811-1823.
- Chong, NHV., Kvant, A., Seregard, S., Bird, AC., Luthert, PJ., Steen, B. 2003. TIMP-3 mRNA is not overexpressed in Sorsby Fundus dystrophy. *Am J Ophthalmol* 136: 954-955.
- Claudio, L., Raine, C.S., Brosnan, C.F. 1995. Evidence of persistent blood-brain barrier abnormalities in chronic-progressive multiple sclerosis. *Acta Neuropathol (Berl)* 90:228-238.
- Colhoun, HM., McKeigue, PM., Davie-Smith, G. 2003. Problems with reporting genetic associations with complex outcomes. *Lancet* 361: 865-872.
- Colón, AL., Menchén, LA., Hurtado, O., De Christóbal, J., Lizasoain, I., Leza, JC., Lorenzo, P., Moro, MA. 2001. Implication of TNF- $\alpha$  convertase (TACE/ADAM17) in inducible nitric oxide synthase expression and inflammation in an experimental model of colitis. *Cytokine* 16: 220-226.
- Compston A., Scolding N., Wren D., Noble M. 1991. The pathogenesis of demyelinating disease: insights from cell biology. *Trends Neurosci* 14: 175-182.
- Contin, C., Pitard, V., Itai, T., Nagata, S., Moreau, JF., Dechanet-Merville, J. 2003. Membrane-anchored CD40 is processed by tumor necrosis factor- $\alpha$ -converting enzyme. *J Biol Chem* 278: 32801-32809.
- Cossins, JA., Clements, JM., Ford, J., Miller, KM., Pigott, R., Vos, W., Van Der Valk, P., De Groot, CJA. 1997. Enhanced expression of MMP-7 and MMP-9 in demyelinating multiple sclerosis lesions. *Acta Neuropathol* 94: 590-598.
- Craner MJ, Newcombe J, Black JA, Hartle C, Cuzner ML, Waxman SG. 2004. Molecular changes in neurons in multiple sclerosis: altered axonal expression of Nav1.2 and Nav1.6 sodium channels and Na<sup>+</sup>/Ca<sup>2+</sup> exchanger. *Proc Natl Acad Sci U S A* 101: 8168-8173.

Crocker. SJ., Pagenstecher, A., Campbel, L. 2004. The TIMPs tango with MMPs and more in the central nervous system. *J Neurosci Res* 75: 1-11.

Cummings, T.J., Strum, J.C., Yoon, L.W., Szymanski, M.H., Hulette, C.M. 2001. Recovery and expression of messenger RNA from post-mortem human brain tissue. *Mod Pathol* 14: 1157-1161.

Cuzner, M.L., Gveric, D., Strand, C., Loughlin, A.J., Paemen, L., Opdenakker, G., Newcombe, J. 1996. The expression of tissue-type plasminogen activator, matrix metalloproteinases and endogenous inhibitors in the central nervous system in multiple sclerosis: comparison of stages in lesion evolution. *J Neuropathol Exp Neurol* 55: 1194-1204.

Dallas, D.J., Genever, P.G., Patton, A.J., Millichip, M.I., McKie, N., Skerry, T.M. 1999. Localization of ADAM10 and Notch receptors in bone. *Bone* 25: 9-15.

Dallasta, L.M., Pisarov, L.A., Esplen, J.E., Werley, J.V., Moses, A.V., Nelson, J.A., Achim, C.L. 1999. Blood-brain barrier tight junction disruption in human immunodeficiency virus-1 encephalitis. *Am J Pathology* 155:1915-1927.

Dalton, C.M., Miszkiel, K.A., Barker, G.J., MacManus, D.G., Pepple, T.I., Panzara, M., Yang, M., Hulme, A., O'Connor, P., Miller, D.H., the International Natalizumab MS trial group. 2004. Effect of natalizumab on conversion of gadolinium enhancing lesions to T1 hypointense lesions in relapsing multiple sclerosis. *J Neurol* 251: 407-413.

Daniel, W.W. 1978. In *Applied nonparametric statistics*. Houghton-Mifflin: Boston, 211-212.

Dawson, R.L., Levien, J.M., Reynolds, R. 2000. NG2-expressing cells in the central nervous system: are they oligodendrocyte progenitors? *J Neurosci Res* 61: 471-479.

De Groot, C.J., Theeuwes, J.W., Dijkstra, C.D., van der Valk, P. 1995. Postmortem delay effects on neuroglial cells and brain macrophages from Lewis rats with acute experimental allergic encephalomyelitis: an immunohistochemical and cytochemical study. *Neuroimmunol* 59: 123-134.

Dejana, E., Lampugnani, M.G., Martinez-Estrada, O., Bazzoni, G.F. 2000. The molecular organisation of endothelial junctions and their functional role in vascular morphogenesis and permeability. *International J developmental Biology* 44:743-748.

DeLuca, G.C., Ebers, G.C., Esiri, M.M. 2004. Axonal loss in multiple sclerosis: a pathological survey of the corticospinal and sensory tracts. *Brain* 127: 1009-1018.

Demeuse, P.H., Kerkhofs, A., Struys-Ponsar, C., Knoops, B., reacle, C., van den Bosch de Aguilar, P.H. 2002. Compartmentalized coculture of rat brain

endothelial cells and astrocytes: a syngenic model to study the blood-brain barrier. *J Neurosci Meth* 121:21-31.

De Simone, R., Giampaolo, A., Giometto, B., Gallo, P., Levi, G., Aloisi, F., 1995. The costimulatory molecule B7 is expressed on human microglia in culture and in multiple sclerosis acute lesions. *J Neuropathol Exp Neurol* 54: 175-187.

De Vries, H.E., Kuiper, J., De Boer A.G., Van Berkel, T.J.C., Breimer, D.D. 1997. The Blood-brain barrier in neuroinflammatory diseases. *Pharma Rev* 49:143-155.

Dietrich, JB. 2004. Endothelial cells of the blood-brain barrier: a target for glucocorticoids and estrogens? *Front Biosci* 9: 684-693.

Dobbie, MS., Hurst, RD., Klein, NJ., Surtees, RAH. 1999. Upregulation of intercellular adhesion molecule-1 expression on human endothelial cells by tumor necrosis factor- $\alpha$  in an in vitro model of the blood-brain barrier. *Brain Res* 830: 330-336.

Doedens, JR., Black, RA. 2000. Stimulation-induced down-regulation of tumor necrosis factor- $\alpha$  converting enzyme. *J Biol Chem* 275: 14598-14607.

Doedens, JR., Mahimkar, RM., Black, RA. 2003. TACE/ADAM-17 enzymatic activity is increased in response to cellular stimulation. *Biochem Biophys Res Commun* 308: 331-338.

Dong, Y., Benveniste, EN. 2001. Immune function of astrocytes. *Glia* 36: 180-190.

Dopp, JM., Brenemann, SM., Olschowka, JA. 1994. Expression of ICAM-1, VCAM-1, L-selectin, and leukosialin in the mouse central nervous system during the induction and remission stages of experimental allergic encephalomyelitis. *J Neuroimmunol* 54: 129-144.

Dore-Duffy, P., Newman, W., Balabanov, R., Lisak, RP., Mainolfi, E., Rothlein, R., Peterson, M. 1995. Circulating, soluble adhesion proteins in cerebrospinal fluid and serum of patients with multiple sclerosis: correlation with clinical activity. *Ann Neurol* 37: 55-62.

Dri P, Gasparini C, Menegazzi R, Cramer R, Alberi L, Presani G, et al. 2000. TNF-Induced shedding of TNF receptors in human polymorphonuclear leukocytes: role of the 55-kDa TNF receptor and involvement of a membrane-bound and non-matrix metalloproteinase. *J Immunol* 165:2165-2172

Drulovic, J., Mostarica-Stojkovic, M., Levic, Z., Stojsavljevic, N., Pravica, V., Mesaros, S. 1997. Interleukin-12 and tumor necrosis factor-alpha levels in the cerebrospinal fluid of multiple sclerosis patients. *147: 145-50.*

Duan, JJ., Lu, Z., Xue, CB., He, X., Seng, JL., Roderick, JJ., Wasserman, ZR., Liu, RQ., Covington, MB., Magolda, RL., Newton, RC., Trzaskos, JM., Decicco, CP. 2003. Discovery of N-hydroxy-2-(2-oxo-3-pyrrolidinyl)acetamides as potent and selective inhibitors of tumor necrosis factor- $\alpha$  converting enzyme (TACE). *Bioorg Med Chem Lett* 13: 2035-2040.

Dyment, DA., Ebers, GC., Sadovnick, AD. 2004. Genetics of multiple sclerosis. *Lancet Neurol* 3: 104-110.

Ebers, GC. 2004. Natural history of primary progressive multiple sclerosis. *Mult Scler* 10: S8-S13.

Ebers, GC., Bulman, DE., Sadovnick, AD, Paty, DW., Warren, S., Hader, W., Murray, TJ., Seland, TP., Duquette, P., Grey, T. 1986. Population based study of multiple sclerosis in twins. *N Eng J Med* 315: 1638-1642.

Eikelenboom, MJ., Killestein, J., Izeboud, T., Kalkers, NF., Baars, PA., van Lier, RAW., Barkhof, F., Uitdehaag, BMJ., Polman, CH. 2005. Expression of adhesion molecules on peripheral lymphocytes predicts future lesion development in MS. *J Neuroimmunol* 158: 222-230.

Endres, K., Anders, A., Kojro, E., Gilbert, S., Fahrenholz, F., Postina, R. 2003. Tumor necrosis factor- $\alpha$  is processed by proprotein-convertases to its mature form which is degraded upon phorbol ester stimulation. *Eur J Biochem* 270: 2386-2393.

Engelhardt, B. 2000. Role of glucocorticoids on T cell recruitment across the blood-brain barrier. *Rheumatol* 59: II/18-II/21.

Engelhardt, B. 2003. Development of the blood-brain barrier. *Cell Tissue Res* 314: 119-129.

Esiri, MM. 1977. Immunoglobulin-containing cells in multiple sclerosis plaques. *Lancet* 2: 478-480.

Esiri, MM., Reading, MC., Squier, MV., Hughes, JT. 1989. Immunocytochemical characterization of the macrophage and lymphocyte infiltrate in the brain in six cases of human encephalitis of varied aetiology. *Neuropathol Appl Neurobiol* 15: 289-305.

Esiri, MM., Gay, D. 1990. Immunological and neuropathological significance of the Virchow-Robin space. *J neurological Sci* 100: 3-8.

Ferguson, B., Matyszak, MM., Esiri, MM., Perry, VH. 1997. Axonal damage in acute multiple sclerosis lesions. *Brain* 120: 393-399.

Etienne-Manneville S, Manneville JB, Adamson P, Wilbourn B, Greenwood J, Couraud PO. 2000. ICAM-1-coupled cytoskeletal rearrangements and transendothelial lymphocyte migration involve intracellular calcium signaling in brain endothelial cell lines. *J Immunol* 6:3375-83

Evangelou, N., Esiri, MM., Smith, S., Palace, J., Mathews, PM. 2000. Quantitative pathological evidence for axonal loss in normal appearing white matter in multiple sclerosis. *Ann Neurol* 47: 391-395.

Evans, JP. 2001. Fertilin  $\beta$  and other ADAMs as integrin ligands: Insights into cell adhesion and fertilization. *BioEssays* 23: 628-639.

Fanning, AS., Mitic, LL., Anderson, JM. 1999. Transmembrane proteins in the tight junction barrier. *J Am Soc Nephrol* 10: 1337-1345.

Faure, E. 2005. Multiple sclerosis and hepatitis B vaccination: Could minute contamination of the vaccine by partial Hepatitis B virus polymerase play a role through molecular mimicry? *Med Hypotheses* 65: 509-520.

Faveeuw, C., Preece, G., Ager, A. 2001. Transendothelial migration of lymphocytes across high endothelial venules into lymph nodes is affected by metalloproteinases. *Blood* 98: 688-695.

Ferguson B, Matyszak MK, Esiri MM, Perry VH. 1997. Axonal damage in acute multiple sclerosis lesions. *Brain* 120: 393-399.

Fife, BT., Huffnagle, GB., Kuziel, WA., Karpus, WJ. 2000. CC chemokine receptor 2 is critical for induction of experimental autoimmune encephalomyelitis. *J exp Med* 192: 899-905.

Filippi, M., Campi, A., Dousset, V., Baratti, C., Martinelli, V., Canal, N., Scotti, G., Comi, G. 1995. A magnetization transfer imaging study of normal-appearing white matter in multiple sclerosis. *Neurology* 45: 478-482.

Filippi, M., Rocca, M.A., Martino, G., Horsfield, M.A., Comi, G. 1998. Magnetization transfer changes in the normal appearing white matter precede the appearance of enhancing lesions in patients with multiple sclerosis. *Ann Neurol* 43:809-814.

Flynn, G., Maru, S., Loughlin, J., Romero, IA., Male, D. 2003. Regulation of chemokines receptor expression in human microglia and astrocytes. *J Neuroimmunol* 136: 84-93.

Ford, AL., Goodsall, AL., Hickey, WF., Sedgwick, JD. 1995. Normal adult ramified microglia separated from other central nervous system macrophages by flow cytometric sorting. Phenotypic differences defined and direct ex vivo antigen presentation to myelin basic protein-reactive CD4+ T cells compared. *J Immunol* 154: 4309-4321.

Fox, RJ., Ransohoff, RM. 2004. New directions in MS therapeutics: vehicles of hope. *Trends Immunol* 25: 632-636.

Franciotta, DM., Grimaldi, LM., Martino, GV., Piccolo, G., Bergamaschi, R., Citterio, A., Melzi d'Eril, GV. 1989. Tumor necrosis factor in serum and

cerebrospinal fluid of patients with multiple sclerosis. *Ann Neurol* 26: 787-789.

Franke, H., Galla, H-J., Beuckmann, C.T. 2000. Primary cultures of brain microvessel endothelial cells: a valid and flexible model to study drug transport through the blood-brain barrier in vitro. *Brain Res Prot* 5:248-256.

Franklin, R.J., Blakemore, W.F. 1997. To what extent is oligodendrocyte progenitor migration a limiting factor in the remyelination of multiple sclerosis lesions? *Mult Scler* 3: 84-87.

Franklin, R.J.M. 2002. Why does remyelination fail in multiple sclerosis? *Nat Rev Neurosci* 3: 705-714.

Franzen, B., Duvefelt, K., Jonsson, C., Engelhardt, B., Ottervald, J., Wickman, M., Yang, Y., Schuppe-Koistinen, I. 2003. Gene and protein expression profiling of human cerebral endothelial cells activated with tumor necrosis factor- $\alpha$ . *Mol Brain Res* 115: 130-146.

Frei, K., Eugster, H., Bopst, M., Constantinescu, C.S., Lavi, E., Fontana, A. 1997. Tumor necrosis factor and lymphotoxin are not required for induction of acute experimental autoimmune encephalomyelitis. *J Exp Med* 185: 2177-2182.

Freyer, D., Manz, R., Ziegenhorn, A., Weih, M., Angstwurm, K., Docke, W.D., Meisel, A., Schumann, R.R., Schonfelder, G., Dirnagl, U., Weber, J.R. 1999. Cerebral endothelial cells release TNF- $\alpha$  after stimulation with cell walls of streptococcus pneumoniae and regulate inducible nitric oxide synthase and ICAM-1 expression via autocrine loops. *J Immunol* 163: 4308-4314.

Fu, L., Matthews, P.M., De Stefano, N., Worsley, K.J., Narayanan, S., Francis, G.S., Antel, J.P., Wolfson, C., Arnold, D.L. 1998. Imaging axonal damage of normal-appearing white matter in multiple sclerosis. *Brain* 121: 103-113.

Furuse, M., Hirase, T., Itoh, M., Nagafuchi, A., Yonemura, S., Tsukita, S. 1993. Occludin: a novel integral membrane protein localizing at tight junctions. *J. Cell Biology* 123:1777-1788.

Furuse, M., Hirase, T., Itoh, M., Nagafuchi, A., Yonemura, S., Tsukita, S., Tsukita, S. 1993. Occludin: a novel integral membrane protein localizing at tight junctions. *J Cell Biol* 123: 1777-1788.

Furuse, M., Itoh, M., Hirase, T., Nagafuchi, A., Yonemura, S., Tsukita, S., Tsukita, S. 1994. Direct association of occludin with ZO-1 and its possible involvement in the localisation of occludin at tight junctions. *J Cell Biology* 127:1617-1626.

Furuse, M., Fujita, K., Hiiragi, T., Fujimoto, K., Tsukita, S. 1998. Claudin-1 and -2: novel integral membrane proteins localizing at tight junctions with no sequence similarity to occludin. *J Cell Biology* 141:1539-1550.

Gale, CR., Martyn, CN. 1995. Migrant studies in multiple sclerosis. *Prog Neurobiol* 47: 425-448.

Garton, KJ., Gough, PJ., Blobel, CP., Murphey, G., Greaves, DR., Dempsey, PJ., Raines, EW. 2001. Tumor necrosis factor- $\alpha$ -converting enzyme (ADAM17) mediates the cleavage and shedding of fractalkine (CX3CL1). *J Biol Chem* 276: 37993-38001.

Garton, KJ., Gough, PJ., Philalay, J., Wille, PT., Blobel, CP., Whitehead, RH., Dempsey, PJ., Raines, EW. 2003. Stimulated shedding of vascular adhesion molecule 1 (VCAM-1) is mediated by tumor necrosis factor- $\alpha$ -converting enzyme (ADAM17). *J Biol Chem* 278: 37459-37464.

Gaultier, A., Cousin, H., Darribere, T., Alfandari, D. 2002. ADAM13 disintegrin and cystein-rich domains bind to the second heparin-binding domain of fibronectin. *J Biol Chem* 277: 23336-23344.

Gay, D., Esiri, M. 1991. Blood-brain barrier damage in acute multiple sclerosis plaques. An immunocytological study. *Brain* 114:557-572.

Gay, FW., Drye, TJ., Dick, GWA., Esiri, MM. 1997. The application of multifactorial analysis in the staging of plaques in early multiple sclerosis indication and characterization of the primary demyelinating lesion. *Brain* 120: 1461-1483.

Ge, S., Song, L., Pachter, JS. 2005. Where is the blood-brain barrier.....really? *J Neurosci Res* 79: 421-427.

Genain, CP., Hauser, SL. 1997. Creation of a model for multiple sclerosis in *Callithrix jacchus* marmosets. *J Mol Med* 75: 187-197.

Genain, CP., Cannella, B., Hauser, SL., Raine, CS. 1999. Identification of autoantibodies associated with myelin damage in multiple sclerosis. *Nature Med* 5: 170-175.

Gerspach, J., Gotz, A., Zimmermann, G., Kollé, C., Bottinger, H., Grell, M. 2000. Detection of membrane-bound tumor necrosis factor (TNF): an analysis of TNF-specific reagents. *Microsc Res Tech* 50: 243-250.

Gijbels, K., Masure, S., Carton, H., Opdenakker, G. 1992. Gelatinase in the cerebrospinal fluid of patients with multiple sclerosis and other inflammatory neurological disorders. *J Neuroimmunol* 41: 29-34.

Gimenez, MAT., Sim, JE., Russell, JH. 2004. TNFR1-dependent VCAM-1 expression by astrocytes exposes the CNS to destructive inflammation. *J Neuroimmunol* 151: 116-125.

Glabinski, AR., Bielecki, B., Ransohoff, RM. 2003. Chemokine upregulation follows cytokine expression in chronic relapsing experimental autoimmune encephalomyelitis. *Scan J Immunol* 58: 81-88.

Glabinski, AR., Bielecki, B., Kawczak, JA., Tuohy, VK., Selmaj, K., Ransohoff, RM. 2004. Treatment with soluble tumor necrosis factor receptor (sTNFR): Fc/p80 fusion protein ameliorates relapsing-remitting experimental autoimmune encephalomyelitis and decreases chemokine expression. *Autoimmunity* 37: 465-471.

Goddard DR, Bunning RA, Woodroffe MN. 2001. Astrocyte and endothelial cell expression of ADAM 17 (TACE) in adult human CNS. *Glia* 34:267-271.

Godiska, R., Chantry, D., Dietsch, G., Gray, P. 1995. Chemokine expression in murine experimental autoimmune encephalomyelitis. *J Neuroimmunol* 58: 167-176.

Goldberg, SH., van der Meer, P., Hesselgesser, J., Jaffer, S., Kolson, DL., Albright, AV., Gonzalez-Scarano, F., Lavi, W. 2001. CXCR3 expression in human central nervous system diseases. *Neuropathol Appl Neurobiol* 27: 127-138.

Goodkin, D.E., Rooney, W.D., Sloan, R., Bacchetti, P., Gee, L., Vermathen, M., Waubant, E., Abundo, M., Majumdar, S., Nelson, S., Weiner, M.W. 1998. A serial study of new MS lesions and the white matter from which they arise. *Neurology* 51:1689-1697.

Grell, M., Douni, E., Wajant, H., Lohden, M., Clauss, M., Maxeiner, B., Georgopoulos, S., Lesslauer, W., Kollias, G., Pfizenmaier, K., Scheurich P. 1995. The transmembrane form of tumor necrosis factor is the prime activating ligand of the 80 kDa tumor necrosis factor receptor. *Cell* 83: 793-802.

Greenwood, J., Pryce, G., Devine, L., Male, DK., dos Santos, WL., Calder, VL., Adamson, P. 1996. SV40 large T immortalised cell lines of the rat blood-brain and blood-retinal barriers retain their phenotypic and immunological characteristics. *J Neuroimmunol* 71: 51-63.

Gumbleton, M., Audus, K.L. 2001. Progress and limitations in the use of In Vitro cell cultures to serve as a permeability screen for the blood-brain barrier. *J Pharm Sci* 90:1681-1698.

Hafler, D. 2004. Multiple sclerosis. *J Clin Invest* 113: 788-794.

Hamm, S., Dehouck, B., Kraus, Wolburg-Buchholz, K., Wolburg, H., Risau, W., Cecchelli, R., Engelhardt, B., Dehouck, M-P. 2004. Astrocyte mediated modulation of the blood-brain barrier permeability does not correlate with a loss of tight junction proteins from the cellular contacts. *Cell tissue Res* 315:157-166.

Harkness, KA., Adamson, P., Sussman, JD., Davies-Jones, GAB., Greenwood, J., Woodroffe, MN. 2000. Dexamethasone regulation of matrix metalloproteinase expression in CNS vascular endothelium. *Brain* 123: 698-709.

Harkness, KA., Sussman, JD., Davies-Jones, GAB., Greenwood, J., Woodroffe, MN. 2003. Cytokine regulation of MCP-1 expression in brain and retinal microvascular endothelial cells. 2003. *J Neuroimmunol* 142: 1-9.

Harris, J.O., Frank, J.A., Patronas, N., McFarlin, D.E., McFarland, H.F. 1991. Serial gadolinium-enhanced magnetic resonance imaging scans in patients with early, relapsing-remitting multiple sclerosis: implications for clinical trials and natural history. *Ann Neurol* 29:548-555.

Hayes GM, Woodroffe MN, Cuzner ML. 1987. Microglia are the major cell type expressing MHC class II in human white matter. *J Neurol Sci* 80: 25-37.

Hensiek AE., Sawcer SJ., Feakes R., Deans J., Mander A., Akesson E., Roxburgh R., Corradu F., Smith S., Compston DA. 2002. HLA-DR 15 is associated with female sex and younger age at diagnosis in multiple sclerosis. *J Neurol Neurosurg Psychiatry*. 72: 184-187.

Herren, B., Raines, EW., Ross, R. 1997. Expression of a disintegrin-like protein in cultured human vascular cells and in vivo. *FASEB J* 11: 173-180.

Herrera BM, Ebers GC. 2003. Progress in deciphering the genetics of multiple sclerosis. *Curr Opin Neurol*. 16: 253-258.

Hickey, WF., Kimura, H. 1988. Perivascular microglial cells of the CNS are bone marrow-derived and present antigen in vivo. *Science* 239: 290-292.

Hickey WF. 2001. Basic principles of immunological surveillance of the normal central nervous system. *Glia* 36: 118-124.

Hinkle, CL., Sunnarborg, SW., Loiselle, D., Parker, CE., Stevenson, M., Russell, WE., Lee, DC. 2004. Selective roles for TACE/ADAM17 in the shedding of epidermal growth factor receptor ligand family. The juxtamembrane stalk determines cleavage efficiency. *J Biol Chem* 279: 24179-24188.

Hirase, T., Staddon, J.M., Saitou, M., Ando-Akatsuka, Y., Itoh, M., Furuse, M., Fujimoto, K., Tsukita, S., Rubin L.L. 1997. Occludin as a possible determinant of tight junction permeability in endothelial cells. *J Cell Science* 110:1603-1613.

Hodgkin PD, Basten A. 1995. B cell activation, tolerance and antigen-presenting function. *Curr Opin Immunol* 7: 121-129.

Hofman, FM., Hinton, DR., Jonhson, K., Merrill, JE. 1989. Tumor necrosis factor identified in multiple sclerosis brain. *J Exp Med* 170: 607-612.

- Hohlfeld, R. 1997. Biotechnological agents for the immunotherapy of multiple sclerosis. Principles , problems and perspectives. *Brain* 120: 865-916.
- Hohol MJ, Orav EJ, Weiner HL. 1995. Disease steps in multiple sclerosis: a simple approach to evaluate disease progression. *Neurology* 45: 251-255.
- Holley, JE., Gveric, D., Newcombe, J., Cuzner, ML., Gutowski, NJ. 2003. Astrocyte characterization in the multiple sclerosis glial scar. *Neuropathol Appl Neurobiol* 29: 434-444.
- Hori, S., Ohtsuki, S., Hosoya, K., Nakashima, E., Terasaki, T. 2004. A pericyte-derived angiopoietin-1 multimeric complex induces occludin gene expression in brain capillary endothelial cells through Tie-2 activation in vitro. *J Neurochem* 89:503-513.
- Howard, L., Lu, X., Mitchell, S., Griffiths, S., Glynn, P. 1996. Molecular cloning of MADM: a catalytically active mammalian disintegrin-metalloprotease expressed in various cell types. *Biochem J* 317: 45-50.
- Howarth, AG., Hughes, MR., Stevenson, BR. 1992. Detection of the tight junction-associated protein ZO-1 in astrocytes and other nonepithelial cell types. *Am J Physiol* 262: C461-469.
- Huang, D, Wang, J., Kivisakk, P., Rollins, BJ., Ransohoff, RM. 2001. Absence of monocyte chemoattractant protein 1 in mice leads to decreased local macrophage recruitment and antigen-specific T helper cell type 1 immune response in experimental autoimmune encephalomyelitis. *J Exp Med* 193: 713-725.
- Huber, J.D., Egleton, R.D., Davis, T.P. 2001. Molecular physiology and pathophysiology of tight junctions in the blood-brain barrier. *Trends Neurosci* 24:719-725
- Hulshof, S., Montagne, L., DeGroot, CJ., Van Der Valk, P. 2002. Cellular localisation and expression patterns of interleukin-10 and interleukin-4, and their receptors in multiple sclerosis. *Glia* 38: 24-35.
- Hulshof, S., van Haastert, ES., Kuipers, HF., van den Elsen, PJ., De Groot, CJ., van der Valk, P., Ravid, R., Biber, K. 2003. CX3CL1 and CX3CR1 expression in human brain tissue: noninflammatory control versus multiple sclerosis. *J Neuropathol Exp Neurol* 62: 899-907.
- Hundhausen, C., Misztela, D., Berkhout, TA., Broadway, N., Saftig, P., Reiss, K., Hartmann, D., Fahrenholz, F., Postina, R., Matthews, V., Kallen, KJ., Rose-John, S., Ludwig, A. 2003. The disintegrin-like metalloproteinase ADAM10 is involved in constitutive cleavage of CX3CL1 (fractalkine) and regulates CX3CL1-mediated cell-cell adhesion. *Blood* 102: 1186-1195.

Hurtado O, Cardenas A, Lizasoain I, Bosca L, Leza JC, Lorenzo P, Moro, MA. 2001. Up-regulation of TNF- $\alpha$  convertase (TACE/ADAM-17) after oxygen-glucose deprivation in rat forebrain slices. *Neuropharmacology* 40:1094-1102.

Hurwitz, AA., Lyman, WD., Guida, MP., Calderon, TM., Berman, JW. 1992. Tumor necrosis factor alpha induces adhesion molecule expression on human fetal astrocytes. *J Exp Med* 176: 1631-1636.

Hyrich, KL., Silman, AJ., Watson, KD., Symmons, DPM. 2004. Anti-tumour necrosis factor  $\alpha$  therapy in rheumatoid arthritis: an update on safety. *Ann Rheum Dis* 63: 1538-1543.

Iba, K., Albrechtsen, R., Gilpin, BK, Frohlich, C., Loechel, F., Wewer, UM. 1999. Cysteine-rich domain of human ADAM12 (meltrin  $\alpha$ ) supports tumor cell adhesion. *Am J Pathol* 154: 1489-1501.

Iglesias, A., Bauer, J., Litzemberger, T., Schubart, A., Linington, C. 2001. T- and B-Cell responses to myelin oligodendrocyte glycoprotein in experimental autoimmune encephalomyelitis and multiple sclerosis. *Glia* 36: 220-234.

Imai, T., Hieshima, K., Haskell, C., Baba, M., Nagira, M., Nishimura, M., Kakizaki, M., Takagi, S., Nomiyama, H., Schall, TJ., Yoshie, O. 1997. Identification and molecular characterisation of fractalkine receptor CX3CR1, which mediates both leukocyte migration and adhesion. *Cell* 91: 521-530.

Imaizumi, T., Itaya, H., Fujita, K., Kudoh, D., Kudoh, S., Mori, K., Fujimoto, K., Matsumiya, T., Yoshida, H., Satoh, K. 2000. Expression of tumor necrosis factor- $\alpha$  in cultured human endothelial cells stimulated with lipopolysaccharide of interleukin-1 $\alpha$ . *Arterioscler Thromb Vasc Biol* 20: 410-415.

Imitola, J., Chitnis, T., Khoury, SJ. 2005. Cytokines in multiple sclerosis: from bench to bedside. *Pharmacol Ther* 106: 163-177.

Issazadeh, S., Mustafa, M., Ljungdahl, A., Hojeberg, B., Elde, R., Dagerlind, A., Olsson, T. 1995a. Interferon- $\gamma$ , interleukin-4 and transforming growth factor- $\beta$  in experimental allergic encephalomyelitis in Lewis rats: dynamics of cellular mRNA expression in the central nervous system and lymphoid cells. *J Neurosci Res* 40: 579-590.

Issazadeh, S., Ljungdahl, A., Hojeberg, B., Mustafa, M., Olsson, T. 1995b. Cytokine production in the central nervous system of Lewis rats with experimental autoimmune encephalomyelitis: dynamics of mRNA expression for interleukin-10, interleukin-12, cytolysin, tumor necrosis factor  $\alpha$  and tumor necrosis factor  $\beta$ . *J Neuroimmunol* 61: 205-212.

Itai, T., Tanaka, M., Nagata, S. 2001. Processing of tumor necrosis factor by the membrane-bound TNF- $\alpha$ -converting enzyme, but not its truncated soluble form. *Eur J Biochem* 268: 2074-2082.

Itoh, M., Morita, K., Tsukita, S. 1999a. Characterization of ZO-2 as a MAGUK family member associated with tight as well as adherens junctions with a binding affinity to occludin and  $\alpha$  catenin. *J Biological Chemistry* 274:5981-5986.

Itoh, M., Furuse, M., Morita, K., Kubata, K., Saitou, M., Tsukita, S. 1999b. Direct binding of three tight junction-associated MAGUKs, ZO-1, ZO-2 and ZO-3, with the COOH termini of claudins. *J Cell Biology* 147:1351-1363.

Jack, C., Ruffini, F., Bar-Or, A., Antel, JP. 2005. Microglia and multiple sclerosis. *J Neurosci Res* 81: 363-373.

Jaworski DM, Fager N. 2000. Regulation of tissue inhibitor of metalloproteinase-3 (TIMP-3) mRNA expression during rat CNS development. *J Neuroscience Research* 61: 396-408.

Jee, Y., Yoon, WK., Okura, Y., Tanuma, N., Matsumoto, Y. 2002. Upregulation of monocyte chemotactic protein-1 and CC chemokine receptor 2 in the central nervous system is closely associated with relapse of autoimmune encephalomyelitis in Lewis rats. *J Neuroimmunol* 128: 49-57.

Jeliazkova-Mecheva, V.V., Bobilya, D.J. 2003. A porcine astrocyte/endothelial cell co-culture model of the blood-brain barrier. *Brain Res Brain Res Protoc* 12:91-98.

Jensen, J., Krakauer, M., Sellebjerg, F. 2005. Cytokines and adhesion molecules in multiple sclerosis patients treated with interferon-beta1b. *Cytokine* 29: 24-30.

Jersild, C., Svejgaard, A., Fog, T. 1972. HLA antigens and multiple sclerosis. *Lancet* 1: 1240-1241.

Jiang, Y., Salafranca, MN., Adhikari, S., Xia, Y., Feng, L., Sonntag, MK., deFiebre, CM., Pennell, NA., Streit, WJ, Harrison, JK. 1998. Chemokine receptor expression in cultured glia and rat experimental allergic encephalomyelitis. *J Neuroimmunol* 86: 1-12.

Jurewicz, AM., Walczak, AK., Selmaj, KW. 1999. Shedding of TNF receptors in multiple sclerosis patients. *Neurology* 53: 1409-1414.

Karen, D., Lin, FC., Bryan, M., Ringel, J., Moniaux, N., Lin, M-F., Batra, SK. 2003. Expression of ADAMs (a disintegrin and metalloproteases) and TIMP-3 (tissue inhibitor of metalloproteinase-3) in human prostatic adenocarcinomas. *Int J Oncol* 23: 1365-1371.

Karkkainen, I., Rybnikova, E., Pelto-Huikko, M., Huovila, AP. 2000. Metalloprotease-disintegrin (ADAM) genes are widely and differentially expressed in the adult CNS. *Mol Cell Neurosci* 15: 547-560.

Karp, C., van Boxel-Dezaire, A., Byrnes, A., Nagelkerken, L. 2001. Interferon- $\beta$  in multiple sclerosis: altering the balance of interleukin-12 and interleukin-10. *Curr Opin Neurol* 14: 361-368.

Karpus, WJ., Lukacs, NW., McRae, BL., Strieter, RM., Kunkel, SL., Miller, SD. 1995. An important role for the chemokine macrophage inflammatory protein-1 $\alpha$  in the pathogenesis of the T cell-mediated autoimmune disease, experimental autoimmune encephalomyelitis. *J Immunol* 155: 5003-5010.

Karpus, WJ., Ransohoff, RM. 1998. Cutting edge commentary: Chemokine regulation of experimental autoimmune encephalomyelitis: Temporal and spatial expression patterns govern disease pathogenesis. *J Immunol* 161: 2667-2671.

Karpus, WJ. 2001. Chemokines and central nervous system disorders. *J Neurovirology* 7: 493-500.

Kassiotis, G., Pasparakis, M., Kollias, G., Probert, L. 1999. TNF accelerates the onset but does not alter the incidence and severity of myelin basic protein-induced experimental autoimmune encephalomyelitis. *Eur J Immunol* 29:774-780.

Kassiotis, G., Kollias, G. 2001. Uncoupling the proinflammatory from the immunosuppressive properties of tumor necrosis factor (TNF) at the p55 TNF receptor level: Implications for pathogenesis and therapy of autoimmune demyelination. *J Exp Med* 193: 427-434.

Kastenbauer, S., Koedel, U., Wick, M., Kieseier, BC., Hartung, HP., Pfister, HW. 2003. CSF and serum levels of soluble fractalkine (CX3CL1) in inflammatory diseases of the nervous system. *J Neuroimmunol* 137: 210-217.

Kaye, JF., Kerlero de Rosbo, N., Mendel, I., Fletcher, S., Hoffman, M., Yust, I., Ben-Nun, A. 2000. The central nervous system-specific myelin oligodendrocyte basic protein (MOBP) is encephalitogenic and a potential target antigen in multiple sclerosis (MS). *J Neuroimmunol* 102: 189-198.

Keirstead, HS., Blakemore, WF. 1999. The role of oligodendrocytes and oligodendrocyte progenitors in CNS remyelination. *Adv Exp Med Biol* 468: 183-197.

Kenealy, SJ., Pericak-Vance, MA., Haines, JL. 2003. The genetic epidemiology of multiple sclerosis. *J Neuroimmunol* 143: 7-12.

Kennedy, K., Strieter, R., Kunkel, S., Lukacs, N., Karpus, W. 1998. Acute and relapsing experimental autoimmune encephalomyelitis are regulated by differential expression of the CC chemokines macrophage inflammatory protein-1 and monocyte chemoattractant protein 1. *J Neuroimmunol* 92: 98-108.

- Kent, S.J., Karlik, S.J., Rice, G.P., Horner, H.C. 1995. A monoclonal antibody to alpha 4-integrin reverses the MR-detectable signs of experimental allergic encephalomyelitis in the guinea pig. *J Magn Reson Imaging* 5: 535-540.
- Kermode, A.G., Thompson, A.J., Tofts, P., MacManus, D.G., Kendall, B.E., Kingsley, D.P., Moseley, I.F., Rudge, P., McDonald, W.I. 1990a. Breakdown of the blood-brain barrier precedes symptoms and other MRI signs of new lesions in multiple sclerosis. Pathogenic and clinical implications. *Brain* 113:1477-1489.
- Kermode, A.G., Tofts, P.S., Thompson, A.J., MacManus, D.G., Rudge, P., Kendall, B.E., Kingsley, D.P., Moseley, I.F., du Boulay, E.P., McDonald, W.I. 1990b. Heterogeneity of blood-brain barrier changes in multiple sclerosis: an MRI study with gadolinium-DTPA enhancement. *Neurology* 40:229-235.
- Kettenmann, H., Steinhauser, C. 2005. In *Neuroglia* (second edition) Ed. H. Kettenmann and B.R. Ransom. Oxford University Press. Chapter 10, Receptors for neurotransmitters and hormones. 131-145
- Kieseier, B.C., Seifert, T., Giovannoni, G., Hartung, H.P. 1999. Matrix metalloproteinases in inflammatory demyelination: targets for treatment (review). *Neurology* 53: 20-25.
- Kieseier, B., Pischel, H., Neuen-Jacob, E., Tortellotte, W.W., Hartung, H.P. 2003. ADAM-10 and ADAM-17 in the inflamed human CNS. *Glia* 42: 398-405.
- Killar, L., White, J., Black, R., Peschon, J. 1999. A family of Metzincins including TNF- $\alpha$  converting enzyme (TACE). *Ann N.Y. Acad Sci* 878: 442-452.
- Kirkegaard, T., Pedersen, G., Saermark, T., Bynskov, J. 2004. Tumour necrosis factor-alpha converting enzyme (TACE) activity in human colonic epithelial cells. *Clin Exp Immunol* 135: 146-153.
- Kivisakk, P., Mahad, D.J., Callahan, M.K., Sikora, K., Trebst, C., Tucky, B., Wujek, J., Ravid, R., Staugaitis, S.M., Lassmann, H., Ransohoff, R.M. 2004. Expression of CCR7 in multiple sclerosis: implications for CNS immunity. *Ann Neurol* 55: 627-638.
- Klein, R.S. 2004. Regulation of neuroinflammation: The role of CXCL10 in lymphocyte infiltration during autoimmune encephalomyelitis. *J Cell Biochem* 92: 213-222.
- Kleine, T.O., Zwerenz, P., Graser, C., Zofel, P. 2003. Approach to discriminate subgroups in multiple sclerosis with cerebrospinal fluid (CSF) basic inflammation indices and TNF- $\alpha$ , IL-1 $\beta$ , IL-6 and IL-8. *Brain Res Bull* 61: 327-346.

Kleinschmidt-DeMasters, BK., Tyler, KL. 2005. Progressive multifocal leukoencephalopathy complicating treatment with Natalizumab and interferon beta-1a for multiple sclerosis. *N Eng J Med* 353: 369-374

Kohm, AP., Miller, SD. 2003. Role of ICAM-1 and P-selectin expression in the development and effector function of CD4<sup>+</sup>CD25<sup>+</sup> regulatory T cells. *J Autoimmun* 21: 261-271.

Kojro, E., Fahrenholz, F. 2005. The non-amyloidogenic pathway: structure and function of alpha-secretases. *Subcell Biochem* 38: 105-127.

Kornek, B., Storch, MK., Weissert, R., Wallstroem, E., Stefferi, A., Olsson, T., Linington, C., Schmidbauer, M., Lassmann, H. 2000. Multiple sclerosis and chronic autoimmune encephalomyelitis. A comparative and quantitative study of axonal injury in active, inactive, and remyelinating lesions. *Am J Pathol* 157: 267-276.

Kornek, B., Lassmann, H. 2003. Neuropathology of multiple sclerosis-new concepts. *Brain Res Bull* 61: 321-326.

Korteweg, T., Barkhof, F., Uitdehaag, BJM., Polman, CH. 2005. How to use spinal cord magnetic resonance imaging in the McDonald diagnostic criteria for multiple sclerosis. *Ann Neurology* 57: 606-607.

Kossakowska AE, Edwards DR, Lee SS, Urbanski LS, Stabler AL, Zhang C-L, Phillips, BW., Zhang, Y., Urbanski, SJ. 1998. Altered balance between matrix metalloproteinases and their inhibitors in experimental biliary fibrosis. *Am J Pathol* 153:1895-1902.

Kouwenhoven, M., Ozenci, V., Gomes, A., Yarilin, D., Giedraitis, V., Press, R., Link, H. 2001. Multiple sclerosis: elevated expression of matrix metalloproteinases in blood monocytes. *J Autoimmun* 16: 463-470.

Kraus, J., Ling, A.K., Hamm, S., Voigt, K., Oschmann, P., Engelhardt, B. 2004. Interferon- $\beta$  stabilizes barrier characteristics of brain endothelial cells in vitro. *Ann Neurol* 56:192-205.

Kuhlmann, T., Lucchinetti, C., Zettl, UK., Bitsch, A., Lassmann, H., Bruck, W. 1999. Bcl-2-expressing oligodendrocytes in multiple sclerosis lesions. *Glia* 28: 34-39.

Kuhlmann, T., Lingfeld, G., Bitsch, A., Schuchardt, J., Bruck, W. 2002. Acute axonal damage in multiple sclerosis is most extensive in early disease stages and decreases over time. *Brain* 125: 2202-2212.

Kurtzke, JF. 1983. Rating neurologic impairment in multiple sclerosis an expanded disability status scale (EDSS). *Neurol* 33: 1444-1452.

Kuruganti, P.A., Hinojoza, J.R., Eaton, M.J., Ehmann, U.K., Sobel, R.A. 2002. Interferon-beta counteracts inflammatory mediator-induced effects on

brain endothelial cell tight junction molecules-implications for multiple sclerosis. *J Neuropathol Exp Neurol* 61:710-724.

Kwon, E.E., Prineas, J.W. 1994. Blood-brain barrier abnormalities in longstanding multiple sclerosis lesions. An immunohistochemical study. *J Neuropathol Exp Neurol* 53:625-636.

Lai M., Hodgson T., Gawne-Cain M., Webb S., MacManus D., McDonald WI., Thompson AJ., Miller DH. 1996. A preliminary study into the sensitivity of disease activity detection by serial weekly magnetic resonance imaging in multiple sclerosis. *J Neurol Neurosurg Psychiatry* 60: 339-341.

Laman, JD., van Meurs, M., Schellekens, MM., de Boer, M., Melchers, B., Massacesi, L., Lassmann, H., Claassen, E., 't Hart, BA. 1998. Expression of accessory molecules and cytokines in acute EAE in marmoset monkeys (*Callithrix jacchus*). *J Neuroimmunol* 86: 30-45.

Langton, KP., Barker, MD., McKie, N. 1998. Localization of the functional domains of human tissue inhibitor of metalloproteinases-3 and the effects of a Sorsby's fundus dystrophy mutation. *J Biol Chem* 273:16778-16781.

Laschinger, M., Engelhardt, B. 2000. Interaction of  $\alpha$ 4-integrin with VCAM-1 is involved in adhesion of encephalitogenic T cell blasts to brain endothelium but not in their transendothelial migration in vitro. *J Neuroimmunol* 102: 32-43.

Laschinger, M., Vajkoczy, P., Engelhardt, B. 2002. Encephalitogenic T cells use LFA-1 for transendothelial migration but not during capture and initial adhesion strengthening in healthy spinal cord microvessels in vivo. *Eur J Immunol* 32: 3598-3606.

Lassmann, H., Bruck, W., Lucchinetti, C., Rodriguez, M. 1997. Remyelination in multiple sclerosis. *Mult Scler* 3: 133-136.

Lassmann, H. 1998. Neuropathology in multiple sclerosis: new concepts. *Mult Scler* 4: 93-98.

Lebar, R., Lubetzki, C., Vincent, C., Lombrail, P., Boutry, JM. 1986. The M2 autoantigen of central nervous system myelin, a glycoprotein present in oligodendrocyte membrane. *Clin Exp Immunol* 66: 423-434.

Lee, MA., Palace, J., Stabler, G., Ford, J., Gearing, A., Miller, K. 1999. Serum gelatinase B, TIMP-1 and TIMP-2 levels in multiple sclerosis; A longitudinal clinical and MRI study. *Brain* 122: 191-197.

Lee, MH., Verma, V., Maskos, K., Becherer, JD., Knauper, V., Dodds, P., Amour, A., Murphy, G. 2002. The C-terminal domains of TACE weaken the inhibitory action of N-TIMP-3. *FEBS Lett* 520: 102-106.

Lee, MH., Verma, V., Maskos, K., Nath, D., Knauper, V., Dodds, P., Murphy, G. 2002. Engineering N-terminal domain of tissue inhibitor of metalloproteinase (TIMP)-3 to be a better inhibitor against tumour necrosis factor- $\alpha$ -converting enzyme. *Biochem J* 364: 227-234

Leib, SL., Clements, JM., Lindberg, RLP., Heimgartner, C., Loeffler, JM., Pfister, L-A., Tauber, MG., Leppert, D. 2001. Inhibition of matrix metalloproteinases and tumor necrosis factor  $\alpha$  as adjuvant therapy in pneumococcal meningitis. *Brain* 124: 1734-1742.

Lenercept Multiple Sclerosis Study Group and The University of British Columbia MS/MRI Analysis Group. 1999. TNF neutralization in MS: results of a randomized, placebo-controlled multicentre study. *Neurology* 53:457-465.

Leonard, JD., Lin, F., Milla, ME. 2005. Chaperone-like properties of the prodomain of TACE and the functional role of its cysteine switch. *Biochem J* 387: 797-805

Leppert, D., Waubant, E., Galardy, R., Bunett, NW., Hauser, SL. 1995. T cell gelatinases mediate basement membrane transmigration in vitro. *J Immunol* 154: 4379-4389.

Leppert, D., Ford, J., Stabler, G., Grygar, C., Lienert, C., Huber, S., Miller, KM., Hauser, SL., Kappos, L. 1998. Matrix metalloproteinase-9 (gelatinase B) is selectively elevated in CSF during relapses and stable phases of multiple sclerosis. *Brain* 121: 2327-2334.

Leppert, D., Lindberg, RLP., Kappos, L., Leib, SL. 2001. Matrix metalloproteinases: multifunctional effectors of inflammation in multiple sclerosis and bacterial meningitis. *Brain Res Rev* 36: 249-257.

Levine, JM., Reynolds, R., Fawcett. 2001. The oligodendrocyte precursor cell in health and disease. *Trends Neurosci* 24: 39-47.

Lichtinghagen, R., Seifert, T., Kracke, A., Marckmann, S., Wurster, U., Heidenreich, F. 1999. Expression of matrix metalloproteinase-9 and its inhibitors in mononuclear cells of patients with multiple sclerosis. *J Neuroimmunol* 99: 19-26.

Liebner, S., Fischmann, A., Rascher, G., Duffner, F., Grote, E.H., Kalbacher, H., Wolburg, H. 2000. Claudin-1 and claudin-5 expression and tight-junction morphology are altered in blood vessels of human glioblastoma multiforme. *Acta Neuropathol* 100:323-331.

Lindberg, RLP., De Groot, CJA., Montagne, L., Freitag, P., Van Der Valk, P., Kappos, L., Leppert, D. 2001. The expression profile of matrix metalloproteinases (MMPs) and their inhibitors (TIMPs) in lesions and normal appearing white matter of multiple sclerosis. *Brain* 124: 1743-1753.

- Lindert, RB., Haase, CG., Brehm, U., Linington, C., Werkle, H., Hohlfels. 1999. Multiple sclerosis: B- and T-cell responses to the extracellular domain of the myelin oligodendrocyte glycoprotein. *Brain* 122: 2089-2099.
- Lindsey JW. 2005. Familial recurrence rates and genetic models of multiple sclerosis. *Am J Med Genet* 135: 53-58.
- Linington, C., Webb, M., Woodhams, PL. 1984. A novel myelin-associated glycoprotein defined by a mouse monoclonal antibody. *J Neuroimmunol* 6: 387-396.
- Linington, C., Lassmann, H. 1987. Antibody responses in chronic relapsing experimental allergic encephalomyelitis: correlation of serum demyelinating activity with antibody titre to the myelin/oligodendrocyte glycoprotein (MOG). *J Neuroimmunol* 17: 61-69.
- Lipton, HL., Dal Canto, MC. 1979. Susceptibility of inbred mice to chronic central nervous system infection by Theiler's murine encephalomyelitis virus. *Infect Immun* 26: 369-74.
- Liu, J., Marino, MW., Wong, G., Grail, D., Dunn, A., Bettadapura, J., Slavin, AJ., Old, L., Bernard, CC. 1998. TNF is a potent anti-inflammatory cytokine in autoimmune-mediated demyelination. *Nat Med* 4: 78-83
- Lohmann, C., Krische, M., Wegener, J., Galla, HJ. 2004. Tyrosine phosphatase inhibition induces loss of blood-brain barrier integrity by matrix metalloproteinase-dependent and -independent pathways. *Brain* 127: 184-196.
- Luabeya, M.K., Dallasta, L.M., Achim, C.L., Pauza, C.D., Hamilton, R.L. 2000. Blood-brain barrier disruption in simian immunodeficiency virus encephalitis. *Neuropathol Appl Neurobiol* 26:454-462.
- Lublin, FD. 1985. Relapsing experimental allergic encephalomyelitis. An autoimmune model of multiple sclerosis. *Springer Semin Immunopathol* 8: 197-208.
- Lucchinetti, C., Bruck, W., Parisi, J., Scheithauer, B., Rodriguez, M., Lassmann, H. 1999. A quantitative analysis of oligodendrocytes in multiple sclerosis lesions. A study of 113 cases. *Brain* 122: 2279-2295.
- Lucchinetti, C., Bruck, W., Parisi, J., Scheithauer, B., Rodriguez, M., Lassmann, H. 2000. Heterogeneity of multiple sclerosis lesions: implications for pathogenesis of demyelination. *Ann Neurol* 47:707-717.
- Lum, L., Wong, BR., Josien, R., Becherer, JD., Erdjument-Bromage, H., Schlondorf, J., Tempst, P., Choi, Y., Blobel, CP. 1999. Evidence for a role of tumor necrosis factor- $\alpha$  (TNF- $\alpha$ ) – converting enzyme-like protease in shedding of TRANCE, a TNF family member involved in osteoclastogenesis and dendritic cell survival. *J Biol Chem* 274: 13613-13618.

- Lunemann, JD., Ruckert, S., Kern, F., Wendling, U., van der Zee, R., Volk, HD., Zipp, F. 2004. Cross-sectional and longitudinal analysis of myelin-reactive T cells in patients with multiple sclerosis. *J Neurol* 251: 1111-1120.
- Lunn, CA., Fan, X., Dalie, B., Miller, K., Zavodny, PJ., Narula, SK., Lundell, D. 1997. Purification of ADAM-10 from bovine spleen as a TNF $\alpha$  convertase. *FEBS Lett* 400: 333-335.
- Mack, CL., Vanderlugt-Casraneda, CL., Neville, KL., Miller, SD. 2003. Microglia are activated to become competent antigen presenting and effector cells in the inflammatory environment of the Theiler's virus model of multiple sclerosis. *J Neuroimmunol* 144: 68-79.
- Maeda, A., Sobel, RA. 1996. Matrix metalloproteinases in the normal human central nervous system, microglial nodules, and multiple sclerosis lesions. *J Neuropathol Exp Neurol* 55: 300-309.
- Mahad, DJ., Howell, SJ., Woodroffe, MN. 2002. Expression of chemokines in the CSF and correlation with clinical disease activity in patients with multiple sclerosis. *J Neurol Neurosurg Psychiatry* 72: 498-502.
- Mahad, DJ., Lawry, J., Howell, SJ., Woodroffe, MN. 2003. Longitudinal study of chemokine receptor expression on peripheral lymphocytes in multiple sclerosis: CXCR3 upregulation is associated with relapse. *Mult Scler* 9: 189-98.
- Mahad, DJ., Trebst, C., Kivisakk, P., Staugaitis, SM., Tucky, B., Wei, T., Lucchinetti, CF., Lassmann, H., Ransohoff, RM. 2004. Expression of chemokine receptors CCR1 and CCR5 reflects differential activation of mononuclear phagocytes in pattern II and pattern III multiple sclerosis lesions. *J Neuropathol Exp Neurol* 63: 262-273.
- Maimone, D., Gregory, S., Arnason, BG., Reder, AT. 1991. Cytokine levels in the cerebrospinal fluid and serum of patients with multiple sclerosis. *J Neuroimmunol* 32: 67-74.
- Mandal, M., Mandal, A., Das, S., Chakraborti, T., Sajal, C. 2003. Clinical implications of matrix metalloproteinases. *Mol Cell Biochem* 252: 305-329.
- Markhlouf, K., Comabella, M., Imitola, J., Weiner, HL., Khoury, SJ. 2001. Oral salbutamol decreases IL-12 in patients with secondary progressive multiple sclerosis. *J Neuroimmunol* 117: 156-165.
- Marrosu, MG., Cocco, E., Lai, M., Spinicci, G., Pischedda, MP., Contu, P I. 2002. Patients with multiple sclerosis and risk of type 1 diabetes mellitus in Sardinia, Italy: a cohort study. *Lancet* 359: 1461-1465.

Martin, D., Near, S.L., 1995. Protective effect of interleukin-1 receptor antagonist (IL-1ra) on experimental allergic encephalomyelitis in rats. *J Neuroimmunol* 61: 241-245.

Martino, G., Consiglio, A., Franciotta, D.M., Corti, A., Filippi, M., Vandenbroeck, K., Sciacca, F.L., Comi, G., Grimaldi, L.M.E. 1997. Tumor necrosis factor  $\alpha$  and its receptors in relapsing-remitting multiple sclerosis. *J Neurol Sci* 152: 51-61.

Martin-Padura, I., Iostaglio, S., Schneemann, M., Williams, L., Romano, M., Fruscella, P., Panzeri, C., Stoppacciaro, A., Ruco, L., Villa, A., Simmons, D., Dejana, E. 1998. Junctional adhesion molecule, a novel member of the immunoglobulin superfamily that distributes at intercellular junction and modulates monocyte transmigration. *J Cell Biology* 142:117-127.

Maskos, K., Fernandez-Catalan, C., Huber, R., Bourenkov, G.P., Bartunik, H., Ellestad, G.A., Reddy, P., Wolfson, M.F., Rauch, C.T., Castner, B.J., Davis, R., Clarke, H.R.G., Peterson, M., Fitzner, J.N., Cerretti, D.P., March, C.J., Paxton, R.J., Black, R.A., Bode, W. 1998. Crystal structure of the catalytic domain of human tumor necrosis factor- $\alpha$ -converting enzyme. *Proc Natl Acad Sci USA* 95: 3408-3412.

Mastronardi, F.G., Moscarello, M.A. 2005. Molecules affecting myelin stability: A novel hypothesis regarding pathogenesis of multiple sclerosis. *J Neurosci Res.* 80: 301-8.

Mayhan, W.G. 2002. Cellular mechanisms by which tumor necrosis factor- $\alpha$  produces disruption of the blood-brain barrier. *Brain Research* 927:144-152.

McDonald, W., Compston, A., Edan, G., Hartung, H-P., Lublin, F., McFarland, H.F., Paty, D.W., Polman, C.H., Reingold, S.C., Sandberg-Wollheim, M., Sibley, W., Thompson, A., van der Noort, S., Weinshenker, B.Y., Wolinsky, J.S. 2001. Recommended diagnostic criteria for multiple sclerosis: guidelines from the international panel on the diagnosis of multiple sclerosis. *Ann Neurol* 50: 121-127.

McFarland, H.F. 1993. Twin studies and multiple sclerosis. *Ann Neurol* 32: 722-723.

McManus, C., Berman, J.W., Brett, F.M., Staunton, H., Farrell, M., Brosnan, C.F. 1998. MCP-1, MCP-2 and MCP-3 expression in multiple sclerosis lesions: an immunohistochemical and in situ hybridization study. *J Neuroimmunol* 86: 20-29.

McQuaid, S., McConnell, R., McMahon, J., Herron, B. Microwave antigen retrieval for immunocytochemistry on formalin-fixed, paraffin-embedded post-mortem CNS tissue. *J Pathol* 176:207-216.

McQuaid, S., Kirk, J. 2005. The blood-brain barrier in multiple sclerosis. In Press

Meli, DN., Loeffler, JM., Baumann, P., Neumann, U., Buhl, T., Leppert, D., Leib, SL. 2004. In pneumococcal meningitis a novel water-soluble inhibitor of matrix metalloproteinases and TNF- $\alpha$  converting enzyme attenuates seizures and injury of the cerebral cortex. *J Neuroimmunol* 151: 6-11.

Menkin, V. 1948. *Newer concepts of inflammation*. Thomas Springfield.

Merrill, JE., Strom, SR., Ellison, GW., Meyers, LW. 1989. In vitro study of mediators of inflammation in multiple sclerosis. *J Clin Immunol* 9: 84-

Merrill, JE. 1991. Effects of interleukin-1 and tumor necrosis factor-alpha on astrocytes, microglia, oligodendrocytes, and glial precursors in vitro. *Dev Neurosci* 14: 1-10.

Merrill, JE., Scolding, NJ. 1999. Mechanisms of damage to myelin and oligodendrocytes and their relevance to disease. *Neuropath Appl Neurobiol* 25: 435-458.

Milla, ME., Leesnitzer, MA., Moss, ML., Clay, WC., Carter, HL., Miller, AB., Su, JL., Lambert, MH., Willard, DH., Sheeley, DM., et al. 1999. Specific sequence elements are required for the expression of functional tumor necrosis factor- $\alpha$ -converting enzyme (TACE). *J Biol Chem* 149: 30563-30570.

Miller, DH., Grossman, RI., Reingold, SC., McFarland, HF. 1998. The role of magnetic resonance imaging in understanding and managing multiple sclerosis. *Brain* 121: 3-24.

Miller, DH., Khan, OA., Sheremata, WA., Blumhardt, LD., Rice, GP., Libonati, MA., Willmer-Hulme, AJ., Dalton, CM., Miszkiel, KA., O'Connor, PW; International Natalizumab Multiple Sclerosis Trial Group. 2003. A controlled trial of natalizumab for relapsing multiple sclerosis. *N Eng J Med* 348: 15-23.

Minagar, A., Shapshak, P., Fujimura, R., Ownby, R., Heyes, M., Eisdorfer, C. 2002. The role of macrophage/microglia and astrocytes in the pathogenesis of three neurologic disorders: HIV-associated dementia, Alzheimer disease, and multiple sclerosis. *J Neurological Sci* 202: 13-23.

Minagar, A., Long, A., Ma, T., Jackson, TH., Kelley, RE., Ostanin, DV., Sasaki, M., Warren, AC., Jawahar, A., Cappell, B., Alexander, JS. 2003. Interferon (IFN)- $\beta$ 1a and IFN- $\beta$ 1b block IFN- $\gamma$ -induced disintegration of endothelial junction integrity and barrier. *Endothelium* 10: 299-307.

Mohammed, FF., Smookler, DS., Taylor, SE., Fingleton, B., Kassiri, Z., Sanchez, OH., English, JL., Matrisian, LM., Au, B., Yeh, WC., Khokha, R. Abnormal TNF activity in TIMP3-/- mice leads to chronic hepatic inflammation and failure of liver regeneration. 2004. *Nat genet* 36: 969-977.

- Moore, GRW. 2003. MRI-clinical correlations: more than inflammation alone - what can MRI contribute to improve the understanding of pathological processes in MS? *J Neurological Sci* 206: 175-179.
- Morita, K., Furuse, M., Fujimoto, K., Tsukita, S. 1999a. Claudin multigene family encoding four-transmembrane domain protein components of tight junction strands. *Proc Natl Acad Sci USA* 96:511-516.
- Morita, K., Sasaki, H., Furuse, M., Tsukita, S. 1999b. Endothelial claudin: claudin-5/TMVCF constitutes tight junction strands in endothelial cells. *J cell Biology* 147:185-194.
- Moss, M.L., Jin, S.L., Milla, M.E., Bickett, D.M., Burkhart, W., Carter, H.L., Chen, W.J., Clay, W.C., Didsbury, J.R., Hassler, D., Hoffman, C.R., Kost, T.A., Lambert, M.H., Leesnitzer, M.A., McCauley, P., McGeehan, G., Mitchell, J., Moyer, M., Pahel, G., Rocque, W., Overton, L.K., Schoenen, F., Seaton, T., Su, J.L., Becherer, J.D. 1997. Cloning of a disintegrin metalloproteinase that processes precursor tumour-necrosis factor-alpha. *Nature* 385(6618):733-736
- Moss, ML., White, JM., Lambert, MH., Andrews, RC. 2001. TACE and other ADAM proteases as targets for drug discovery. *DDT* 6: 417-426.
- Muir, EM., Adcock, KH., Morgenstern, DA., Clayton, R., von Stillfried, N., Rhodes, K., Ellis, C., Fawcett, JW., Rogers, JH. 2002. Matrix metalloproteases and their inhibitors are produced by overlapping populations of activated astrocytes. *Brain Res Mol Brain Res* 100: 103-117.
- Murphy, PM., Baggiolini, M., Charo, IF., Herbert, CA., CA., Horuk, R., Matsushima, K., Miller, LH., Oppenheim, JJ., Power, CA. 2000. International union of pharmacology. XXII. Nomenclature for chemokine receptors. *Pharmacol Rev* 52: 145-176.
- Murray, JM. 1992. Neuropathology in depth: the role of confocal microscopy. *J Neuropathol Exp Neurol* 52: 475-487.
- Myers, KJ., Witchell, DR., Graham, MJ., Koo, S., Butler, M., Condon, TP. 2005. Antisense oligonucleotide blockade of alpha 4 integrin prevents and reverses clinical symptoms in murine experimental autoimmune encephalomyelitis. *J Neuroimmunol* 160: 12-24.
- Neumann, H., Misgeld, T., Matsumuro, K., Werkle, H. 1998. Neurotrophins inhibit major histocompatibility class II inducibility of microglia: Involvement of the p75 neurotrophin receptor. *Proc Natl Acad Sci USA* 95: 5779-5784.
- Nguyen, KB., Pender, MP. 1998. Phagocytosis of apoptotic lymphocytes by oligodendrocytes in experimental autoimmune encephalomyelitis. *Acta Neuropathol* 95: 40-46.

Nico, B., Frigeri, A., Nicchia, GP., Corsi, P., Ribatti, D., Quondamatteo, F., Herken, R., Girolamo, F., Marzullo, A., Svelto, M., Roncali, L. 2003. Severe alterations of the endothelial and glial cells in the blood-brain barrier of dystrophic mdx mice. *Glia* 42: 235-251.

Nitta, T., Hata, M., Gotoh, S., Seo, Y., Sasaki, H., Hasimoto, N., Fyruze, M., Tsukita, S. 2003. Size-selective loosening of the blood-brain barrier in claudin-5-deficient mice.

Nishiyori, A., Minami, M., Ohtani, Y., Takami, S., Yamamoto, J., Kawaguchi, N., Kume, T., Akaike, A., Satoh, M. 1998. Localization of fractalkine and CX<sub>3</sub>CR1 mRNAs in rat brain: does fractalkine play a role in signalling from neuron to microglia? *FEBS Lett* 429: 167-172.

Norton, W. 1996. Do oligodendrocytes divide? *Neurochem Res* 21: 495-503.

Numan, J., Small, DH. 2000. Regulation of APP cleavage by  $\alpha$ -,  $\beta$ - and  $\gamma$ -secretases. *FEBS Lett* 483: 6-10.

Ohta, S., Harigai, M., Tanaka, M., et al. 2001. Tumor necrosis factor- $\alpha$  (TNF- $\alpha$ ) converting enzyme contributes to production of TNF- $\alpha$  in synovial tissues from patients with rheumatoid arthritis. *J Rheumatol* 28: 1756-1763.

O'Connor, P.W., Goodman, A., Willmer-Hulme, A.J., Libonati, M.A., Metz, L., Murray, R.S., Sheremata, W.A., Vollmer, T.L., Stone, L.A., Natalizumab multiple sclerosis study group. 2004. Randomized multicenter trial of natalizumab in acute MS relapses: clinical and MRI effects. *Neurology* 62:2038-2043.

Ohgoh, M., Hanada, T., Smith, T., Hashimoto, T., Ueno, M., Yamanishi, Y., Watanabe, M., Nishizawa, Y. 2002. Altered expression of glutamate transporters in experimental autoimmune encephalomyelitis. *J Neuroimmunol* 125: 170-178.

Okada, K., Kuroda, E., Yoshida, Y., Yamashita, U., Suzumura, A., Tsuji, S. 2005. Effects of interferon- $\beta$  on the cytokine production of astrocytes. *J Neuroimmunol* 159: 48-54.

Olerup, O., Hillert, J. 1991. HLA class II-associated genetic susceptibility in multiple sclerosis: a critical evaluation. *Tissue Antigens* 38: 1-15.

Ota, K., Matsui, M., Milford, EL., Mackin, GA., Weuner, HL., Hafler, DA. 1990. T-cell recognition of an immunodominant myelin basic protein epitope in multiple sclerosis. *Nature* 346: 183-187.

Ozawa, K., Suchanek, Breitschopf, H., Bruck, W., Budka, H., Jellinger, K., Lassmann, H. 1994. Patterns of oligodendroglia pathology in multiple sclerosis. *Brain* 117: 1311-1322.

- Ozenci V, Rinaldi L, Teleshova N, Matusevicius D, Kivisakk P, Kouwenhoven M, et al. 1999. Metalloproteinases and their tissue inhibitors in multiple sclerosis. *J Autoimmun*; 12: 297-303.
- Pagenstecher, A., Stalder, AK., Kincaid, CL., Shapiro, SD., Campbell, IL. 1998. Differential expression of matrix metalloproteinase and tissue inhibitor of matrix metalloproteinase genes in the mouse central nervous system in normal and inflammatory states. *Am J Pathol* 152: 729-741.
- Palucka KA, Taquet N, Sanchez-Chapuis F, Gluckman J-C. 1998. Dendritic cells as the terminal stage of monocyte differentiation. *J Immunol* 160: 4587-4595.
- Pan, Y., Lloyd, C., Zhou, H., Dolich, S., Deeds, J., Gonzalo, JA., Vath, J., Gosselin, M., Ma, J., Dussalt, B., Woolf, E., Alperin, G., Culpepper, J., Gutierrez-Ramos, JC., Gearing, D. 1997. Neuroactin, a membrane-anchored chemokine upregulated in brain inflammation. *Nature* 387: 611-617.
- Pan, D., Rubin, GM. 1997. Kuzbanian controls proteolytic processing of notch and mediates lateral inhibition during *Drosophila* and vertebrate neurogenesis. *Cell* 90: 271-280.
- Panitch, HS., Hirsch, RL., Haley, AS., Johnson, KP. 1987. Exacerbations of multiple sclerosis in patients treated with gamma interferon. *Lancet* 1: 893-895.
- Park, KW., Lee, DY., Joe, EH., Kim, SU., Jin, BK. 2005. Neuroprotective role of microglia expressing interleukin-4. *J Neurosci Res* 81: 397-402.
- Patel, IR., Attur, MG., Patel, RN., Stuchin, SA., Abagyan, RA., Abramson, SB., Amin, AR. 1998. TNF- $\alpha$  convertase enzyme from human arthritis-affected cartilage: Isolation of cDNA by differential display, expression of the active enzyme, and regulation of TNF- $\alpha$ . *J Immunol* 160: 4570-4579.
- Paul, R., Lorenzi, S., Koedel, U., Sporer, B., Vogel, U., Frosch, M., Pfister, HW. 1998. Matrix metalloproteinases contribute to the blood-brain barrier disruption during bacterial meningitis. *Ann Neurol* 44: 592-600.
- Peiretti, F., Canault, M., Deprez-Beauclair, P., Berthet, V., Bonardo, B., Juhan-Vague, I., Nalbone, G. 2003. Intracellular maturation and transport of tumor necrosis factor alpha converting enzyme. *Exp Cell Res* 285: 278-285.
- Pellerin, L., Magistretti, PJ. 2005. In *Neuroglia* (second edition) Ed. H. Kettenmann and B.R. Ransom. Oxford University Press. Chapter 29 The central role of astrocytes in neuroenergetics 367-376.
- Pender, MP. 1988. The pathophysiology of myelin basic protein-induced acute experimental allergic encephalomyelitis in the Lewis rat. *J Neurol Sci* 86: 277-289.

- Pender, MP., Rist, MJ. 2001. Apoptosis of inflammatory cells in immune control of the nervous system: Role of glia. *Glia* 36: 137-144.
- Perry, V.H., Anthony, D.C., Bolton, S.J., Brown, H.C. 1997. The blood-brain barrier and the inflammatory response. *Molecular Medicine Today* 3:335-341.
- Peschon, JJ., Slack, JL., Reddy, P., Stocking, KL., Sunnarborg, SW., Lee, DC., Russell, WE., Castner, BJ., Johnson, RS., Fitzner, JN., Boyce, RW., Nelson, N., Kozlosky, CJ., Wolfson, MW., Rauch, CT., Cerretti, DP., Paxton, RJ., March, CJ., Black, RA . 1998. An essential role for ectodomain shedding in mammalian development. *Science* 282: 1281-1284.
- Petty, A.M., Lo, E.H. 2002. Junctional complexes of the blood brain barrier: permeability changes in neuroinflammation. *Prog Neurobiol* 68:311-323.
- Philips, LM., Lampson, LA. 2000. Local neurochemicals and site-specific immune regulation in the CNS. *J Neuropathol Exp Neurol* 59: 177-187.
- Pitzalis, C., Pipitone, N., Perretti, M. 2002. Regulation of leukocyte-endothelial interactions by glucocorticoids. *Ann N Y Acad Sci* 966: 108-118.
- Plant, SR., Arnett, HA., Ting, JPY. 2004. Astroglial-derived lymphotoxin- $\alpha$  exacerbates inflammation and demyelination, but not remyelination. *Glia* 49: 1-14.
- Plumb, J., Armstrong, MA., Mirakhur, M., McQuaid, S. 2003. CD83-positive dendritic cells are present in occasional perivascular cuffs in multiple sclerosis lesions. *Multiple Sclerosis* 9: 142-147.
- Ponchel, F., Toomes, C., Bransfield, K., Leong, FT., Douglas, SH., Field, SL., Bell, SM., Combaret, V., Puisieux, A., Mighell, AJ., Robinson, PA., Inglehearn, CF., Isaacs, JD., Markham, AF. 2003. Real-time PCR based on SYBR-Green I fluorescence: an alternative to the TaqMan assay for a relative quantification of gene rearrangements, gene amplifications and micro gene deletions. *BMC Biotechnol* 3:18.
- Ponomarev, ED., Novikova, M., Maresz, K., Shriver, LP., Dittel, BN. 2005. Development of a culture system that supports adult microglia cell proliferation and maintenance in the resting state. *Immunol Methods* 300: 32-46.
- Poser CM. 2004. Multiple sclerosis trait: the premorbid stage of multiple sclerosis. A hypothesis. *Acta Neurol Scand.* 109: 239-243.
- Poser, C., Paty, D., Scheinberg, L., McDonald, W., Davis, F., Ebers, G., Johnson, KP., Sibley, WA., Silberberg, DH., Tourtellotte, WW. 1983. New diagnostic criteria for multiple sclerosis: guidelines for research protocols. *Ann Neurol* 13: 227-231.

- Poser, CM., Brinar, VV. 2004. Diagnostic criteria for multiple sclerosis: an historical review. *Clin Neurol Neurosurg* 106: 147-158.
- Prat, A., Biernacki, K., Wosik, K., Antel, J.P. 2001. Glial cell influence on the human blood-brain barrier. *Glia* 36:145-155.
- Priller, J., Flugel, A., Wehner, T., Boentert, M., Haas, CA., Prinz, M., Fernandez-Klett, F., Prass, K., Bechmann, I., de Boer, BA., Frotscher, M., Kreutzberg, GW., Persons, DA., Dirnagl, U. 2001. Targeting gene-modified hematopoietic cells to the central nervous system: use of green fluorescent protein uncovers microglial engraftment. *Nat Med* 7: 1356-1361.
- Prineas, JW., Wright, RG. 1978. Macrophages, lymphocytes and plasma cells in the perivascular compartment in chronic multiple sclerosis. *Lab Invest* 38: 409-421.
- Probert L, Akassoglou K. 2001. Glial expression of tumor necrosis factor in transgenic animals: How do these models reflect the "normal situation"? *Glia* 36: 212-19
- Qi, JH., Ebrahim, Q., Moore, N., Murphy, G., Claesson-Welsh, L., Bond, M., Baker, A., Anand-Apte, B. 2003. A novel function for tissue inhibitor of metalloproteinases-3 (TIMP3): inhibition of angiogenesis by blockage of VEGF binding to VEGF receptor-2. *Nat Med* 9: 407-415.
- Racke, MK., Bonomo, A., Scott, DE., Cannella, B., Levine, A., Raine, CS., Shevach, EM., Rocken,, M. 1994. Cytokine-induced immune deviation as a therapy for inflammatory autoimmune disease. *J Exp Med* 180: 1961-1966.
- Raine, CS. 1995. Multiple sclerosis: TNF revisited, with promise. *Nat Med* 1: 211-214.
- Raine, CS., Bonnetti, B., Cannella, B. 1998. Multiple sclerosis: expression of molecules of the tumor necrosis factor ligand and receptor families in relationship to the demyelinated plaque. *Rev Neurol* 154: 577-585.
- Raine, CS., Cannella, B., Hauser, SL., Genain, CP. 1999. Demyelination in primate encephalomyelitis and acute multiple sclerosis lesions: a case for antigen-specific antibody mediation. *Ann Neurol* 46: 144-160.
- Raivich, G., Banati, R. 2004. Brain microglia and blood-derived macrophages: molecular profiles and functional roles in multiple sclerosis and animal models of autoimmune demyelinating disease. *Brain Res Rev* 46: 261-281.
- Randolph GJ., Beaulieu, S., Lebecque, S., Steinman, RM., Muller, WA. 1998. Differentiation of monocytes into dendritic cells in a model of transendothelial trafficking. *Science* 282: 480-483.

Ransohoff RM, Hamilton TA, Tani M, Stoler MH, Shick HE, Major JA, Estes ML, Thomas DM, Tuohy VK. 1993. Astrocyte expression of mRNA encoding cytokines IP-10 and JE/MCP-1 in experimental autoimmune encephalomyelitis. *FASEB J* 7: 592-600.

Ransohoff RM. 1999. Mechanisms of inflammation in MS tissue: adhesion molecules and chemokines. *Neuroimmunol* 98: 57-68.

Rauh, J., Meyer, J., Beuckmann, C., Galla, H.J. 1992. Development of an in vitro cell culture system to mimic the blood-brain barrier. *Prog Brain Res* 91:117-121.

Rausch, M., Hiestand, P., Baumann, D., Cannet, C., Rudin, M. 2003. MRI-based monitoring of inflammation and tissue damage in acute and chronic relapsing EAE. *Magn Reson Med* 50: 309-314.

Richert, N.D., Ostuni, J.L., Bash, C.N., Leist, T.P., McFarland, H.F., Frank, J.A. 2001. Interferon beta-1b and intravenous methylprednisolone promote lesion recovery in multiple sclerosis. *Mult Scler* 7:49-58.

Rieckmann, P., Altenhofen, B., Riegel, A., Kallmnn, B., Felgenhauer, K. 1998. Correlation of soluble adhesion molecules in blood and cerebrospinal fluid with magnetic resonance imaging activity in patients with multiple sclerosis. *Mult Scler* 4: 178-182.

Risch, NJ. 2000. Searching for genetic determinants in the new millennium. *Nature* 405: 847-856.

Rivers, TM., Sprunt, DH., Berry, GP. 1933. Observations on the attempts to produce acute-disseminated encephalomyelitis in monkeys. *J Exp Med* 58: 39-53.

Rivers, TM., Schwenkter, FF. 1935. Encephalomyelitis accompanied by myelin destruction experimentally produced in monkeys. *J Exp Med* 61: 698-703.

Roberts, L., McColl, GJ. 2004. Tumor necrosis factor inhibitors: risks and benefits in patients with rheumatoid arthritis. *Int Med J* 34: 687-693.

Robertshaw, HL., Brennan, FM. 2005. Release of tumor necrosis factor  $\alpha$  (TNF $\alpha$ ) by TNF $\alpha$  cleaving enzyme (TACE) in response to septic stimuli in vitro. *Br J Anaesth* 94: 222-228.

Romanic, AM., White, RF., Arleth, AJ., Ohlstein, EH., Barone, FC. 1998. Matrix metalloproteinase expression increases after cerebral focal ischemia in rats. *Stroke* 29: 1020-1030.

Romera, C., Hurtado, O., Botella, SH., Lizasoain, I., Cardenas, A., Fernandez-Tome, P., Leza, JC., Lorenzo, P., Moro, MA. 2004. In vitro ischemic tolerance involves upregulation of glutamate transport partly

mediated by the TACE/ADAM17-Tumor necrosis factor- $\alpha$  pathway. *J Neurosci* 24: 1350-1357.

Romero IA, Radewicz K, Jubin E, Michel CC, Greenwood J, Couraud PO, Adamson P. 2003. Changes in cytoskeletal and tight junctional proteins correlate with decreased permeability induced by dexamethasone in cultured rat brain endothelial cells. *Neurosci Lett* 344: 112-116.

Rosenberg, GA., Dencoff, JE., Correa, N., Reiners, M., Ford, CC. 1996. Effects of steroids on CSF matrix metalloproteinases in multiple sclerosis: relation to blood-brain barrier injury. *Neurology* 46: 1626-1632.

Rosenberg GA, Estrada EY, Dencoff JE. 1998. Matrix metalloproteinases and TIMPs are associated with blood-brain barrier opening after reperfusion in rat brain. *Stroke* 29: 2189-2195.

Rosenberg, GA. 2002. Matrix metalloproteinases in neuroinflammation. *Glia* 39: 279-291.

Rott, O., Fleischer, B., Cash, E. 1994. Interleukin-10 prevents experimental allergic encephalomyelitis in rats. *Eur J Immunol* 24: 1434-1440.

Rottmann, JB., Ganley, KP., Williams, K., Wu., L., Mackay, CR., Ringler, DJ. 1997. Cellular localisation of the chemokine receptor CCR5. Correlation to cellular targets of HIV-1 infection. *Am J Pathol* 151: 1341-1351.

Rovida, E., Paccagnini, A., Del Rosso, M., Peschon, J., Dello Sbarba, P. 2001. TNF- $\alpha$  converting enzyme cleaves the macrophage colony-stimulating factor receptor in macrophages undergoing activation. *J Immunology* 166: 1583-1589.

Rubin, L.I., Hall, D.E., Porter, S., Barbu, K., Cannon, C., Horner, C., Janatpour, M., Liaw, C.W., Manning, K., Morales, J., Tanner, L.I., Tomaselli, K.J., Bard, F. 1991. A cell culture model of the blood-brain barrier. *J Cell Biol* 115:1725-1735.

Sadovnick, AD., Ebers, GC., Dyment, D., Risch, NJ., and Canadian collaborative study group. 1996. Evidence for the genetic basis of multiple sclerosis. *Nature* 347: 1728-1730.

Saitou, M., Furuse, M., Sasaki, H., Schulzke, J.-D., Fromm, M., Takano, H., Noda, T., Tsukita, S. 2000. Complex phenotype of mice lacking occludin, a component of tight junction strands. *Molecular Biology of the Cell* 11:4131-4142.

Sanders, V., Conrad, A.K., Tourtellotte, W.W. 1993. On classification of post-mortem multiple sclerosis plaques for neuroscientists. *J Neuroimmunol* 46:201-216.

Satoh, J., Onoue, H., Arima, K., Yamamura, T. 2005. Nogo-A and nogo receptor expression in demyelinating lesions of multiple sclerosis. *J Neuropathol Exp Neurol* 64: 129-138.

Sawcer, S., Compston, A. 2003. The genetic analysis of multiple sclerosis in Europeans (GAMES): concepts and design. *J Neuroimmunol* 143: 13-16.

Schenkel, AR., Mamdouth, Z., Muller, WA. 2004. Locomotion of monocytes on endothelium is a critical step during extravasation. *Nat Immunol* 5: 393-400.

Schiffenbauer, J., Streit, WJ., Butfiloski, E., LaBow, M., Edwards III, C., Moldawer, LL. 2000. The induction of EAE is only partially dependant on TNF receptor signalling but requires the IL-1 type 1 receptor. *Clin Immunol* 95: 117-123.

Schlörndorff, J., Becherer, JD., Blobel, CP. 2000. Intracellular maturation and localisation of the tumour necrosis factor  $\alpha$  convertase (TACE). *Biochem J* 347: 131-138.

Schlondorff J, Lum L, Blobel CP. 2001. Biochemical and pharmacological criteria define two shedding activities for TRANCE/OPGL that are distinct from the tumor necrosis factor alpha convertase. *J Biol Chem* 276:14665-14674

Schulze, C., Firth, J.A. 1993. Immunohistochemical localisation of adherens junction components in blood-brain-barrier microvessels of the rat. *J Cell Sci* 104:773-782.

Schwaebel, WJ., Stover, CM., Schall, TJ., Dairaghi, DJ., Trinder, PK., Linington, C, Iglesias, A., Schubart, A., Lynch, NJ., Weihe, E., Schafer, MK. 1998. Neuronal expression of fractalkine in the presence and absence of inflammation. *FEBS Letts* 439: 203-207.

Scolding, N., Franklin, R., Stevens, S., Helden, C., Compston, A., Newcombe, J. 1998. Oligodendrocyte progenitors are present in the normal adult CNS and in the lesions of MS. *Brain* 121: 2221-2228

Scott, GS., Kean, RB., Fabis, MJ., Mikeeva, T., Brimer, CM., Phares, TW., Spitsin, SV., Hooper, DC. 2004. ICAM-1 upregulation in the spinal cords of PLSJL mice with experimental allergic encephalomyelitis is dependent upon TNF- $\alpha$  production triggered by loss of blood-brain barrier integrity. *J Neuroimmunol* 155: 32-42.

Seals, DF., Courtneidge, SA. 2003. The ADAMs family of metalloproteases: multidomain proteins with multiple functions. *Genes and development* 17: 7-30.

Seifert, T., Kieseier, BC., Ropele, S., Strasser-Fuchs, S., Quehenberger, F., Fazekas, F., Hartung, HP. 2002. TACE mRNA expression in peripheral

mononuclear cells precedes new lesions on MRI in multiple sclerosis. *Mult Scler* 8: 447-451.

Selmaj, KW., Raine, CS. 1988. Tumor necrosis factor mediates myelin and oligodendrocyte damage in vitro. *Ann Neurol* 23: 339-346.

Selmaj, KW., Farooq, M., Norton, WT., Raine, CS., Brosnan, CF. 1990. Proliferation of astrocytes in vitro in response to cytokines. A primary role for tumor necrosis factor. *J Immunol* 144: 129-135.

Selmaj, K., Raine, CS., Cannella, B., Brosnan, CF. 1991a. Identification of lymphotoxin and tumor necrosis factor in multiple sclerosis lesions. *J Clin Invest* 87: 949-954.

Selmaj, K., Raine, CS., Farooq, M., Norton, WT., Brosnan, CF. 1991b. Cytokine cytotoxicity against oligodendrocytes. Apoptosis induced by lymphotoxin. *J Immunol* 147: 1522-1529.

Selmaj, K., Shafit-Zagardo, B., Aquino, DA., Farooq, M., Raine, CS., Norton, WT., Brosnan, CF. 1991c. Tumor necrosis factor-induced proliferation of astrocytes from mature brain is associated with down-regulation of glial fibrillary acidic protein mRNA. *J Neurochem* 57: 823-830.

Selmaj, K., Papierz, W., Glabinski, A., Kohno, T. 1995. Prevention of chronic relapsing experimental autoimmune encephalomyelitis by soluble tumor necrosis factor receptor I. *J Neuroimmunol* 56: 135-141.

Selmaj, KW., Raine, CS. 1995. Experimental autoimmune encephalomyelitis: immunotherapy with anti-tumor necrosis factor antibodies and soluble tumor necrosis factor receptors. *Neurology* 45: S44-49.

Selmaj, KW. 2000. Tumour necrosis factor and anti-tumour necrosis factor approach to inflammatory demyelinating diseases of the central nervous system. *Ann Rheum Dis* 59: i94-i102

Shapiro, S., Miller, A., Lahat, N., Sobel, E., Lerner, A. 2003. Expression of matrix metalloproteinases, sICAM-1 and IL-8 in CSF from children with meningitis. *J Neurological Sci* 206: 43-48.

Sharief, MK., Thompson, EJ. 1992. In vivo relationship of tumor necrosis factor-alpha to blood-brain barrier damage in patients with active multiple sclerosis. *J Neuroimmunol* 38: 27-33.

Shin, WH., Lee, DY., Park, KW., Kim, SU., Yang, MS., Joe, EH., Jin, BK. 2004. Microglia expressing interleukin-13 undergo cell death and contribute to neuronal survival in vivo. *Glia* 46: 142-152.

Shinde, S., Wu, Y., Guo, Y., Niu, Q., Xu, J., Grewal, IS., Flavell, R., Liu, Y. 1996. CD40L is important for induction of, but not response to, costimulatory

activity. ICAM-1 as the second costimulatory molecule rapidly up-regulated by CD40L. *J Immunol* 157: 2764-2768.

Sicotte NL, Voskuhl RR. 2001. Onset of multiple sclerosis associated anti-TNF therapy. *Neurology* 57:1885-88.

Simmons, DL. 2005. Anti-adhesion therapies. *Curr Opin Pharmacol* 5: 1-7.

Simpson, JE., Newcombe, J., Cuzner, ML., Woodroffe, MN. 1998. Expression of monocyte chemoattractant protein-1 and other beta-chemokines by resident glia and inflammatory cells in multiple sclerosis lesions. *J Neuroimmunol* 84: 238-249.

Simpson, JE., Rezaie, P., Newcombe, J., Cuzner, ML., Male, D., Woodroffe, MN. 2000a. Expression of the beta-chemokine receptors CCR2, CCR3 and CCR5 in multiple sclerosis central nervous system tissue. *J Neuroimmunol* 108: 192-200.

Simpson, JE., Newcombe, J., Cuzner, ML., Male, D., Woodroffe, MN. 2000b. Expression of interferon-gamma-inducible chemokines IP-10 and Mig and their receptor CXCR3, in multiple sclerosis lesions. *Neuropathol Appl Neurobiol* 26: 133-142.

Skovronsky, DM., Fath, S., Lee, VM-Y., Milla, M. 2001. Neuronal localization of the TNF $\alpha$  converting enzyme (TACE) in brain tissue and its correlation to amyloid plaques. *J Neurobiol* 49: 40-46.

Small, J., Rottner, K., Hahne, P., Anderson, KI. 1999. Visualising the actin cytoskeleton. *Microsc Res Tech* 47: 3-17.

Smith, T., Groom, A., Zhu, B., Turski, L. 2000. Autoimmune encephalomyelitis ameliorated by AMPA antagonists. *Nat Med* 6: 62-66.

Sobel, RA., Van Der Veen, RC., Lees, MB. 1986. The immunopathology of chronic experimental encephalomyelitis induced in rabbits with bovine proteolipid protein. *J Immunol* 136: 157-163.

Sobel, RA., Mitchell, ME., Fondren, G. 1990. Intercellular adhesion molecule-1 (ICAM-1) in cellular immune reactions in the human central nervous system. *Am J Pathol* 136: 1309-1316.

Soldan, SS., Berti, R., Salem, N., Secchierom, P., Flamand, L., Calabresi, PA., Brennan, MB., Maloni, HW., McFarland, HF., Lin, HC., Patnaik, M., Jacobson S. 1997. Association of human herpes virus 6 (HHV-6) with multiple sclerosis: increased IgM response to HHV-6 early antigen and detection of serum HHV-6 DNA. *Nat Med* 3: 1394-1397.

Song, L., Pachter, JS. 2004. Monocyte chemoattractant protein-1 alters expression of tight junction-associated proteins in brain microvascular endothelial cells. *Microvasc Res* 67: 78-89.

Sørensen, TL., Tani, M., Jensen, J., Pierce, V., Lucchinetti, C., Folcik, VA., Qin, S., Rottmann, J., Selleberg, F., Strieter, RM., Frederiksen, JL., Ransohoff, RM. 1999. Expression of specific chemokines and chemokine receptors in the central nervous system of multiple sclerosis patients.

Sotgiu S., Pugliatti M., Fois ML., Arru G., Sanna A., Sotgiu MA., Rosati G. 2004. Genes, environment, and susceptibility to multiple sclerosis. *Neurobiol Dis.* 17: 131-143.

Sriram, S., Mitchell, W., Stratton, C. 1998. Multiple sclerosis associated with *Chlamydia pneumoniae* infection of the CNS. *Neurology* 50: 571-572.

Srour, N., Lebel, A., McMahon, S., Fournier, I., Fugere, M., Day, R., Dubois CM. 2003. TACE/ADAM-17 maturation and activation of sheddase activity require proprotein convertase activity. *FEBS Lett* 554: 275-283.

Stangel, M., Hartung, HP. 2002. Remyelinating strategies for the treatment of multiple sclerosis. *Prog Neurobiol* 68: 361-376.

Stevenson, BR., Siliciano, JD., Mooseker, MS., Goodenough, DA. 1986. Identification of ZO-1: a high molecular weight polypeptide associated with the tight junction (zonula occludens) in a variety of epithelia. *J Cell Biol* 103: 755-766.

Stinissen, P., Medaer, R., Raus, J. 1998. Myelin reactive T cells in the autoimmune pathogenesis of multiple sclerosis. 4: 203-211.

Stoll G, Jander S. 1999. The role of microglia and macrophages in the pathophysiology of the CNS. *Prog Neurobiol* 58: 233-247.

Stone, L.A., Smith, M.E., Albert, P.S., Bash, C.N., Maloni, H., Frank, J.A., McFarland, H.F. 1995. Blood-brain barrier disruption on contrast-enhanced MRI in patients with mild relapsing-remitting multiple sclerosis: relationship to course, gender and age. *Neurology* 45:1122-1126.

Storch, MK., Piddlesden, S., Haltia, M., Livanainen, M., Morgan, P., Lassmann, H. 1998. Multiple sclerosis: in situ evidence for antibody- and complement-mediated demyelination. *Ann Neurol* 43: 465-471.

Streit, WK. 2005. In *Neuroglia* (second edition) Ed. H. Kettenmann and B.R. Ransom. Oxford University Press. Chapter 5 Microglial cells 60-71.

Swanborg, RH., Whittum-Hudson, JA., Hudson, AP. 2003. Infectious agents and multiple sclerosis--are *Chlamydia pneumoniae* and human herpes virus 6 involved? *J Neuroimmunol* 136: 1-8.

Swingler, RJ., Compston, D. 1986. The distribution of multiple sclerosis in the United Kingdom. *J Neurol* 234: 1115-1124.

Tanuma, N., Shin, T., Kogure, K., Matsumoto, Y. 1999. Differential effects of TNF- $\alpha$  and IFN- $\gamma$  in chronic relapsing autoimmune encephalomyelitis. *J Neuroimmunol* 96: 73-79.

Tao-Chen, J.H., Nagy, Z., Brightman, M.W. 1987. Tight junctions of the brain endothelium in vitro are enhanced by astroglia. *J Neuroscience* 76:3293-3299.

Terasaki, T., Ohtsuki, S., Hori, S., Takanaga, H., Nakashima, E., Hosoya, K-I. 2003. New approaches to in vitro models of blood-brain barrier drug transport. *Drugs Discovery Today* 8:944-954.

't Hart, BA., Amor, S. 2003. The use of animal models to investigate the pathogenesis of neuroinflammatory disorders of the central nervous system. *Curr Opin Neurol* 16: 375-383.

't Hart, BA., Amor, S., Jonker, M. 2004. Evaluating the validity of animal models for research into therapies for immune-based disorders. *DDT* 9: 517-524.

Theien, BE., Vanderlugt, CL., Eager, TN., Nickerson-Nutter, C., Nazzreno, R., Kuchroo, VK., Miller, SD. 2001. Discordant effects of anti-VLA-4 treatment before and after onset of relapsing experimental autoimmune encephalomyelitis. *J Clin Invest* 107: 995-1006.

Thompson, AJ., McDonald, WA. 1996. Multiple sclerosis. *Medicine* 69-75  
Tsou, C-L., Haskell, CA., Charo, IF. 2001. Tumor necrosis factor- $\alpha$ -converting enzyme mediates the inducible cleavage of fractalkine. *J Biol Chem* 48: 4462-44626.

Tobin, AM., Kirby, B. 2005. TNF $\alpha$  inhibitors in the treatment of psoriasis and psoriatic arthritis. *BioDrugs* 19: 47-57.

Trapp, BD., Peterson, J., Ransogoff, RM., Rudick, R., Mork, S., Bo, L. 1998. Axonal transection in the lesions of multiple sclerosis. *N Eng J Med* 338: 278-285.

Trapp, BD., Bö, L., Mörk, S., Chang, A. 1999. Pathogenesis of tissue injury in MS lesions. *J Neuroimmunol* 98: 49-56.

Trebst, C., Sørensen, TL., Livisakk, P., Cathcart, MK., Hesselgesser, J., Horuk, R., Sellebjerg, F., Lassmann, H., Ransohoff, RM. 2001. CCR1+/CCR5+ mononuclear phagocytes accumulate in the central nervous system of patients with multiple sclerosis. *Am J Pathol* 159: 1701-1710.

Trebst, C., Staugaitis, SM., Kivisakk, P., Mahad, D., Cathcart, MK., Tucky, B., Wei, T., Rani, MRS., Horuk, R., Aldape, KD., Pardo, CA., Lucchinetti, CF., Lassmann, H., Ransohoff, RM. 2003. CC chemokine receptor 8 in the central nervous system is associated with phagocytic macrophages. *Am J Pathol* 162: 427-438.

Tsou, CL., Haskell, CA., Charo, IF. 2001. Tumor necrosis factor- $\alpha$ -converting enzyme mediates the inducible cleavage of fractalkine. *J Biol Chem* 276: 44622-44626.

Tsukita, S., Furuse, M. 1999. Occludin and claudins in tight-junction strands: leading or supporting players? *Trends Cell Biol* 9:268-273.

Tuohy, VK., Yu, M., Weinstock-Guttman, B., Kinkel, RP. 1997. Diversity and plasticity of self recognition during the development of multiple sclerosis. *J Clin Invest* 99: 1682-1690.

Tzeng, SF., Kahn, M., Liva, S., De Vellis, J. 1999. Tumor necrosis factor- $\alpha$  regulation of the Id gene family in astrocytes and microglia during CNS inflammatory injury. *Glia* 26: 189-152.

Vaillant C, Didier-Bazes M, Hutter A, Belin M-F, Thomasset N. 1999. Spatiotemporal expression patterns of metalloproteinases and their inhibitors in the postnatal developing rat cerebellum. *J Neuroscience*; 19: 4994-5004.  
van der Valk, P., De Groot, C.J. 2000. Staging of multiple sclerosis (MS) lesions: pathology of the time frame of MS. *Neuropathol Appl Neurobiol* 26:2-10.

Van Assche, G., Van Ranst, M., Sciot, R., Dubois, B., Vermeire, S., Noman, M., Verbeek, J., Geboes, K., Robberecht, W., Rutgeerts, P. 2005. Progressive multifocal leukoencephalopathy after Natalizumab therapy for Crohn's disease. *N Eng J Med* 353: 362-368.

van Boxel-Dezaire AH., Hoff SC., van Oosten BW., Verweij CL., Drager AM., Ader HJ., van Houwelingen JC., Barkhof F., Polman CH., Nagelkerken L. 1999. Decreased interleukin-10 and increased interleukin-12p40 mRNA are associated with disease activity and characterize different disease stages in multiple sclerosis. *Ann Neurol* 45: 695-703.

VandenBerg, E., Reid, MD., Edwards, JD., Davis, HW. 2004. The role of the cytoskeleton in cellular adhesion molecule expression in tumor necrosis factor-stimulated endothelial cells. *J Cell Biochem* 9: 926-937.

Van der Goes, A., Kortekaas, M., Hoekstra, K., Dijkstra, CD., Amor, S. 1999. The role of anti-myelin (auto)-antibodies in the phagocytosis of myelin by macrophages. *J Neuroimmunol* 101: 61-67.

Van der Laan, LJW., van der Goes, A., Wauben, MHM., Ruuls, SR., Dopp, EA., De Groot, CJA., Kuijpers, TW., Elices, MJ., Dijkstra, CD. 2002. Beneficial effect of modified peptide inhibitor of  $\alpha$ 4 integrins on experimental allergic encephalomyelitis in Lewis rats. *J Neurosci Res* 67: 191-199.

Vanderlugt, CT., Begolka, WS., Neville, KL., Katz-Levy, Y., Howard, LM., Eagar, TN., Bluestone, JA., Miller, SD. 1998. The functional significance of

epitope spreading and its regulation by co-stimulatory molecules. *Immunol Rev* 164: 63-73.

Van der Meer, SH., Ulrich, AM., Gonzalez-Scarano, F., Lavi, E. 2000. Immunohistochemical analysis of CCR2, CCR3, CCR5 and CXCR4 in the human brain: potential mechanisms for HIV dementia. *Exp Mol Pathol* 69: 192-201.

van der Valk, P., De Groot, C.J. 2000. Staging of multiple sclerosis (MS) lesions: pathology of the time frame of MS. *Neuropathol Appl Neurobiol* 26:2-10.

Van der Voorn, P., Tekstra, J., Beelen, RH., Tensen, CP., Van de Valk, P., De Groot, CJ. 1999. Expression of MCP-1 by reactive astrocytes in demyelinating multiple sclerosis lesions. *Am J Pathol* 154: 45-51.

Van Itallie, C.M., Fanning, A.S., Anderson, J. M. 2003. Reversal of charge selectivity in cation or anion-selective epithelial lines by expression of different claudins. *Am. J. Physiol Renal Physiol* 285:1078-1084.

Van Noort, JM. 1996. Multiple sclerosis: an altered immune response or altered stress response? *J Mol Med* 74: 285-296.

van Oosten, BW., Barkhof, F., Truyen, L., Boringa, JB., Bertelsmann, FW., von Blomberg, BM., Woody, JN., Hartung, HP., Polman, CH. 1996. Increased MRI activity and immune activation in two multiple sclerosis patients treated with the monoclonal anti-tumor necrosis factor antibody cA2. *Neurology* 47:1531-1534.

Van Wart, HE., Birkedal-Hansen, H. 1990. The cystein switch: A principle regulation of metalloproteinase activity with potential applicability to the entire matrix metalloproteinase gene family. *Proc Natl Acad Sci* 87: 5578-5582.

Villarroya, H., Violleau, K., Ben Younes-Chennoufi, A., Baumann, N. 1996. Myelin induced experimental autoimmune encephalomyelitis in Lewis rats : Tumor necrosis factor  $\alpha$  levels in serum and cerebrospinal fluid. Immunohistochemical expression in glial cells and macrophages of optic nerve and spinal cord. *J Neuroimmunol* 64 :55-61

Virgintino D, Errede, M., Robertson, D., Capobianco, C., Girolamo, F., Virmercati, A., Bertossi, M., Roncali, L. 2004. Immunolocalization of tight junction proteins in the adult and developing human brain. *Histochem Cell Biol* 122:51-59.

Visse, R., Nagase, H. 2003. Matrix metalloproteinases and tissue inhibitors of metalloproteinase, structure function and biochemistry. 2003. *Circ Res* 92: 827-839.

Von Budingen, HC., Tanuma, N., Villoslada, P., Ouallet, JC., Hauser, SL., Genain, CP. 2001. Immune responses against the myelin/oligodendrocyte

glycoprotein in experimental autoimmune demyelination. *J Clin Immunol* 21: 155-170.

Vora, A.J., Kidd, D., Miller, D.H., Perkin, G.D., Hughes, R.A., Ellis, B.A., Dumonde, D.C., Brown, K.A. 1997. Lymphocyte-endothelial cell interactions in multiple sclerosis: disease specificity and relationship to circulating tumour necrosis factor-alpha and soluble adhesion molecules. *Mult Scler* 3: 171-179.

Vorbrodt, A.W., Dobrogowska, D.H. 2003. Molecular anatomy of intercellular junctions in brain endothelial and epithelial barriers: electron microscopist's view. *Brain Res Rev* 42: 221-242.

Wagnerova, J., Cervenakova, L., Balabanov, R., Zitron, I., Dore-Duffy, P/ 2002. Cytokine regulation of E-selectin in rat CNS microvascular endothelial cells: differential response of CNS and non-CNS vessels. *J Neurological Sci* 195: 51-62.

Wallace, J.A., Alexander, S., Estrada, E.Y., Hines, C., Cunningham, L.A., Rosenberg, G.A. 2002. Tissue inhibitor of metalloproteinase-3 is associated with neuronal death in reperfusion injury. *J Cereb Blood Flow Metab* 22: 1303-1310.

Wallach, D., Bigda, J., Engelmann, H. 1999. The tumor necrosis factor (TNF) family and related molecules. In *The cytokine network and immune functions*. Oxford university press, ed Jacques Thèze.

Walsh, S.V., Hopkins, A.M., Nusrat, A. 2000. Modulation of tight junction structure and function by cytokines. *Advanced Drug Delivery Reviews* 41:303-313.

Wang, X., Feuerstein, G.Z., Xu, L., Wang, H., Schumacher, W.A., Ogletree, M.L., Taub, R., Duan, J.J., Decicco, C.P., Liu, R.Q. 2004. Inhibition of tumor necrosis factor-alpha-converting enzyme by a selective antagonist protects brain from focal ischemic injury in rats. *Mol Pharmacol* 65:890-896.

Washington, R., Burton, J., Todd, R.F., Newman, W., Dragovic, L., Dore-Duffy, P. 1994. Expression of immunologically relevant endothelial cell activation antigens on isolated central nervous system microvessels from patients with multiple sclerosis. *Ann Neurol* 35: 89-97.

Weber, B.H., Vogt, G., Pruetz, R.C., Stohr, H., Felbor, U. 1994. Mutations in the tissue inhibitor of metalloproteinases-3 (TIMP3) in patients with Sorsby's fundus dystrophy. *Nat Genet* 8: 352-56.

Weerth, S., Berger, T., Lassmann, H., Linington, C. 1999. Encephalitogenic and neuritogenic T cell responses to myelin-associated glycoprotein (MAG) in the Lewis rat. *J Neuroimmunol* 95: 157-164.

- Weerth, SH., Rus, H., Shin, ML., Raine, CS. 2003. Complement C5 in experimental autoimmune encephalomyelitis (EAE) facilitates remyelination and prevents gliosis. *Am J Pathol* 163: 1069-1080.
- Weinshenker, B. 1994. Natural history of MS. *Ann Neurol* s6-s11.
- Weishaupt A, Kreiss M, Gold R, Herrmann T. 2004. Modulation of experimental autoimmune encephalomyelitis by administration of cells expressing antigenic peptide covalently linked to MHC class II. *J Neuroimmunol* 152: 11-19.
- Werring, DJ., Brassat, D., Droogan, AG., Clark, CA., Symms, MR., Barker, GJ., MacManus, DG., Thompson, AJ., Miller, DH. 2000. The pathogenesis of lesions and normal-appearing white matter changes in multiple sclerosis a serial diffusion MRI study. *Brain* 123: 1667-1676.
- Wetzel, M., Rosenberg, GA., Cunningham, LA. 2003. Tissue inhibitor of metalloproteinase-3 and matrix metalloproteinase-3 regulate neuronal sensitivity to doxorubicin-induced apoptosis. *Eur J Neurosci* 18: 1050-1060.
- Wilhelm, J., Pingoud, A. 2003. Real-time polymerase chain reaction. *Chembiochem* 4: 1120-1128.
- Willer, C J., Dyment, DA., Risch, NJ., Sadovnick AD., Ebers GC., The Canadian Collaborative Study Group. 2003. Twin concordance and sibling recurrence rates in multiple sclerosis. *Proc Natl Acad Sci U S A.* 100:12877-82.
- Windhagen, A., Newcombe, J., Dangond, F., Strand, C., Woodroffe, MN., Cuzner, ML., Hafler, DA. 1985. Expression of costimulatory molecules B7-1 (CD80), B7-2 (CD86), and Interleukin 12 cytokine in multiple sclerosis lesions. *J Exp Med* 182: 1995-1996.
- Wingerchuk, D.M., Lucchinetti, C.F., Noseworthy, J.H. 2001. Multiple sclerosis: current pathophysiological concepts. *Lab Invest* 81:263-281.
- Wittchen, E., Haskins, J., Stevenson, B. 1999. Protein interactions at the tight junction: Actin has multiple binding partners, and ZO-1 forms independent complexes with ZO-2 and ZO-3. *J Biol Chemistry* 274:35179-35185.
- Wolburg, H., Neuhaus, J., Kniessel, U., Kraus, B., Schmid, E.-M., Ocalan, M., Farrell, C., Risau, W. 1994. Modulation of tight junction structure in the blood-brain barrier ECs. Effects of tissue culture, second messengers and cocultured astrocytes. *J Cell Science* 107:1347-1357.
- Wolburg, H., Wolburg-Buchholz, K., Kraus, J., Rascher-Eggstein, G., Liebner, S., Hamm, S., Duffner, F., Grote, E.-H., Risau, W., Engelhardt, B. 2003. Localisation of claudin-3 in tight junctions of the blood-brain barrier is

selectively lost during experimental autoimmune encephalomyelitis and human glioblastoma multiforme. *Acta Neuropathol* 105:586-592.

Wolburg, H., Wolburg-Buchholz, K., Engelhardt, B. 2005. Diapedesis of mononuclear cells across cerebral venules during experimental autoimmune encephalomyelitis leaves tight junctions intact. *Acta Neuropathol* 109: 181-190.

Wolburg, H., Lippoldt, A. 2002. Tight junctions of the blood-brain barrier: Development, composition and regulation. *Vascular Pharmacology* 38:323-337.

Wolka, AM., Huber, JD., Davis, TP. 2003. Pain and the blood-brain barrier: obstacles to drug delivery. *Adv Drug Del Rev* 55: 987-1006.

Wolswijk, G. 2000. Oligodendrocyte survival, loss and birth in lesions of chronic-stage multiple sclerosis. *Brain* 123: 105-115.

Wong, D., Dorovini-Zis, K. 1992. Upregulation of intercellular adhesion molecule-1 (ICAM-1) expression in primary cultures of human brain endothelial cells by cytokines and lipopolysaccharide. *J Neuroimmunol* 39: 11-21.

Wong, D., Dorovini-Zis, K. 1995. Expression of vascular cell adhesion molecule-1 (VCAM-1) by brain microvessel endothelial cells in primary culture. *Microvasc Res* 49: 325-339.

Woodroffe, MN., Bellamy, AS., Feldmann, M., Davison, AN., Cuzner, ML. 1986. Immunocytochemical characterisation of the immune reaction in the central nervous system in multiple sclerosis: possible role for microglia in lesion growth. *J Neurol Sci* 74: 135-152.

Woodroffe, M.N., Cuzner, M.L. 1993. Cytokine mRNA expression in inflammatory multiple sclerosis lesions: detection by non-radioactive in situ hybridization. *Cytokine* 5:583-588.

Wucherpfennig, KW., Strominger, JL. 1995. Molecular mimicry in T-cell mediated autoimmunity: viral peptides activate human T cell clones specific for myelin basic protein. *Cell* 80: 695-705.

Wucherpfennig, KW. 2001a. Mechanisms for the induction of autoimmunity by infectious agents. *J Clin Invest* 108: 1097-1104.

Wucherpfennig, KW. 2001b. Insights into autoimmunity gained from structural analysis of MHC-peptide complexes. *Curr Opin Immunol* 13: 650-656.

Xia, MQ., Bacskai, BJ., Knowles, RB., Qin, SX., Hyman, BT. 2000. Expression of chemokine receptor CXCR3 on neurons and the elevated

expression of its ligand IP-10 in reactive astrocytes: in vitro ERK1/2 activation and role in Alzheimer's disease. *J Neuroimmunol* 108: 227-235.

Yang, J., Lindsberg, P.J., Hukkanen, V., Seljelid, R., Gahmberg, C.G., Meri, S. 2002. Differential expression of cytokines (IL-2, IFN- $\gamma$ , IL-10) and adhesion molecules (VCAM-1, LFA-1, CD44) between spleen and lymph nodes associates with remission in chronic relapsing experimental autoimmune encephalomyelitis. *Scand J Immunol* 56: 286-293.

Yamamoto, S., Higuchi, Y., Yoshiyama, K., Shimizu, E., Kataoka, M., Hijiya, N., Matura, K. 1999. ADAM family proteins in the immune system. *Immunology Today* 20: 278-284.

Ying, C., Zang, Q., Samanta, A.K., Halder, J.B., Hong, J., Tejada-Simon, M.V., Rivera, V.M., Zhang, J.Z. 2000. Aberrant T cell migration towards RANTES and MIP-1 $\alpha$  in patients with multiple sclerosis overexpression of chemokine receptor CCR5. *Brain* 123: 1874-1882.

Yong, V.W., Krekoshi, C.A., Forsyth, P.A., Bell, R., Edwards, D. 1998. Matrix metalloproteinases and diseases of the CNS. *TINS* 21: 75-80.

Young, L.S., Eliopoulos, A.G. 2004. TNF receptors and their ligands: in sickness and in health, in life and death. *Curr Opin Pharmacology* 4: 311-313.

Yoshiyama, K., Higuchi, Y., Kataoka, M., Matsuura, K., Yamamoto, S. 1997. CD156 (human ADAM-8): expression, primary amino acid sequence, and gene location. *Genomics* 41: 56-62.

Yu WH, Yu S, Meng Q, Brew K, Woessner JF Jr. 2000. TIMP-3 binds to sulfated glycosaminoglycans of the extracellular matrix. *J Biol Chem* 275:31226-1232.

Zhao, L.C., Shey, M., Farnsworth, M., Dailey, M.O. 2001. Regulation of membrane metalloproteolytic cleavage of L-selectin (CD62L) by epidermal growth factor domain. *J Biol Chem* 276: 30631-30640.

Zheng, J., Lan, Y., Guo, Y., Luo, Y. 2000. Vitro culture and immunohistochemical identification of astrocytes of infantile optic nerve. *Eye Sci* 16: 203-207.

Zivadinov, R., Bakshi, R. 2004. Role of MRI in multiple sclerosis I: inflammation and lesions. *Front Biosci* 9: 665-683.